

TESTING THE SECOND AUSTRALOPITHECINE
SPECIES HYPOTHESIS FOR THE SOUTH AFRICAN
SITE OF STERKFRONTEIN: GEOMETRIC MORPHOM
ETRIC ANALYSIS OF MAXILLARY MOLAR TEETH

Cinzia Fornai

A dissertation submitted to the Faculty of Science, University of the
Witwatersrand, in fulfillment of the requirements for the degree of Master of
Science

Johannesburg, 2009

DECLARATION

I declare that this dissertation is my own, unaided work. It is being submitted for the Degree of Master of Science in the University of the Witwatersrand, Johannesburg. It has not been submitted before for any degree or examination in any other University.

CINZIA FORNAI

Johannesburg, 27 August 2009

ABSTRACT

The morphological variability of the australopithecine fossil record from Sterkfontein Member 4, generally regarded as *Australopithecus africanus*, has been interpreted in various ways by different authors. However, R. J. Clarke originally put forward the hypothesis that such variability can be explained with the occurrence of a distinct and new *Australopithecus* species showing notable affinities with *Paranthropus*.

Focusing on the study of maxillary molar morphology, through the geometric morphometric analysis of data gathered from three-dimensional virtual images from CT-scanning, the aim of this project was to establish a new methodology for the study of hominid dentition, with the particular goal of contributing to the issue of Clarke's "second australopithecine species hypothesis" for Sterkfontein Member 4 site.

The methods applied have been demonstrated to be statistically valid. Likewise, the procedure for landmark collection has been shown to be repeatable.

The results obtained have provided further information with regard to the variability of the South African Plio-Pleistocene hominids attributed to the genera *Australopithecus*, *Paranthropus* and *Homo*, as shown by their maxillary molars. Most importantly the research supports, with new evidence, the hypothesis of the occurrence of a second australopithecine species in Sterkfontein Member 4.

*To my son Niccolò,
the greatest joy in my life.*

ACKNOWLEDGMENTS

I am deeply grateful to Necsa for providing me with the CT-scans, and in particular I thank Mr. Frikkie de Beer and Mr. Mabuti Radebe who not only operated at the facility, but supported this research with their professional skills and great enthusiasm.

A sincere acknowledgment goes to Mr. Jason Hemingway for his precious support during the statistical analysis. I also thank Dr. Silvia Boccone for sharing pictures, data and information in relation to her doctoral thesis.

I express my gratitude to Dr. Lucinda Backwell and Mr. Peter Montja for suggestions and support with regard to the casting procedures, and to Dr. Geeske Langejans who assisted with the carrying out of the experiment for the assessment of the effect of the use of a digitizer on the enamel surface.

I thank Prof. Bernard Wood and Dr. Katerina Harvati for contributing to this project with precious suggestions.

I am grateful to the Curators of the Wits fossil collection (Dr. Bernard Zipfel) and Transvaal Museum (Prof. Francis Thackeray and Ms. Stephany Potze) for permission to study the fossils and assistance. I show appreciation toward all the academic, administrative and technical staff at the School of Anatomical Sciences, University of the Witwatersrand and Dr. Kathleen Kuman for their kindness and continuous support. Last but not least, I thank Luca, my husband, for supporting me through the carrying out of this project.

This project was financially supported by:

- Necsa (refund for fuel expenses) 2007
- J.J.J. Smieszek bursary, 2007 and 2008
- Palaeontological Scientific Trust - PAST, 2007 and 2008
- Italian Government scholarship (Jan-Sep 2008)
- Postgraduate Merit Award 2008, University of the Witwatersrand
- Bradlow Scholarship 2009, University of the Witwatersrand

CONTENTS

LIST OF FIGURES.....	iv
LIST OF TABLES.....	x

CHAPTER ONE - VARIABILITY IN MAXILLARY MOLAR MORPHOLOGY IN THE AUSTRALOPITHECINE SPECIMENS FROM STERKFORTEIN MEMBER 4

1.1 <i>Australopithecus africanus</i> : taxonomic attributions and the issue of the high morphological variability among the hominid remains from the ancient cave infill of Member 4 breccia at Sterkfontein site.....	1
1.2 The second australopithecine species hypothesis.....	4
1.3 Why teeth?	9
1.4 Previous studies on the subject.....	11
1.5 Thesis structure.....	13

CHAPTER TWO - TRADITIONAL METHODS FOR THE STUDY OF TOOTH MORPHOLOGY

2.1 Tooth gross anatomy and definitions.....	15
2.2 Analytical methods.....	18
2.2.1 The descriptive approach.....	18
2.2.2 Odontometrics.....	20
2.2.3 Two-dimensional image analysis.....	23

CHAPTER THREE - ADVANCED TECHNOLOGIES FOR THE STUDY OF TOOTH MORPHOLOGY

3.1 Scanning systems for three-dimensional reconstruction.....	27
3.2 X-ray Computed Tomography (CT).....	29
3.3 Definitions and technical features of CT scan.....	30
3.4 Three-dimensional CT imaging.....	32
3.5 Drawbacks of CT-based three-dimensional imaging.....	34
3.6 Brief review of Computed Tomography (CT) properties compared to those of Neutron Tomography (NT).....	36

CHAPTER FOUR - QUANTITATIVE ANALYSIS OF DATA FROM CT BASED TECHNIQUES: GEOMETRIC MORPHOMETRICS

4.1 Landmark definition.....	38
4.2 Geometric morphometrics.....	40
4.3 Superimposition-based morphometrics, coordinate-free methods and visualization.....	42

4.4	Analyses of landmark data.....	45
-----	--------------------------------	----

CHAPTER FIVE - MATERIALS

5.1	Introduction.....	48
5.2	The sample.....	50

CHAPTER SIX - METHODS

6.1	Procedures for the collection of landmark coordinates to be used in geometric morphometric analysis.....	60
6.1.1	Acquisition of landmarks on the original specimens (or casts).....	61
6.1.2	Sampling of landmarks on pictures and casts	62
6.1.3	Collection of data on Optical Coherence Tomography – OCT.....	63
6.1.4	X-ray tomography.....	64
6.2	SANRAD facility.....	65
6.3	Tomography procedure.....	67
6.4	Image reconstruction.....	68
6.5	Tomography set up and expedients for the safety of the fossils.....	70
6.6	Other security measures for the safety of the fossils.....	71
6.7	Set of landmarks.....	72
6.8	Tooth alignment.....	74
6.9	Landmark coordinate sampling.....	76
6.10	Statistical analyses.....	82

CHAPTER SEVEN - ASSESSMENT OF THE METHODS USED, ADVANTAGES AND LIMITATIONS

7.1	Introduction.....	85
7.2	First molars. <i>Paranthropus</i> vs. early <i>Homo</i>	87
7.3	Second molars. <i>Paranthropus</i> vs. early <i>Homo</i>	97
7.4	Repeatability of the landmark collection.....	101
7.5	Advantages and limitations.....	109
7.5.1	CT scan through the SANRAD facility, Necsa.....	109
7.5.2	Tooth orientation.....	110
7.5.3	Acquisition of landmark data through VGStudio MAX 2.1.....	112
7.5.4	Analysis of landmark data.....	114
7.6	Final remarks.....	114

CHAPTER EIGHT - RESULTS

8.1	Introduction.....	116
8.2	First molars.....	118
8.3	Second molars.....	125
8.4	Third molars.....	131
8.5	Joint first and second molars.....	137
8.6	Final remarks.....	139

CHAPTER NINE – DISCUSSION

9.1	On the methodology.....	141
9.2	Other potential uses of the methods.....	143
9.3	On the second species hypothesis.....	147
9.4	Additional results.....	158
	9.4.1 First molars.....	159
	9.4.2 Second molars.....	162
	9.4.3 Third molars.....	163
	9.4.4 Remarks on the correlation between size and shape.....	164
	9.4.5 Joint first and second molar configurations.....	165
9.5	Uncertain attributions.....	165
9.6	The case of StW 151.....	167
9.7	Morphological variability within <i>Paranthropus</i>	168

CHAPTER TEN – CONCLUSIONS.....170

APPENDIIX A - Maxillary molar morphology in the taxa under study.....175

APPENDIX B - Experiment on animal teeth: testing the risk of enamel damage related to the use of the standard and extra fine tips of the digitizer.....180

APPENDIX C - Casting procedures for tooth replicas.....182

APPENDIX D - Landmark collection: image gallery.....184

REFERENCES.....217

LIST OF FIGURES

	Page
Fig. 1.1 Specimen StW 252 before and after the reconstruction of Ronald J. Clarke.....	3
Fig. 1.2 The comparison between OH 5, <i>P. boisei</i> from Tanzania (a. and b.) and Sts 5, <i>A. africanus</i> (c. and d.) helps in the identification of some of the cranial features of <i>Paranthropus</i> among those highlighted by Clarke (1996; pp. 94-95) with respect to other genera of the same family Hominidae.....	5
Fig. 2.1 Tooth anatomy.....	15
Fig. 2.2 Upper and lower dental arches and associated terminology.....	16
Fig. 2.3 Occlusal views of a maxillary molar showing its anatomical features and their names.....	17
Fig. 2.4 Identification of mesio-distal and bucco-lingual diameters.....	21
Fig. 2.5 A M ¹ showing the occlusal polygon. The lines connect the cusp tips of the protocone (A), paracone (B), metacone (C) and hypocone (D).....	23
Fig. 2.6 – A. Image illustrating the points (interlandmarks) sampled for the study of P4 occlusal surface. B. and C. illustrate further elaboration of landmark coordinates in two different steps of the geometric morphometric analysis.....	24
Fig. 3.1 Surface models of teeth (upper left to lower right: <i>Afropithecus</i> , <i>Dryopithecus</i> , <i>Gorilla</i> , <i>Pan</i> , <i>Pongo</i>).....	28
Fig. 3.2 Chimpanzee’s molar occlusal surface. Shaded relief model with superimposed contour lines and with triangulated irregular network.....	29
Fig. 3.3 Transversal slice of the skull Saccopastore 1 (<i>Homo neanderthalensis</i>). The image shows the stone matrix included in the endocranial cavity.....	31
Fig. 3.4 Models of australopithecine molars in occlusal view produced through the 3D imaging method of surface rendering.....	33
Fig. 3.5 Midsagittal CT scans of KNM-ER406 (<i>Paranthropus boisei</i>) showing high noise levels and ‘frozen noise’ streak artifacts.....	35
Fig. 4.1 Transformation grids as conceived by D’Arcy Thompson.....	40

Fig. 4.2	Schematic of the three-step process of Procrustes analysis performed on triangles.....	43
Fig. 4.3	Thin Plate Spline (TPS) deformation grid between the midsagittal profiles of a human skull and a chimpanzee skull.....	44
Fig. 4.4	Vector plot for the visualization three-landmarks configurations..	45
Fig. 4.5	Representation of Kendall's shape space for triangles and projection of points representing triangles in Kendall's shape space into a space tangent to the mean triangle and the principal components of shape variability in this tangent space.....	46
Fig. 5.1	Fossil hominid sites within the Cradle of Humankind, north of Krugersdorp and Makapansgat.....	59
Fig. 6.1	Digitizer: Immersion's MicroScribe® G2X	61
Fig. 6.2	Slice of a cast of a first molar (StW 151) as built through OCT....	64
Fig. 6.3	Schematic top view of the beam line facilities at SAFARI-1.....	66
Fig. 6.4	Schematic illustration of the tomography set up at the SANRAD facility.....	68
Fig. 6.5	Set up of the partial mandible of <i>Theropithecus oswaldi</i> fixed with putty onto the rotary disk and positioned between the X-ray source and the scintillator screen.....	70
Fig. 6.6	Three-dimensional virtual image where the main axes of the scene box are not parallel to those of the teeth	74
Fig. 6.7	Section of the virtual image showing Line 1 and Line 2 which connect respectively points P2-P3 and P4-P5.....	77
Fig. 6.8	Transverse section of SK 829 LM ¹ at the level of Plane P1 showing two different procedures for the collection of point on the crown outline.....	78
Fig. 6.9	Transverse section on Plane P1 where points P2 and P4, P4 and P3, P3 and P5, P5 and P2 are connected with lines.....	80
Fig. 7.1	PCA: M ¹ – <i>Paranthropus</i> (SK 55A, SK 89, SK 102, SK 829, SK 832, SK 838, SK 839). Percentage of total variance explained from PC1: 47.22% and PC2: 20.17%.....	88
Fig. 7.2	PCA: M ¹ – <i>Paranthropus</i> and early <i>Homo</i> (SK 27). Percentage of total variance explained from PC1: 41.77% and PC2: 20.58%.....	90

Fig. 7.3	PCA: M ¹ – <i>Paranthropus</i> and early <i>Homo</i> (SK 27; SKW 3114). Percentage of total variance explained from PC1: 37.87% and PC2 21.31%.....	92
Fig. 7.4	PCA: M ¹ – <i>Paranthropus</i> and early <i>Homo</i> (SK 27; SKW 3114; SKX 268 cast). Percentage of total variance explained from PC1: 34.07% and PC2: 20.63%.....	94
Fig. 7.5	PCA: M ¹ – <i>Paranthropus</i> and early <i>Homo</i> ; PC1 against centroid size. No significant correlation between size and shape is shown ($r = 0.45162$; $P = 0.19011$).....	96
Fig. 7.6	PCA: M ² – <i>Paranthropus</i> and early <i>Homo</i> . Percentage of total variance explained from PC1: 32.55% and PC2: 19.14% ($r = 0.23701$; $P = 0.50969$).....	98
Fig. 7.7	PCA: M ² – <i>Paranthropus</i> and early <i>Homo</i> ; PC1 against centroid size. No significant correlation between size and shape is shown.....	100
Fig. 7.8	PCA: M ³ – Repeatability test. The seven pairs of repeats are plotted together.....	103
Fig. 7.9	PCA: M ³ full sample – Repeatability test. The seven pairs of repeats are plotted together with the rest of M ³ specimens.....	104
Fig. 7.10	Results of the investigation of the Euclidean distances for the evaluation of intra-observer error	106
Fig. 7.11	Pairwise comparison of the landmark configurations which show a difference in a visual inspection.....	108
Fig. 7.12	Axial view of a virtual image showing the measuring tool of VGStudio MAX 2.1 software.....	114
Fig. 8.1	PCA: M ¹ – Full sample. Percentage of total variance explained: PC1 22.65% and PC2 19.10%.....	121
Fig. 8.2	Wire frame images (as built from <i>Morphologika</i> software) showing the mean shapes of the first molars at the extremes scores for PC1 and PC2 as well as the mean shape.....	122
Fig. 8.3	PC1 against centroid size. With regards to first molars, any significant correlation exists between size and shape ($r = -0.31078$, $P = 0.15921$).....	123
Fig. 8.4	Morphing along the regression line of centroid size and PC1 for first molars.....	124

Fig. 8.5	PCA: M ² – Full sample. Percentage of total variance explained from PC1: 24.18% and PC2 15.15%.....	127
Fig. 8.6	Wire frame images (as built from <i>Morphologika</i> software) showing the mean shapes of the second molars at the extremes scores for PC1 and PC2 as well as the mean shape.....	128
Fig. 8.7	PC1 against centroid size. With regards to second molars a significant correlation exists between size and shape ($r = 0.43487$, $P = 0.043116$).....	129
Fig. 8.8	Morphing along the regression line of centroid size and PC1 for second molars.....	130
Fig. 8.9	PCA: M ³ – Full sample. Percentage of total variance explained from PC1: 20.81% and PC2 15.78%.....	133
Fig. 8.10	Wire frame images (as built from <i>Morphologika</i> software) showing the mean shapes of the third molars at the extremes scores for PC1 and PC2 as well as the mean shape.....	134
Fig. 8.11	PC1 against centroid size. With regards to third molars, any significant correlation exists between size and shape ($r = ,0.089808$, $P = 0.69103$).....	135
Fig. 8.12	Morphing along the regression line of centroid size and PC1 for third molars.....	136
Fig. 8.13	PCA: M ¹ and M ² as a single object. Percentage of total variance explained from PC1: 58.24% and PC2 20.14%.....	138
Fig. 9.1	Images from VGStudio MAX 2.1 showing the degree of modification due to the previous invasive investigation on StW 280 fossil molar compared to its cast which preserve the original form of the specimen.....	145
Fig. 9.2	Visualization features showing the (subtle) differences between the morph of StW 280 cast and StW original but damaged specimen.....	146
Fig. 9.3	Wire frame images showing the general morphology of M ¹ for the different hominid taxa through the mean shapes at the extremes scores for PC1 and PC2.....	160
Fig. 9.4	Wire frame images showing the general morphology of M ² for the different hominid taxa through the mean shapes at the extremes scores for PC1 and PC2.....	161

Fig. 9.5	Occlusal photographs of M ² of Sts 22 and StW 183 which show notable differences in overall crown morphology.....	163
Fig. 9.6	Wire frame images showing the general morphology of M ³ for the different hominid taxa through the mean shapes at the extremes scores for PC1 and PC2.....	164
Fig. B.1	Portion of the tooth surface of <i>Theropithecus oswaldi</i> before and after the use of the extra-fine tip.....	181
Fig. D.1	Point i. Palatal aspect.....	184
Fig. D.2	Point ii. Buccal aspect.....	185
Fig. D.3	Point iii. Mesial aspect	186
Fig. D.4	Point iv. Distal aspect	187
Fig. D.5	Tooth image before alignment	188
Fig. D.6	Tooth image after alignment	189
Fig. D.7	P1. Lowest point of central fossa.....	190
Fig. D.8	P2. Contact between Pr-Hy on the plane P1 outline.....	191
Fig. D.9	P3. Contact between Pa-Me on the plane P5 outline.....	192
Fig. D.10	P4. Contact between Pr-Pa on the plane P5 outline.....	193
Fig. D.11	P5. Contact between Hy-Me on the plane P5 outline.....	194
Fig. D.12	Line 1 (connecting P2-P4).....	195
Fig. D.13	Line 2 (connecting P4-P3).....	196
Fig. D.14	Line 3 (connecting P3-P5).....	197
Fig. D.15	Line 4 (connecting P5-P2).....	198
Fig. D.16	Lines 1-4.....	199
Fig. D.17	P6. The furthest point projecting from Line 1 to the Pr outline...200	
Fig. D.18	P7. The furthest point projecting from Line 2 to the Pa outline...201	
Fig. D.19	P8. The furthest point projecting from Line 3 to the Me outline..202	
Fig. D.20	P9. The furthest point projecting from Line 4 to the Hy outline..203	

Fig. D.21	P10. Pr apex.....	204
Fig. D.22	P11. Pa apex.....	205
Fig. D.23	P12. Me apex.....	206
Fig. D.24	P13. Hy apex.....	207
Fig. D.25	P14. Central groove mesial terminus on the mesial crest.....	208
Fig. D.26	P15. Lowest point on central groove between P1 and P14.....	209
Fig. D.27	P16. Intersection between the distal central groove and the transverse groove.....	210
Fig. D.28	P17. Lowest point of distal fossa.....	211
Fig. D.29	P18. Central groove distal terminus on the distal crest.....	212
Fig. D.30	P19. Highest point of contact between Pr and Hy.....	213
Fig. D.31	P20. Highest point of contact between Pa and Me.....	214
Fig. D.32	Comprehensive views of the set of landmarks collected.....	215

LIST OF TABLES

	Page
Table 2.1 Anthropometric indexes calculated from the fundamental variables MD and BL diameters.....	20
Table 5.1 Specimens considered in this study: species attribution and site of provenience.....	51
Table 5.2 Number of maxillary molars analysed/Number of maxillary molars scanned at Necca.....	53
Table 5.3 Specimens divided by tooth typology and listed in alphabetical order. Descriptions of the level of wear and the state of preservation are provided together with relevant notes.....	54
Table 6.1 Characteristics of the X-ray beam and image properties at SANRAD facility.....	67
Table 6.2 Resolution parameters applied for the calibration of image size....	70
Table 6.3 Set of landmarks.....	73
Table 7.1 M ¹ . <i>Paranthropus</i> , Swartkrans (sample: SK 55A, SK 89, SK 102, SK 829, SK 832, SK 838, SK 839): eigenvalues and percentage of variance explained for all the PCs.....	89
Table 7.2 M ¹ . <i>Paranthropus</i> (sample: SK 55A, SK 89, SK 102, SK 829, SK 832, SK 838, SK 839) and early <i>Homo</i> (sample: SK 27): eigenvalues and percentage of variance explained for all the PCs.....	91
Table 7.3 - M ¹ . <i>Paranthropus</i> (sample: SK 55A, SK 89, SK 102, SK 829, SK 832, SK 838, SK 839) and early <i>Homo</i> (sample: SK 27, SKW 3114): eigenvalues and percentage of variance explained for all the PCs.....	93
Table 7.4 - M ¹ . <i>Paranthropus</i> (sample: SK 55A, SK 89, SK 102, SK 829, SK 832, SK 838, SK 839) and early <i>Homo</i> (sample: SK 27, SKW 3114, SKX 268 cast): eigenvalues and percentage of variance explained for all the PCs.....	95
Table 7.5 – M ² . <i>Paranthropus</i> , (sample: SK 13/14, SK 16, SK 47, SK 48 cast, SK 49 cast, SK 98, SK 834, SK 837, SKW 11) and early <i>Homo</i> (sample: SK 27): eigenvalues and percentage of variance explained for all the PCs.....	99
Table 7.6 Euclidean distances between pairs of repeats in ascendant order.....	106

Table 8.1	Significant linear correlations between centroid size and landmark coordinate for first molars.....	124
Table 8.2	Significant linear correlations between centroid size and landmark coordinate for second molars.....	130
Table 8.3	Significant linear correlations between centroid size and landmark coordinate for third molars.....	136

CHAPTER 1

VARIABILITY IN MAXILLARY MOLAR MORPHOLOGY IN THE AUSTRALOPITHECINE SPECIMENS FROM STERKFORTEIN MEMBER 4

1.1 - *Australopithecus africanus*: taxonomic attributions and the issue of the high morphological variability among the hominid remains from the ancient cave infill of Member 4 breccia at Sterkfontein site

Several hundred early hominid specimens were recovered from the first excavations at Sterkfontein Caves between 1936 to the present (see Schwartz and Tattersall, 2005 for a general review of the site and of the specimens). The most fruitful deposit in Sterkfontein seems to be the Member 4 breccia, within which the area known as the “Type site” provided the type specimen of *Australopithecus transvaalensis* which is represented by a partial cranium and endocast (TM 1511) that came to light through the mining operations at the site. Broom (1936) considered it to be generally similar to the juvenile specimen from Taung for which Raymond A. Dart had created the new genus and species *Australopithecus africanus* (1925). Subsequently, Broom (1938), being impressed by the differences he noted between the Taung child and a child mandible from Sterkfontein (TM 1516 and associated left canine Sts 50), placed the individuals from Sterkfontein in the new genus *Plesianthropus*. Later findings had led Broom and Schepers (1946) to the conclusion that australopithecines are closely related

to humans, a belief that was strengthened by the remarkable finding of the fairly complete skull Sts 5 (Broom, 1947). In the 1940s, this wisdom was brought to the attention of the international scientific community and led to the extreme viewpoint of Mayr (1950) who lumped all the australopithecines into *Homo transvaalensis*. Although this view was supported by some authors, from the 1950s the specimens from Sterkfontein were generally considered as members of *A. africanus*. By the mid 1960s there was wide acceptance also in including in the same taxon *A. africanus* the individuals recovered from the Makapansgat Limeworks site (Day, 1965; Reed, *et al.*, 1993) which were initially attributed by Dart to a new species *A. prometheus* (1948a,b; 1949a,b,c; 1954; 1959; 1962). Nevertheless, both the assemblages from Sterkfontein Member 4 and Makapansgat include individuals with diverse cranial morphologies and tooth sizes (Clarke, 1988; 1994), which is the reason why the various forms present have been interpreted in different ways by different authors. Some (e.g. Broom, 1947) saw them as males and females of one species. Robinson (1967) and Olson (1985) have stressed the *Homo*-like features and considered *A. africanus* as the direct *Homo* ancestor and, therefore, classified it as *Homo*. A different viewpoint interprets *A. africanus* as ancestor of both *Homo* and *Paranthropus* (Tobias, 1980; Skelton, *et al.*, 1986). Others believe *A. africanus* is a *Paranthropus* ancestor, focusing primarily on *Paranthropus*-like features (Johanson and White, 1979; White, *et al.*, 1981; Rak, 1983).

The fossil assemblage from Makapansgat is also known for its morphological variability. For example, Aguirre (1970) considered that it is indubitable that there

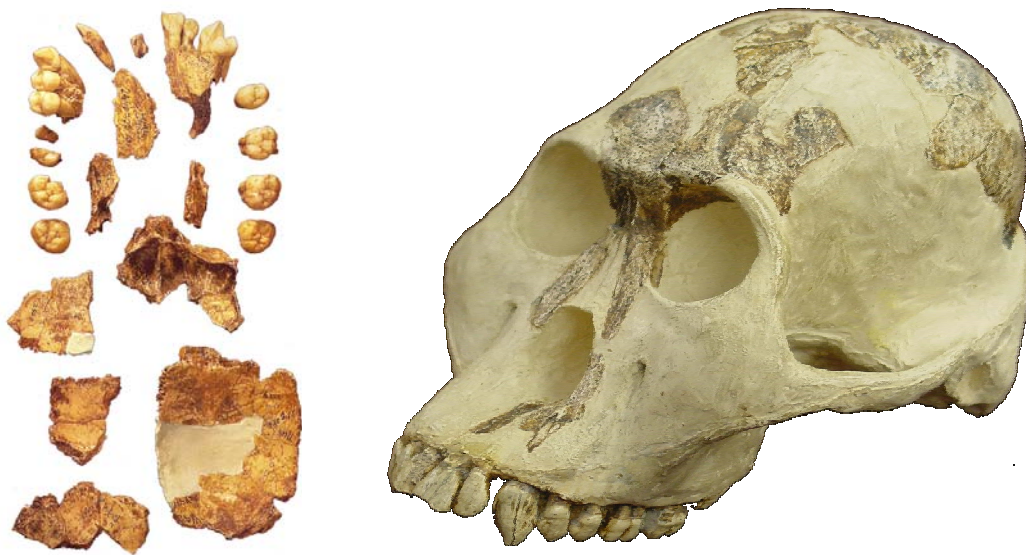


Fig. 1.1 – Specimen StW 252 before (left) and after (right) the reconstruction of Ronald J. Clarke (1988)

is more than one hominid species at Makapansgat as well as at Sterkfontein and he classified the Makapansgat MLD 2 mandible as *Paranthropus*.

A further explanation of the high variability found among the specimens of Member 4 and Makapansgat has been proposed by Clarke (1985a,b; 1988; 1994; 1996; 2008). He believes that both sites contain two *Australopithecus* species. This second species is exemplified by a fragmentary partial cranium from Sterkfontein Member 4, labelled StW 252 (Clarke 1988; Figure 1.1). After being reconstructed, it showed a number of cranial and dental features that suggested a morphology not akin to that of *A. africanus*. Other specimens he thinks can be grouped with StW 252, and could represent a large number of individuals. These include the partial cranium Sts 71, StW 183, StW 498, the fairly complete cranium StW 505, and a large number of tooth remains from Sterkfontein and MLD 2 from Makapansgat.

1.2 - The second australopithecine species hypothesis

Among the Sterkfontein Member 4 remains, Clarke (1988) recognised a new hominid form which is characterised by a large sized dentition (especially in the postcanine teeth), thin supraorbital margin and flat nasal region associated with anteriorly prominent cheek bones, features that make it distinguishable from the other small-toothed form, with thick supraorbital margin, and prominent nasal area relative to cheek bones. On the basis of considerations of the morphology of this specimen and others allied to it and on the stratigraphy of Sterkfontein, Clarke rejected with confidence the possibility of explaining the variability observed through sexual dimorphism, individual variation, or change through time. On the contrary, he argued the bigger-toothed morph trends towards the condition of the australopithecine genus *Paranthropus*, and suggested the recognition of a new second species of *Australopithecus* in Member 4 and Makapansgat.

The genus *Paranthropus* was first recognized by Robert Broom (1938) at Kromdraai and later found at other South African sites (Swartkrans has yielded the most numerous sample) and in East Africa. The features that characterise *Paranthropus* are principally related to the presence of a very massive masticatory apparatus, making it a highly specialised primate form (Clarke, 1996). The apomorphous characters specific to *Paranthropus* and identifiable in the cranium have been described in detail by Robinson (1962) and later extended by Clarke (1996; see Figure 1.2). Diagnostic features include a very pronounced flatness of the face, small incisors and canines, molarised premolars and very large molars, in total a different tooth morphology when compared to *A. africanus* (Broom, 1938; Robinson, 1962; Clarke, 1996) which is characterised by a less robust masticatory

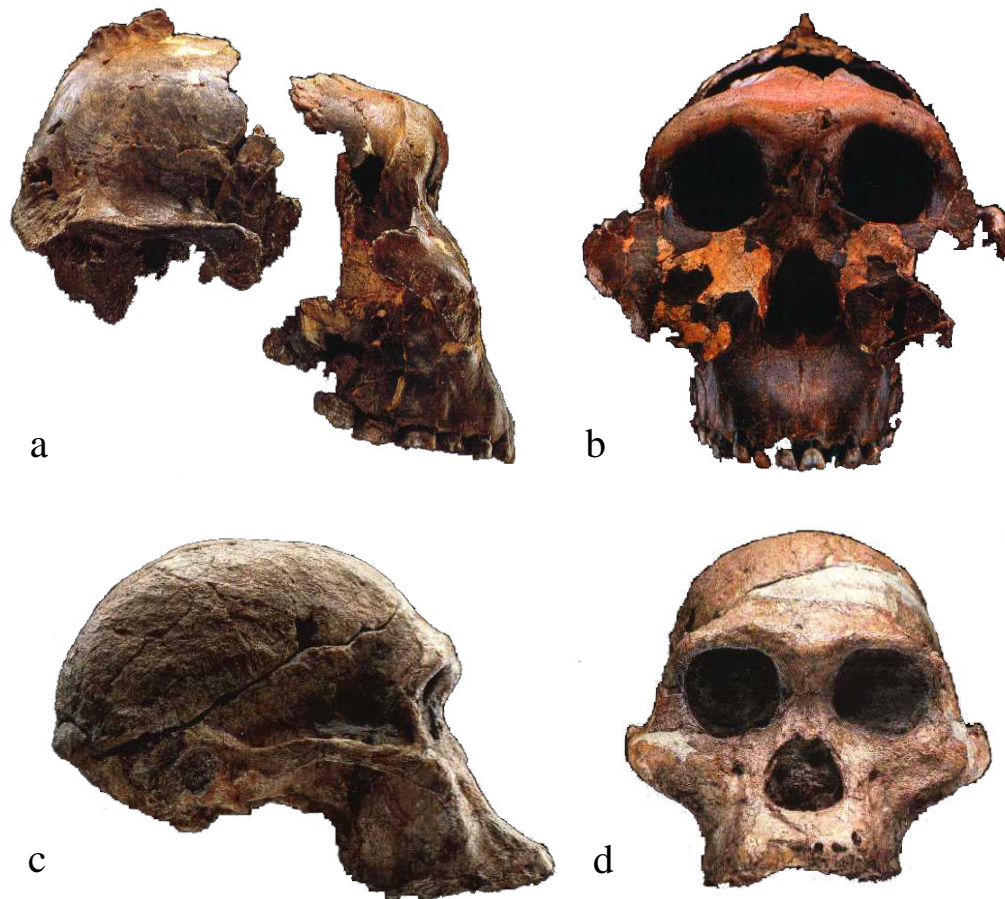


Fig. 1.2 – The comparison between OH 5, *P. boisei* from Tanzania (a. and b.) and Sts 5, *A. africanus* (c. and d.) helps in the identification of some of the cranial features of *Paranthropus* among those highlighted by Clarke (1996; pp. 94-95) with respect to other genera of the same family Hominidae

apparatus. In particular, Clarke (1996; pp. 94-95) describes the following cranio-facial traits characteristic to *Paranthropus*:

- A brain that is on the average larger than that of *Australopithecus*, yet not as large as that of *Homo*
- Formation of a central facial hollow associated with a completely flat nasal skeleton and a cheek region which is situated anterior to the plane of the piriform aperture
- Great increase in the size of the masticatory musculature and attachments, relative to the size of the skull

- Formation of a broad gutter on the superior surface of the posterior root of the zygoma
- A low forehead with a frontal trigone delimited laterally by posteriorly converging temporal crests
- Presence of a flattened “rib” of bone across each supraorbital margin
- A glabella that is situated at a lower level than the supraorbital margin
- A naso-alveolar clivus which slopes smoothly into the nasal cavity
- Temporal fossa capacious and mediolaterally expanded

As stated by Clarke (1988), the hominid form represented by the individual StW 252, Sts 71 and other large-toothed specimens from Member 4 of Sterkfontein and from Makapansgat is comparable to *Paranthropus* in overall cranial morphology and tooth size, except for the anterior dentition that seems to retain the plesiomorphic condition of prognathism with a wide intercanine region. Considering the dating of the Member 4 site, which is approximately between 2.6 and 2.1 Myr old (Vrba, 1985; Kuman and Clarke, 2000; Partridge, 2005) and the fact that the most ancient *Paranthropus* cranium yet discovered (*P. boisei* or *P. aethiopicus*; Walker, *et al.*, 1986; Walker and Leakey, 1988; Kimbel, *et al.*, 1988) is dated at 2.5 Myr and presents the same characteristic of massiveness but also a remarkable prognathism, Clarke believes the second australopithecine species at Sterkfontein might be closely associated with the lineage leading to *Paranthropus* based on the observations made on specimens such Sts 71, StW 252 and StW 505. Indeed, Schwartz and Tattersall (2005) did acknowledge the high morphological variability observed within the Sterkfontein Member 4 assemblage by grouping

the fossil remains according to their morphological affinities rather than assigning them to specific taxa. In particular, they decided to use the degree of development of the molar cingula as the major criterion to allocate the different kind of dentitions observed in the different morphs. However, their grouping does not coincide with that of Clarke (1998, 2008). Schwartz and Tattersall (2005) also found the specimens from Makapansgat of difficult taxonomic attribution because of the variety of unconnected cranial and dental regions represented. Interestingly, they considered some of the specimens as allied to the *A. africanus* type specimen and others, such as MLD2 mandible, morphologically close to TM1517b *Paranthropus* specimen, while they thought some other isolated teeth match with the StW 252 morphology.

Kimbel and White (1988) examined cranial and dental features for a wide sample of australopithecines from southern and eastern Africa and compared it with the variability known for modern apes. They found the variability expressed within *A. africanus* impossible to be explained either with individual variation or sexual dimorphism; therefore they considered two not necessarily mutually exclusive potential explanations: the presence of a second hominid species at Sterkfontein Member 4 and/or the presence of a temporally mixed population of an evolving lineage.

However, other viewpoints have been advanced on the matter. Lockwood and Tobias (2002) provided a description of 27 hominid cranial remains recovered from Member 4 between 1968 and 1994. They recognised the majority of the specimens as *A. africanus*, and others of uncertain attribution. They also identified two specimens (StW 183 and StW 255, plausibly related to StW 252) that clearly

do not fall into the range of variation of *A. africanus* but rather show affinities with *Paranthropus*. Other individuals also exhibit interesting and possibly significant differences. Lockwood and Tobias (2002) concluded that a second species may occur at Sterkfontein; however, they did not infer its phyletic role and show doubt with regard to a new species. For example, elsewhere (1999), they considered StW 505 a large male belonging to the species *A. africanus*, rather than an individual of a different species. Furthermore, Lockwood and Tobias (2002) disagreed with Clarke (1988; 1994) about the number of the specimens diverging from *A. africanus*, and considered it to be smaller. On the contrary, they agreed with Kimbel and Rak (1993), and Moggi-Cecchi, *et al.* (1998), who underlined the occurrence of individual differences within the *A. africanus* hypodigm, as a possibility for some specimens to represent *Homo* (namely, Sts 19, and StW 151 respectively). Elsewhere, Moggi-Cecchi, *et al.*, (2006) analyzed a large tooth sample from Sterkfontein Member 4 in its coefficients of variation of the linear mesio-distal and bucco-lingual dimensions, with those collected on *A. africanus*, *P. robustus* and *Homo sp.* from other sites in southern Africa. They did not find sufficient reason to support the occurrence of multiple species in the Sterkfontein Member 4 sample since their results did not show a sufficiently high degree of variability for the Member 4 assemblage. Nevertheless, Moggi-Cecchi and Boccone (2007) identified some individuals among the remains from Member 4 that do not fit the pattern of variability of *A. africanus*. They suggested in conclusion that further diverse statistical techniques and analytical approaches could be used to analyse Sterkfontein Member 4 variability.

1.3 - Why teeth?

The partial, fragmented and/or deformed status of the fossil remains represents one limitation to the interpretation of the morphological and therefore biological and taxonomical meaning of the various hominid forms present at sites. However, fossils represent the only evidence of extinct hominids and therefore the major source of information for a palaeoanthropologist. Thus, it is inevitable that the study of fossil material cannot improve our knowledge on the genetic, behavioural, feeding and reproductive patterns of the extinct forms. Nonetheless, by focusing on the skeletal and dental morphology it is still possible to distinguish between different biological morphotypes assuming that some morphological features are more distinctive and reliable than others. However, it is to be noted that the application of diverse species concepts may also lead to very different results, where, for example, different chronospecies are clustered into a single lineage (e.g. Wolpoff, *et al.* 1994) while others have considered the traditional taxa to be divided since the hard tissues underestimate the actual variability represented (e.g. Tattersall, 1986; 1992; 1994).

This research focuses on the dentition which is considered a very informative form of fossil remains in that the hominid (and primate dentition in general) is rather conservative. Thus, when notable morphological differences are observable between fossil dental remains it is legitimate to consider that these may represent different taxa, especially when coupled with the observations made on craniofacial and mandibular fossils. This represents an application of the phylogenetic species concept where a species is defined as “an irreducible cluster

of organisms, diagnosably distinct from other such clusters, and within which there is a parental pattern of ancestry and descent” (Cracraft, 1989; pp. 34-35).

The present project was motivated by a previous analysis carried out by Boccone (2004) for her Doctoral research under the supervision of Prof. Jacopo Moggi-Cecchi at Università degli Studi di Firenze, Italy the results of which were later published in a paper by Moggi-Cecchi and Boccone (2007). Boccone provided a comparative and integrated analysis of South African australopithecine maxillary molars. She assessed the metrical variation among the sample studied on the basis of cusp areas. Boccone highlighted the differences in the patterns of dental growth and development among the different forms studied and identified a diverse metrical pattern for those specimens that are elsewhere (Clarke, 1988) considered as a different species. Since such analysis provided interesting preliminary results on the matter, the opportunity to examine the same sample with advanced methods and powerful statistical techniques was a main focus.

Another reason in support of the choice of teeth as materials for this research is that Clarke (1996) identifies the molar crown morphology as one of the several tangible characteristics (in terms of both degree of expression and number of fossil examples) on which he bases his hypothesis. In particular, the cusps of the cheek teeth are very low and bulbous, with cusp tips situated closer to the centre of the crown than in *A. africanus* and *Homo*. Furthermore, cheek teeth are characterised by the formation of flat occlusal wear surface, with smoothly rounded borders between the occlusal surfaces and the sides of the crowns. Considering that variation in tooth shape and cusp form between closely related primate species is not easy to quantify or even to visualise, and regular criteria of

variation between species do not exist for all those aspects of morphology seen in the totality of the individual, it was an encouraging fact that there are clearly visible dental distinctions between individual molars in the Sterkfontein and Makapansgat samples suggesting that there may be a specific difference especially when taken in conjunction with the cranial morphological distinctions. The morphological analysis proposed for this study is in order to elucidate the matter.

1.4 - Previous studies on the subject

Previous studies have already highlighted the dental morphological variability within the australopithecine forms (Grine, *et al.*, 2003; Hills, *et al.*, 1983; Suwa, *et al.*, 1994; Wood and Abbott, 1983; Wood, *et al.*, 1983; Wood and Engleman, 1988; see also appendix A for the description of maxillary molar morphology of the taxa considered in this study). It is also known that a diverse masticatory function is reflected in a different dental arcade shape (Clarke, 1996) and dental size, and relative tooth dimensions are both significantly different within the australopithecines.

Most of the studies (see the latest Moggi-Cecchi, *et al.*, 2006) are based on the analysis of linear dental dimensions (namely, mesio-distal and bucco-lingual diameters). Other works have also highlighted the relations between the different cusp areas (Moggi-Cecchi and Boccone, 2007; Wood, 1984; Wood and Abbott, 1983; Wood, *et al.*, 1983; Wood and Engleman, 1988), cross sectional shape of the crown and crown features such as fissure pattern (Wood, *et al.*, 1983). However, the variables that have been used were not suitable for the description

of those morphological differences that can be clearly detected through a visual inspection of the molars. Calcagno, *et al.* (1997; 1999) studied the variability on posterior dental morphology within two different samples of individuals commonly assigned to *A. africanus* from Sterkfontein Member 4 (“StW” specimens for the study of 1997 and “Sts” specimens for the study of 1999) through the analysis of bucco-lingual and mesio-distal diameters. They found contrasting results with regard to the hypothesis of multiple species at Sterkfontein by applying different methodologies to samples different in sizes. Their results show the problem with the description of the morphology through application of linear statistical analyses.

No previous research on this topic has provided results based on the analysis of the crown morphology considered in its totality and in its three-dimensional shape. The aim of the present project is to highlight the variability expressed within the sample studied in terms of crown and cusp morphology and cusp relative position, rather than tooth size. Observations and descriptions of authoritative scholars (Clarke, 1985a,b; 1988; 1994; 1996; 2008; but see also Lockwood and Tobias, 2002) have commented on the likelihood of a second species in addition to *A. africanus*. Thus, this project was conceived with the aim of evaluating the differences in shape, quantifying morphological and thus phylogenetic distances between the hominid forms under consideration, by studying dental morphology through accurate and powerful techniques.

Particularly, this project has two main objectives: the first is the establishment and assessment of a new methodology for the study of hominid molar crown morphology where the null hypothesis is that the molars belonging to two

different hominid genera cannot be distinguished by the method applied. The second is the test of the hypothesis of the occurrence of a second *Australopithecus* species at Sterkfontein Member 4 through the analysis of maxillary molar morphology by applying the methods previously outlined. Thus, with regard to the latter statement, the null hypothesis that the molars of the specimens from Sterkfontein Member 4 do form only one cluster, will be tested.

1.5 - Thesis structure

The main problem here investigated and the purposes of the present study are treated above. In the following chapters a review of the current methods available for the study of human remains in general and tooth morphology in particular is presented: chapter 2 is devoted to the description of the traditional approaches, for which advantages and limitations are discussed; in chapter 3 the state of art methods such as tomographic techniques, which have been lately applied to overcome problems and limitations of the traditional methodologies, are illustrated and evaluated. Chapter 4 explains how data obtained from CT-scans can be analyzed through geometric morphometrics, an innovative statistical technique for the quantitative study of the shape of living objects which is applied in this work.

Chapters 5 describes the materials used and chapter 6 illustrates the methods and procedures applied for the carrying out of the present study.

Chapter 7 is dedicated to the assessment of the methods chosen as preliminary and basic step before they were applied in chapter 8 which shows the results of the

analyses performed on the full sample of hominids taken into consideration. The discussion is given in chapter 9 and the conclusions are reported in chapter 10.

Additional information on certain aspects already presented in the body of the thesis is given in the appendices following chapter 10. Appendix A provides a description of the maxillary molar morphology of the taxa considered in this research (reference in the present chapter). Appendix B illustrates an experiment conducted at an early stage of this work in order to evaluate the effects of the use of a metallic tip (such as that of an electromagnetic digitizer for the collection of landmark coordinates) on a tooth surface. Appendix C describes the procedure and materials used for casting some of the fossil teeth included in the sample. Appendix D reports template images that show the processes of virtual tooth alignment and landmark collection on 3D images. The appendices from B to D are linked to chapter 6.

CHAPTER 2

TRADITIONAL METHODS FOR THE STUDY OF TOOTH MORPHOLOGY

2.1 - Tooth gross anatomy and definitions

Teeth are composed of different anatomical regions and made up of different biological tissues (Figure 2.1). A tooth mainly consists of a crown and a root

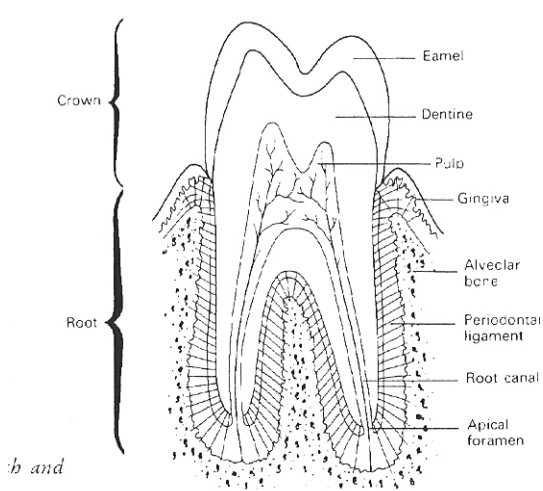


Fig. 2.1 – Tooth anatomy (from Aiello and Dean 1990)

system, mostly formed of dentine. The anatomical crown is that region of a tooth covered with enamel and clinically corresponds to that part that emerges from the gum into the mouth with the pulp chamber found in the centre. A root system may be composed of a single or multiple roots. Roots are covered with cementum, and are mostly embedded into alveolar bone; they normally have pulp canals. The limit between the crown and the root(s) is called the cervical margin, while the area of contact between the inner enamel surface and the crown is known as enamel-dentine junction (EDJ). Tooth tissues are made of particularly durable biological material, however both cementum and dentine are not as tough and white as enamel which

is the hardest biological material known (it is in fact formed of tightly packed bundles of apatite crystals).

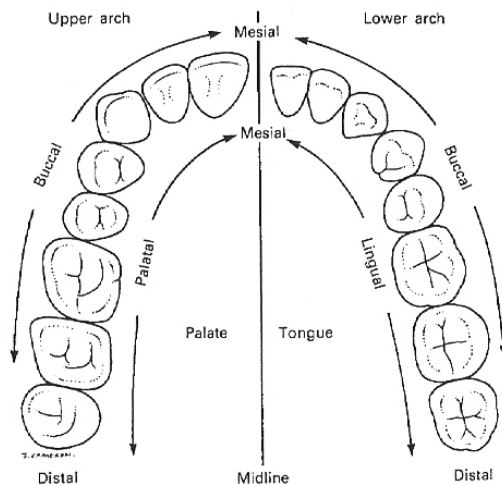


Fig. 2.2 – Upper and lower dental arches and associated terminology (from Aiello and Dean, 1990)

surface of the mouth that they face: palatal (faces the palate), lingual (faces the tongue), buccal (faces the cheek), labial (faces the lips). However, very often only lingual and buccal are used to refer to the internal and external surfaces of a tooth. The area of a tooth that occludes with the teeth of the opposite jaw is called the occlusal surface.

Hominids, like all hominoids, have eight permanent incisors, four canines, eight premolars and twelve molars, distributed in rows of two incisors, one canine, two premolars and three molars for each quadrant of the mouth (Figure 2.2). Since maxillary molars constitute the sample considered in the present work, the description of the other tooth typologies will be left out. Molar teeth have a rather complex morphology (Figure 2.3). Their crown is composed of cusps that are both joined by ridges of enamel and separated by fissures that run at the base of the

The surface of a tooth facing the anterior end of the sagittal plane of the jaw is called the mesial aspect of the tooth. The distal aspect is the surface that faces away from the anterior end of mid-line and is thus at the opposite side of the mesial aspect.

The remaining aspects of a tooth are named according to the

crown. In particular, maxillary molar crowns are composed of four main cusps: protocone (Pr in this work; mesio-palatal); paracone (Pa; mesio-buccal); metacone (Me; disto-buccal); hypocone (Hy; disto-palatal). Minor cusps may occur on ridges that connect main cusps. Their names are formed using the name of the main closest cusp adding the suffix “conule” (for example, metaconule). Ridges occur and connect the main cusps: Pr and Pa are linked by the mesial marginal ridge, while the distal marginal ridge connects Hy and Me; Pr and Me can be joined by a ridge of enamel known as transverse or oblique ridge which separates Hy from the rest of the crown. The area included between the two mesial cusps and Me forms the occlusal basin (central fossa); the mesial marginal ridge represents its mesial limit while the transverse ridge bounds it distally. Mesially to this, the anterior fovea could be either well demarcated from the central fossa or merged with it. A posterior fovea is also present between the distal cusps and it is mesially closed by the transverse ridge and distally delimited by the distal marginal ridge. The fissure pattern may show some variation; nevertheless the

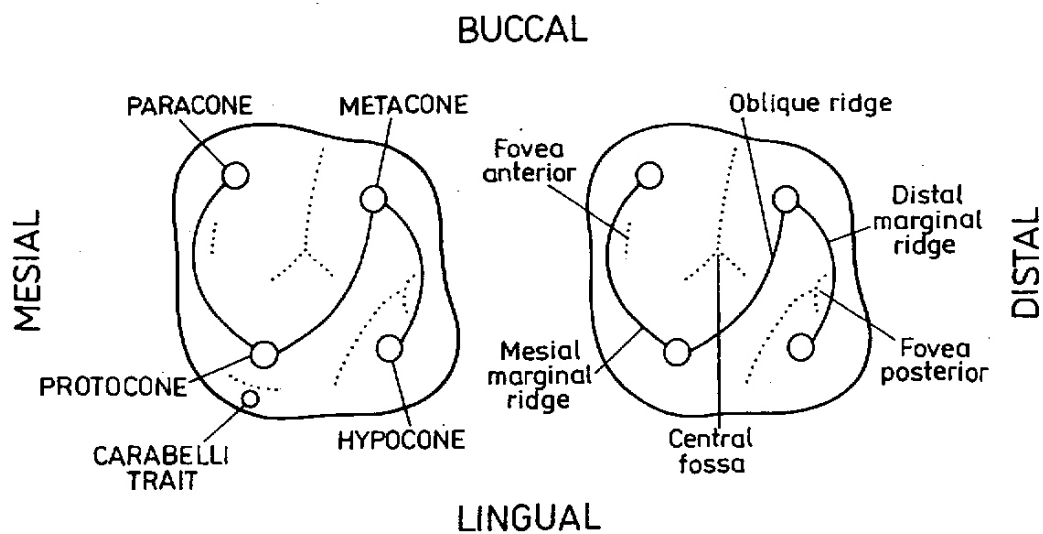


Fig. 2.3 – Occlusal views of a maxillary molar showing its anatomical features and their names (from Kaszycka, 2006)

identification of the main fissures that separate the cusps is possible. A triradiate system of grooves in the central fossa separates Pr from Pa (central groove); Pa from Me (buccal groove) and Pr from Hy (lingual groove); a transverse groove and sometimes a central groove are present in the posterior fovea.

The morphology and the position of the cusps are species specific, and once a tooth is completely formed it does not go through morphological changes and remodelling, except for wear (Aiello and Dean, 1990). It is possible to infer about the functional meaning of teeth, diet and thus palaeoecology and phylogenetic relationships of extinct species by interpreting the tooth shape, type of wear and tooth eruption stage (Ungar, 2004). Moreover, the biological material which forms the dentition, their small dimensions and compact shape make of teeth durable remains, more easily preserved in a fossil assemblage than bones. For these reasons, teeth are traditionally considered very informative palaeontological remains.

2.2 - Analytical methods

2.2.1 - The descriptive approach

Teeth represent an important source of information for the study of both modern humans and ancient hominids. They have been studied through different approaches and methodologies; among these some have not gone through significant changes since the beginning of the 20th century. One of the long-established ways to study teeth is the descriptive analysis which represents the first (both historically and methodologically) and fundamental approach in anatomical studies. Beside the morphological approach, morphometrics, which is

based on three fundamental measurements, is the other major tool for the analysis of tooth morphology. As stated by Hillson (1986), teeth have a peculiar and complex shape that is difficult to measure. Not having flat surfaces and right angles, teeth involve a high degree of subjectivity in the description of certain features, in their orientation or in the location of significant points. In the light of this, the main advantage of the descriptive approach is that it enables researchers to take into account the tooth in its wholeness, considering not only its general shape but also all of those qualitative features that cannot be measured (e.g., the Carabelli trait and the fissures pattern). Thus, the morphological description requires an accurate observation of dental aspects but unlike morphometrics it does not involve the use of measuring devices. This is at the same time the strong and weak point of this approach. In fact, the development of morphometrics is highly influenced by the development of measuring tools, but the descriptive approach suffers limitations due to the subjectivity with which each morphological trait can be interpreted or the degree of expression by which a certain feature can be evaluated. One way around this problem is the creation of standardized systems for the description of teeth such as the Arizona State University Dental Anthropology System, ASUDAS, which is a well articulated compendium for the analysis of human dental morphology with detailed description of non-metrical traits (Turner, *et al.*, 1991). Even though ASUDAS started in support of the study of the dentition of modern human populations on the basis of a movement that begun well before (Hrdlička, 1920), more recently it has been widely applied for the study of ancient populations and hominids (see for

example, Haeussler, 1995; Coppa, *et al.*, 1998; Bailey, 2000; Irish and Guatelli-Steinberg, 2003).

2.2.2 – Odontometrics

Traditional morphometrics basically concerns the comparison of three fundamental measurements also called “diameters”, namely the mesio-distal diameter (MD), the bucco-lingual diameter (BL) and the cusp height. Since the latter is very much affected by the presence of wear it is rarely considered, while the first two diameters can be used to obtain further variables as detailed in Table 2.1.

Table 2.1 – Anthropometric indexes calculated from the fundamental variables MD and BL diameters

Name	Formula	Meaning
Crown module (CM)	$(MD + BL)/2$	It is the average diameter for each tooth
Crown index (CI)	$(BL / MD)*100$	It is the relative breath of the crown, expressed as a percentage. CI = 100, BL=MD CI > 100 BL > MD CI < 100 BL < MD
Robustness index (RI)	$MD*BL$	It is the area of the occlusal surface (assuming it to be rectangular)

Even though MD and BL diameters are the main variables used in traditional morphometric studies, they are far from being of certain identification on a tooth. First of all, it is to be considered that they are measured by means of a calliper (either manual or digital) and this could imply a certain bias. Secondly, both wear and damages can interfere with the correct sampling of these variables. Third and most importantly, the definition of the variables themselves is not unequivocally

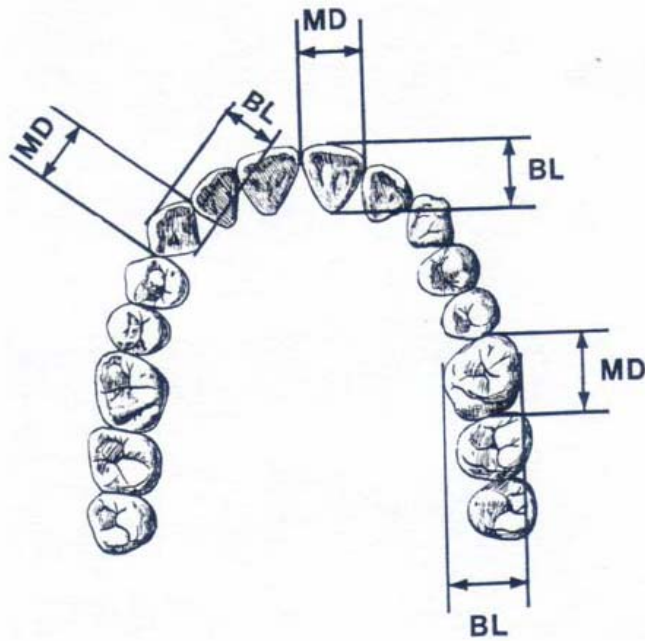


Fig. 2.4 – Identification of mesio-distal and bucco-lingual diameters, according to Brace (1979)

standardised since different authors have suggested diverse ways to collect such measurements. Moreover there is confusion on the definitions of these variables, alternatively considered as length, breadth, diameter, or thickness (the latter for BL only) according to the

different scholars' interpretations (Kieser, 1990; and references therein). However, it seems that the term "diameter" might be applied with confidence taking into account that the other terms are often used to describe other parts of the body (Goose, 1963). A synthetic review of the different approaches to the sampling of BL and MD is outlined as follow.

While these variables had been variously interpreted in works of the first half of the 20th century, in 1954, Moorrees and Reed provided a revision of the morphometric method based on tooth diameters. They defined MD measurement as the greatest mesio-distal length of the crown measured on a plane parallel to the occlusal surface with BL perpendicular to it. This criterion started for the study of modern human dentition, but was borrowed from Palaeoanthropology, as well (Hillson, 1986). A different point of view sees MD as the distance between the points of contact with the adjacent teeth of the same dental arch, measured on a

plane parallel to the occlusal surface (Nelson, 1938) while BL is perpendicular to MD and measured at right angle with respect to the median vertical axis of the crown (Brace, 1979; see also Figure 2.4). Since the interproximal facets of contact in premolars and molars may not correspond to the maximum mesio-distal extension of the crown, further suggestions as a compendium for the collection of MD have been advanced (Goose, 1963; Thoma, 1985). Furthermore, Tobias (1967) provided an alternative interpretation of MD defining it as the distance between two parallel lines which run perpendicularly to the mesio-distal axial plane of the tooth. Even though BL has been often considered a variable dependent (perpendicular) to MD, it is to be noted that in molars this measurement does not correspond to the maximum diameter. To fit both conditions of perpendicularity to MD and maximum length in bucco-lingual direction, at least two measurements must be taken and their average is to be considered. In order to avoid confusion, Tobias (1967) considered the maximum diameter the condition to be preferred to that of perpendicularity, since the former provides researchers with a more accurate repeatability.

From what is said above, it is evident that the issue of linear measurements is not straightforward. Moreover, the presence of occlusal and interproximal wear makes the collection of these variables even more difficult and uncertain. Thus, some authors (Hillson, *et al.*, 2005) explored the possibility of introducing new variables such as the diameters measured from the mesio-buccal to the disto-lingual and from the mesio-lingual to the disto-buccal corners or to collect MD and BL at level of cervical margin since it is rarely affected by wear. For this

purpose they developed a special calliper with extra fine tips which could be inserted between teeth when in place.

Furthermore, both the complex and irregular morphology of teeth and the error linked to the use of mechanical and digital callipers make the use of such variables even more problematic. Most importantly, being based only on few (linear) variables, morphometrics does not enable to define a tooth neither in some of its important aspects of form (for example, cusps size and shape) nor in its general dimensions. To overcome the limitations proper to traditional linear morphometrics new methods based on two-dimensional imaging have been applied to the study of tooth morphology.

2.2.3 – Two-dimensional image analysis

Analyses of tooth morphology based on the study of two-dimensional images have been carried out since 1970s (Biggerstaff, 1970; Hanihara, *et al.*, 1970; Le

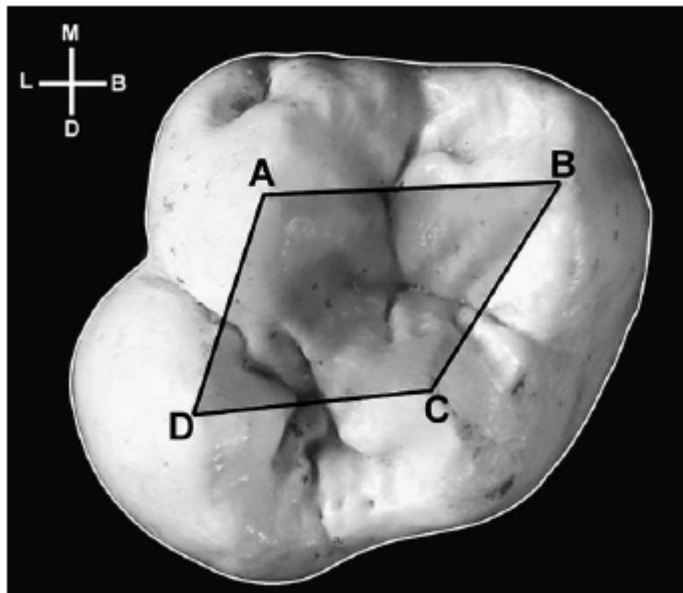


Fig. 2.5 - A M¹ showing the occlusal polygon. The lines connect the cusp tips of the protocone (A), paracone (B), metacone (C) and hypocone (D) (from Bailey 2004)

Blanc and Black, 1974; Williams, 1979) and have made it possible to gather a large number of information from teeth. The first studies focused on the assessment and comparison of the occlusal outline or on the estimation of crown

surface measuring the area inside the profile using a planimeter. However, different kinds of information have been sourced from two-dimensional dental images. Among these, important works in the field of Palaeoanthropology were dedicated to the analysis of cusp areas and cusp tip distances (occlusal polygon; see Figure 2.5) and its internal angles following the effort of Bernard Wood and colleagues (Wood and Abbott, 1983; Wood, *et al.*, 1983; Wood, 1984; Bailey, 2004; Moggi-Cecchi and Boccone, 2007; Quam, *et al.*, in press). Recently, an innovative method for the assessment of Neanderthals and modern humans P₄ crown profile was applied by Bailey and Lynch (2005), who used the Elliptical Fourier analysis as a process for the description of the outline of a two-dimensional closed curve (Kuhl and Giardina, 1982; Lestrel, 1997). Another novel use of two-dimensional dental images was carried out by Martín-Torres, *et al.* (2006) who applied geometric morphometric techniques to a set of landmarks collected from pictures of P₄ occlusal surface for the study of tooth variation in the genus *Homo* (Figure 2.6). Each analysis carried out on pictures of teeth (from traditional or digital cameras) is based on two major assumptions:

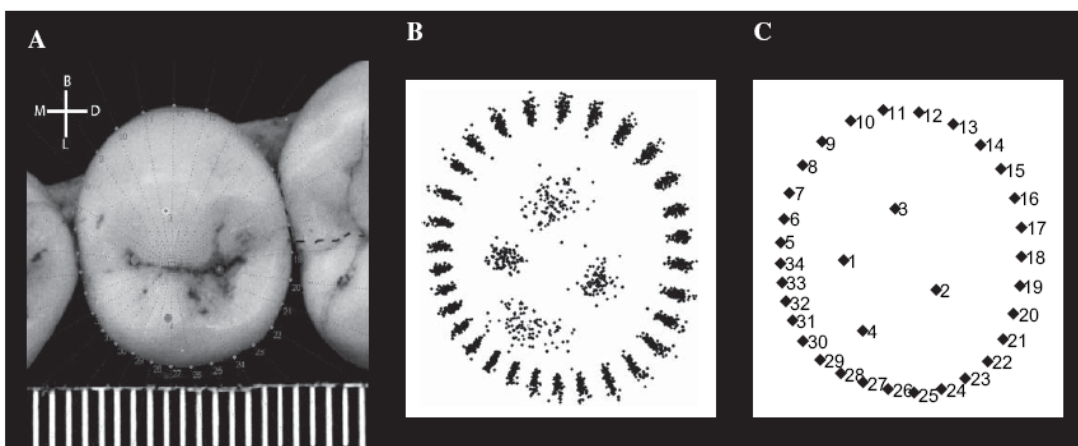


Fig. 2.6 – A. Image illustrating the points (interlandmarks) sampled for the study of P₄ occlusal surface. B. and C. illustrate further elaboration of landmark coordinates in two different steps of the geometric morphometric analysis (from Martín-Torres, *et al.*, 2006)

first, the tooth must be positioned with its occlusal surface as much as possible parallel to the lens of the camera; second, a metric scale of reference must be positioned next to the specimen. Compared to other methodologies, two-dimensional image analysis presents a number of advantages that have made of it a tool of research very often used for the study of tooth morphology. First of all, the equipment consists simply of a camera with its support, and a metric scale, thus it is portable and easy to use. Furthermore, pictures are a reliable model of the object under study and are source of a number of information. In addition, expenses related to this kind of approach are highly affordable. Moreover, photos collected from different researchers can be compared and a record of images can be created at Museums and Institutes of research. Nevertheless, this technique presents also limitations that must be taken into account while carrying out an examination. First of these, is a problem inherent in the photographic technique itself: if the optical axis is not exactly orthogonal to the reference plane, the image shows a distortion (parallax error) that invalidates the next calibration and the measurements into the image. A second technical aspect that must be considered is the sensitiveness to details of the software used for the elaboration of the images and for the sampling of landmarks and/or measurements, property that makes the software more or less reliable. There exist also problems related to methodological aspects. The major limitation of two-dimensional image analysis is the loss of information that comes from the fact that a three-dimensional object is projected onto a plane enabling for the collection of linear and quadratic measurements only. Therefore, tooth features which are expanded into the space, cannot be precisely evaluated when represented in two dimensions and an error

during to the identification of points and features can occur. Another critical issue that must be taken into account when dealing with teeth is orientation. Although there are different procedures established for the orientation of teeth, in practical use teeth are orientated positioning the occlusal surface, as much as possible parallel to the camera, taking as a reference the cervical margin as well. Since both aspects (occlusal surface and cervical margin) present an irregular morphology this procedure may become difficult, especially for worn or damaged teeth. In addition to this, it must be noted that there is no standard method for the positioning of the metric scale device, which has been variously placed at the level of the occlusal plane, or on buccal cusp, or buccal and lingual cusps, or next to the cervical margin (see for example, Robinson, *et al.*, 2002; Bailey, 2004; Harris and Dinh, 2006; Martín-Torres, *et al.*, 2006; Moggi-Cecchi and Boccone, 2007), even though the best option is the use of cameras which acquire scaled images that do not need further calibration (Ferrario, *et al.*, 1999).

In conclusion, two-dimensional image analysis is a suitable technique for the study of dental remains; nevertheless some limitations due to technical and methodological issues and to the intrinsic nature of teeth make the use of advanced techniques desirable for a better understanding of the anthropological and palaeoanthropological dental record.

CHAPTER 3

ADVANCED TECHNOLOGIES FOR THE STUDY OF TOOTH

MORPHOLOGY

3.1 - Scanning systems for three-dimensional reconstruction

The use of systems that make it possible to render a three-dimensional model of an object is increasing in several fields of research. These methodologies, which were traditionally conceived for medical and industrial purposes, have been applied in palaeoanthropological research focused on the analysis of tooth morphology, as well. There are different scanning systems and software for three-dimensional restitution and virtual geometric models analysis. Most of the scanning facilities available allow for the acquisition of a three-dimensional model of the outer morphology only (for example: laser scanners, mechanical and piezoelectric digitizers, confocal microscopes), but within the study of small biological objects, such as primate or hominid teeth, problems arise which are unknown in other fields of research. For example, in one of the first three-dimensional dental analysis, Zuccotti, *et al.* (1998) presented a new method for the description and comparison of primate tooth morphology in order to make inferences about their diet and feeding behaviour. They gathered landmarks using an electromagnetic digitizer and then imported data in Geographic Resources Analysis Support System (GRASS) software which is used to interpolate points of the occlusal surface and to gather data on volumes, slopes, and aspects of each cusp (Figure 3.1). In view of the low spatial resolution (capacity to resolve fine

details) of the digitizer (0.13 mm), they had to perform thin-plate spline (see chapter 4 - *Quantitative analysis of data from CT based techniques* for discussion about this function) for the reconstruction of the three-dimensional occlusal surface models. For this reason and for the fact that a device with such a resolution would be unsuitable for small-sized teeth, the authors highlighted the importance of using a facility with a higher spatial resolution such as a laser scanner. In 1999, Jernvall and Selänne presented a technique for the study of mammalian tooth crowns based on the use of laser confocal microscopy, capable of generating digital elevation models (DEMs) that can be transferred to Geographic Information System (GIS) software. Although they found the confocal microscopy to be very effective for the study of small teeth, it is to be noted that its use is restricted to tooth diameters less than 10 mm, thus smaller than that of many mammals. Other scholars have recognised the potential of GIS in the study of tooth morphology (Figure 3.2), but instead, used laser scanners for the collection of data (Ungar and Williamson, 2000; Kirera and Ungar, 2003;

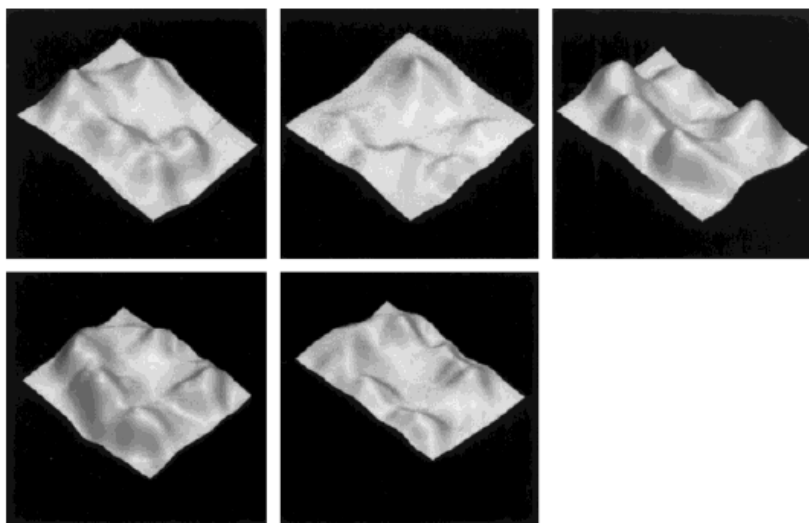


Fig. 3.1 - Surface models of teeth (upper left to lower right: *Afropithecus*, *Dryopithecus*, *Gorilla*, *Pan*, *Pongo*) examined in Zuccotti, *et al.*, 1998

Ungar and Kirera, 2003). A laser scanner presents technical characteristics that make it a suitable tool for

the study of small objects such as teeth, even though a new perspective in the study of dental and fossil remains in general is provided by techniques utilising penetrating radiation, such as X-ray Computed Tomography (CT) and Neutron Tomography (NT) (Alt and Buitrago-Téllez, 2004). Through CT and NT the inner features of a certain object that otherwise would be accessible only with an invasive approach, can be recorded and can allow researchers to study biological objects with a wide range of dimensions with high spatial resolution. CT and NT have been used since the 1970s (Lehmann, *et al.*, 2000), and in particular CT scanning, which started as a tool for three-dimensional diagnostic examination of humans based on the properties of radiography (Hounsfield, 1973), is now in very common usage in several fields of research.

3.2 - X-ray Computed Tomography (CT)

CT has provided a range of new opportunities in the qualitative and quantitative study of fossil morphology (Spoor, *et al.*, 2000a,b), and the sophisticated

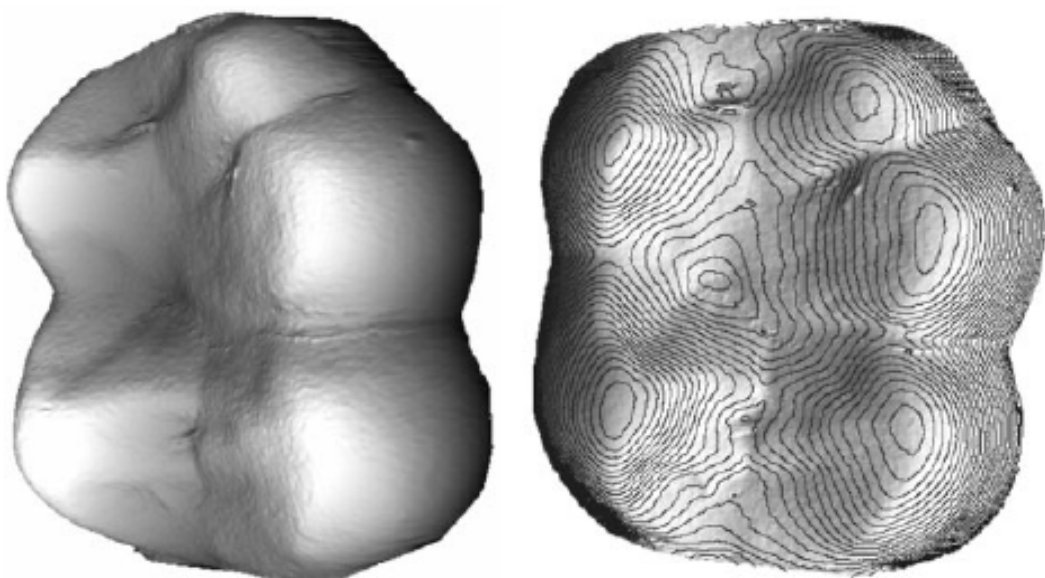


Fig. 3.2 – Chimpanzee's molar occlusal surfaces. Shaded relief model with superimposed contour lines (left) and with triangulated irregular network (right) as presented by Kirera and Ungar, 2003

computer graphics applications currently available make CT of great value for palaeontological and human evolutionary studies. CT scanning does not have the limits inherent in conventional radiography. First of all, a CT scan is not affected by parallel distortion since the object is measured in multiple directions. Second, a radiography produces a superimposition of structures that makes it difficult to interpret the inner morphology, while a CT scan not only allows for the visualisation of each distinct slice of an object, but a three-dimensional image reconstructed thereof gives a realistic rendering of the overall morphology. Moreover, although conventional radiography has a good spatial resolution, its contrast resolution (capacity to resolve small differences in density) is low relative to that of CT scan. This means, for example, that in CT images boundaries between the fossilised bone and cavities filled with sediments are more sharply marked and therefore more easily discernible than in a radiograph (Schwarz, *et al.*, 2005).

3.3 - Definitions and technical features of CT scan

The expression “CT scan” is commonly used to indicate either digital data and a virtual image of one slice, or a full CT examination. A CT scan is a result of a multiple scanning through X-rays, where the object is positioned between the source and a detector, the latter measuring the attenuation of the beam energy passing throughout the specimen. X-rays interact mainly with the electron shell of atoms that constitute the sample. In medical CT scanners the source/detector system rotates about the specimen, whilst in most of the non-medical CT scanners it is the object that rotates. The procedure for the scanning of skeletal remains is

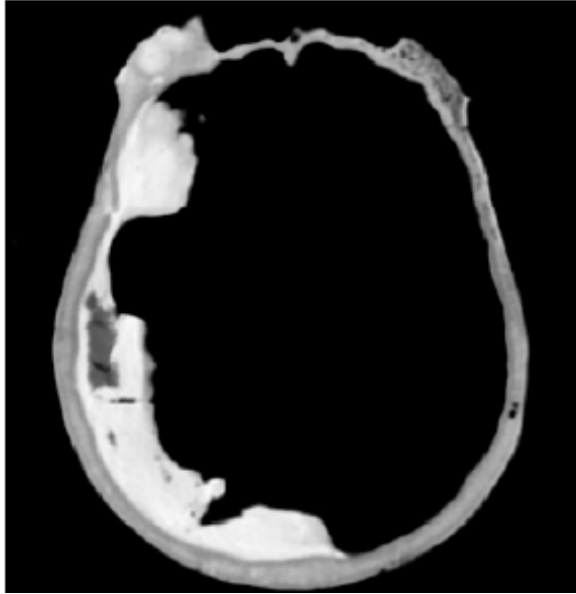


Fig. 3.3 – Transversal slice of the skull Saccopastore 1 (*Homo neanderthalensis*). The image shows the stone matrix included in the endocranial cavity (from Bruner, *et al.*, 2002)

similar to the one used for clinical practise with some differences due to the nature of the specimens scanned and to the purposes of the examination. For example, a fossil can be positioned in the most convenient way for the beam penetration, while the possibilities in the case of a living human body are limited.

Moreover radiologists use several

kinds of filters to highlight the inner morphology of a human body, which are not suitable for the observation of a fossilised structure. Furthermore, being that a human body's density and overall mass are different from those of a fossil, a CT scanner designed for medical practice might be unsuitable for research.

Scanning produces a series of cross-sectional images, each of them recording different areas of attenuation (indicated as "CT numbers") proper to the correspondent slice of the specimen so that a CT scan appears as a grey scale image on a monitor, with black representing the lowest density and white the highest one, as shown in Figure 3.3 (see Newton and Potts, 1981; Swindell and Webb, 1992, for technical aspects of CT). The spatial resolution of a CT scan is due, first of all, to the technical characteristics of the facility used. Currently, it is possible to achieve remarkable spatial resolution: for example, the spatial resolution of an X-ray Computed microTomography (μ CT) system ranges on a

scale of a few μm (Bernard, 2005) while the European Synchrotron Radiation Facility (ESRF) in Grenoble reaches a spatial resolution even $< 1 \mu\text{m}$ (<http://ieeexplore.ieee.org/iel1/23/6853/00277459.pdf>). However, the spatial resolution could be not as high as potentially possible. In fact, considering that the image is composed of an array of two-dimensional elements called pixels (with a pixel associated volume element named voxel), when the fixed image matrix covers a large area (field of view or FOV) the pixel size is relatively large determining a lower spatial resolution. Some kind of scanners produces a better two-dimensional spatial resolution while the slice thickness is much bigger than the pixel size. Others, among the non-medical scanners, give isometric voxels. It is impossible to map different CT numbers (namely variations in beam attenuation) within a pixel, but an average of the different values is recorded. This means that small variations of density between the fossilised bone and the matrix cannot be detected (see paragraph *Drawbacks of CT-based three-dimensional imaging* for further details).

3.4 - Three-dimensional CT imaging

Computer graphic techniques can be used to stack a series of CT images to provide a three-dimensional data set of the scanned object. This technique is commonly applied in medical practice and more recently adopted for Palaeoanthropology. One of the most common methods of three-dimensional imaging is surface rendering, in which surfaces are extracted from the data volume and imaged. It is a three-step process consisting of segmentation, interpolation and illumination by means of one or more virtual lights (Figure 3.4).

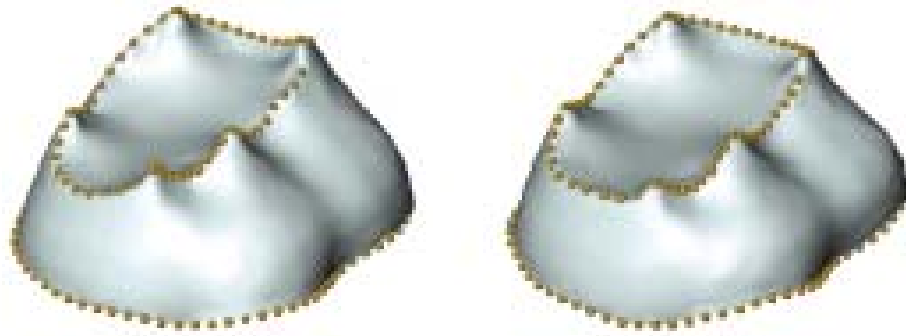


Fig. 3.4 – Models of australopithecine molar crowns produced through the three-dimensional imaging method of surface rendering. The segmentation process made it possible to separate the dentine (shown in the images) from the enamel which was eliminated through a cut-away process (modified from Skinner, *et al.*, 2008)

This data provides the base for the construction of stereolithographic models which are resin models that can be handled (Zollikofer and Ponce de León, 1995). Another method of three-dimensional visualisation is by volume rendering, where all of the data volume contributes to the image. This technique presents a number of advantages. First of all, it allows for the visualisation of internal and external features that can be shown in relation to each other, avoiding the laborious segmentation process. Therefore, three-dimensional imaging has been used in Palaeoanthropology in order to describe the morphology of internal features (Mafart, *et al.*, 2004). Moreover the matrix that obscures the morphology of a specimen can be electronically removed. Another application of CT based three-dimensional images is the reconstruction of missing parts of damaged fossils, and the production of physical models, as aforementioned. Furthermore, it is noteworthy that CT can be the basis for quantitative analyses: either the single scan or the three-dimensional reconstruction can be used to obtain data such as landmark coordinates, distances, angles, surface areas and volumes. Recently, geometric morphometrics has enabled the analysis of shape differences using

techniques such as the Procrustes projection and “thin-plate spline” (see chapter 4 - *Quantitative analysis of data from CT based techniques* for discussion). CT has been applied in Palaeoanthropology and comparative Primatology to study extant and fossil skeletal morphology; such as cranial and facial features (Ross and Henneberg, 1995; Hublin, *et al.*, 1996; Spoor, 1997; Spoor, *et al.*, 1998; Spoor and Zonneveld, 1998, Bruner, *et al.*, 2002; Bruner and Manzi, 2005; among the others) or long bones (for example, Ruff and Leo, 1986; Ruff, 1989; Ohman, *et al.*, 1997) and has been also widely applied to examine the dentition (Ward, *et al.*, 1982; Conroy and Vannier, 1987; Conroy, 1988; Conroy and Vannier, 1991a,b; Macho and Thackeray, 1992; Conroy, *et al.*, 1995; Schwartz, *et al.*, 1998; Skinner, *et al.*, 2008). The use of these methodologies has been often limited to two-dimensional analysis of CT images and more rarely to a certain number of points extracted from three-dimensional images.

3.5 - Drawbacks of CT-based three-dimensional imaging

Although the three-dimensional imaging has remarkably improved in the past years allowing researchers to reconstruct the inner structure of fossilised materials with increasing accuracy, this technique is affected by five common technical pitfalls, as recently reviewed by Zonneveld (2002; and references therein). One of these happens when the object scanned is too thick in a certain direction and the fossilised material is dense due, for example, to mineralization. If the slice is too thin it may happen that the signal in the direction of the highest attenuation is too weak when it reaches the detector, causing a noise in the raw data that may be fixed into the reconstruction of the CT image. Because of this phenomenon the

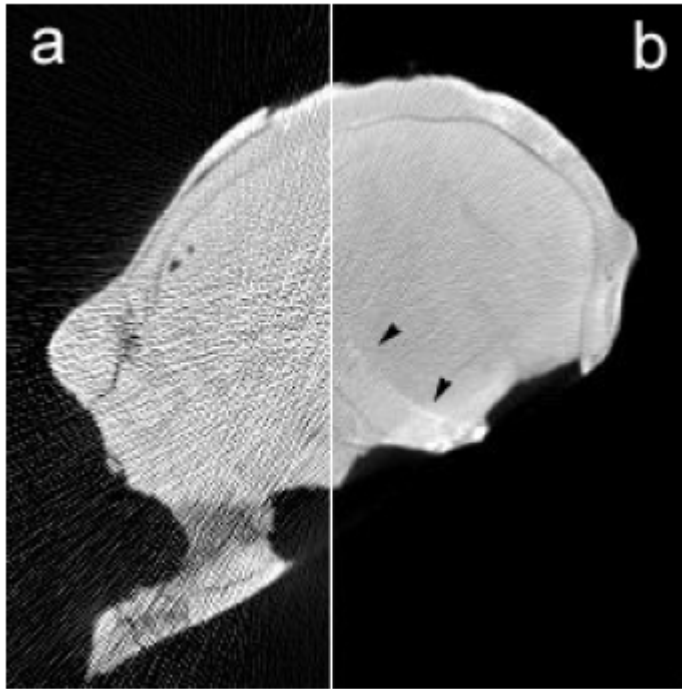


Fig. 3.5 – Midsagittal CT scans of KNM-ER406 (*Paranthropus boisei*) with a slice thickness of (a) 1 mm and (b) 3 mm. The high density and mass of the matrix-filled fossil result in a lack of detector signal causing high noise levels and ‘frozen noise’ streak artefacts when using a 1 mm slice thickness. Image in (b) is more clear but less defined (from Spoor, *et al.*, 2000a)

process of segmentation is impossible and the image is affected by a lack of surface definition (Figure 3.5). Problems arise also when the density of the object exceeds the range of CT density range. When an

object is of small dimension as in the case of teeth, where the enamel causes very weak attenuation of the beam, it

may happen that part of the object will be shown as white, resulting in a displacement of the boundaries and therefore in a wrong volume rendering. If the object is too dense (at least in part) some areas could appear as black spots, which do not contribute to the total volume rendering. The fact that CT scanners are often not calibrated for fossils causes another kind of problem because beam hardening is more severe in mineralised structures. It happens that the tissues lying deep in the object appear more dense than those just under the surface, because of the strong attenuation of the beam before it reaches the inside of the object. This results in a false lack of homogeneity of the image and in the formation of accidental interfaces of segmentation. Another common pitfall that

can occur in CT imaging is known as “partial volume rendering”. An averaging of the densities that fall into a voxel is represented in the final image. This produces a smoothing effect and artefacts caused by the mixing of two different signals, especially in the worst case of mineral (high density) and air (low density) present in the same volume element. The three-dimensional image will show a displacement of true interfaces and a loss of details.

3.6 - Brief review of Computed Tomography (CT) properties compared to those of Neutron Tomography (NT)

NT has been successfully applied in palaeontological studies as a technique for the study of internal structures of fossil remains (Schwarz, *et al.*, 2005). In the technique of NT neutrons, emanating from a nuclear research reactor or spallation source interact with the nucleus of the elements. Some light materials like hydrogen, boron or lithium attenuate (absorb and/or scatter) neutrons the most but can penetrate, with minimum attenuation, through dense materials such as lead, iron, copper and compositions of dense materials and is very suitable in a case where metals contaminate the sample. On the other hand CT can usually penetrate a thicker layer of rock or fossilised materials. The image quality of CT is generally higher than that of NT which provides a lesser contrast resolution. Moreover, NT examinations are strongly attenuated by the presence of some materials like glues and resins used for the restoration of the fossils or by special combination of materials constituting skeletal remains and sediment matrix. However, this property of neutrons can result in an advantage when the purpose of the examination is the analysis of the distribution of sediment filling internal cavities or when the state of preservation of a museum specimen is to be

investigated in a historical light. The time and effort for the carrying out of CT and NT scanning and image reconstruction are also different, with NT taking much longer than CT due to the fact that less neutrons are being produced than X-rays and that the quantum efficiency of the X-ray detectors are higher than the detector for neutrons. In conclusion, the choice of which of the two techniques might be used depends upon the physical and chemical properties and state of preservation of the fossil remains, as well as the research questions that have to be answered.

CHAPTER 4

QUANTITATIVE ANALYSIS OF DATA FROM CT BASED TECHNIQUES: GEOMETRIC MORPHOMETRICS

4.1 - Landmark definition

Geometric morphometrics is a method for the description of the shape of biological objects and is based on the analysis of the relative position of specific points (called landmarks) identified over the object itself. More precisely, the purpose of geometric morphometrics is to describe forms in terms of landmark configurations, where a landmark is “a specific point on a biological form or image of a form located according to some rule. Landmarks with the same name, homologues in the purely semantic sense, are presumed to correspond in some sensible way over the forms of a data set” (Slice, *et al.*, 1998, p.31). Sets of landmarks represent models of the specimens and report on the variation within a sample. It is evident that it is not possible to fully describe an object through landmarks. Nevertheless, it is very important to choose a set of points that are biologically and geometrically significant but also suggestive of biological insight. Of major interest for biological and palaeontological scholars is the individualisation, if any, of covariance between form and some factors, and the nature of the covariance (Bookstein, 1991). In other words it is the study of the relationship between extrinsic and intrinsic factors and pattern of form variation (O'Higgins, 2000).

Landmarks are points of equivalence between different objects that match between and within populations (Bookstein, 1991; Zelditch, *et al.*, 2004), and have both coordinates and biological significance (Bookstein, 1991). Biological Equivalence is often termed homology. There are several definitions of homology (see for example, Hall 1994, Van Valen 1982, Wagner 1994), even if in a pragmatic sense, landmarks are identified thanks to previous knowledge of mechanisms underlying morphogenesis. In this way, the only difficulties which arise concern finer details of an anatomical region.

Landmarks are generally classified as follows (Bookstein, 1991; Marcus, *et al.*, 1996):

- Type I landmarks: homology is supported by strong anatomical evidence (for example: meeting of structures)
- Type II landmarks: homology is supported geometrically (for example: cusp tips), but not by local or histological evidence. Therein are included landmarks equivalent functionally, but not homologous in an evolutionary meaning.
- Type III landmarks: can be located on a surface or an outline.

Of course type I landmarks are preferable because of their definite biological meaning and slim chance of displacement. Even though the use of all landmark types is not precluded, it is important to consider the nature of the set of landmarks used when interpreting the results.

Landmark data can be sampled using different procedures. Two dimensional coordinates obtained from specimens or images is fairly straightforward through the use of digitising tablets or graph paper. With respect to 3 dimensional coordinates the matter has, in the past, been more problematic since digitizing

devices and mechanical arms have only recently become more user-friendly and less expensive. However, it has also become possible to collect landmark data from 3 dimensional computer generated CT, NT, and Magnetic Resonance Imaging (MRI) images.

4.2 - Geometric morphometrics

Geometric morphometrics represents a new quantitative approach for the study of morphological variation (O'Higgins, 2000). Its origin can be traced back to D'Arcy Thompson's insight: in 1917 he wrote the book titled "On growth and form" in which he considered how mathematical functions could be applied to pictures of living organisms to transform them into others (Figure 4.1). From the synthesis between this descriptive approach and the biometrics of Karl Pearson,

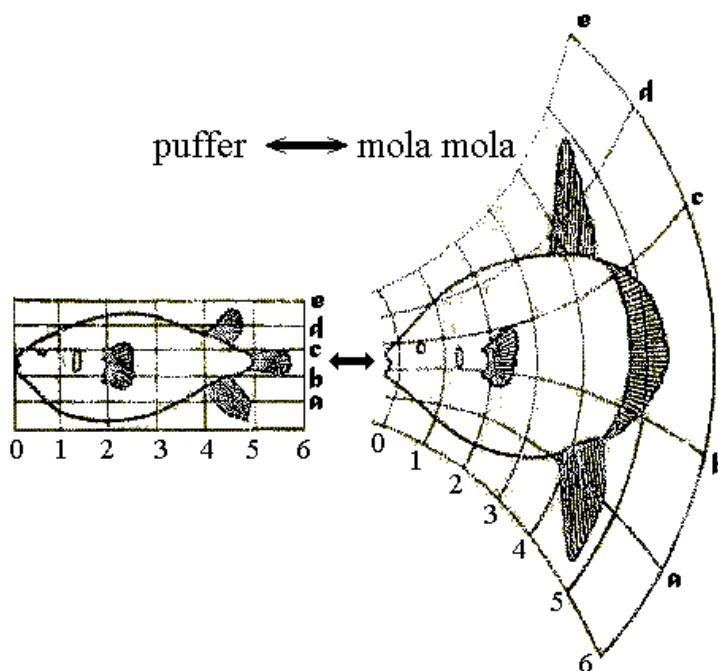


Fig. 4.1 – Transformation grids as conceived by D'Arcy Thompson (1917). He used mathematical functions to show morphological relationships among biological objects; in this particular case a transformation between a puffer fish and a mola mola is illustrated

Sewall Wright, and Ronald A. Fisher together with the introduction of computer-assisted techniques, in the 1980's geometric morphometrics arose thanks to Fred Bookstein, Jim Rohlf and a small group of researchers. Geometric

morphometrics focuses on methods for the analysis of landmark configurations, which are generally described as a “form” that occupies a 2 or 3 dimensional space. Geometric morphometrics assesses the shape that, according to Kendall’s definition (1986, p. 222), is “what remains when location, size and rotational effects are filtered out” from a landmark configuration of a certain object. Like conventional morphometrics, these methods are conceived for the analysis of individual and group differences and sample variation, but have the additional advantage of allowing for their visualization as well. Furthermore, with linear dimensions or angles and indices the spatial relationship among the measured variables is lost, while a coordinate dataset gives a pictorial model of the biological object which retains its anatomical meaning. On the other hand, statistical analyses of landmark configurations are not as straightforward as in traditional morphometrics, since they are preserved throughout and operate in Kendall’s shape space (Rohlf, 1999). This shape space is defined as “the set of all possible values of the variables” (Dryden and Mardia, 1991, p. 259). This is a non-Euclidean space that has a unit hemispherical shape for triangles but it is more complex and high dimensional for configurations of more than three landmarks (Rohlf, 1999). Moreover, configurations of landmarks are more difficult to compare statistically, due to the problem of registration (Bookstein, 1978), namely the way in which landmark locations of different specimens are superimposed (through reflection, rotation and translation) and scaled with respect to each other. In fact, the apparent displacement of a landmark from one specimen to another depends upon the way they are registered.

4.3 - Superimposition-based morphometrics, coordinate-free methods and visualization

Most of the statistical studies are structured on a basic model in which shape variation is expressed by landmark distribution around a mean form (perturbation model; O'Higgins, 2000). Nevertheless, the estimation of the mean form is not straightforward (Lele, 1993) and the distance metric between specimens depends upon the calculated mean shape (Rohlf, 2000a). There are different methods for landmark registration, each of them with peculiar applications or problems and limitations (Slice, 2005). Among these, the simplest is that of base-line registration especially suitable for two-dimensional landmarks (Bookstein, 1986; 1991), where location is defined identifying the coordinates of one landmark while orientation and scale are defined specifying length and direction of a line segment between that point and another.

The so called Procrustes superimposition is a least-squares method that takes into account the entire set of landmarks rather than only two. The theoretical work on Procrustes methods is, to a great extent, due to Kendall's investigations (1984; 1985; 1989), especially in response to questions that arose in the field of Archaeology (Kendall and Kendall, 1980). Procrustes superimposition estimates the parameters for location and orientation minimising the sum of squared distances between corresponding landmarks on two configurations, so that all the configurations are fit to that of a reference form. Scaling can be done through a least-square estimate (full Procrustes analysis) but in the case of configurations of different sizes its use does not lead to symmetric results. Otherwise, and more commonly, specimens can be scaled to a common standard size (partial Procrustes

analysis). When the mean is iteratively computed the term used to describe the fitting of the sample around the mean form is Generalised Procrustes Analysis (GPA; Gower, 1975). GPA is a process of normalization that allows for the estimation of the mean shape minimising the differences in size. It operates through three different steps translating the centroids on a common value, scaling the centroid size to a unit value and rotating the objects, minimising the sum of square distances between the equivalent landmarks of forms (Figure 4.2).

According to Siegel and Benson (1982), one of the major limitations of Procrustes superimposition methods lies in its use of the least-squares criterion itself that happen when one or few landmarks in an individual or in the sample are greatly displaced relatively to the others. This causes a large local difference to be spread across all of the other landmarks, resulting in many smaller differences and suggesting differences in the whole shape instead of only in that particular region. This is called the “Pinocchio effect” with reference to the puppet’s head shape

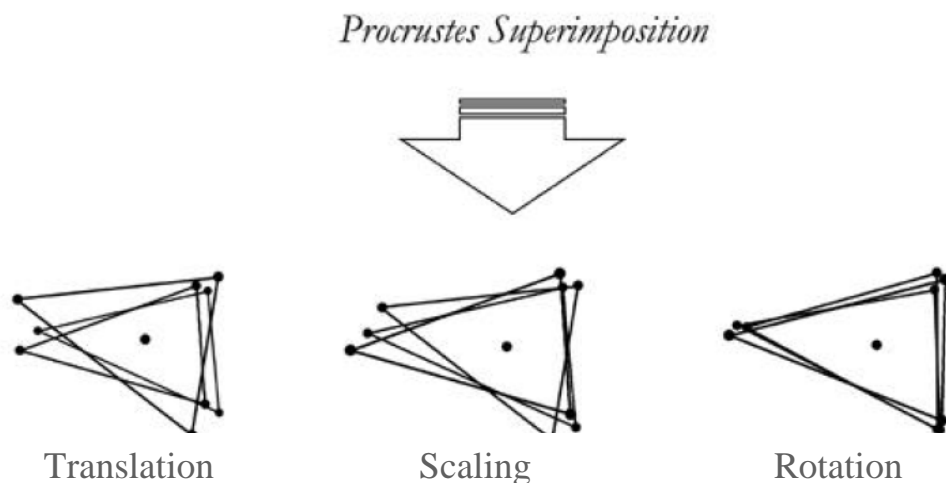


Fig. 4.2 – Schematic of the three-step process of Procrustes analysis performed on triangles (modified from Bruner, 2003)

before and after lying.

A possible alternative to overcome this problem is the method of resistant fit, based on the use of medians and repeated medians for the estimation of rotation, translation and scaling. This is not a statistical approach as sophisticated as the Procrustes superimposition, but could be used to highlight local differences that go unnoticed using a least-squares method (Slice, 2005).

To avoid problems related to registration dependent approaches, several “coordinate-free” methodologies have been suggested. Among these, the most used is based on the Euclidean Distance Matrix Analysis (EDMA; Lele 1993), in which form is described by matrix of all possible interlandmark distances. A recent study by Rohlf (2000b) seems to indicate that such a method for the assessment of differences between means, which is also quite complex to deal with mathematically, is still to be improved.

Differences between landmark datasets can be expressed also in terms of deformation instead of absolute movement. These methods describe stretching and contraction of the space in the vicinity of a certain landmark configuration in order for it to match the landmark configuration of a reference specimen and measure the bending energy associated to this transformation. One of the

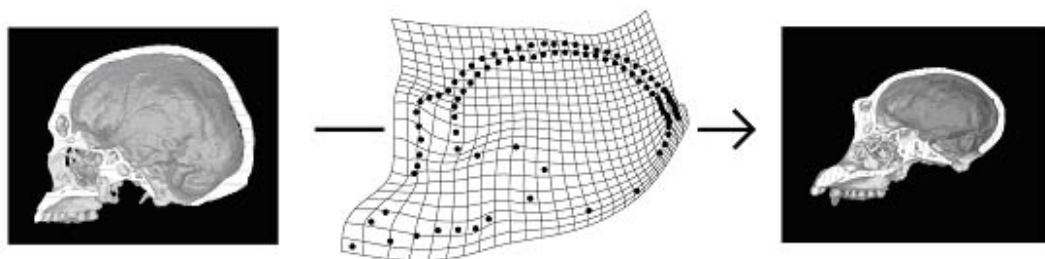


Fig. 4.3 - Thin Plate Spline (TPS) deformation grid between the midsagittal profiles of a human skull and a chimpanzee skull (from <http://www.virtual-anthropology.com/virtual-anthropology/geometric-morphometrics/thin-plate-splines>)

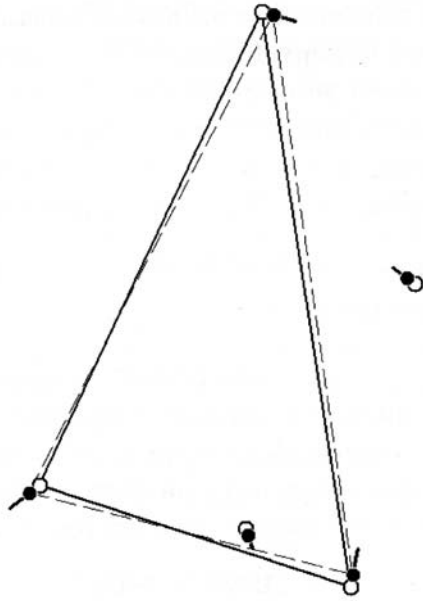


Fig. 4.4 – Vector plot for the visualization three-landmarks configurations (from Slice, 2005)

functions recently in use is called Thin Plate Spline (TPS; Bookstein, 1989; Dryden and Mardia, 1998; Marcus, *et al.*, 1996) which can be applied to draw Cartesian transformation grids (Figure 4.3) that resemble those proposed by Thompson (1917) and is

therefore suitable for the visualization of the results. However the simplest way to visualise shape differences is through vector plots, with vectors pointing from the landmarks of the reference shape to that of the target configuration (Figure 4.4).

4.4 - Analyses of landmark data

Once the landmark configurations have been registered, the resulting data is suitable for exploration of shape differences. The most frequently used statistical tools for the analysis of distances from the mean shape are standard multivariate methods (Rao and Suryawanshi, 1996). Once the complete set of scaled interlandmark distances have been obtained it is possible to carry out analyses such as Principal Component Analysis (PCA), to assess variation, and regression, to investigate allometric, functional, and phylogenetic aspects related to shape variation of biological objects. It must be highlighted that multivariate statistical techniques are conceived for linear data, whilst landmark configurations operate

in the non-Euclidean Kendall's space. One way around this problem is to analyse the Procrustes coordinate projections onto a linear space, tangent either to Kendall's space or to the Procrustes hemisphere (Rohlf, 1999; Slice, 2001). In fact the projection of Procrustes coordinates into a linear space seems to preserve the distances between specimens, when shapes do not differ excessively (Figure 4.5). The combined use of Procrustes superimposition, multivariate statistical analysis and TPS visualization is what Bookstein (1993) defined the "Morphometric synthesis" which represents the basis of most coordinate-based analyses that have been carried out. However, not all the statistical tools of multivariate analysis are considered applicable to Procrustes data (Klingeberg and Monteiro, 2008). For example, Bookstein (1991) considered discriminant-function analysis to be inherently incompatible with morphometric and so is its extension to multiple

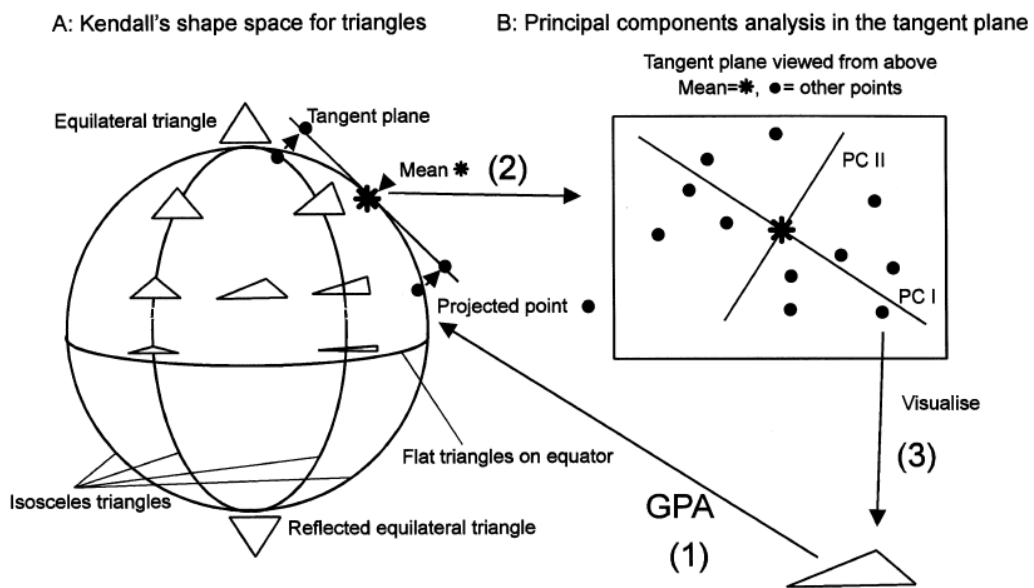


Fig. 4.5 – A. Representation of Kendall's shape space for triangles. B. Projection of points representing triangles in Kendall's shape space into a space tangent to the mean triangle (arrows) and the principal components of shape variability (PC I, PC II) in this tangent space. The steps indicated in the image are (1) generalised Procrustes analysis (GPA) to register figures, that are then represented as points in the shape space; (2) projection of points into a space tangent to the mean and the principal components (PCs) of shape variation in this space are extracted; (3) visualisation of the shape variability represented by PCs is achieved by reconstructing (from O'Higgins, 2000)

groups, canonical-variates analysis. Nonetheless, this assertion is controversial, being that canonical-variates analysis is one of the most frequently used techniques in morphometrics (e.g. Lague and Jungers, 1998; Harvati, 2003; Pan and Oxnard, 2004; McNulty, 2005; Nicholson and Harvati, 2006; Perez, *et al.*, 2006).

At present, there are numerous software packages available for the carrying out of geometric morphometric analysis of landmark configurations. A comprehensive source of software, information and links is available on the website <http://life.bio.sunysb.edu/morph/>, maintained by F James Rohlf. For example, the software suite *APS* by Xavier Penin for the analysis of covariances with shape can be downloaded. The website includes links to a program, *Morpheus et al.*, by Dennis E. Slice that provides a comprehensive, cross-platform environment for two- and three-dimensional morphometric data analysis; finally it provides access to the *Morphologika* web site. This program was developed by Paul O'Higgins and Nicholas Jones (see O'Higgins and Jones, 1998) to enable straightforward geometric morphometric analyses of two- and three-dimensional landmark configurations in a PC environment, allowing for the visualization of shape variation.

CHAPTER 5

MATERIALS

5.1 - Introduction

The present project is designed to study the South African Plio-Pleistocene australopithecines generally regarded as *A. africanus* (*A. africanus sensu lato*, *s. l.* in this project) through the analysis of dental morphology in order to contribute to the extant debate about the possible presence of a further australopithecine species in Sterkfontein Member 4 (and Makapansgat). Through the analysis of shape and characteristics of molars, using geometric morphometric techniques applied on data gathered from three-dimensional images, the main objective is to verify if, among the hominid remains from the cave infill of Member 4 breccia, the morphology of some specimens is significantly distinguishable from the others. It is my intent to analyse the degree of variation showed within the assemblage from Sterkfontein Member 4 (and Makapansgat) using as a test groups the fairly homogeneous and distinct taxonomic group of *Paranthropus* from the South African sites of Swartkrans and Kromdraai and some specimens attributed to early *Homo* from Sterkfontein (see Moggi-Cecchi, *et al.*, 1998 for StW 151) and Swartkrans (see Clarke, 1977 for SK 27; and Grine, 2004 for SKX 268 and SKW 3114). These two groups were chosen for the assessment of the discriminant power of the method used since they are clearly morphologically distinguishable. Furthermore, they are quite distinct in size (*Homo*) and shape (both *Paranthropus*

and *Homo*) to those of *Australopithecus*. Moreover, this comparison is of extreme interest since these two genera are those that have been frequently related to *Australopithecus*, both for their morphological affinities and their chronological and geographical distribution. However, it must be said that there has been a big and longstanding controversy also about the taxonomic attribution of *Paranthropus* which some authors have not considered as a separate genus from *Australopithecus* (for example, Simpson, 1945; Howell, 1955, 1968; Wallace, 1972; Wolpoff, 1974; Wolpoff and Lovejoy, 1975; Lockwood and Tobias, 2002; Moggi-Cecchi, *et al.*, 2006). Nevertheless, most researchers have agreed that this hominid form is characterised by a peculiar massive jaw and masticatory apparatus, the biomechanical significance and function of which were extensively explained by Broom (1938; 1939) and Robinson (1952; 1954a,b; 1956; 1962; 1963; 1967; 1972), in support of generic distinction. This position was then widely accepted by other authors (see for example, Clarke, 1985a; 1988; 1990; 2006; Aiello and Dean, 1990; Grine and Martin, 1988; Grine and Strait, 1994; Kuman and Clarke, 2000) and furtherly sustained by Clarke (1996). Moreover, there is no general consensus on the specific attribution of the *Paranthropus* specimens from the diverse South African sites. It has generally now become conventional to consider them as belonging to the species *P. robustus*, denying specific distinction (see Le Gros Clark, 1967; and references therein), although others have at time distinguished the Kromdraai specimens from those of Swartkrans on the basis of cranial and dental differences (Broom, 1949; 1950; followed by Howell, 1978; Grine, 1982; 1984; 1985; Clarke, 1996; as reviewed by Kaszycka, 2002) and therefore recognize two different species (*P. robustus*

and *P. crassidens*, respectively), while Robinson (1954b) distinguished the two morphotypes only at a subspecific level.

In spite of the above, it is still evident that this specialised hominid form is well distinguishable from the comparatively less specialised hominid (*Australopithecus*) known mainly from Sterkfontein Member 4 and Makapansgat. Nevertheless, the analysis performed in this study will contribute to this issue, as well.

A *Paranthropus* specimen from Cooper's Cave and a specimen of *A. africanus* from Gladysvale were also added to the sample in order to observe their variation with respect to the other individuals considered. However, due to its state of preservation the molar from Gladysvale could not be included in the statistical analysis (see Table 5.3 for further details).

5.2 - The sample

The sample preliminarily considered and which had gone through CT scanning was composed of 80 permanent maxillary M¹s, M²s and M³s coming from the Plio-Pleistocene South African sites of Cooper's Cave, Gladysvale, Kromdraai, Makapansgat, Swartkrans and Sterkfontein. Of these, 65 had been quantitatively analysed. The specimens which are the object of the present work are listed in Table 5.1 where the provenience, the species attribution, the tooth typology and maxillary side is also indicated. Table 5.2 shows the number of specimens that were scanned at Necsa and that of the specimens that could be also statistically analysed detailed by tooth typologies and by fossil sites. The notes of Table 5.3

explain why the CT scan of certain individuals could not be successfully used to perform the statistical analysis.

A general review of the sites of Kromdraai, Makapansgat, Sterkfontein and Swartkrans is given by Schwartz and Tattersall (2005; and references therein; see also Clarke, 2006, who provides new data and insights on Sterkfontein stratigraphy). Middleton Shaw (1939); Berger and Pickford (1995) Berger, *et al.* (2003) contain information about Cooper’s Cave while Berger (1992); Berger, *et al.* (1993); and Schmid (2002) provide information on Gladysvale.

Table 5.1 – Specimens considered in this study: species attribution and site of provenience. The specimens highlighted in grey could not be included in the statistical analysis

SPECIMEN	PROVENIENCE	M¹	M²	M³
<i>Paranthropus</i>				
CD 5774	Cooper’s Cave, Coopers D		L	
KB 5383	Kromdraai, KB	R		
TM 1517A	“		L	R
TM 1517B	“			R
TM 1601	“	L		
TM 1603	“			L
SK 13/14	Swartkrans		R	R
SK 16	“		L	
SK 31	“			R
SK 36	“			R
SK 47	“		L	
SK 48	“		L	L
SK 49	“		R	R
SK 55A	“	L		
SK 89	“	L		
SK 98	“		L	
SK 102	“	L		
SK 105	“			L
SK 829	“	L		
SK 831A	“			L

SK 832	“	L		
SK 834	“		R	
SK 835	“			L
SK 836	“			L
SK 837	“		R	
SK 838	“	R		
SK 839	“	R		
SK 3975	“			L
SK 3977	“			R
SKW 11	“		R	R
SKW 14	“		L	
SKW 29	“			R
SKX 21841	“			R
<i>Australopithecus</i>				
MLD 6	Makapansgat	R	R	
MLD 28	“			R
GVH 2	Gladysvale		R	
STS 1	Sterkfontein, Member 4	L	L	
STS 8	“	L	L	
STS 22	“		L	
STS 24A	“	R		
STS 37	“		L	L
STS 52	“		L	L
STS 56	“	L		
STS 57	“	L		
STW 59	“	R		
STW 179	“			L
STW 183	“	L	L	R
STW 188	“		R	
STW 189	“			L
STW 204	“		R	
STW 252 J, K, L	“	L	L	L
STW 280	“	L	L	
STW 280 cast	“		L	
STW 402	“	R		
STW 447	“		R	
STW 450	“	R		
STW 498A	“			R
STW 530	“		L	
TM 1511	“			R
<i>Early Homo</i>				

STW 151	Sterkfontein, Member 4	R	R
SK 27	Swartkrans	R	R
SKW 3114	“	L	
SKX 268	“	R	

Table 5.2 - Number of maxillary molars analysed/Number of maxillary molars scanned at Necca

		M¹	M²	M³	Total per species
<i>A. africanus s.l.</i>	Gladysvale	-	-/1	-	
	Makapansgat	-/1	-/1	1/1	
	Sterkfontein, M4	9/11	8/13	7/8	
	Subtotal	9/12	8/15	8/9	25/36
<i>P. robustus</i>	Cooper's Cave	-	1/1	-	
	Kromdraai	2/2	1/1	3/3	
	Swartkrans	7/7	9/10	11/14	
	Subtotal	9/9	11/12	14/17	34/38
Early <i>Homo</i>	Sterkfontein, M4	1/1	1/1	-	
	Swartkrans	3/3	1/1	-	
	Subtotal	4/4	2/2	-	6/6
Total per tooth typology		22/25	21/29	22/26	65/80

The teeth included in the statistical analysis are those where the collection of the whole set of landmarks could be done (for details about the set of landmarks see chapter 6 - *Methods*). Therefore, in the majority of the teeth included at least the crown is complete. In addition, they are unworn or slightly worn, and only a few of them are moderately worn. Where antimeres were present the one in a better state of preservation was used. In Table 5.3 information of tooth wear and description of the state of preservation of the sample are provided.

Table 5.3 – Specimens divided by tooth typology and listed in alphabetical order. It is indicated where a cast was used and where the specimen was scanned but for some reason was not used for the statistical analysis (Specimen Not Analysed, SNA). Descriptions of the level of wear and the state of preservation are provided. Some notes are added when relevant (abbreviations: CF: Cinzia Fornai; JMC: Jacopo Moggi-Cecchi; MMR: mesial marginal ridge)

Specimens	Cast	SNA	Wear	State of preservation	Notes
M¹					
KB5383			Slight	The cervical aspect of the Hy is missing	The position of a landmark on the Hy profile was estimated considering the morphology of the rest of the cusp
MLD6		X	Heavy	Minor matrix-filled cracks	
SK 27			Slight	Minor matrix-filled cracks	
SK 55 A			Moderate	Well preserved	
SK 89			Unworn	Well preserved	
SK 102			Unworn	Some matrix-filled cracks	
SK 829			Unworn	Well preserved	
SK 832			Slight	Well preserved	
SK 838			Slight	Some matrix-filled cracks	
SK 839			Unworn	Well preserved	
SKW 3114			Moderate MMR worn out	Well preserved	
SKX 268	X (by JMC)		Slight	Well preserved	
STS 1			Slight	Well preserved	
STS 8			Moderate	Well preserved	
STS 24 A			Slight	Some matrix-filled cracks	
STS 56			Moderate MMR worn out	Mesial cusps crossed by a minor matrix-filled crack	
STS 57			Slight	Major matrix-filled cracks	
STW 59		X	Unworn	Several matrix-filled cracks	Damages and peculiar morphology due to incomplete eruption led to its exclusion from the sample
STW 151			Slight	Very well preserved	
STW 183			Slight	Well preserved	
STW 252 J			Moderate	Well preserved	

STW 280		X	Moderate	Well preserved	Relevant crown features are worn out
STW 402	X		Slight	Well preserved. It was sectioned by Grine and Martin (1988); from that comes also a lack of a thin portion of the crown	
STW 450			Unworn	Well preserved	
TM 1601			Unworn	Well preserved	
M ²					
CD 5774			Unworn	Well preserved	
GVH 2		X	Unworn	The Pa is largely missing	Incompleteness caused the set of landmarks to be partial
MLD 6		X	Moderate	Well preserved	
SK 13/14			Slight	A thin crack runs bucco-lingually between mesial and distal cusps	
SK 16			Moderate	Some minor matrix-filled cracks	
SK 27			Slight	Well preserved	
SK 47			Unworn	Well preserved	
SK 48	X (by CF)		Moderate	Some matrix-filled cracks	
SK 49	X (by CF)		Moderate	Several matrix-filled cracks	
SK 98			Unworn	Well preserved	
SK 834			Moderate	Several major matrix-filled cracks	
SK 837			Moderate	Several major matrix-filled cracks	
SKW 11			Slight	Well preserved	
SKW 14		X	Slight	A wedge of enamel is missing from Me	Incompleteness caused the collection of 1 landmark to be inaccurate
STS 1		X	Slight	Distal margin reconstructed	Missing landmarks
STS 8			Slight	Well preserved	
STS 22		X	Moderate	Well preserved	The scanning did not succeed due to a temporary malfunctioning of the facility
STS 37		X	Moderate MMR worn out	Several matrix-filled cracks with the corner of Pa dislocated	

STS 52	X	Slight. MMR slightly worn out	Well preserved	The scanning did not succeed due to a temporary malfunctioning of the facility
STW 151		Unworn	Very well preserved (unerupted)	
STW 183		Unworn	Well preserved	
STW 188		Slight	It is broken in two halves (roughly mesial cusps detached from distal ones)	The scanning was done keeping the two halves together with putty
STW 204		Unworn	Well preserved. Still under development	
STW 252 K		Slight		
STW 280		Unworn	Well preserved. It was sectioned by Grine and Martin (1988); from that comes also a lack of a thin portion of the crown	The scanning was done keeping the two halves together with putty
STW 280	X	See line above		
STW 447	X	Unworn	Well preserved. The lingual aspect of the Hy is missing	Incompleteness caused the set of landmarks to be partial
STW 530		Moderate	Well preserved	
TM 1517 A	X (by CF)	Moderate	Well preserved	
M ³				
MLD 28		Moderate	Well preserved	
SK 13/14		Slight	Well preserved	The surface is very crenulated, therefore the crown anatomy is difficult to interpret. The internal features give the possibility to understand its morphology
SK 31		Slight	Some minor matrix-filled cracks	
SK 36		Slight	Some major cracks. Two of them caused a displacement of the crown portion placed between the corners of the lingual cusps.	

SK 48	X (by CF)		Slight	A matrix-filled crack follows the course of the transverse groove	
SK 49	X (by CF)	X	Slight	A matrix-filled crack visibly separates the corner of Pa from the rest of the crown	The cast lacks completely the cervical margin. That made orientation of the tooth impossible
SK 105 SK 831 A SK 835			Unworn Moderate Moderate	Well preserved Well preserved Some matrix-filled cracks. One caused the detachment of Pa and part of Me from the rest of the crown	
SK 836			Slight	A matrix-filled crack runs bucco-lingually between mesial and distal cusps. A flake of enamel is missing from the Hy	
SK 3975 SK 3977 SKW 11			Slight Slight Very slight	Well preserved Some minor cracks Well preserved	
SKW 29		X	Moderate	Lingual surface of the Pr missing	The fossilised bone obscured the X-ray penetration, therefore the scan is not of good quality.
SKX 21841		X	Unworn	Well preserved. It was sectioned by Grine and Martin (1988); from that comes also a lack of a thin portion of the crown	The scanning was done keeping the two halves together with putty. One of the two parts moved during the acquisition of the image making the scan unsuitable
STS 37			Unworn	A thin crack runs mesio-distally cutting the crowns in two halves. The crack caused a slight shifting of the two parts.	
STS 52		X	Moderate MMR slightly worn out	Well preserved	The scanning did not succeed due to a temporary malfunctioning of the facility

STW 179		Unworn	Some minor matrix-filled cracks
STW 183		Unworn	Well preserved
STW 189		Unworn	Well preserved
STW 252 L		Unworn	Well preserved
STW 498 A		Slight	Damaged. The lingual cusps are crossed from a crack that runs mesio-distally and produced a displacement of the lingual aspect respect to the rest of the crown
TM 1511	X (by CF)	Slight	Well preserved
TM 1517 A	X (by CF)	Moderate	Well preserved
TM 1517 B	X (by CF)	Unworn	Well preserved
TM 1603		Unworn	Well preserved

All the specimens considered come from the Cradle of Humankind World Heritage Site. The Cradle of Humankind was named by UNESCO in 1999 and Makapansgat was included later, in 2005 (<http://whc.unesco.org>) following the remarkable Plio-Pleistocene hominid and non-hominid fossil discoveries at the sites inscribed. The Cradle of Humankind is located 50 Km northwest of Johannesburg, in Gauteng and North-West Province of South Africa, and occupies an area of 447 Km². It includes a number of Plio-Pleistocene sites of paleontological and paleoanthropological importance. Most of the initial discoveries of these deposits were associated with mining operations, and the fossil remains at the Cradle of Humankind are embedded in a matrix of calcium carbonate-cemented sediments called breccia (Robinson, 1956). A map of the sites is shown in Figure 5.1.



Fig. 5.1 - Fossil hominid sites within the Cradle of Humankind, north of Krugersdorp and Makapansgat (modified from McKee, *et al.*, 1995)

CHAPTER 6

METHODS

6.1 - Procedures for the collection of landmark coordinates to be used in geometric morphometric analysis

Shape analysis has traditionally used methods that are today called “traditional” morphometric (Marcus, 1990). These methods deal with morphometric data such as distances, distance ratios, and angles, and are characterised by the application of multivariate statistical procedures. Morphometric data used in traditional morphometrics fail to describe the full geometry of a biological object, making it difficult to assess shape variability and geometric relationships among the structures under analysis (Slice, 2005).

By contrast, geometric morphometrics which is a series of statistical techniques for the assessment of landmarks distribution preserves full information about the relative spatial arrangements of landmarks throughout an analysis and therefore allows for the evaluation but also visualization of morphological differences between individuals and groups.

Landmark coordinates can be obtained with the use of a digitizer directly applied on the object or on pictures. Alternatively, landmarks can be collected on virtual images. To commence with the present project, the opportunity to collect data either on the original specimens (or casts), or on pictures with the use of a digitizer was considered. In addition, a protocol for the acquisition of three-

dimensional images based on a laser technique called OCT - Optical Coherence Tomography, at the National Laser Centre - CSIR, Pretoria was tested. However, these techniques were excluded due to the following problems and limitations related to these protocols.

6.1.1 - Acquisition of landmarks on the original specimens (or casts)

This procedure is preferable for accuracy, rather than using a substitute such as a picture. Nevertheless, for some specimens it would be necessary to use a cast, when the original is not available, or in the cases of very fragile or important individuals (such as a type specimen), and this would bring an inherent error into the results of the research.

Landmarks are easily identifiable on the crown surface, which is an area well characterised by anatomical and geometric features (for example, cusp tips,



Fig. 6.1 – Digitizer: Immersion's MicroScribe® G2X

foveae, intersection of two different foveal fissures). These landmarks are collected with the use of a digitizer (see Figure 6.1), which has an articulated arm supplied with an electromagnetic tip that converts physical objects (collecting the spatial coordinates of the selected points) into digital three-dimensional models for virtual manipulation and editing. It is supported by a digitizing software application and can be also

linked to a three-dimensional graphic application. Although this procedure landmark collection is intrinsically safe in terms of preserving and safeguarding the fossils (see appendix B), some crucial difficulties were faced as it is evident

that the three-dimensional shape of a tooth is very hard to describe. Complications arise in describing the peripheral area of the tooth as the bulbous nature of a tooth tends to make an operator not to trust his/her eyes in determining the most external outline of the tooth. A solution to this problem can be the collection of a series of landmarks at a set distance on the mesio-distal and bucco-lingual sides of the teeth on selected meridians. Manually, this consists of setting the digitizer to acquire landmarks at a defined distance (for example, 0.1 mm.), and tracing an uninterrupted line on each meridian with its tip. As a following step the most outstanding point from the bisector passing from the highest and lower point of the meridian can be selected. One of the weak points of this procedure can be represented by the definition of the meridians itself on the teeth: it must be a systematic and repeatable sampling. Another important limitation is related to the small dimension of the objects under study since the Immersion's MicroScribe® G2X, currently in use at the School of Anatomical Science at the University of the Witwatersrand, has an accuracy of 0.23 mm. The results of a study on small objects such as teeth can be affected when the area observed is smaller than the possible error. In order to bypass that problem many authors (see Martín-Torres et al., 2006 among the others) have chosen to work on pictures of the specimens.

6.1.2 - Sampling of landmarks on pictures and casts

A picture is a good model of the objects under study. It can be enlarged, thus resolving complications related to minute objects. In the case of teeth, a photograph helps to identify those tricky points such as the ones in the crown outline. The sampling has a high repeatability and taking picture is absolutely non-invasive for the fossils. To prevent the loss of information from three-

dimensional objects to two dimensional images, the combination of the picture of the occlusal surface with two vertical sections of the tooth, one passing through the mesial cusps and the other through the distal cusps and perpendicular to the occlusal plane was considered. In so doing more information on tooth morphology can be acquired, especially in relation with the cusp position and shape. Alternatively, the sections could be obtained from casts (for discussion about casting materials and procedures see appendix C), especially when dealing with such important fossil sample. Very good sections could be done using a high precision cutting machine commonly kept at the Dental Research Department of the University of the Witwatersrand, able to cut any kind of material with the maximum accuracy. Such kind of facility is equipped with different sort of holding supports and with a laser guide that leads the operator in finding the right positioning of the object before it reaches the blade. Landmarks can be collected directly on the section of the cast (over the profile) or, in case the size affects significantly the results, the cast could be scanned and the image enlarged. This protocol is extremely laborious and thus requires a long time for the acquisition of the data set. Also the orientation of the tooth appears very critical for the producing of the sections and it is to be taken into account that the cut always leads to a loss of material.

6.1.3 – Collection of data on Optical Coherence Tomography – OCT

A further option is the acquisition of landmark data on virtual images rendered through Optical Coherence Tomography – OCT (Figure 6.2). This technique uses a laser beam which allows the scanning of small objects and has a varying degree of penetration depending on the type of material. It is generally applied in medical

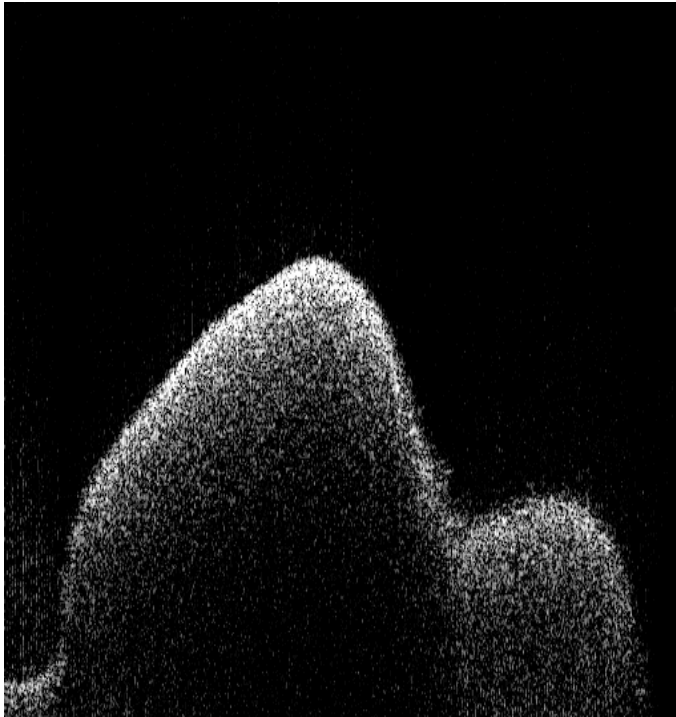


Fig. 6.2 – Slice of a cast of a first molar (StW 151) as built through OCT

and especially ophthalmological field. After a trial performed at CSIR – South African Laser Centre, in Pretoria on faunal fossil teeth, it was realised that the procedure is not applicable for this project. In fact a

good resolution can be obtain scanning a square

5x5 mm, 2 mm deep, therefore it is necessary to scan each tooth several times, choosing several overlapping squares. Each square can be “stitched” to the adjacent one(s) using the common points in the overlapping areas with the adequate software. Both the acquisition of the portions of images and their merging would require a very long time, without any assurance of accurate results.

6.1.4 - X-ray tomography

I then chose X-ray tomography as a means to obtain clear and accurate three-dimensional images. Indeed, this technique provides CT scans which are similar to those for medical purposes but with a higher spatial resolution.

For the purposes of the current project, X-ray tomography shows characteristics that make it preferable to neutron tomography. In fact, X-rays are not invasive, do

not irradiate the sample and do not overheat it. These safeguard the state of preservation of the fossils as well as their inner structure.

The facility utilised is the South African Neutron Radiography (SANRAD) facility, located at the Nuclear Research Reactor (SAFARI-1) which is owned and operated by the South African Nuclear Energy Corporation (Necsa), Pelindaba, South Africa (de Beer, 2005). Although research in the field of Palaeontology and Anthropology has been often carried out with the collaboration of the Johannesburg Hospital, it was found that the collaboration with Necsa was much more suitable. First of all, Necsa has been involved in paleontological research in the past; thus, the facility and technique was utilised on fossils. The Necsa CT system provides CT-scans with a much higher resolution (up to ~50 microns) whilst scanning parameters used in clinical settings are usually unsuitable especially for fossils of small dimensions and bearing fine details as teeth. It is also noteworthy that the beam time for research purposes at Necsa is free, whereas a student is charged for the use of the CT-scanner facility at Johannesburg Hospital. The latter is also rarely available for students, because understandably the priority is given to the patients. Necsa however provided beam time within the period scheduled for the carrying out of the present project.

6.2 - SANRAD facility

The No. 2 beam tube of the SAFARI-1 (SANRAD facility) is equipped to utilise thermal neutrons from the nuclear reactor or alternatively utilises up to 100kV X-

rays from an X-ray source built into the experimental containment. The facility is positioned at the beam port floor area of the reactor as illustrated in Figure 6.3.

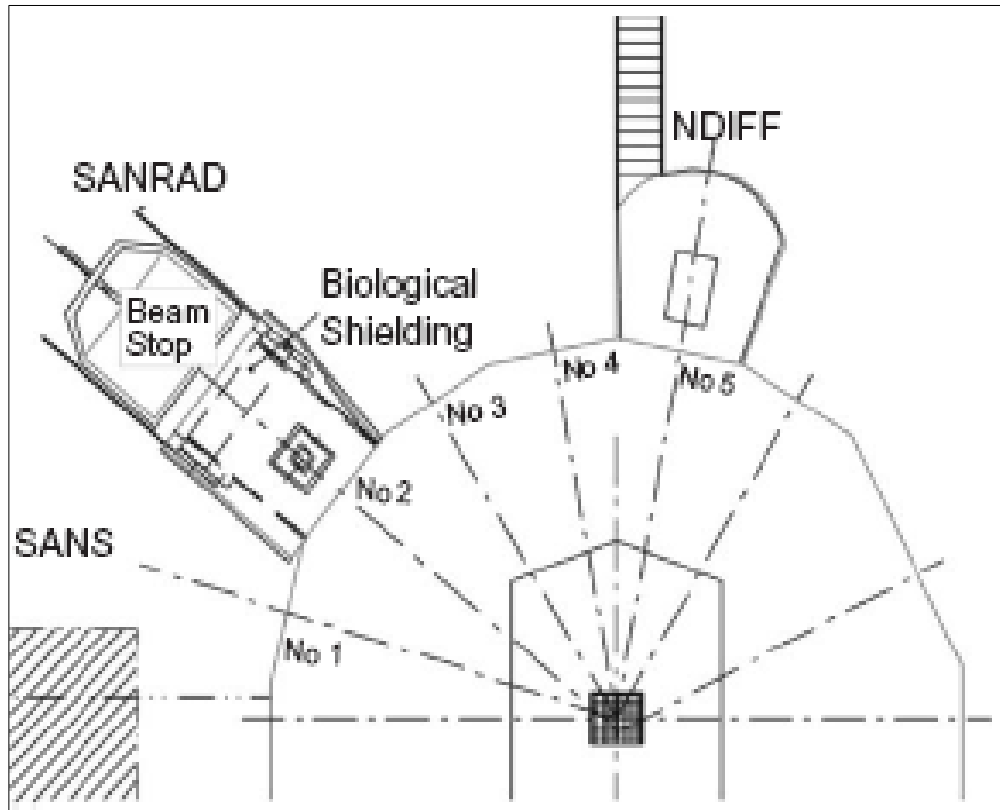


Fig. 6.3 - Schematic top view of the beam line facilities at SAFARI-1 (from de Beer, 2005)

The SANRAD facility consists of a containment specially built for stopping the neutrons and X-rays in which it is possible to allocate the sample. The containment also hosts, at the opposite side, a beam detector (neutrons or X-ray sensitive scintillator screen) for the formation of photon images. The photons generated by the scintillator screen are then reflected by a mirror onto a special CCD-camera (Charged Coupled Device). The spatial resolution is improved with a system of lenses, especially suitable for scanning small objects. Table 6.1 shows the characteristics of the X-ray beam and imaging properties.

The control to release neutrons onto the sample, the X-ray power supply as well as two PCs, one containing the frame grabber card and the other for the coordination of the rotation of the sample for the purpose of tomography, are located in the laboratory outside the containment (Figure 6.4).

Table 6.1 – Characteristics of the X-ray beam and image properties at SANRAD facility (from de Beer, 2005)

Distance from aperture to scintillator (L) (mm)		1000
Cone beam diameter at scintillator (mm)		~728
X-ray tube voltage (Continues)		0–100 kV
Approximate collimation ratio L/D for focal spot D		
	D = 1 mm	800
	D = 3 mm	266
Geometric unsharpness [mm] with sample thickness 5 cm and sample distance = 600 mm from focal spot:		
	D = 1 mm	0.07 mm
	D = 3 mm	0.20 mm
Beam divergence		40°

6.3 - Tomography procedure

The correct positioning of the sample inside the containment is checked through the imaging software and displayed on the PC (de Beer, 2005). The number of angular sampling intervals can be set within the range of 360° for the X-ray tomography. After the image acquisition, at least 3 background images (taken when the beam is closed) and 3 flat field images (images without a sample in the

beam) must be taken for the image correction due to beam fluxuation. Speckle noise and exposure normalization are also applied for each projection.

6.4 - Image reconstruction

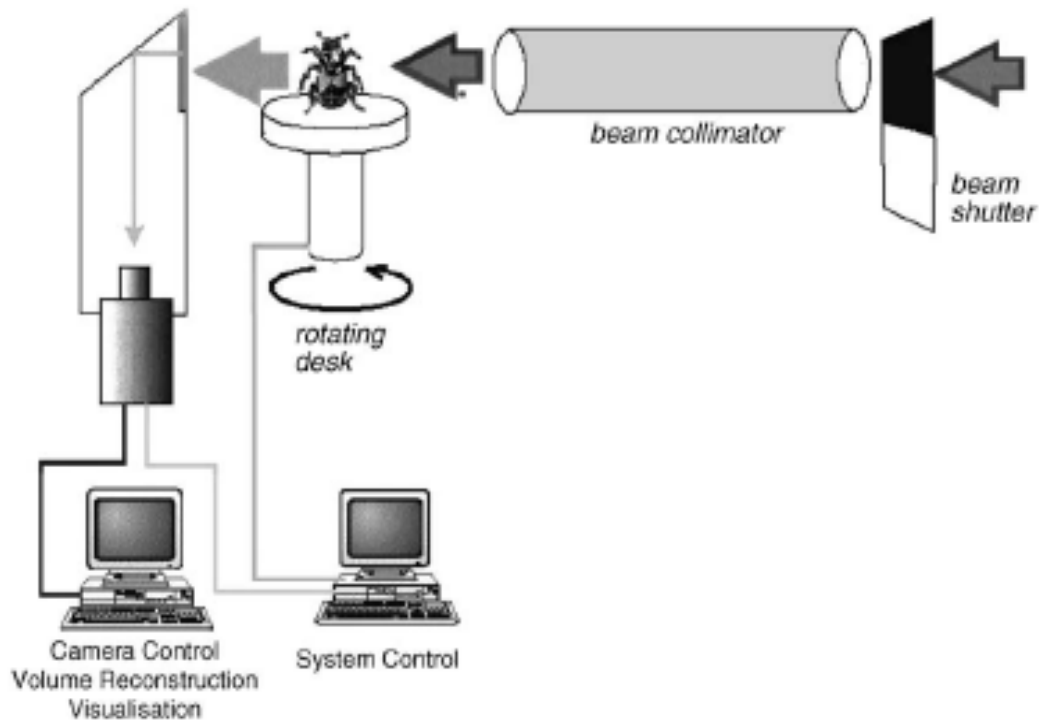


Fig. 6.4 – Schematic illustration of the tomography set up at the SANRAD facility (from de Beer, 2005)

The method of three-dimensional CT imaging by volume rendering has been used within the scope of the present project, and three-coordinates landmarks have been sampled for the purposes of geometric morphometric analysis. The scanning procedure produces many (depends on the size) sections per specimen; those needed to be merged together in order to render three-dimensional virtual images. The reconstruction was performed through *Octopus* software¹, which first converts the raw projections into TIFF image stacks of two-dimensional cross-

¹ Octopus is a commercial tomography reconstruction package for cone beam CT, spiral CT, parallel beam CT (synchrotron or neutron beam). Pre-processing steps are included in the package, such as ring filtering, normalisation, automatic beam hardening correction, axis tilt correction (<http://www.xraylab.com/>)

sections through the sample. A number of corrections were performed in order to facilitate the analysis of the three-dimensional data. Among the artefacts and noise reduction functions, the algorithms for correcting the ring artefacts, beam hardening, detector or stage tilt and Centre of Rotation (COR) misalignment were applied. The reconstruction was finally performed through a mathematical Fourier Transformation method which produces two-dimensional axial slices of the sample. In the next stage, the slices were stacked to produce a virtual voxel volume representing the sample in three-dimensions in a software package VGStudio MAX 2.1, which is a voxel data visualization and analysis software system (<http://www.volumegraphics.com/>). Initially, the visualisation of the images appeared like the original specimen. In a second phase, the three-dimensional images were cut in different planes to expose the adjacent teeth and to isolate each molar of interest from the others. In addition, every right side molar was mirrored into a left side one. The procedure consisted in loading the image stacks, setting several parameters such as resolution, surface lighting and resultant image size due to geometric enlargement of different magnitudes between the samples. Every tooth needed to be calibrated with respect to the others in order to be comparable in size. Thus, the resolution was set according to the distance of the object from the source, as schematized in Table 2. The calibration of grey values was necessary prior to the positioning of any landmarks on the image. Every tooth was re-aligned according to its major axes (see paragraph *Tooth alignment* in this chapter for further details) before the coordinate data could be sourced.

Table 6.2 – Resolution parameters applied for the calibration of image size

Source Object Distance	Resolution (mm/pixel)
920	0.091
680	0.067
480	0.047
250	0.024

6.5 - Tomography set up and expedients for the safety of the fossils

The X-ray tomography was performed using a CCD camera (Pentax lens FA 135mm: F2.8, FOV= 9 cm x 9 cm). 400 projections were taken along 360°; with a time of exposure of 1 sec per projection. The time for the scanning was about 20 minutes per sample. Every specimen was located in the containment of SANRAD



Fig. 6.5 - Set up of the partial mandible of *Theropithecus oswaldi* fixed with putty onto the rotary disk and positioned between the X-ray source (the yellow tube in the picture) and the scintillator screen (not visible here)

facility on a support consisting of a rotary stage, which represents the target area. Several expedients were applied in order to assure a high standard of safety of the fossils. Every sample was firmly placed on the support using an adequate putty (UHU® Tac Reusable Adhesive Putty), in the position that better allowed the penetration of the rays through the sample, but always considering its stability and avoiding any contact with the putty above particularly fragile regions (Figure 6.5). The putty itself is particularly satisfactory for this specific use because does not leave any greasy residue, does not melt with heat even though it is highly mouldable and easily removable, thus it is safe on fossil surface.

Different diameter disks were used for the positioning of the samples of diverse sizes in a way that the specimen was fully housed inside the disk area. In some cases, when the teeth were part of a complete or almost complete skull, the fossil was cradled in a cavity within a piece of foam rubber. This helped in finding the correct position of the specimen in absolute safe condition.

6.6 - Other security measures for the safety of the fossils

For the nature of the technique used for data collection, the fossils had to be obligatorily moved from the safe and transferred to Pelindaba. For security reasons a strict protocol was observed. Only a small number of fossils was moved at any one time, with care taken in grouping different tooth typology together (for example not only M¹s at once) and taking the teeth belonging to the same individual during different trips. The fossils were bubble-wrapped and placed in an anti-shock case embedded in holes shaped in a block of foam rubber. The case was secured with elastic bands inside the car and hidden with a rug in order to not

call attention to it. The speed was always kept below 90 km/h. During the staying at Necsa, the fossils were kept inside the case and handled one at a time only when necessary for the scanning session. Each fossil was set in a support of foam rubber when moved from the case.

Even though the X-ray tomography does not cause the sample to be radioactive, the security protocol at Necsa calls for a double monitoring of the radioactivity level which must not be higher when the sample leaves the SAFARI-1 reactor than it was at the time of admission. Only after this is the sample permitted to exit the area. At the end of each working day the sample was returned to the Museum of provenience. Only when some specimens could not be scanned within a certain day, were they stored in a safe at Necsa in order to avoid the exposure of the fossils to double risks of accidents during transport.

6.7 - Set of landmarks

The set of landmarks utilized (see list on Table 6.3, discussion in *Landmark coordinate sampling* below, and illustrations in appendix D) reflects the aim to describe the morphology of the crown in a better way, which is considered to be that portion of the tooth between the cervical line and the cusp tips. However, the nature of the statistical analysis performed implied some limitation in the choice of the points selected as well as in their number. In fact, the crown of a molar has an irregular form and some of the dental features detectable do not occur regularly or vary remarkably in their expression (see for example the Carabelli trait or supernumerary cusps, among the others).

Each landmark was collected by integrating the information provided by the three-dimensional image together with the axial, sagittal and frontal views which

show the xy, yz and xz slices respectively. In the case of scans performed on casts the identification of the points was based on the three-dimensional image mostly, since a cast obviously does not preserve the inner structure of a fossil.

Table 6.3 - Set of landmarks (Abbreviation: P = Point)

- P1. The deepest point of the central fovea (which determines Plane P1*)
 - P2. The point of contact between Pr and Hy on the outline at level of Plane P1
 - P3. The point of contact between Pa and Me on the outline at level of Plane P1
 - P4. The point of contact between Pr and Pa on the outline at level of Plane P1
 - P5. The point of contact between Hy and Me on the outline at level of Plane P1
 - P6. The furthest point projecting from Line 1 (bisecting P2 and P4) to the Pr outline
 - P7. The furthest point projecting from Line 2 (bisecting P4 and P3) to the Pa outline
 - P8. The furthest point projecting from Line 3 (bisecting P3 and P5) to the Me outline
 - P9. The furthest point projecting from Line 4 (bisecting P5 and P2) to the Hy outline
 - P10. Pr cusp tip
 - P11. Pa cusp tip
 - P12. Me cusp tip
 - P13. Hy cusp tip
 - P14. Central groove mesial terminus on the mesial margin
 - P15. Lowest point on central groove between P1 and P14
 - P16. Intersection between distal central groove and transverse groove
 - P17. Lowest point of distal fovea
 - P18. Central groove distal terminus on the distal margin
 - P19. Highest point of contact between Pr and Hy
 - P20. Highest point of contact between Pa and Me
-

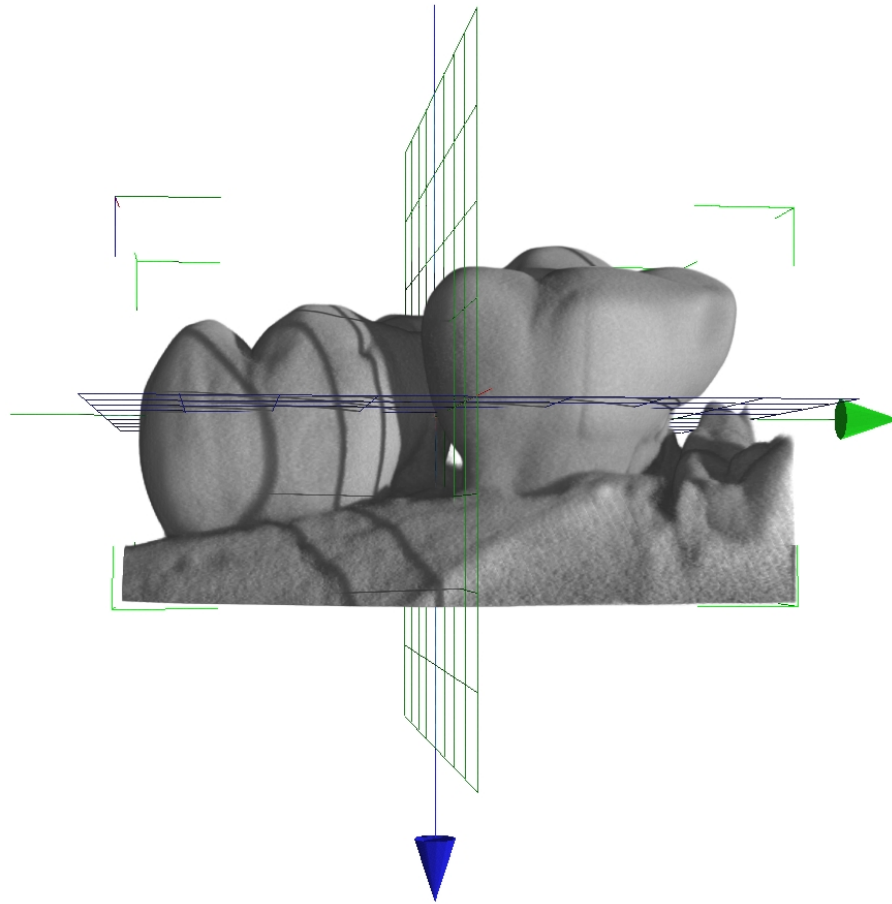


Fig. 6.6 – Three-dimensional virtual image where the main axes of the scene box (represented by grids and arrows) are not parallel to those of the teeth

6.8 - Tooth alignment

To obtain a good quality scan it is important to allow the highest penetration possible through the material. This means that each specimen must be positioned such that the bulk of the fossilised bone or matrix does not obscure the penetration of the rays in the region of interest. In the case of this project, such expedients meant that the teeth could not be positioned according to their major axes during most of the scannings. In the visualisation of the images, the teeth appear not to be

well oriented with respect to the scene box as illustrated in Figure 6.6. Even though the position of the object in the space does not affect the results of the geometric morphometric analyses (see chapter 4 - *Quantitative analysis of data from CT based techniques* for more details), it was necessary to re-align the images of the teeth (through VGStudio MAX 2.1) before the landmark coordinate sampling could proceed. In fact, VGStudio MAX 2.1 slices the object in accordance with the main axes of the scene box. This would result in a misplacing of some of the landmarks considered, such as those sampled on the so called Plane P1 as discussed below (paragraph *Landmark coordinate sampling*).

Different procedures for the identification of the correct orientation had been considered (for problems related to tooth orientation see Benazzi, 2007). Among these, there is the orientation based on cusp tips method that was left out because the sample is composed of worn teeth. Finally a method was outlined taking into account possible constraints such as tooth incompleteness and wear but also the helpfulness of the virtual tools available. The alignment was thus realised by identifying 4 points on the cervical margin which fulfil the following definitions:

- i. The point of contact between Pr and Hy
- ii. The point of contact between Pa and Me
- iii. The point of contact between Pr and Pa
- iv. The point of contact between Hy and Me

The object would be re-oriented according to the plane that interpolates the aforementioned points. Sometimes, the state of preservation of the fossils made the identification of one or more of those points not possible or too inaccurate. When one aspect of the tooth was damaged over the cervical margin, the

matchpoints used for tooth alignment were reduced from 4 to 3. If more than one landmark was missing, the point(s) in a different location than over the region between cusps were chosen, in particular more mesially or more distally for points i and ii; more lingually or buccally for points iii and iv (Samples: SK 27 RM¹; SK 832 LM¹; SK 829 RM¹; Sts 1 LM²; TM 1603 LM³).

The identification of these points could be particularly difficult on a CT-scan obtained from a cast, where the information on the external morphology cannot be integrated with that of inner morphology. In these events the three-dimensional view only was utilised. For a small number of specimens the re-alignment was not performed, in so far as the points i – iv could not be detected and the original orientation was considered acceptable or the re-aligned and original image overlapped (Sample: KB 5383 RM¹; SK 831A LM³; SKW 3114 LM¹; Stw 151 LM¹; Stw 204 LM²; Stw 252 LM¹).

6.9 - Landmark coordinate sampling

The landmarks collected and procedure and problems related to the acquisition of each of them are described in the following paragraphs and are illustrated in a series of template images in appendix D.

P1. Lowest point of central fovea

It is located in the deepest point of the central fovea. It is generally positioned in the region of contact between the Pr, Pa and Me. Being anatomically well distinct, its sampling was straight forward. Its placement was based on the observation of the 3 slice views. This point provides for the definition of the following 8 landmarks (P2-P9), which are located on the axial plane passing for P1 (“plane P1” for short) and which all together describe the crown outline at a fixed level.

P2. Contact between Pr and Hy on the plane P1 outline

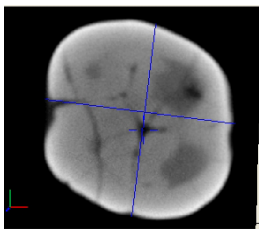
This landmark is positioned on the point of contact between the palatal cusps, and lies on plane P1. It is placed at the base of the fissure between these cusps, thus it is easily identified in the axial view. The simultaneous examination of the three-dimensional image helps in determining exactly where the landmark should be positioned.

P3. Contact between Pa and Me on the plane P1 outline

Everything said for P2 is true for P3 as well, except that P3 lies on the buccal aspect instead.

P4. Contact between Pr and Pa on the plane P1 outline

The identification of this point, which is placed on the mesial side of the crown, is not as straightforward as P2 and P3, in so far as the fissure is not always present



or

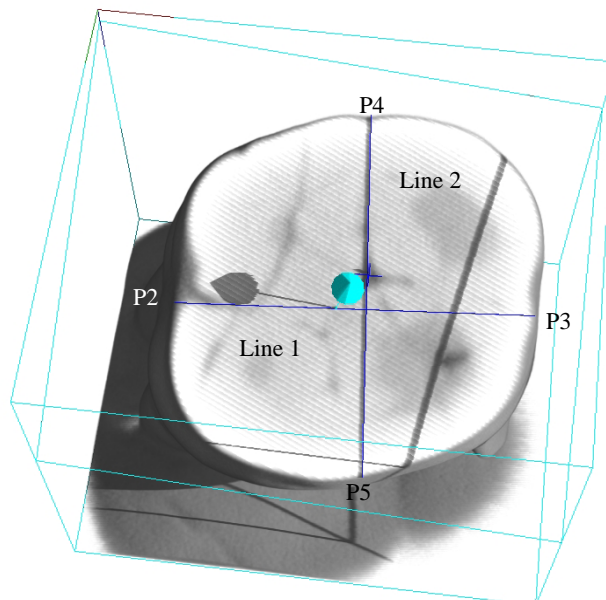


Fig. 6.7 – Section of the virtual image showing Line 1 and Line 2 which connect respectively points P2-P3 and P4-P5

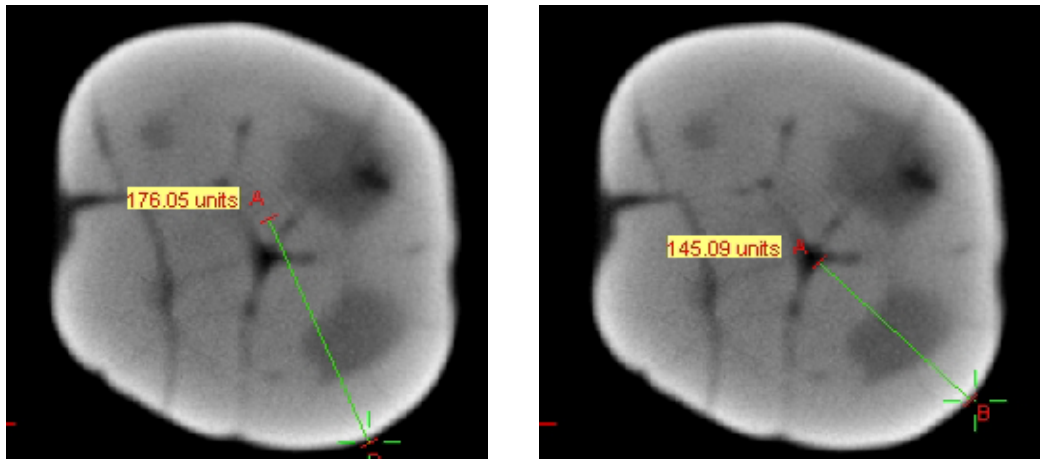


Fig 6.8 – Transverse section of SK 829 LM¹ at the level of Plane P1. a. The picture shows the sampling of Me cusp most projecting point in accordance with the procedure based on the use of the pivot at the intersection between Line 1 and Line 2. The point seems not to be correct when looking at the general shape of the cusp. In b. it is shown an alternative way of sampling that leads to a completely different positioning of the landmark on the same cusp

sharply defined. The examination of the three-dimensional representation is essential together with the slices above and below Plane P1 in axial view.

P5. Contact between Hy and Pa on the plane P1 outline

Also for this point located on the distal side, the identification could be difficult for the same reason as P4, and must be based on the observation of the three-dimensional representation and slices above and below Plane P1, as well.

The landmarks P2-P5 were also used as points of reference for the sampling of the landmarks P6-P9 which are defined as follows:

P6-P9. Most projecting point on Pr – Pa – Me - Hy outline (respectively) on plane 1

These landmarks represent the points of maximum projection of the four major cusps on the axial plane P1. They are identified on the region of maximum curvature, far from the area of contact between cusps. For their detection various alternatives and geometric construction had to be taken into account. In a first attempt, two lines roughly perpendicular bisecting P2 and P3 (Line 1) and P4 and

P5 (Line 2), were used (Figure 6.7). The point of intersection between those two lines was considered as a pivot for a measuring tool which helped in the identification of the longest distance detectable along the outline. This landmark collection procedure turned out to be unsuitable in a certain number of samplings where, for the particular morphology of the cusp, the longest distance ended up being too close to one of the adjacent cusp. This was the case in laterally reduced cusps especially, the profile of which tends to have a straight margin rather than strongly convex margin. In such instances should have the pivot been positioned in accordance with the shape of the cusp in order to detect a point that could be consistent with the one identifiable by a visual inspection? (Note the case of Me in a M¹ of *Paranthropus robustus*, as shown in Figure 6.8). In particular, the fixed extremity of the measuring tool would have been positioned on either Line 1 or Line 2 on that point considered the centre of the ideal arch described by the cusp profile. This procedure could not be considered satisfactory because it implies a high level of subjectivity of the sampling and therefore it is neither precise nor repeatable.

The second and final (definitive) procedure used consists in connecting P2-5 as in the picture showed in Figure 6.9. A line connecting the points of contact of each cusp to its adjacent cusp was drawn. Then the subtense from this line to the crown outline was drawn.

P10-P13. Pr, Pa, Me, Hy apices (respectively)

These points were sampled basically with reference to the axial view, using the mouse-scroll until the slice with the last pixel(s) available was found on the peak of each cusp. The sampling of these points did not present complications in

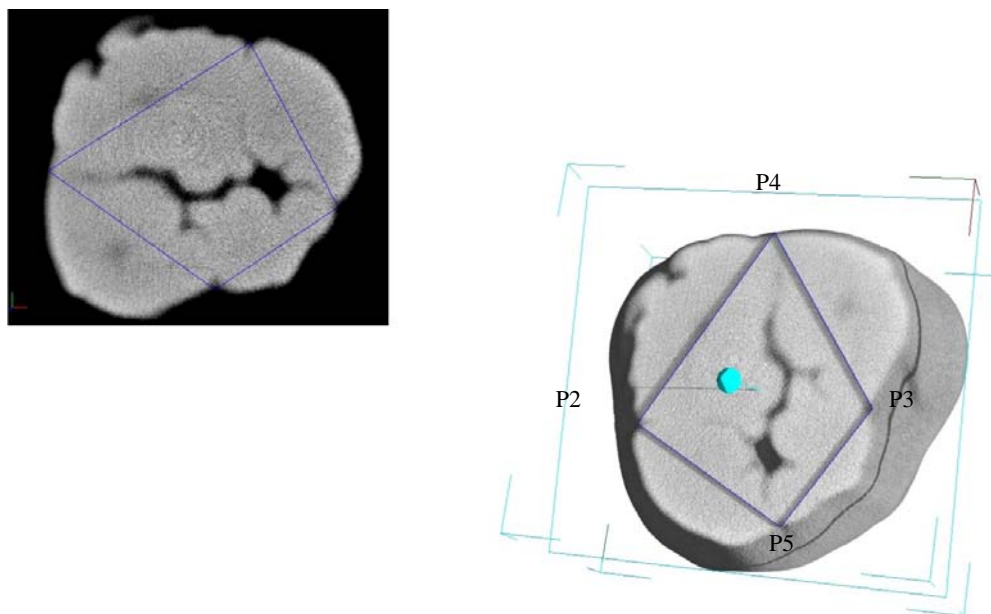


Fig. 6.9 – Transverse section on Plane P1 where points P2-P4, P4-P3, P3-P5; P5-P2 are connected with lines

unworn specimens. It is noteworthy that the wear affects very much the position of these landmarks. Not only has the height varied, but the location in the axial plane as well, due to the modification of cusp shape.

Concerning Pr, it was noted that within unworn teeth, the apex is in correspondence to the peak of its dental pulp cavity, but this is not always true anymore for those teeth affected by wear, in which the highest point of the cusp is generally shifted more toward the centre. The Pa of an unworn tooth follows a different pattern and the cusp apex is more mesio-buccally positioned than is the peak of its dental pulp cavity. Being that teeth are not uniform in wear and the various cusp typologies are different in the response to the wear, I decided to always collect the actual highest point of the cusp, whether or not it corresponded to the original cusp tip position on the coronal plane. In any case it should be emphasised that wear compromises the sampling of these landmarks very much, both in the cusps height and on the axial coronal plane.

P14. Central groove mesial terminus on the mesial margin

This is identifiable by following the course of the central groove and is positioned on the highest point of the mesial margin. The three-dimensional and axial views were mainly used. For some specimens the sampling could be difficult as the area was worn away. When the tooth presented an extra cusp, the landmark was located at its highest point.

P15. Lowest point on central groove between P1 and P14

This can be described as a point of flexum, morphologically well defined and situated along the central groove between P1 and P14.

P16. Intersection between distal central groove and transverse groove

This landmark falls in the distal fovea where the distal and transverse grooves meet. It was sampled in the deepest point of the transverse groove. In not all of the specimens is this feature well outlined, but it is always somehow expressed. Only marked wear caused uncertainty in the sampling.

P17. Lowest point of distal fovea

It is the deepest point of the distal fovea and is identified with the same method as P1. It is generally easily detectable even in the most worn specimens included in the sample.

P18. Central groove distal terminus on the distal margin

The central groove distal terminus corresponds to P14 on the distal side (see the discussion regarding P14, above).

P19. Highest point of contact between Pr and Hy

This landmark is situated between the palatal cusps and corresponds to their highest point of contact on the tooth sagittal plane. It is well defined in unworn

teeth, while the identification is problematic in cases of wear, where the landmark is shifted toward the centre of the tooth and appears to be represented by a region instead of a point. In these cases the landmark was selected in the midpoint of this region in the sagittal axis.

P20. Highest point of contact between Pa and Me

It is the same as P19, but for the buccal cusps (see the discussion regarding P19, above).

6.10 – Statistical analyses

The geometric morphometric analysis on landmark coordinates was done using *Morphologika* software. PCA on full tangent space projection (see O’Higgins and Jones, 1998 for details about this function and its meaning) was performed on GPA residuals. The visualization of variance along PCs was possible through the visualization features available through *Morphologika*. However the plots shown in this work were obtained using *PAST* software. *PAST* was used for basic statistic, as well.

Two different sets of analysis were performed: first the validity of the method chosen was assessed, then the null hypothesis (i.e., only one australopithecine species exists among the remains at Sterkfontein Member 4 and Makapansgat) was test as fully disclosed in chapters 7 – *Assessment of the method used, advantages and limitations*, and 8 - *Results*, respectively. Here a brief report of the statistical analyses conducted is provided.

In chapter 7, M¹s and M²s of *Paranthropus* and early *Homo* from Swartkrans were compared through a geometric morphometric analysis in order to verify whether the different morphologies of these two taxa were somehow captured and

reflected by applying the methods conceived for this project. Furthermore, the intra-observer error for landmark collection was assessed and discussed at different levels. Seven repeats were sampled from M³s. The seven pairs of landmark configurations underwent geometric morphometric analysis and then were plotted together with the full M³ sample. Since this approach gives a visual impression of the variance shown, but does not allow to quantify the error, the Euclidean distances between landmark coordinates were calculated in order to verify whether or not the error was significant (namely if the Euclidean distance between each of the seven pairs of repeats was out of the interval of confidence (= 95%)). Moreover, PCA does not give information about the landmark displacement, nor does the Euclidean distances matrix, thus, the images of the seven pairs of landmark configurations (as rendered through VGStudio MAX 2.1) were compared and the landmark displacement were discussed.

In chapter 8 the full subsamples grouped per tooth typology were investigated through geometric morphometric analyses. In addition, the visualization of the variance along the first two PCs was rendered through the shape morphs.

The relationship between shape and size was also investigated by plotting each PC against the centroid size² (through *Morphologika*), the latter representing an estimate of overall size. Since for none of the other PCs a significant correlation was found, only the plot of every PC1 against the centroid size was presented. The allometric trend was further investigated by applying a linear correlation analysis

² **Definition:** Centroid size is the square root of the sum of squared distances of a set of landmarks from their centroid, or, equivalently, the square root of the sum of the variances of the landmarks about that centroid in *x*- and *y*-directions. Centroid size is used in geometric morphometrics because it is approximately uncorrelated with every shape variable when landmarks are distributed around mean positions by independent noise of the same small variance at every landmark and in every direction. Centroid size is the size measure used to scale a configuration of landmarks so they can be plotted as a point in Kendall's shape space. The denominator of the formula for the Procrustes distance between two sets of landmark configurations is the product of their centroid sizes (Slice, *et al.*, 1998; from <http://www.paleo.geos.vt.edu/geos5384/Gloss.htm>)

between GPA residuals and centroid sizes (through *PAST*) in order to quantify the relationship between variables (calculating the correlation coefficient r and the P-value). With the aim to strengthen the results obtained in chapter 8 - *Results*, M¹ and M² belonging to the same individual (5 in total) were analyzed as a single object through a geometric morphometric analysis.

CHAPTER 7

ASSESSMENT OF THE METHODS USED, ADVANTAGES AND LIMITATIONS

7.1 - Introduction

In this chapter the protocol applied to the acquisition of data is tested. An evaluation of the strength of the proposed methods is necessary before the full sample of maxillary molars is analyzed in terms of crown and cusp morphology and relative position (see chapter 8 - *Results*). In order to demonstrate that the methods are able to capture the differences in terms of tooth form and that these are sufficient to separate the groups under study it is necessary to test the methods on hominid tooth samples known to be taxonomically distinct. Qualitative features, such as fissure patterns, supernumerary cusps, Carabelli trait expression, etc. are not considered here.

For this purpose, the samples of *Paranthropus* and *Homo* (both from Swartkrans) are compared, providing the analysis for M¹ and M² tooth types separately but not including any M³ attributed to early *Homo*. The validity of the methods applied in this project will be confirmed if the results obtained are those expected, namely that the specimens of *Paranthropus* and those of *Homo* do not cluster on the plot. In fact, general tooth morphology and molar morphology in particular are clearly distinguishable in these two groups even in a visual inspection. Moreover, the

taxonomical distinction between these two hominids is broadly acknowledged as well as accepted here.

In view of the necessity for certainty about the specific attribution of the specimens, the molars belonging to *Paranthropus* from Cooper's Cave and Kromdraai are not considered at this stage of the research as there is no consensus that they belong to the same species as that from Swartkrans (see Broom, 1949, 1950; and later Howell 1978; Grine 1982, 1984, 1985; Clarke, 1996 but also Robinson, 1954 for a different point of view. For a comprehensive discussion see Kaszycka, 2002). For an analogous reason, StW 151 is not included in the analysis, since there is also no general consensus of this specimen's attribution to the genus *Homo* (Spoor, 1993; Moggi-Cecchi, *et al.*, 1998). For each analysis, the plot showing the distribution of the specimens along PC1 and PC2 is provided (Figures 7.1-7.4 and 7.6). The percentage of the total variance explained by the first two PCs is shown in the heading of the graphs and is also discussed in the text, but a full disclosure of the PCs' eigenvalue¹, percentage of the total variance explained and cumulative variance explained is given in the table pertinent to each analysis (Tables 7.1-7.5). The relationship between the size and shape of molar crowns was investigated by looking for indications of a significant correlation between the scores of individuals on each PC and centroid size. This procedure allowed for the effective examination for signs of allometry by the analysis of principal vectors of variation in shape space. Since no allometric trend was found

¹ Definition: in mathematics, given a linear transformation, an eigenvector of that linear transformation is a non-zero vector which, when the transformation is applied to it, may change length but not direction. For each eigenvector of a linear transformation, there is a corresponding scalar value called **eigenvalue** for that vector, which determines the amount the eigenvector is scaled under the linear transformation.

for any of the PCs, only the plots of PC1 against centroid size are shown below (Figure 7.5 for M¹ and Figure 7.7 for M²).

7.2 – First molars. *Paranthropus* vs. early *Homo*

Firstly, the distribution of the *Paranthropus* specimens from Swartkrans was checked (sample: SK 55A, SK 89, SK 102, SK 829, SK 832, SK 838, SK 839; Figure 7.1; Table 7.1).

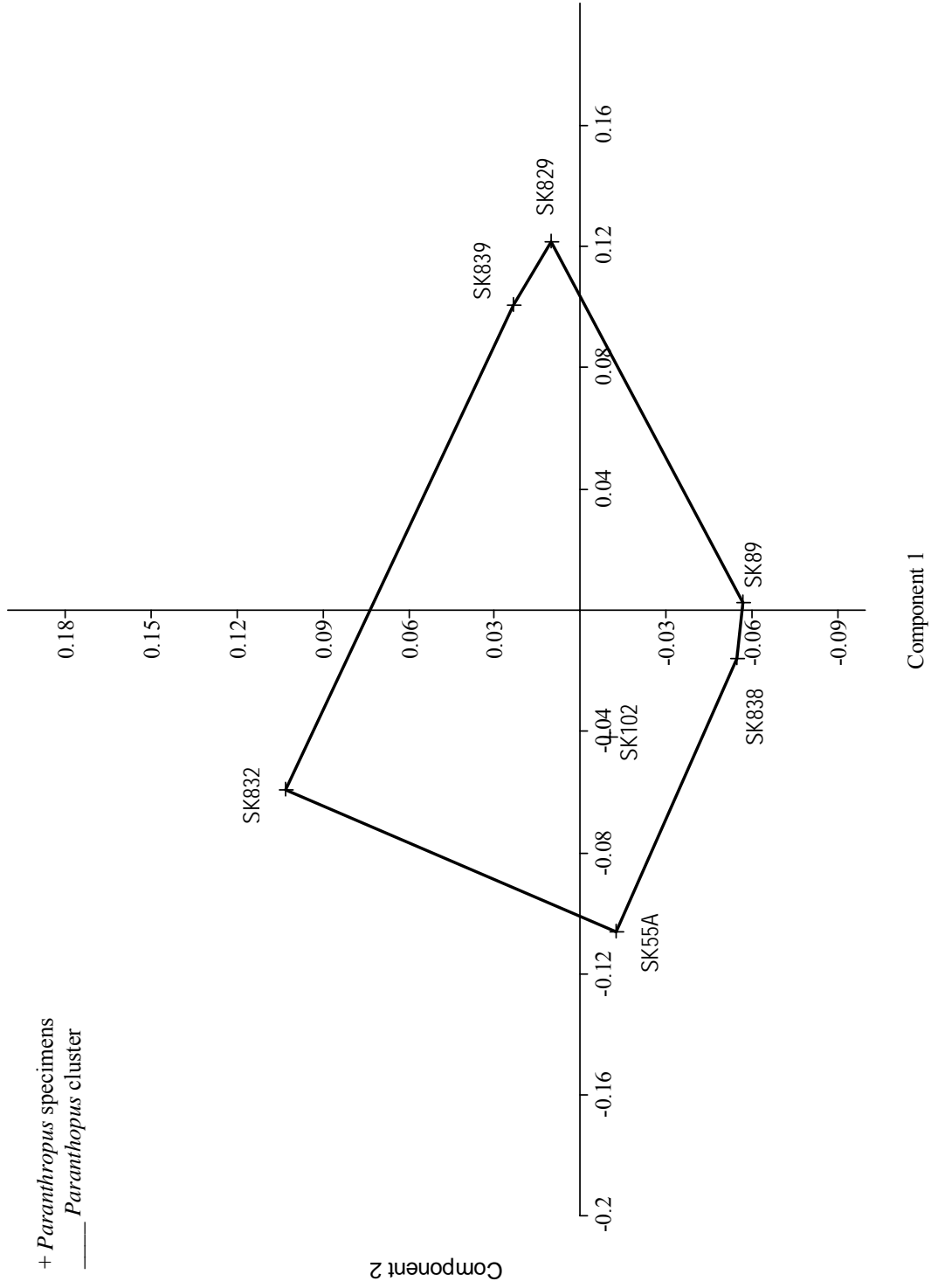


Fig. 7.1 – PCA: M¹ – *Paranthropus* (SK 55A, SK 89, SK 102, SK 829, SK 832, SK 838, SK 839). Percentage of total variance explained from PC1: 47.22% and PC2: 20.17%

Table 7.1 - M¹. *Paranthropus*, Swartkrans (sample: SK 55A, SK 89, SK 102, SK 829, SK 832, SK 838, SK 839): eigenvalues and percentage of variance explained for all the PCs

	Eigenvalue	Percentage of total variance explained	Cumulative variance explained
PC1	0.006958432211	47.22	47.22
PC2	0.002972135411	20.16	67.38
PC3	0.001861332146	12.63	80.01
PC4	0.001523614278	10.34	90.35
PC5	0.000948302474	6.44	96.79
PC6	0.000473813707	3.21	100.00

Along PC1, the first upper molars of *Paranthropus* cluster quite tightly in the positive half of the plot with the maximum score of +0.11 (where the x coordinate score of SK 89 is slightly negative), whilst SK 829, SK 839 plot rather distant from the rest of the group and set in the negative part of the horizontal axis (score -0.12). The distribution along PC2 is narrower and scores between +0.6 and -0.10.

The tooth specimens of early *Homo* from Swartkrans (sample: SK 27, SKW 3114, SKX 268 cast) are gradually included in the sample with the aim to investigate the discriminant power of the methods applied (Figures 7.2 – 7.4).

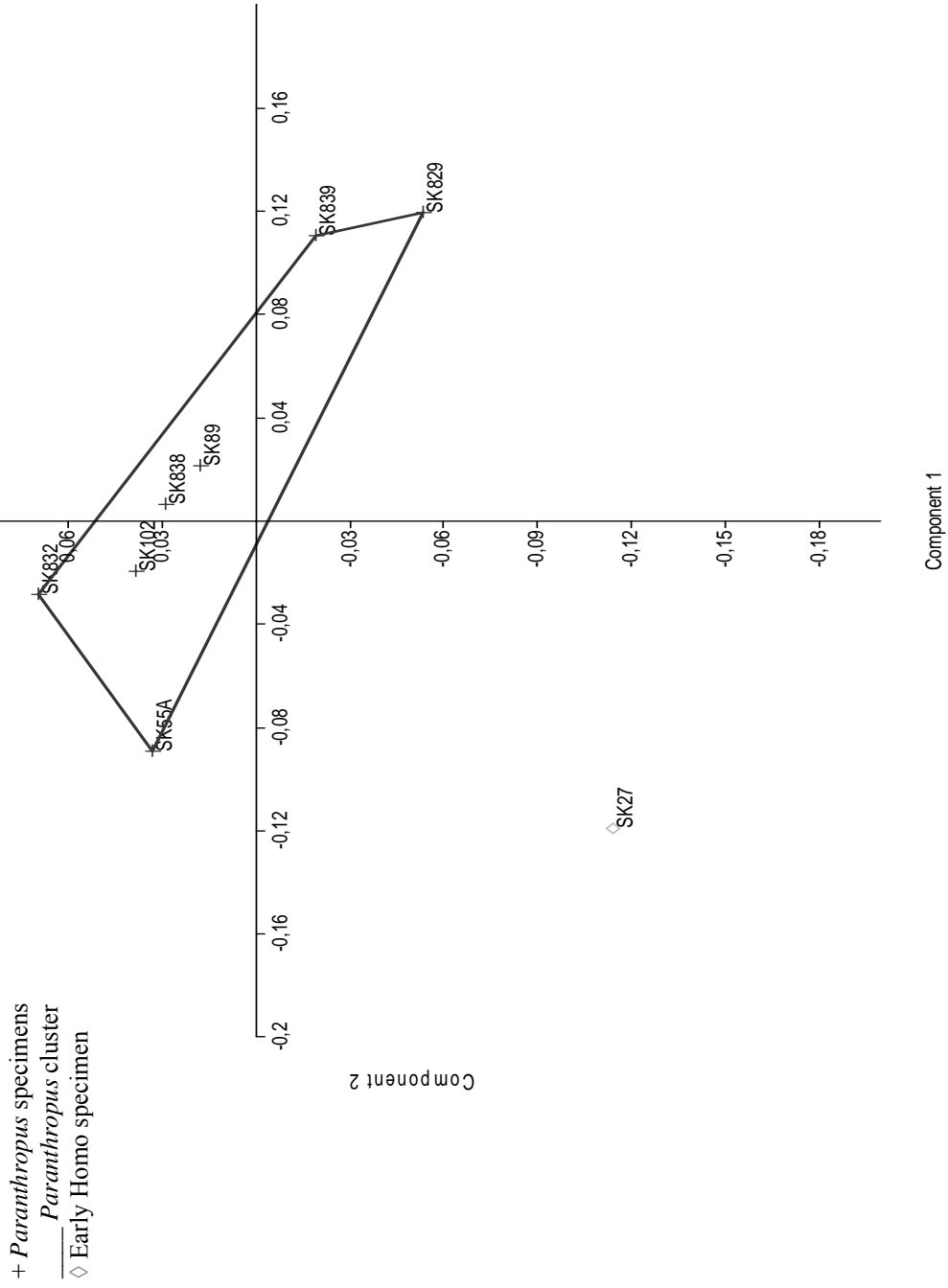


Fig. 7.2 – PCA: M¹ – *Paranthropus* and early *Homo* (SK 27). Percentage of total variance explained from PC1: 41.77% and PC2: 20.58%

Table 7.2 - M¹. *Paranthropus* (sample: SK 55A, SK 89, SK 102, SK 829, SK 832, SK 838, SK 839) and early *Homo* (sample: SK 27): eigenvalues and percentage of variance explained for all the PCs

	Eigenvalue	Percentage of total variance explained	Cumulative variance explained
PC1	0.007184333356	41.77	41.77
PC2	0.003539145778	20.58	62.35
PC3	0.002528918264	14.70	77.05
PC4	0.00145571941	8.46	85.51
PC5	0.00128813163	7.49	93.00
PC6	0.000802220209	4.67	97.67
PC7	0.000401604747	2.33	100.00

The M¹ of SK 27 plots far from the specimens of *Paranthropus*. SK 27 is positioned out of the range of distribution of *Paranthropus* on PC1 and especially on PC2 where the maximum positive score on PC1 of *Paranthropus* is +0.06 and that of SK 27 is well beyond it, at +0.12. It is to be noted that the relative position on the plot of the specimens of *Paranthropus* does not change after including in the sample the specimen of early *Homo*.

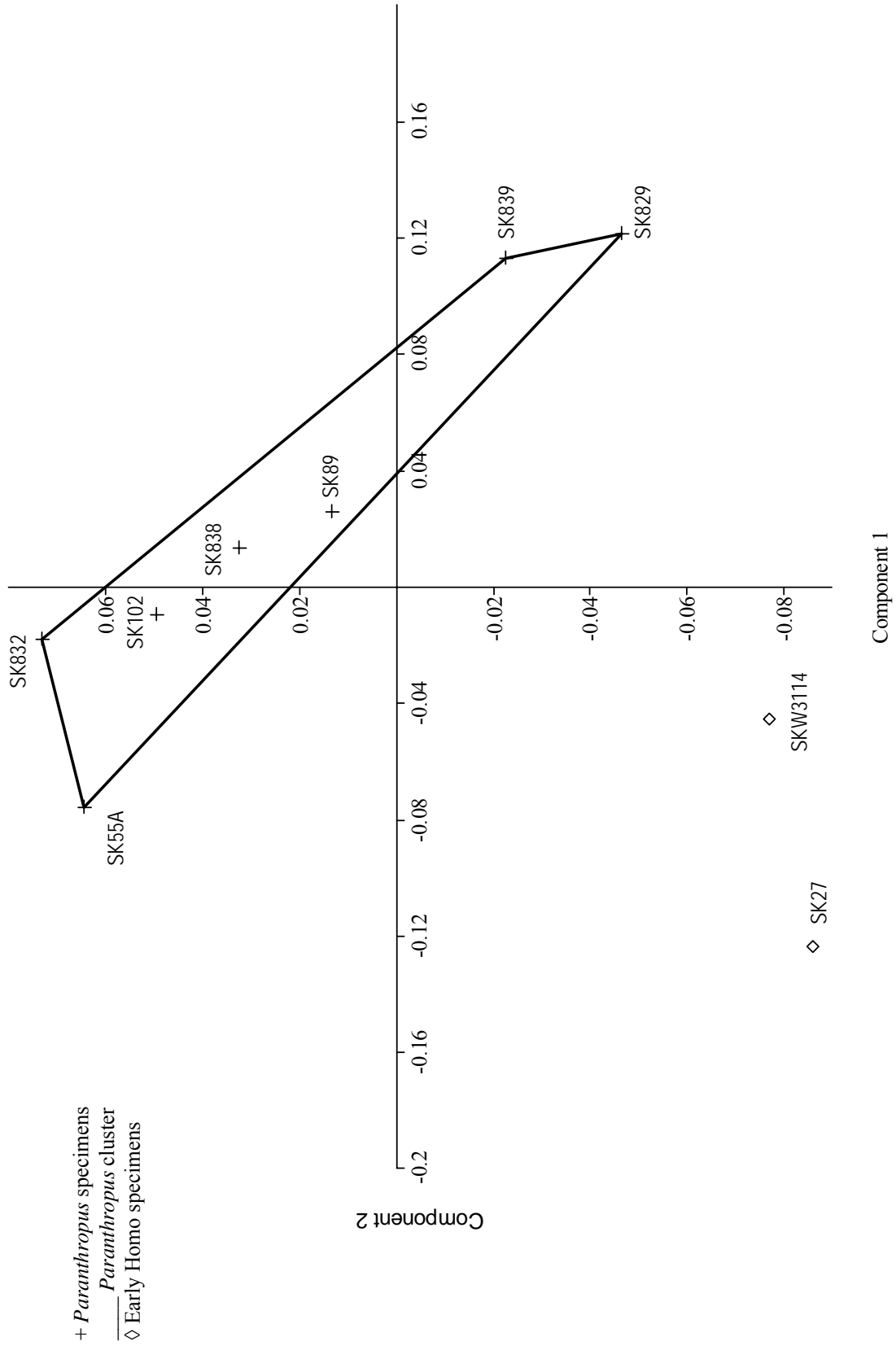


Fig. 7.3 – PCA: M¹ – *Paranthropus* and early *Homo* (SK 27; SKW 3114). Percentage of total variance explained from PC1: 37.87% and PC2: 21.31%

Table 7.3 - M¹. *Paranthropus* (sample: SK 55A, SK 89, SK 102, SK 829, SK 832, SK 838, SK 839) and early *Homo* (sample: SK 27, SKW 3114): eigenvalues and percentage of variance explained for all the PCs

	Eigenvalue	Percentage of total variance explained	Cumulative variance explained
PC1	0.006478903919	37.87	37.87
PC2	0.00364661141	21.31	59.18
PC3	0.002213607487	12.94	72.12
PC4	0.00177963861	10.40	82.52
PC5	0.001208037385	7.06	89.58
PC6	0.000778133797	4.55	94.13
PC7	0.00068168831	3.98	98.11
PC8	0.000323650082	1,89	100.00

Including SKW 3114 (another M¹ classified as belonging to early *Homo*) in the sample the general picture described as in Figure 7.2 does not change significantly and the relative position of the individuals does not vary. When considering PC1 and PC2 together, SKW 3114 plots close to SK 27 and far from the other hominid form, whilst there is a certain superimposition along PC1.

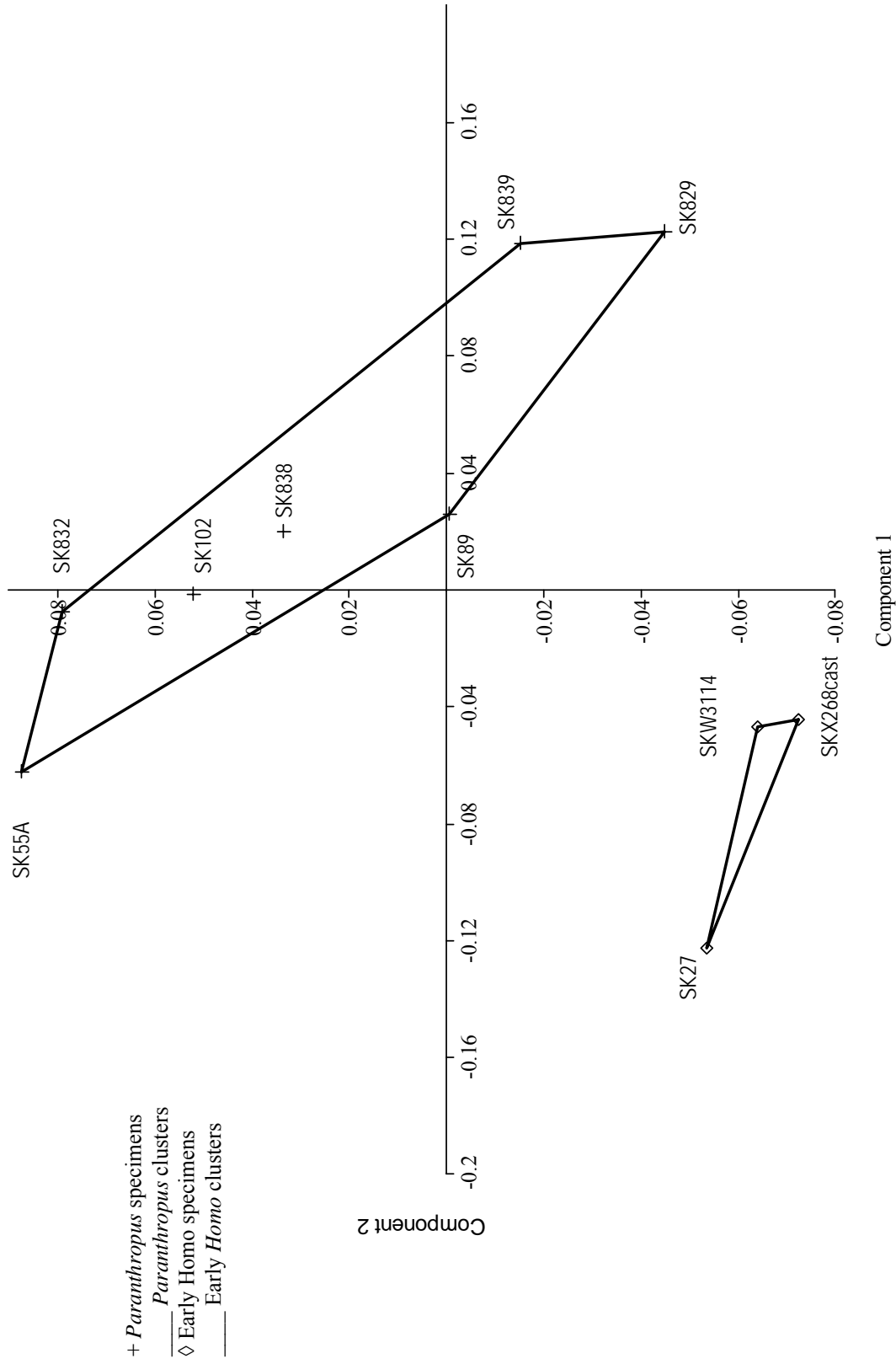


Fig. 7.4 – PCA: M¹ – *Paranthropus* and early *Homo* (SK 27; SKW 3114; SKX 268 cast). Percentage of total variance explained from PC1: 34.07% and PC2: 20.63%

Table 7.4 - M¹. *Paranthropus* (sample: SK 55A, SK 89, SK 102, SK 829, SK 832, SK 838, SK 839) and early *Homo* (sample: SK 27, SKW 3114, SKX 268 cast): eigenvalues and percentage of variance explained for all the PCs

	Eigenvalue	Percentage of total variance explained	Cumulative variance explained
PC1	0.005909581664	34.07	34.07
PC2	0.003578898706	20.63	54.70
PC3	0.002247162829	12.95	67.65
PC4	0.001858854071	10.71	78.36
PC5	0.001340574881	7.73	86.09
PC6	0.001073678831	6.19	92.28
PC7	0.000636258252	3.67	95.95
PC8	0.000426325906	2.46	98.41
PC9	0.000276584445	1.59	100.00

Figure 7.4 shows how the specimen SKX 268 (represented from a cast) is situated close to the other M¹ of early *Homo* and sets apart from those of *Paranthropus*, at least along PC2. Taking into consideration PC1 and PC2 together, there is a reasonably neat separation of the M¹ of early *Homo*. Along PC1 there is a slight superimposition with SK 55. Except for this case, PC1, which explains 34.07% of the total variance, discriminates well between the two genera. PC2 (20.63% of the total variance) also seems to separate the two groups quite well, even though the score of SK 829 on the vertical axis is quite similar to those of early *Homo* specimens. In conclusion, the specimens of *Paranthropus* and those of early *Homo* appear quite well separated on the plot.

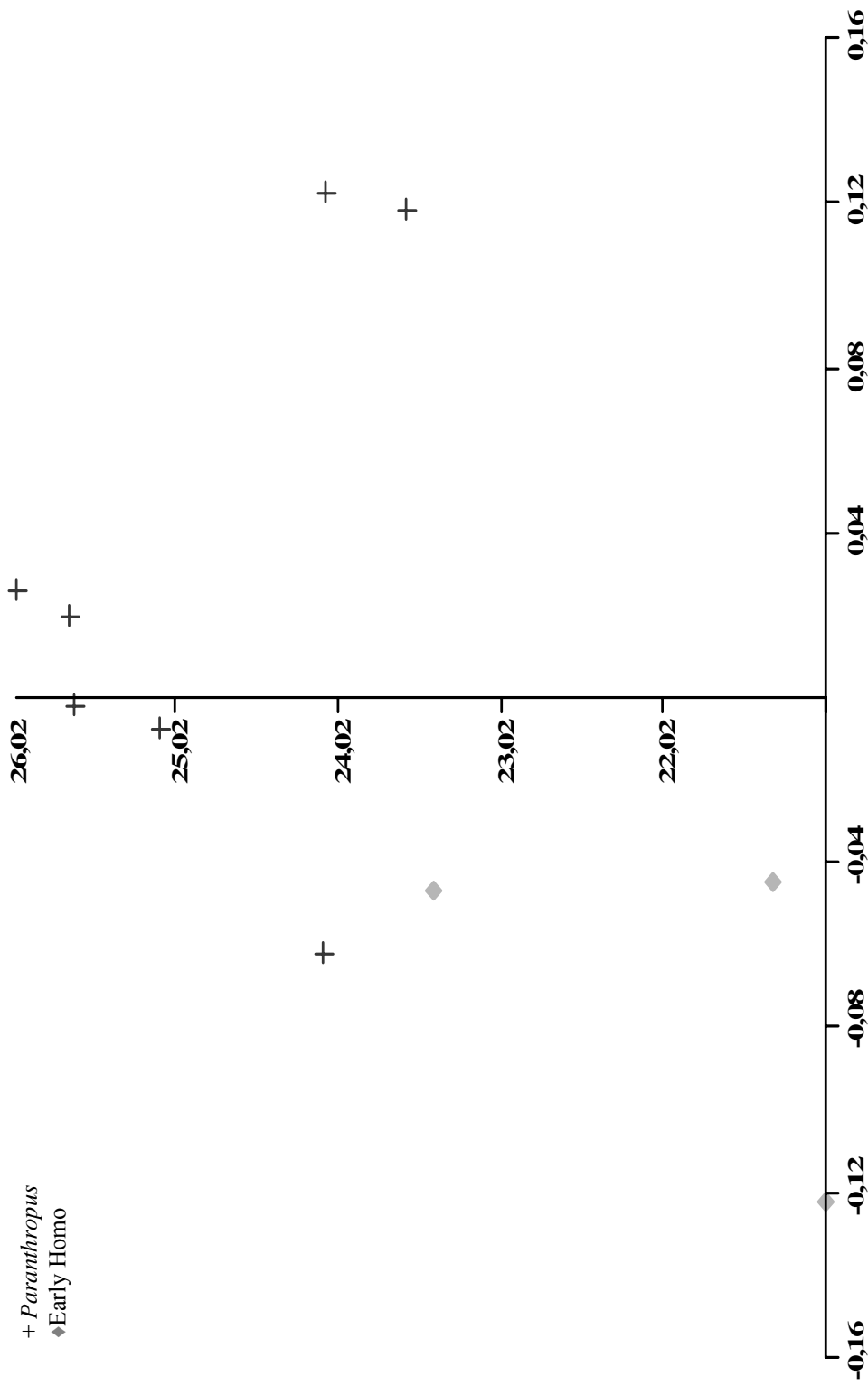


Fig. 7.5 – PCA: M¹ – Paranthropus and early Homo; PC1 against centroid size. No significant correlation between size and shape is shown ($r = 0.45162$; $P = 0.19011$)

Figure 7.5 represents the plot of PC1 (horizontal axis) from PCA vs centroid size for the sample of M¹. It does not show a linear correlation of the specimens, thus it is reasonable to think that there is not a linear correlation between the change in shape and that in size, namely there is not an allometric trend characterizing the sample.

7.3 – Second molars. *Paranthropus* vs. early *Homo*

Since the analysis performed for the M¹ demonstrated that the relative position of the specimens does not change when adding others to the sample, the distribution of *Paranthropus* M² only is not shown here. Figure 7.5 shows the plotting of SK 27 (early *Homo* from Swartkrans) relative to the *Paranthropus* sample (SK 13/14, SK 16, SK 47, SK 48 cast, SK 49 cast, SK 98, SK 834, SK 837, SKW 11), while further information is detailed in Table 7.5.

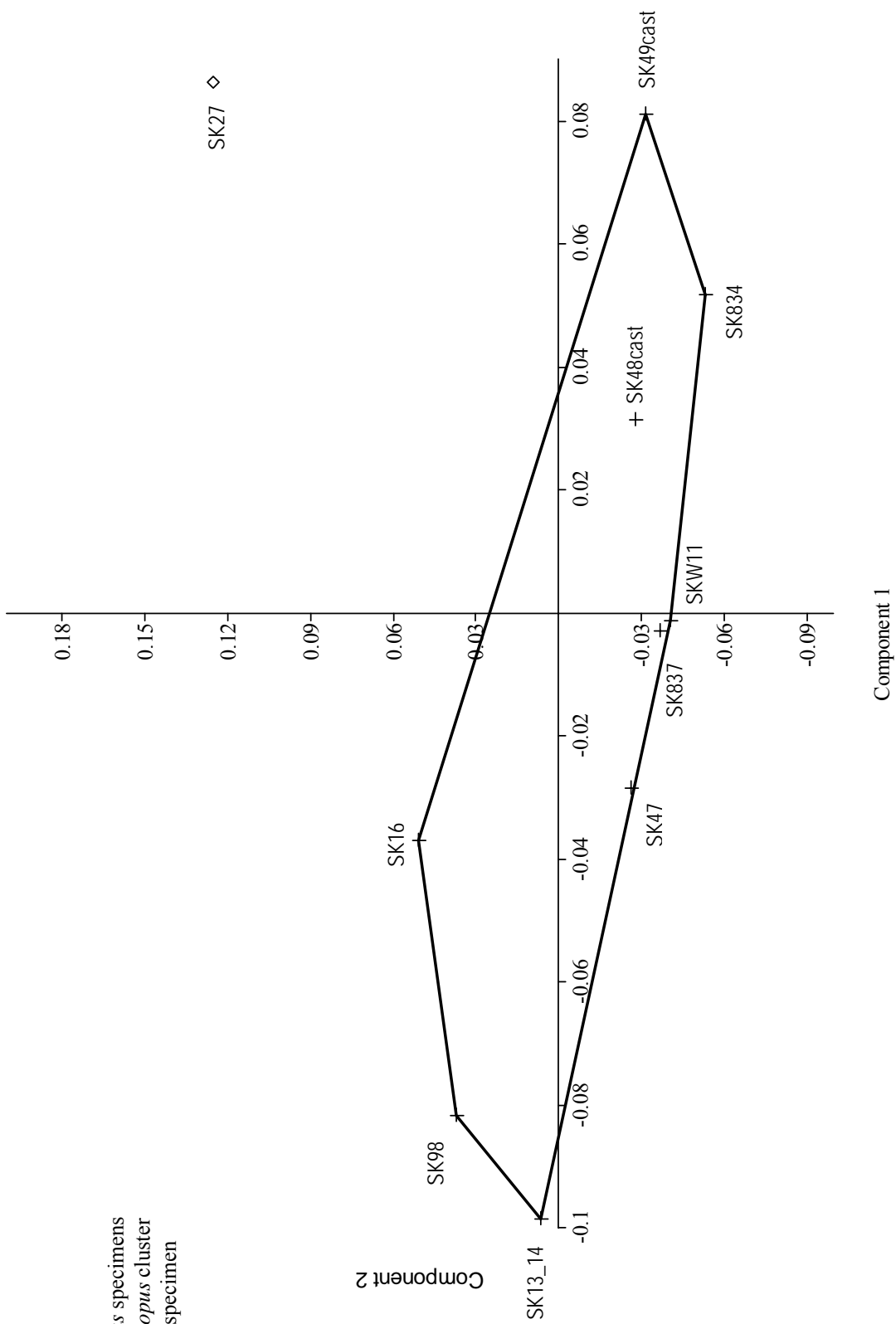


Fig. 7.6 – PCA: M² – *Paranthropus* and early *Homo*. Percentage of total variance explained from PC1: 32.55% and PC2: 19.14%

Table 7.5 – M². *Paranthropus*, (sample: SK 13/14, SK 16, SK 47, SK 48 cast, SK 49 cast, SK 98, SK 834, SK 837, SKW 11) and early *Homo* (sample: SK 27): eigenvalues and percentage of variance explained for all the PCs

	Eigenvalue	Percentage of total variance explained	Cumulative variance explained
PC1	0.004027369203	27.32	27.32
PC2	0.003108572351	21.09	48.41
PC3	0.0021757777	14.76	63.18
PC4	0.001527307564	10.36	73.54
PC5	0.001157255275	7.85	81.39
PC6	0.000917879037	6.23	87.62
PC7	0.000756039001	5.13	92.75
PC8	0.00060383203	4.09	96.84
PC9	0.00046542652	3.16	100.00

SK 27 is well distinct from the rest of M². However, the score of SK 27 on PC1 and that of SK 49 cast is approximately the same. Nevertheless, there is a good separation from the rest of the specimens of *Paranthropus* as well as a neat distinction on PC2.

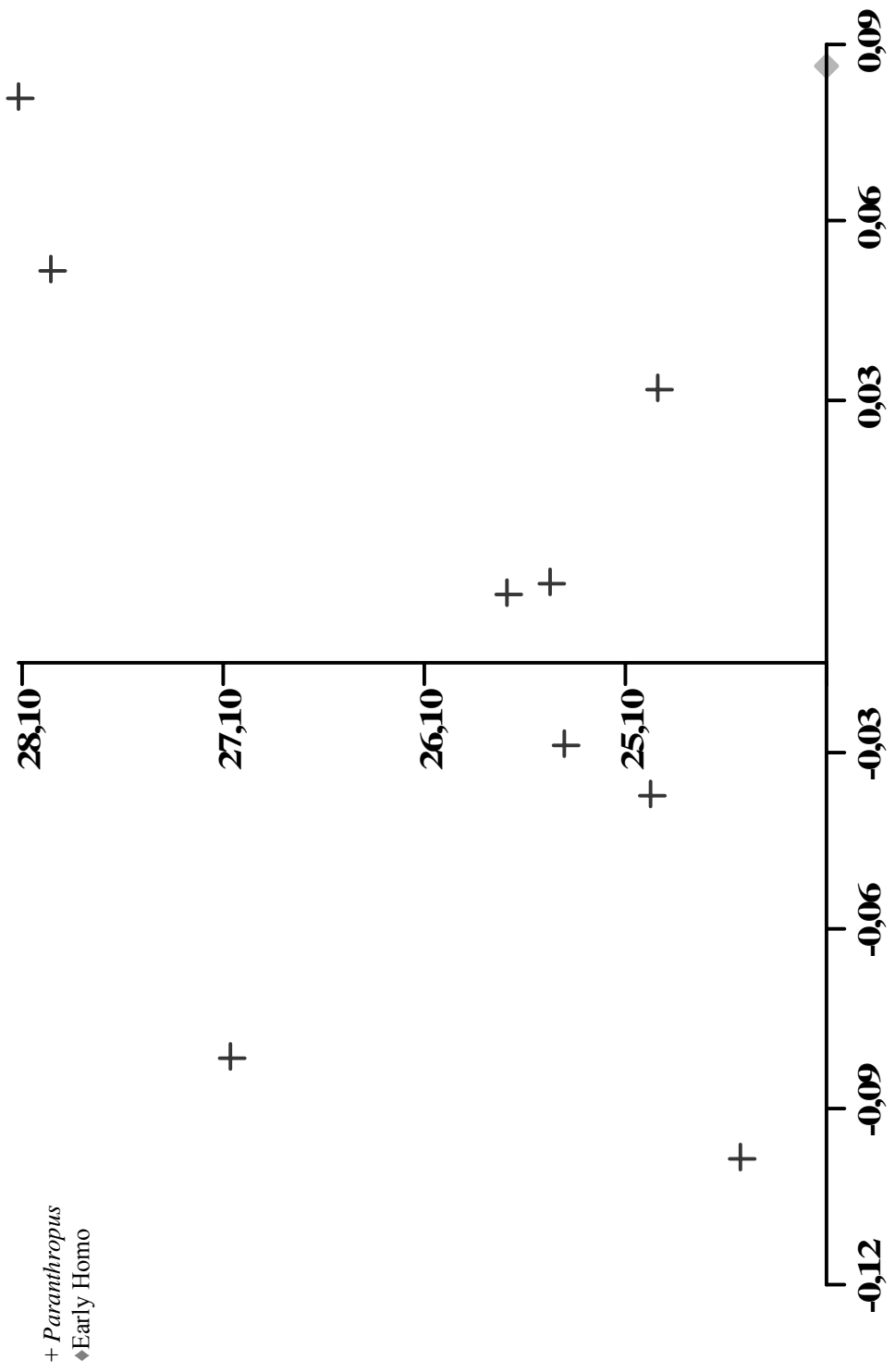


Fig. 7.7 – PCA: M² – Paranthropus and early Homo; PC1 against centroid size. No significant correlation between size and shape is shown (r = 0.23701; P = 0.50969)

Scores on PC1 vs. centroid size are plotted in Figure 7.7. This plot indicates that no convincing linear relationship between size and shape exists, thus an allometric trend is excluded.

In summary, the analyses performed at this stage of the research have demonstrated that the methods applied can discriminate between two taxa (*Paranthropus* and *Homo*) under study. Although there is not a sharp-cut separation on both PCs between groups, there is evident formation of diverse clusters between the specimens of *Paranthropus* and those of early *Homo* for both M¹ and M².

7.4 - Repeatability of the landmark collection

One of the major issue in an experimental study is the repeatability of the method applied, which must led, under the same conditions, to the same results when the data recording is repeated by the same investigator or by others. Repeatability is crucial for a procedure to be validated as a systematic method and it is tested by performing the sampling of the variables after certain temporal intervals and/or by means of different operators. The different data sets are then analyzed and the results compared in order to evaluate the intra- and inter-observer error. In traditional morphometrics, the issue of error assessment is straightforward: univariate analyses, first (see Dahlberg, 1926; Davemport, *et al.*, 1935; among the others), and multivariate analyses, later (Spielman, *et al.*, 1972; Jamison and Zegura, 1974; Jamison and Ward, 1993; White and Folkens, 2000) such as analysis of variance, canonical variates analysis and product-moment correlations

have been employed to assess intra- and inter-observer error. The major advantages of geometric morphometrics over traditional methods are the preservation of the full geometry of the biological object under study and the generation of a clear graphical output. Nevertheless, the observer-induced measurement variation of landmark configurations is difficult to assess and quantify. One of the causes of error in sampling landmark points is that self-assessment is rather difficult since coordinates are not as easily legible as distances. Moreover, type I landmarks represent a more straightforwardly detectable entity than type II and III landmarks (as discussed in chapter 4 – *Quantitative analysis of data from CT based techniques: Geometric morphometrics*), of more uncertain identification. However, different approaches have been applied for the evaluation of the inter- and intra-observer error (reviewed and integrated by Cramon-Taubadel, Frazier and Lahr, 2006).

Among those, the one that employs GPA was used in the present project (following O'Higgins and Jones, 1998; Lockwood, *et al.*, 2002; Viðarsdóttir, *et al.*, 2002; Harmon, 2007) for an empirical assessment of the impact of measurement error. In particular, the sampling was repeated for seven specimens from the M³ sample, preferred to M¹ and M² samples because taken as a whole it is in a better state of preservation, namely it is less worn. The seven pairs of landmark coordinate configurations were computed through GPA and PCA in order to evaluate the overall effect of error. The same analyses were performed using a sample composed of the seven pairs of repeats plus all the M³s.

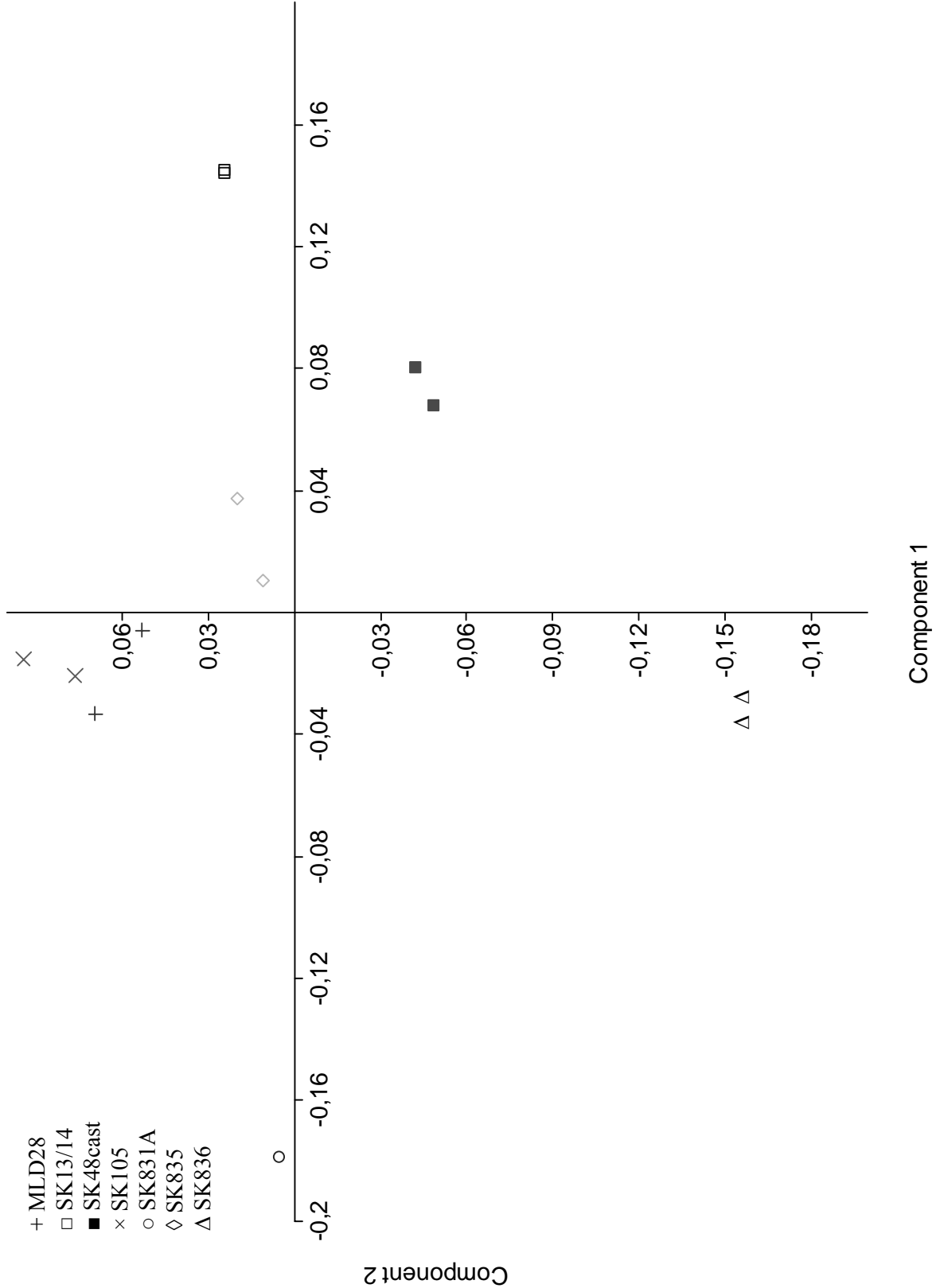
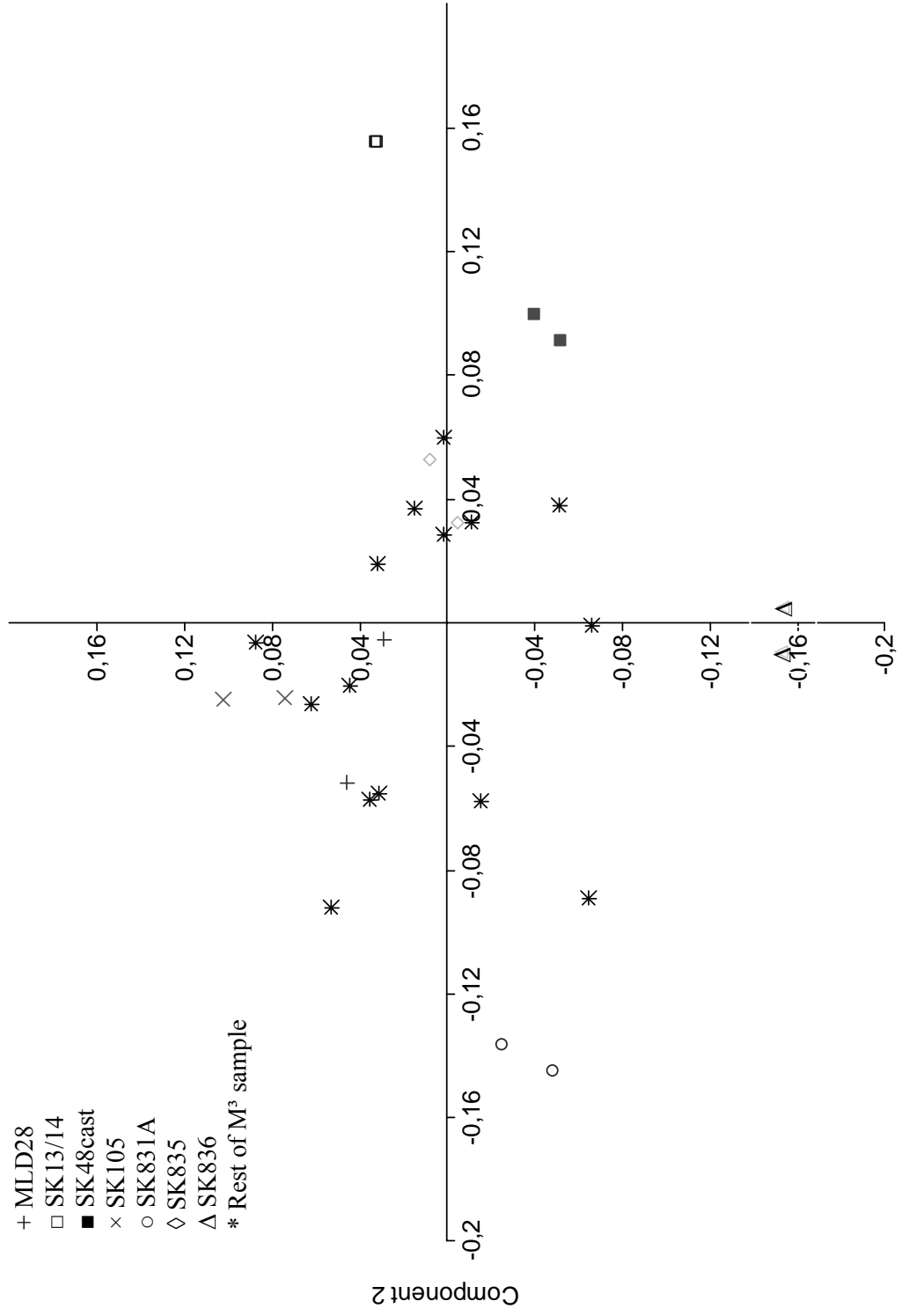


Fig. 7.8 – PCA: M³ – Repeatability test. The seven pairs of repeats are plotted together



Component 1
 Fig. 7.9 – PCA: M³ full sample – Repeatability test. The seven pairs of repeats are plotted together with the rest of M³ specimens

Figures 7.8 and 7.9 show that the two configurations related to the same individual cluster tightly in almost all the cases compared to the variation of the entire sample, and even overlap in the case of SK 13/14. However, in some instances the distance of the two pairs of landmark configurations of the same specimen seems to need further investigation. (as per MLD 28, SK 48 cast, SK 105, SK 831A).

Thus, the method of Euclidean distances was applied in order to ascertain whether or not the error recorded was significant. All the Euclidean distances between the three-coordinates sets of landmark were calculated and the threshold value between significant and not-significant error among all the Euclidean distances was identified at 0.15452 mm ($P < 0.05$). The Euclidean distances between each pair of repeats is smaller than that value, as shown in Table 7.6 and Figure 7.10, with the exception of the repeats of MLD 28 for which the sampling seems to be not accurate. This case will be discussed below.

Although the accuracy of the sampling was estimated using geometric morphometrics and the method of Euclidean distances, as is clear from what is illustrated above, these approaches do not allow for the assessment of the landmark-by-landmark displacement. In fact, GPA results are affected by the “Pinocchio effect” which distributes the difference of one or few landmark displacement/s over the whole set of landmarks. Instead, through the method of Euclidean distances it is possible to quantify the distance between configurations of landmarks taken as a whole, but it does not give indication of what landmark/s has/have caused it.

Table 7.6 - Euclidean distances between pairs of repeats in ascendant order. The threshold value between not significant and significant error is also indicated in bold. Only for the specimen MLD 28 the error is significant

Specimens	Euclidean distances
SK13_14	0.007116
SK48cast	0.047838
SK831A	0.061098
SK105	0.068967
SK836	0.074042
SK835	0.085851
Threshold value	0,15452
MLD28	0.17248

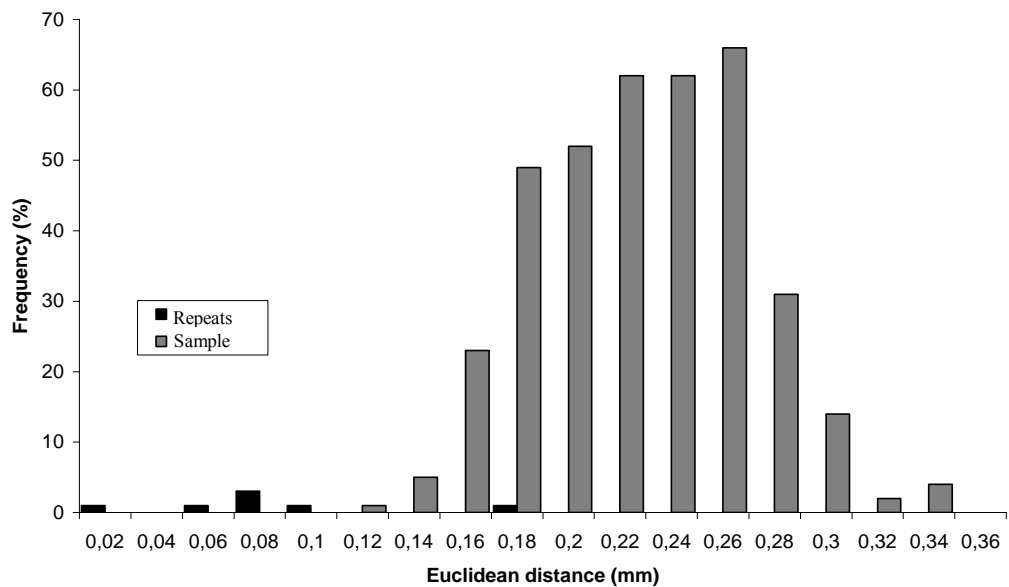


Fig. 7.10 – Results of the investigation of the Euclidean distances for the evaluation of intra-observer error. Most of the Euclidean distances between different individuals range between 0.18 mm and 0.26 mm, while the distances between repeats are smaller (≤ 0.1 mm) than any distance between different individuals, except in the case of one pair of repeats (MLD 28) in which reciprocal distance (0.18 mm) falls in the interval of confidence of the sample

For this reason, the major differences in distribution of landmarks between the two configurations were investigated through a visual inspection of the three-dimensional snapshots of teeth showing the landmarks collected (Figure 7.11: the cases shown are those of the specimens which show higher Euclidean distances, which is significant only in the case of MLD 28). It seems that an error in the sampling of P6 (Intersection between distal central groove and transverse groove) is recurrent (4 times / 5 cases reported), and this could be linked either to a less than rigorous definition of the landmark or to the nature of the landmark itself. Other landmarks that present a displacement are those on cusp tips (3 displacements, 2/3 on Pa); while in the case of SK 835 a crack on Pa could have caused confusion. The displacement of Pr and Pa cusp tips in the case of MLD 28 is quite evident. This could reflect the difficulty in sampling such landmarks where the tooth shows a moderate level of wear. As said elsewhere in this thesis (chapter 6 – *Methods*) when a certain degree of wear is present the summit of the cusp may appear as an area rather than a point (formed of one or few pixels).

In conclusion, it can be affirmed that the intra-observer error is unlikely to confound the discrimination of specimens in the sample while stressing that particular attention must be paid in the sampling of landmark where the specimen is affected by wear and/or damage in a region of interest.

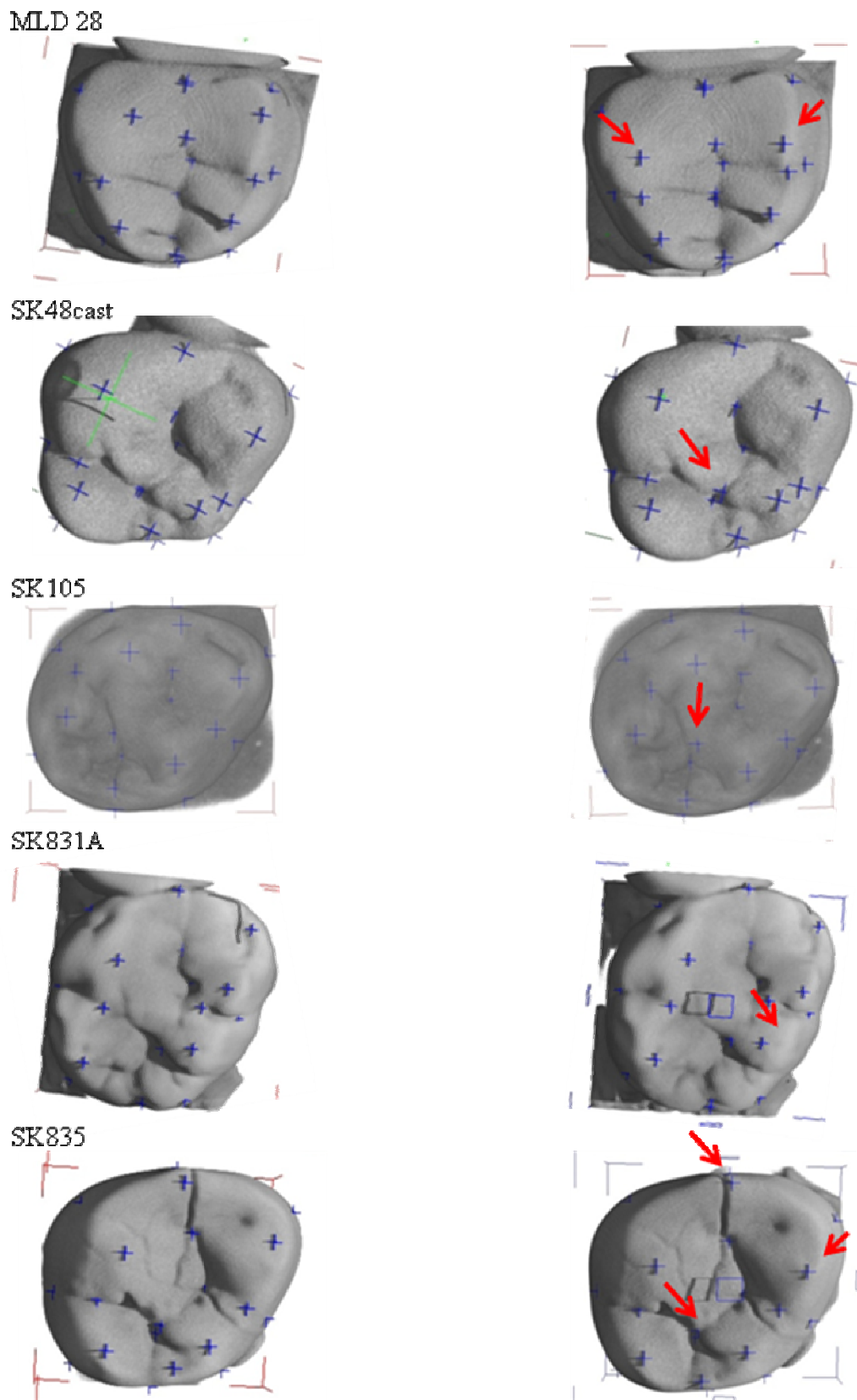


Fig. 7.11 – Pairwise comparison of the landmark configurations which show a difference in a visual inspection. The landmark displacement due to intra-observer error is shown in the images on the right (arrows). See the text for discussion. Images are not to scale

7.5 - Advantages and limitations

The experimentation carried out has demonstrated that the methods proposed in this project discriminate well between diverse hominid forms (namely *Paranthropus* and *Homo*) based on shape differences of the different genera. Therefore, the procedures applied are here judged as statistically valid and applicable to the study of hominid molar cusp morphology as a diagnostic feature for the assessment of their phyletic relationships. However, an extension of the range of applicability of the same methods to other tooth types or to the study of primates and other mammal tooth morphology in general is desirable, and further studies devoted to the testing of its validity are recommended.

Nevertheless, certain limitations of the methods used need to be stressed and problems that have arisen in various stages of the research must be discussed. (Problems and limitations related to the procedures for the collection of landmark data which were tested but not used for this project have already been discussed in chapter 6 - *Methods*).

7.5.1 - CT scan through the SANRAD facility, Necsca

As per their nature and technical characteristics (discussed in chapter 4 - *Advanced methods for the study of tooth morphology*), the CT scans obtained through the SANRAD facility at Necsca resulted in extremely suitable, high resolution three-dimensional models of the fossils under consideration. Even though this technique has led to extremely good results, some drawbacks are discussed as follows. One of the major limitations of the facility used is that it is not movable; therefore the sample had to be transported to the facility. This caused the fossils to be exposed to potential risks of damage, loss or theft, even

though circumstances and most of all the precautions used (detailed in chapter 6 - *Methods*) meant that each specimen was returned safely to its location.

Given the size of the sample studied, the scanning, reconstruction and visualization of the specimens resulted in very time-consuming procedures. Above all, in order to comply with the strict rules that regulate the loan of the fossils, the specimens had to be preferably collected and returned the same day. However, it would have been desirable to have them available later for finalizing the image reconstruction in order to ascertain the exact correspondence with the original specimens.

Another issue that has to be mentioned is that a few of the CT examinations performed were not successful. In the case of SK 49 the teeth were not well enough exposed to the X-rays due to the superimposition of other regions of the fossil itself. This precluded the possibility of reconstructing the tooth images, thus, as a way around this problem, casts of the teeth of interest were produced. In two cases the instruments had some temporary technical problems and produced data that could not to be correctly reconstructed. These specimens (Sts 22, Sts 52) were eventually not included in the statistical analysis since there was no opportunity to perform the scanning again, due to the paucity of time.

7.5.2 - Tooth orientation

The lack of a tooth orientation standard system causes measurements to be imprecise and data gathered by different authors to be not rigorously comparable. The issue of tooth orientation has been briefly dealt with in chapter 2 - *Traditional methods for the analysis of tooth morphology* with respect to the problems related to two-dimensional dental image analysis. Nevertheless, problems related to tooth

orientation have arisen in the case of this project as well, since the three-dimensional tooth image had to be oriented aligning the tooth major axes to those of the reference system (i.e. scene box).

There are two kinds of variables: those for which an orientation is not necessary since their value is not dependent on the position of the object in the space, and others that require a previous orientation according to certain criteria. The same is true in the case of the landmarks used in the present study: those detectable on the crown surface did not need previous orientation, while those positioned on the plane P1, namely the plane passing for the lowest point of the central fossa, did require an orientation in the space. However, the need for a re-alignment comes from the definition of the landmarks considered and from the technical features inherent in both the CT scan and the software for the image visualization (VGStudio MAX 2.1), rather than from the nature of the statistical analysis performed. The latter, in fact, through the process of normalization (i.e. rotation and translation) of the landmark configurations eliminates problems related to the position in the space.

However, the system used to orientate the tooth images presented some limitations due to two major aspects inherent in the nature of teeth. First of all, the cervical margin line is not regular. In addition to this, in several cases the cervix was partially or totally damaged or sometimes it was still under formation at the time of death. The procedure chosen, therefore, seems not to be completely adequate, as in several cases an alternative sampling had to be performed (namely, orientation on the base of three points instead of four and/or sampling of the landmark in the only trait of the cusp cervical margin available which did not

necessarily correspond to the point of contact with the adjacent cusp). However, other possibilities such as those mentioned below, were discounted because they were considered to be less satisfactory. For example, the orientation based on all or three of the major cusp tips (i.e. Pr, Pa and Me) would have led to a certain bias, since the sample did not present a uniform wear (ranging from unworn to moderately worn). Likewise, taking the buccal margin only as reference would have caused difficulties in the orientation of those teeth where that region is damaged or missing. In conclusion, the system used for the alignment of tooth images, also discussed and proposed by Benazzi (2007), but independently thought of in this study, is considered the best system that could be used with respect to the nature of the sample under analysis.

7.5.3 - Acquisition of landmark data through VGStudio MAX 2.1

VGStudio MAX 2.1 is high technology software which ensured a very accurate landmark collection. In spite of this, the identification of landmark points was not straightforward. Sometimes the impression that the observer has of tooth morphology can change according to the positioning of the image in the virtual space, namely according to its position respective to the source of a light introduced for better visualization. For this reason, each landmark was collected with reference to the inner surface as well, whilst looking simultaneously at one or more slice views in addition to the three-dimensional image.

Since the software used is very expensive, this operation was performed at Necsa, which kindly offered the use of their computer lab for the purposes of this research, when the alternative was to use much less sophisticated “freeware” software for the visualization of three-dimensional images. This fortunate

situation led to the acquisition of very reliable data. However, the fact that the image reconstruction had to be performed at Necsa made the landmark collection more difficult, because it would have been desirable to look at the original specimens. For reason of safety the fossils could be transferred at Necsa for the scanning only, as already discussed.

Moreover, even though the resolution offered by the SANRAD facility made it possible to obtain extremely good results, a higher resolution such as that possible with a micro-focus X-ray tomography system (spatial resolution of $\sim 1\text{-}5\ \mu\text{m}$) - which hopefully will be available at Necsa in the future - is recommended for further complementary studies. In fact, a better resolution would help in the identification of certain landmarks, such as cusps tips especially in the case of worn teeth, where those landmarks are often represented by an area, rather than a single pixel.

Problems related to the technical properties of the software were also present. It happened that the procedure of grey scale calibration, required for the subsequent step of coordinates sampling, caused the tooth three-dimensional image to fade away (specimen Stw 447). It happened sometimes that the whole set of landmarks collected turned out to be displaced with respect to the original positioning on the tooth surface. In this case the sampling had to be performed again. One of the limitations of the software with respect to the purposes of this particular study lies in the properties of the measuring tool, which connects and measures the distance between two points as shown in Figure 7.12. In view of the fact that the measuring tool cannot be shifted, therefore, it had to be re-positioned for each of the numerous attempts to identify the most projecting points on the cusp's outline.

7.5.4 - Analysis of landmark data

It is inherent in geometric morphometric techniques that the set of landmark coordinates analyzed must be complete, where the null values are not accepted. This caused some of the specimens to be excluded from the sample even in the

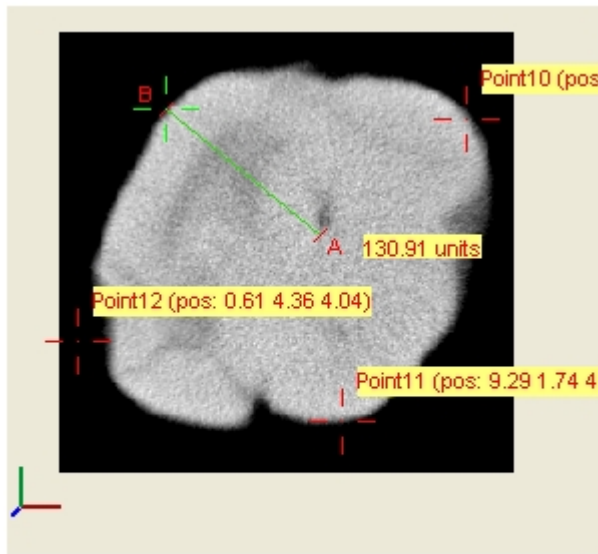


Fig. 7.12 – Axial view of a virtual image showing the measuring tool of VGStudio MAX 2.1 software, namely the line connecting points A (fixed end) and B (free end)

case of GVH-2 and SKW 14 where only one landmark was missing.

The software utilized to perform the geometric morphometric analysis is very user-friendly and is the only one available at the moment that allows for the analysis of sets of three dimensional coordinates visualizing the results through

plots and TPS grids. In spite of this, some of the properties of *Morphologica* are rather basic, thus the operation of editing and labeling of plots would have resulted in a very time-consuming and repetitive procedure. For this reason, the graphs were produced using *PAST* software.

7.6 – Final remarks

The methodological procedures conceived for this project have been demonstrated to be scientifically valid. Moreover, it has been proved that these methods can be successfully applied for further analyses aimed at investigating the morphological

variation of hominid dentition and therefore, their taxonomic affinities. However, it is recommended that further analysis will be done in order to verify the strength of the method when dealing with different species belonging to the same genus. Other primate taxa can be included in the sample as an outgroup provided that the sample available is sufficiently big (at least 15-20 specimens per tooth typology). Since for most of the hominid taxa the fossil record is sparse, and there is no general consensus on the taxonomic attribution, chimpanzee (*Pan paniscus* and *P. troglodytes*) seems to be the most suitable outgroup to extend and improve this project. Nevertheless, other primates could be considered such as baboons (the extinct *Theropithecus oswaldi* and the living *T. gelada*) or other species among the family Cercopithecidae.

In the light of what was discussed in the present chapter, it is also recommended that, under optimal conditions, the sample used would be composed of unworn and undamaged specimens, where originals are preferred to casts. Moreover, scanning isolated teeth presents the advantage of avoiding the occurrence of beam attenuation through fossilised bone and/or matrix, though teeth *in situ* can be more readily classified.

Moreover, it would be desirable to perform the reconstruction of the images and landmark sampling, whilst looking at the original fossil for comparison, thus avoiding the possibility of misinterpretations of the features observed on the three-dimensional images.

CHAPTER 8

RESULTS

8.1 - Introduction

The experimentation carried out has demonstrated that the methods outlined in this project are suitable for a study with the aim to investigating the morphological relationship between the South African hominid forms taken into consideration for this project. In this chapter, the statistical analysis will focus on the assemblage from Sterkfontein Member 4 in order to test the single-species null hypothesis. In this stage of the research, teeth from various sites are considered, including individuals of *A. africanus s.l.* from Makapansgat (MLD28; in the case of M³) beside the specimens from Sterkfontein Member 4, and *Paranthropus* from Kromdraai (for all tooth typologies) and Cooper's Cave (for M²) together with those from Swartkrans. Furthermore, the individual StW 151 from Sterkfontein was also included in the M¹ and M² samples.

The distributions of the full samples of M¹, M² and M³, and of the M¹ + M² joint spatial configurations are investigated separately. The plots showing the variance along PC1 (horizontal axis) and PC2 (vertical axis) are here reported and discussed (Figures 8.2, 8.5, 8.8 and 8.13). The third principal components (variance explained for M¹: 11.14%; M²: 9.94%; M³: 12.90%; M¹ + M² 13.69%) were also analyzed but did not add suitable information to what already observed for PC1 and PC2.

Those individuals from Sterkfontein Member 4 that are elsewhere considered as belonging to a further species than *A. africanus* (Clarke, 1988; 2008; and personal communication; individuals: Sts 1, Sts 8, StW 183, StW 188, StW 189, StW 252, StW 280, StW 450, StW 498a) and indicated here as “second species” were differently labeled from those that are here considered as *A. africanus* (*s.s.*) (individuals: Sts 57, StW 179, StW 402, StW 447, TM 1511), as shown in the notes accompanying each plot. Where there was an uncertainty in the species attribution (with reference to Clarke, 1988; 2008; and personal communication; individuals: Sts 24a, Sts 37, Sts 56, StW 204, StW 530), the specimens were labeled as *A. africanus*. Since we are testing the hypothesis of the occurrence of a new australopithecine species, as mainly proposed by Clarke we accept the taxonomic classification of the specimens from the *Australopithecus*-bearing sites, as per Clarke’s attribution (1988; 2008; personal communication). This approach is justifiable by the well distinct dental morphology observed within the Sterkfontein Member 4 and by the nature of the systematic topic of this research.

The visualization of variance along PCs was done using the animation features (wire frame images) of *Morphologika* software suite to morph the mean shape along the axes. This visualization technique relates variation along any chosen PC to a deformation of the mean shape. Thus, the mean shape is deformed in a way such that it comes to adopt the shape with score 0 on all PCs except the one under investigation. The wire frame images are very informative and give an immediate impression of shape variation since they approximately delineate the crown morphology. In particular the occlusal and buccal views of the wire frame images representing the mean shape of each subsample, and the mean shapes at the

positive and negative extremities of PC1 and PC2 are provided (Figure 8.2 for M¹, Figure 8.6 for M² and Figure 8.10 for M³).

The scores of individuals on each PC against centroid size are also observed with the aim to investigating any possible allometric trend within the sample. Only the plots of PC1 against centroid size are shown below, since for none of the other PCs a significant correlation between shape and size was found (Figure 8.3 for M¹, Figure 8.7 for M² and Figure 8.11 for M³). However, a further investigation on allometry was conducted through a correlation test between the centroid size and the GPA scores, as discussed for each tooth typology.

Moreover, for the individuals represented by both M¹ and M², the geometric morphometric analysis of the joint landmark configurations was performed; thus, the first two molars of certain specimens were considered as a single object. Any other possible combination (e.g. M¹ + M³, M² + M³; M¹ + M² + M³) was not considered for the paucity or absence of cases within the sample. In this case, the visualization features representing the occlusal and lingual views are shown.

8.2 – First molars

Figure 8.1 shows how the first two PCs account for a similar amount of variance (where their scores range from -0.08 to +0.13 for PC1 and from -0.12 to +0.09 for PC2) as it is also reflected from the percentage of total variance explained (PC1: 22.65%; PC2: 19.09%). PC1 quite well separates *Paranthropus* from the rest of the sample, whilst PC2 seems to discriminate *Paranthropus* and the “second species” from *A. africanus* and early *Homo*. Thus, looking at the plot four main groups corresponding to the four hominid forms considered are distinguishable,

although there is a partial superimposition between *A. africanus* and early *Homo*. On the contrary, there is quite a neat separation between the specimens considered as *A. africanus* and those considered as “second species”. *A. africanus* is also well distinct from *Paranthropus* with the only exception of Sts 57 which falls within the range of variation of *Paranthropus* (however, it must be noticed that this tooth is characterized by a moderate wear and presents matrix-filled cracks). The “second species” appears on the plot as it extends the range of distribution of *Paranthropus* toward the negative values of the horizontal axis (conversely, StW 450 is within *Paranthropus* specimens), whilst they overlap to a great extent along PC2.

The wire frame images (Figure 8.2) show that the morph along PC1 changes from the positive to negative scores from a square profile of the crown (as it can be described from the landmark collected) towards a more mesiodistally elongated one. At the same time, there can be observed a remarkable cusp height reduction and a shift of the cusp tips toward the buccal side except for Hy tip which moves toward the palatal side. Along PC2 as well, a variation in cusp height (which decreases towards the positive scores) plays an important role in determining the change of the morphs, with the mesial cusps principally involved. Another remarkable change occurs with regard to the cusp tips, which mutual distances increase when moving from negative to positive scores.

Plotting each PC against the centroid size, no allometric trend was found as shown by the plot of PC1 versus centroid size in Figure 8.3. Subsequently, a linear correlation between the centroid sizes and GPA residuals for all the landmarks were performed. A significant correlation was found for some landmark

coordinates as reported in Table 8.1 and illustrated in Figure 8.4. The visualization features suggest that the major changes in relation to the increase of size, in the case of first molars, is represented by a bigger distal cusps height at their distal portion, which include the deepest point of distal fossa, as well (points 5z, 8z, 9z and 17z are farther to point 18z). Moreover, the highest point of distal margin shifts mesialwards (coordinate 18x) so that the slope between P18 and P5 is slightly less steep. P15 (y coordinate), which is located between Pr and Pa, shifts towards Pa, making Pr slightly bigger and Pa smaller.

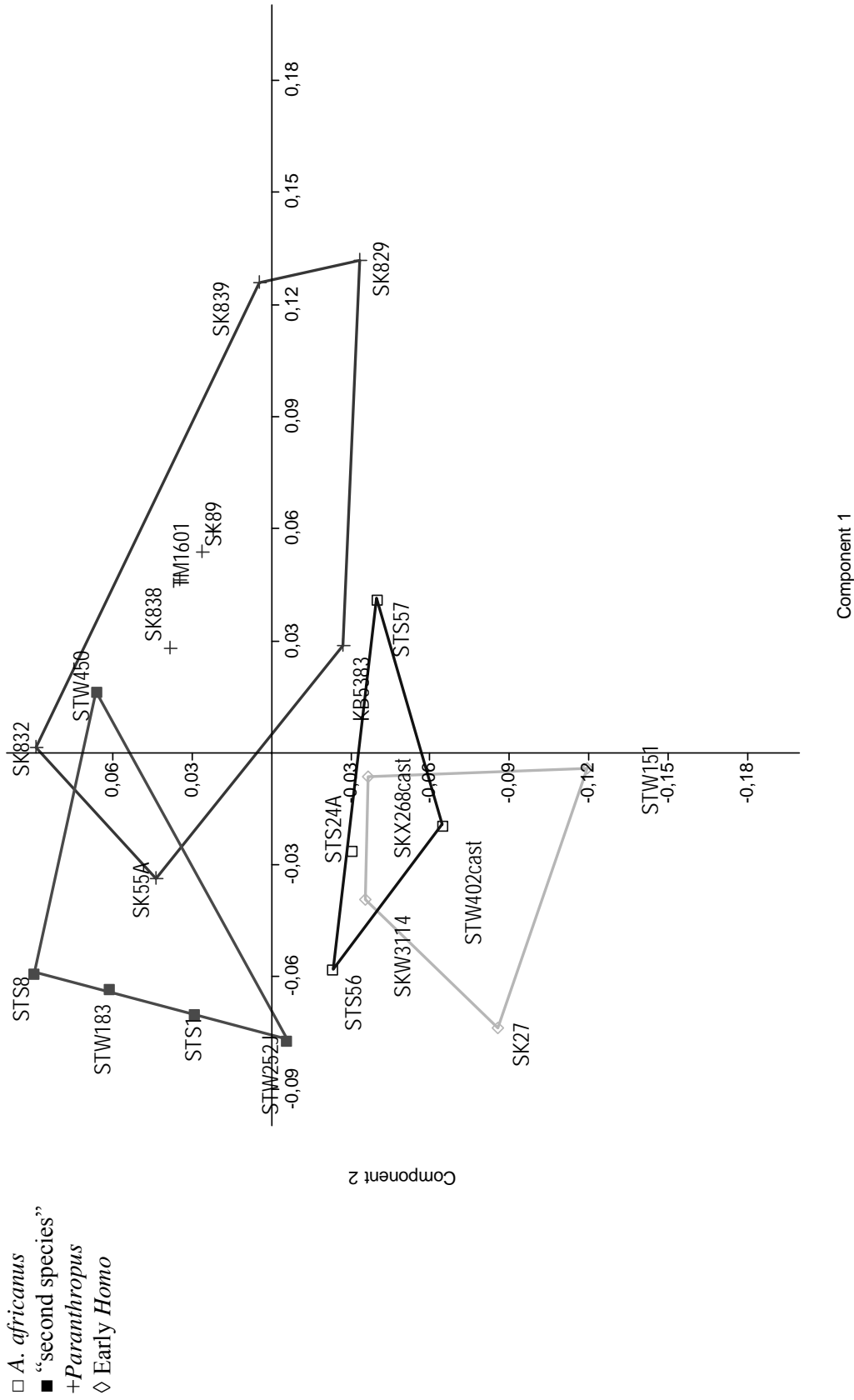
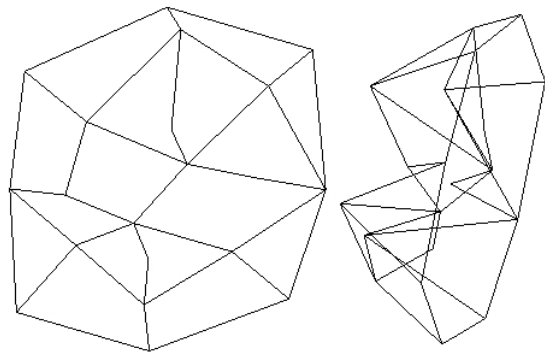
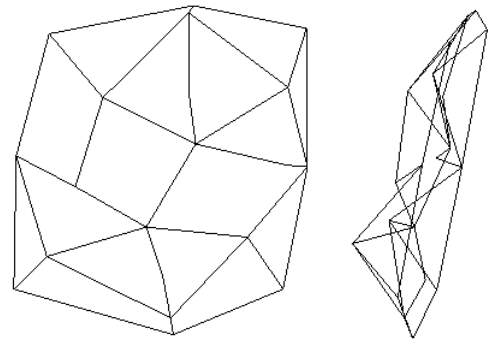


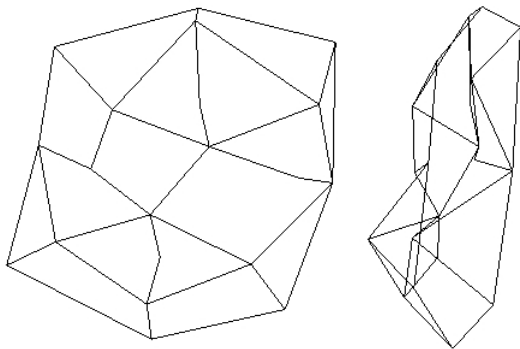
Fig. 8.1 - PCA: M¹ - Full sample. Percentage of total variance explained: PC1 22.65% and PC2 19.10%



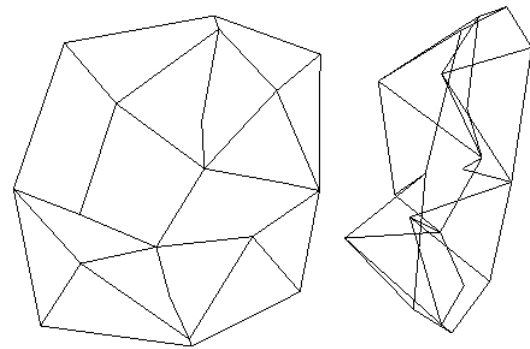
PC1 score +0.13



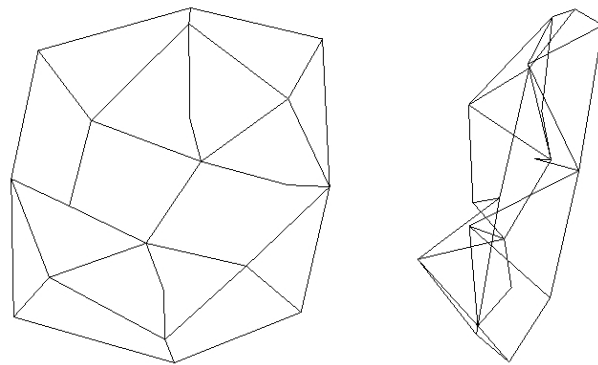
PC1 score -0.8



PC2 score +0.9



PC2 score -0.12



Mean shape

Fig. 8.2 – Wire frame images (as built from *Morphologika* software) showing the mean shapes of the first molars at the extremes scores for PC1 (top line) and PC2 (middle line) as well as the mean shape (bottom line)

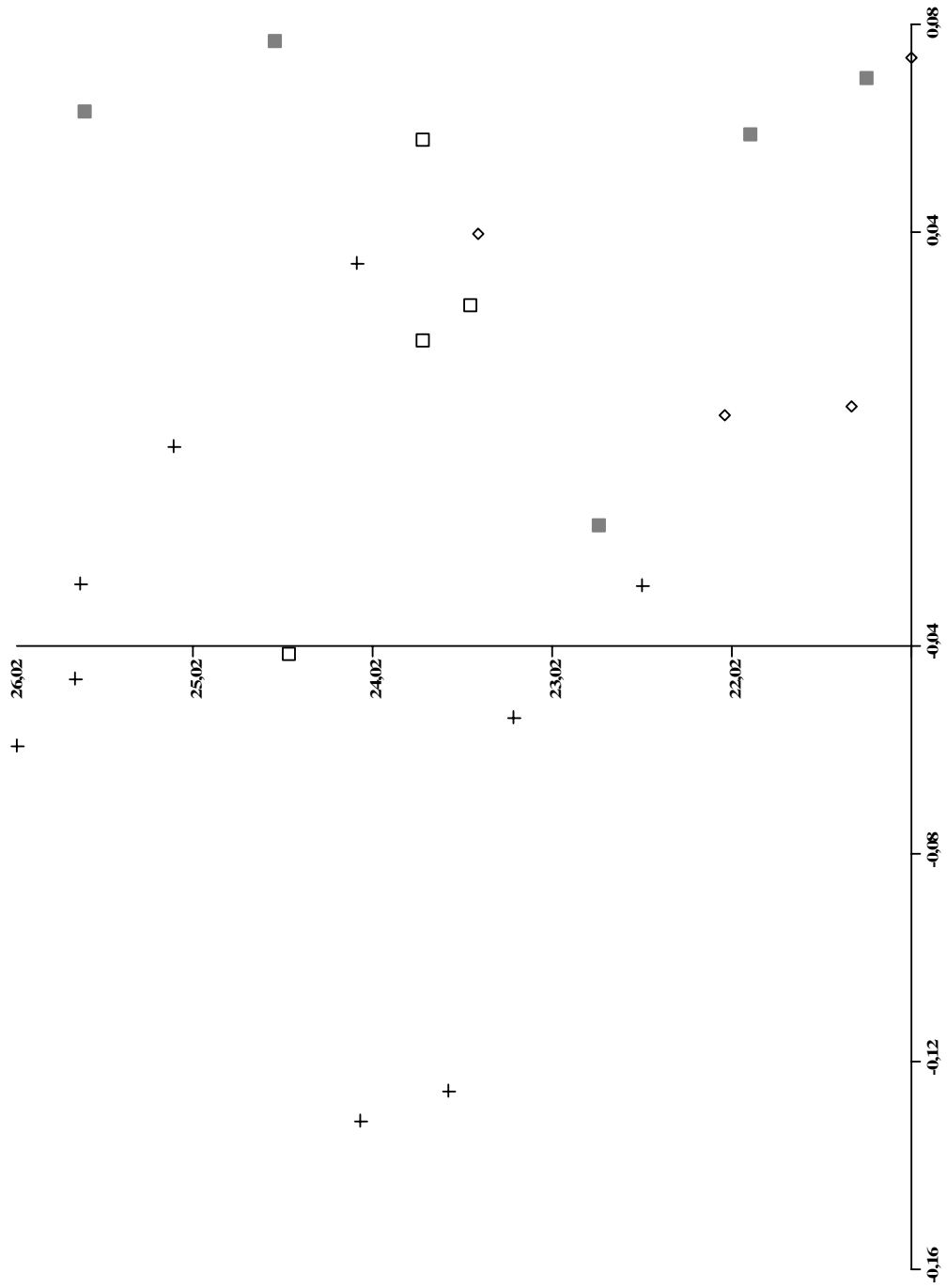


Table 8.1 – Significant linear correlations between centroid size and landmark coordinate for first molars

Landmark coordinate	P
5 z	0.0062721
8 z	0.044338
9 z	0.0048842
15 y	0.037235
17 z	0.039694
18 x	0.00075299
18 z	0.0044768

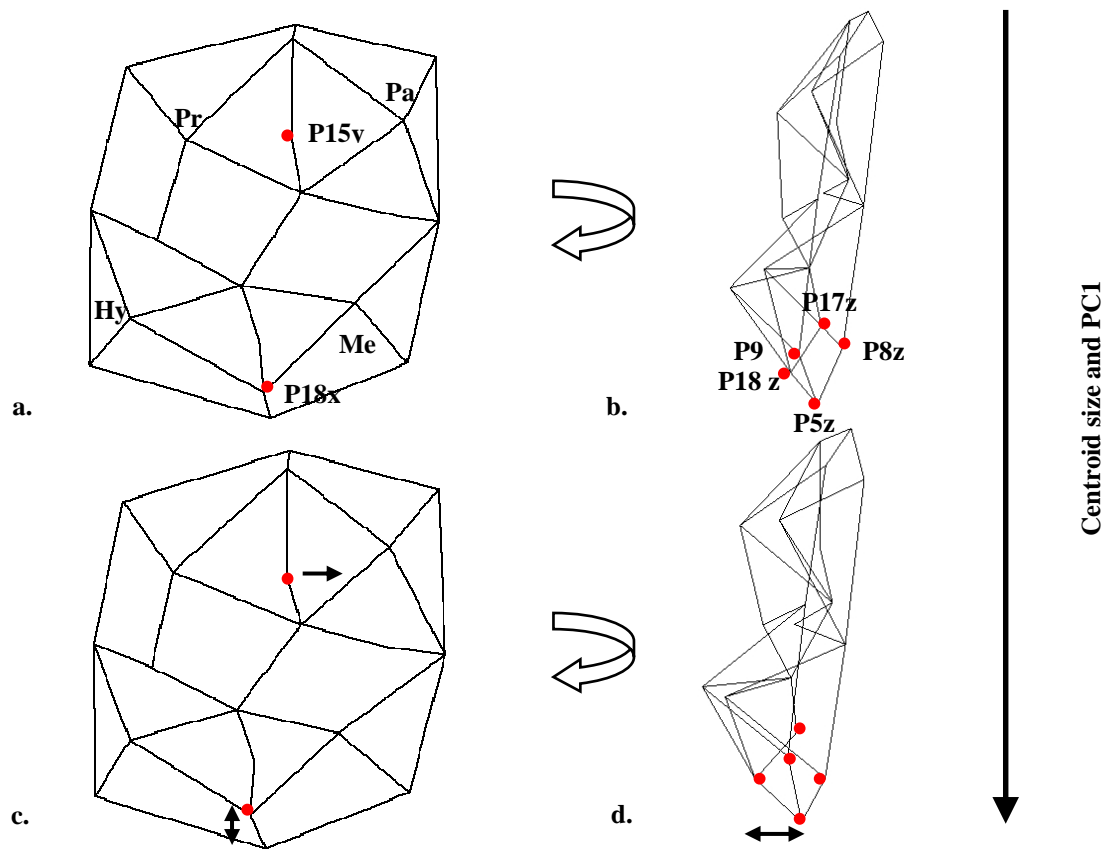


Fig. 8.4 – Morphing along the regression line of centroid size and PC1 for first molars. Red dots represent the landmark coordinates that vary from a. and b. (occlusal and buccal views of the morph for the lowest values of the variables), and c. and d. (occlusal and buccal views of the morph for the highest values of the variables). The black arrows illustrate the direction of the landmark displacement. Further information is provided in the text

8.3 – Second molars

Figure 8.5 shows the distribution of the full sample of second molars along PC1 and PC2. PC1 explains 24.18% of the total variance and separates early *Homo* from the rest of the sample. As per M¹, the range of distribution of *Paranthropus* is quite wide, especially along PC1 (scores -0.06 to +0.05 on -0.11 to +0.12 total variance). *A. africanus* and the “second species” plot at the two extremities of this distribution, and only partially superimpose with *Paranthropus*. Thus, *A. africanus* and the “second species” are neatly separated from each other.

PC2, which explains only 15.15% of variance, distinguishes early *Homo* from all the others, while the rest of the sample is not discriminated.

The visualizing features help describing the morphological changes that occur along the first two PCs (Figure 8.6). The mean shape at the highest negative score of PC1 is characterized from expanded distal cusps with respect to the mesial cusps. Their relative dimensions are remarkably reversed at the positive extremity of horizontal axis. Simultaneously, central fossa becomes smaller and all cusp tips appear closer to each others, or, in other words, they are closer to the centre of the crown. Major changes along PC2 occur at level of general shape of the crown, which is a mesio-distally elongated rectangle at the most negative score and progressively becomes a bucco-lingually elongated rectangle at the most positive score. At the change in general shape seem to contribute all four cusps, although distal cusps also remarkably vary in their cusp height, whilst mesial cusps show mainly a variation in their profile as seen in occlusal view. To the change in each cusp outline (as described by the wire frame images) from mesio-distally to bucco-lingually elongated, it corresponds also a different position of cusp tips. In

particular, morphing from negative to positive scores of PC2, Pr cusp tip shifts buccalwards; Pa and Me cusp tips shift distalwards; Hy cusp tip shifts lingualwards. In summary, mesial cusp tips are closer to each others and the central fossa results to be narrower, whilst the distance between distal cusp tips becomes bigger.

It exist a not very strong correlation between size and shape for PC1 ($P = 0.043116$) as shown in Figure 8.7. Thus, the small teeth have a mesio-distally elongated profile of the crown, whilst big teeth have a bucco-lingually elongated crown. Investigating this correlation more in detail through a linear correlation of centroid size and GPA residuals for all the specimens in the sample (Table 8.2 and Figure 8.8), the landmark coordinates which are significantly involved in the shape transformation are identified. These points mostly corresponds to landmarks that are located between cusps (P2 between Pr and Hy and P3 between Pa and Me both on plane P1; P14 between Pr and Pa on mesial margin; P17 between Me and Hy on distal margin) and represent sort of joints between cusps. Previous description of wire frame images for second molars emphasized the role of cusp's change in determining the general transformation observed along PC1. On the contrary, this analysis put the stress on those points which serve as pivots between cusps. P8 (x coordinate) is also significantly correlated to size: it shifts buccalwards with size increase, making of Me a more laterally reduced cusp, the profile of which tends to have a straight margin.

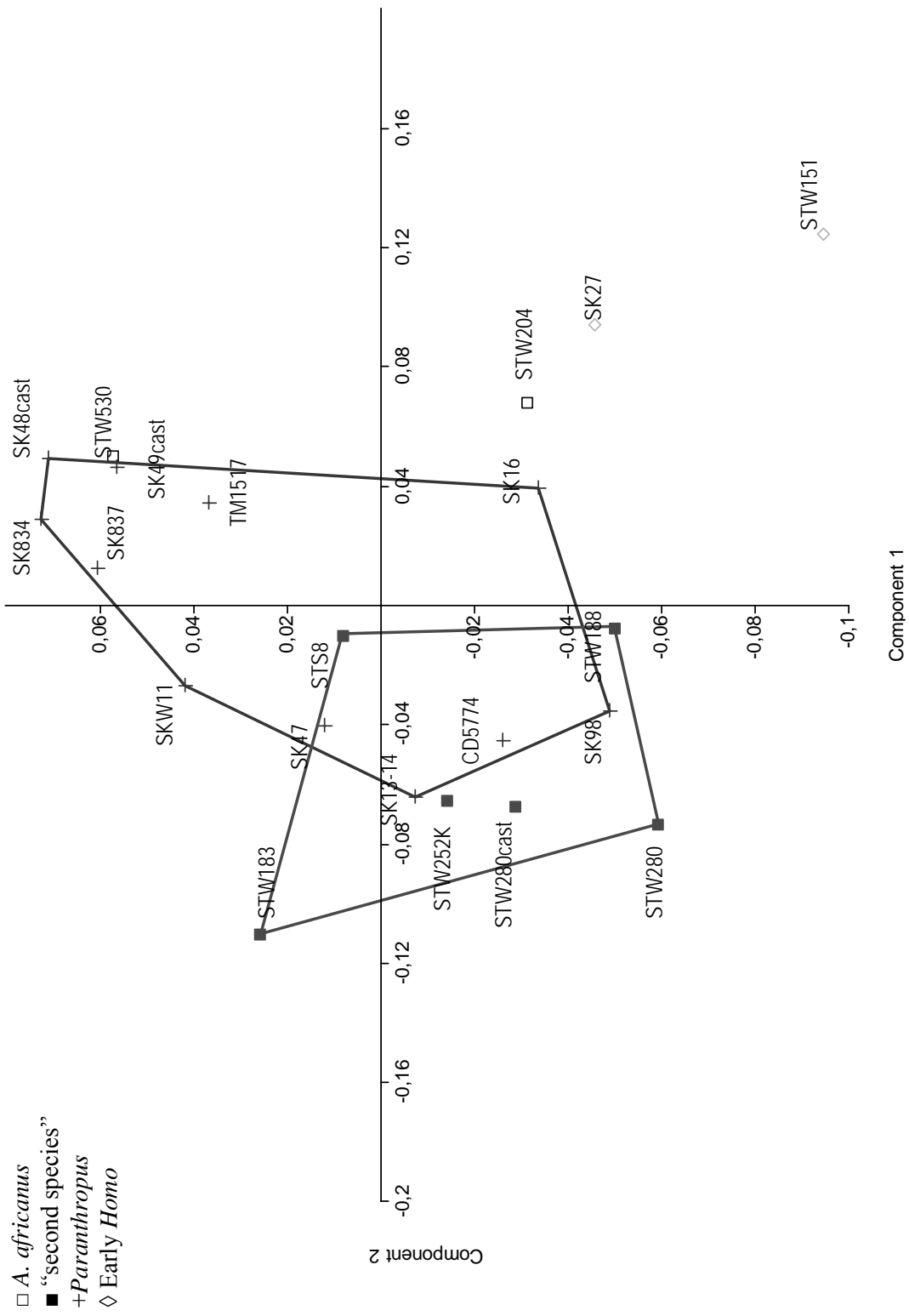


Fig. 8.5 - PCA: M² – Full sample. Percentage of total variance explained from PC1: 24.18% and PC2 15.15%

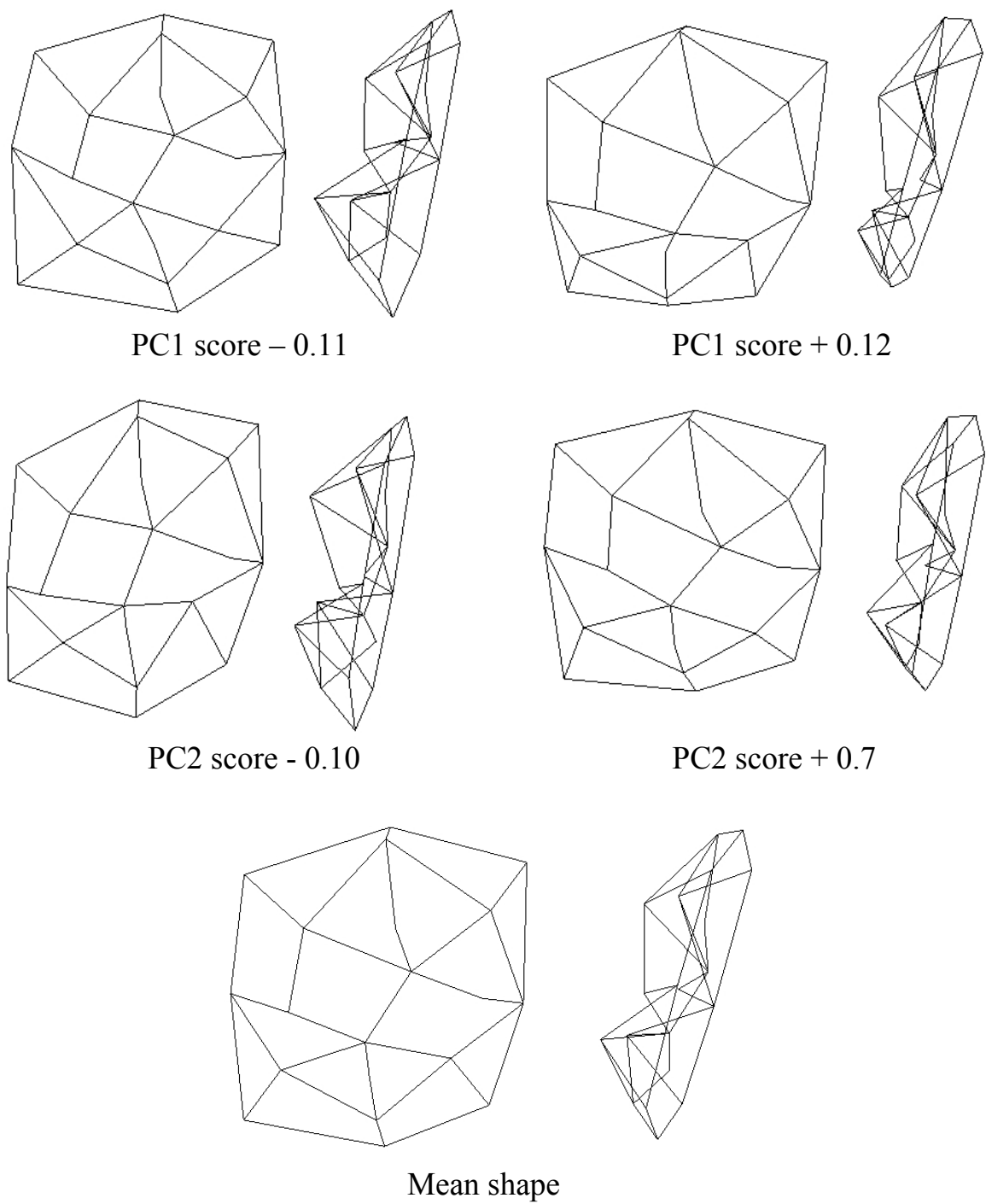


Fig. 8.6 – Wire frame images (as built from *Morphologika* software) showing the mean shapes of the second molars at the extremes scores for PC1 (top line) and PC2 (middle line) as well as the mean shape (bottom line)

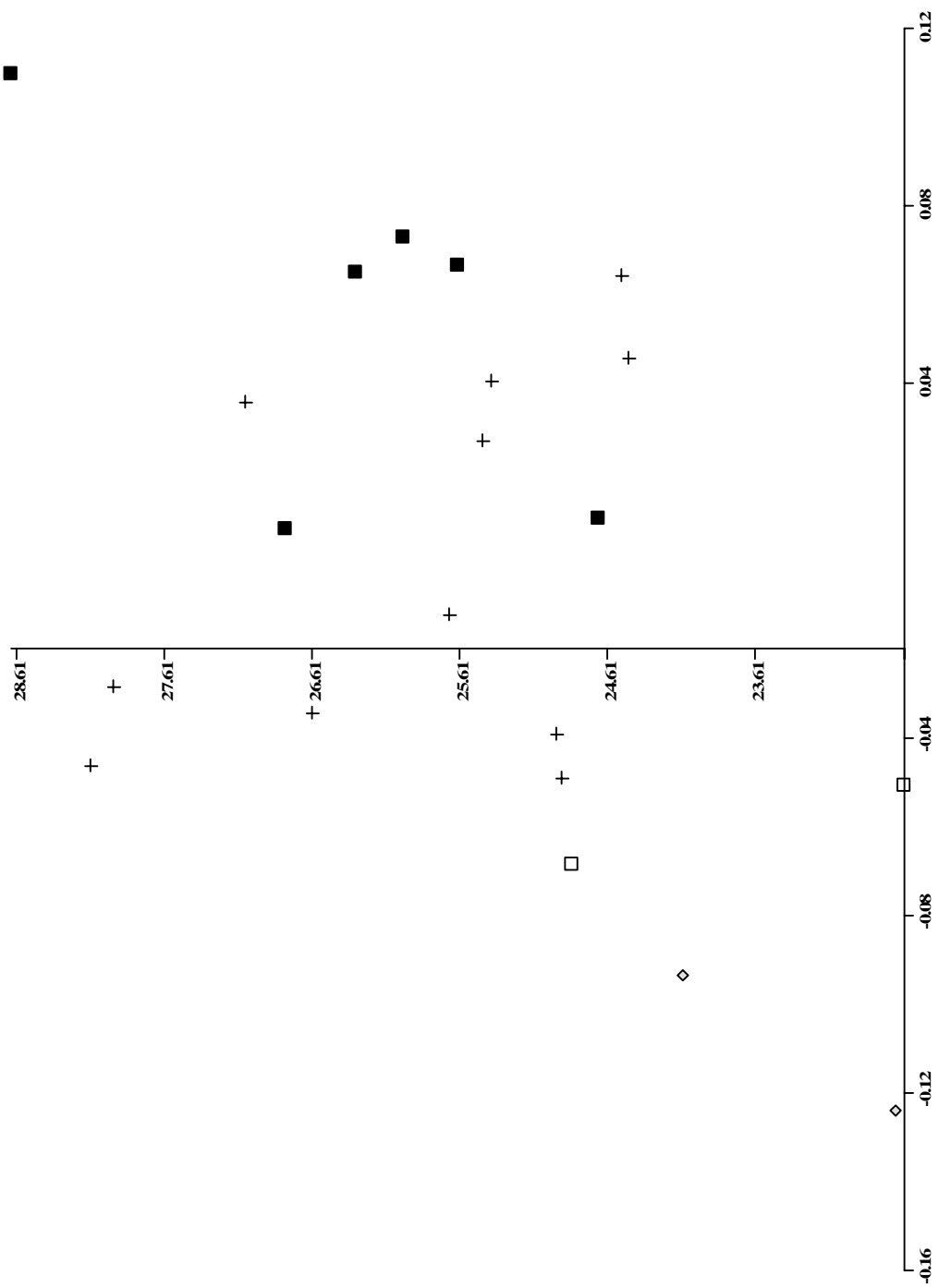


Table 8.2 – Significant linear correlations between centroid size and landmark coordinate for second molars

Landmark coordinate	P
2 x	0.018181
2 z	0.022677
3 x	0.00075445
8 x	0.041366
14 x	0.033634
17 y	0.038801

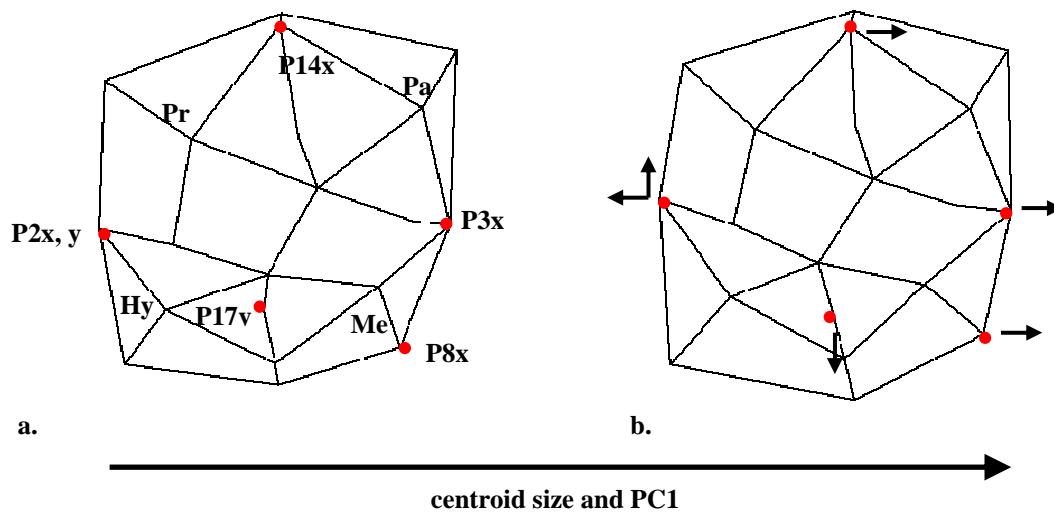


Fig. 8.8 –Morphing along the regression line of centroid size and PC1 for second molars. Red dots represent the landmark coordinates that vary from a. (occlusal view of the morph for the lowest values of the variables) and b. (occlusal view of the morph for the highest values of the variables). The black arrows illustrate the direction of the landmark displacement. Further information is provided in the text

8.4 – Third molars

Figure 8.9 report the results of PCA on third molars. The variance expressed is greater compared to that of first and second molars, where PC1 scores range from -0.16 to +0.12 and PC2 scores range from to -0.11 to +0.14.

In the case of M³ the picture presented is less clear as it is that illustrated for M¹ and M². Along both PC1 and PC2 there is a superimposition of the specimens belonging to the different forms, although *Paranthropus* show a wider distribution on the plot, whilst *A. africanus* and the “second species” mainly set in the two quadrants with positive values of the horizontal axis.

The separation between the latter two forms is not very clear. However, with a certain approximation it can be said that the “second species” is positioned toward the positive values of PC2 where the bulk of the *Paranthropus* specimens are, whilst *A. africanus* is placed more toward the negative part of the vertical axis. Nevertheless, there are two remarkable exceptions. One is represented by StW 489A which presents a certain degree of deformation due to a crack across the lingual cusps with consequent shifting of their lingual portion with respect to the rest of the crown. The other, Sts 37, is one of the teeth labelled as *A. africanus* but of uncertain attribution (according to Clarke, personal communication).

The morphological variation along the first two axes is represented through the visualization features of *Morphologika* software (Figure 8.10): along PC1, third molars' general outline changes from a bucco-lingually elongated shape (negative scores) to mesio-distally elongated rectangle (positive scores). The shape for negative scores does not approximate a rectangle since the mesial cusps are remarkably bigger than the distal cusps, and especially Me is particularly laterally

reduced. The central fossa width decreases from negative to positive scores and so does the cusps' height. Along PC2, the morph changes from a bucco-lingually elongated rectangle (negative scores) to a mesio-distally elongated pentagonal shape (positive scores), in which the distal cusps are bigger than the others. Between the distal cusps, the Hy presents a major reduction, although that is not as marked as in the morph at the negative extremity of PC1; distal cusps remarkably reduce in height, as well.

The linear correlation analysis does not show a significant correlation between size and shape for all the PCs (Figure 8.11 shows the plot of centroid size against PC1). Investigating the allometric trend in detail, only few variables were highlighted as those correlated to size, as reported in Table 8.3 and illustrated in Figure 8.12. They seem to reflect a positive correlation between size and mesial cusps' height. A shifting of P17 (deepest point of distal fossa) towards the lingual side, seems to indicate a different relation between the distal cusps: in particular, a reduction of Hy correlated to an increased general size.

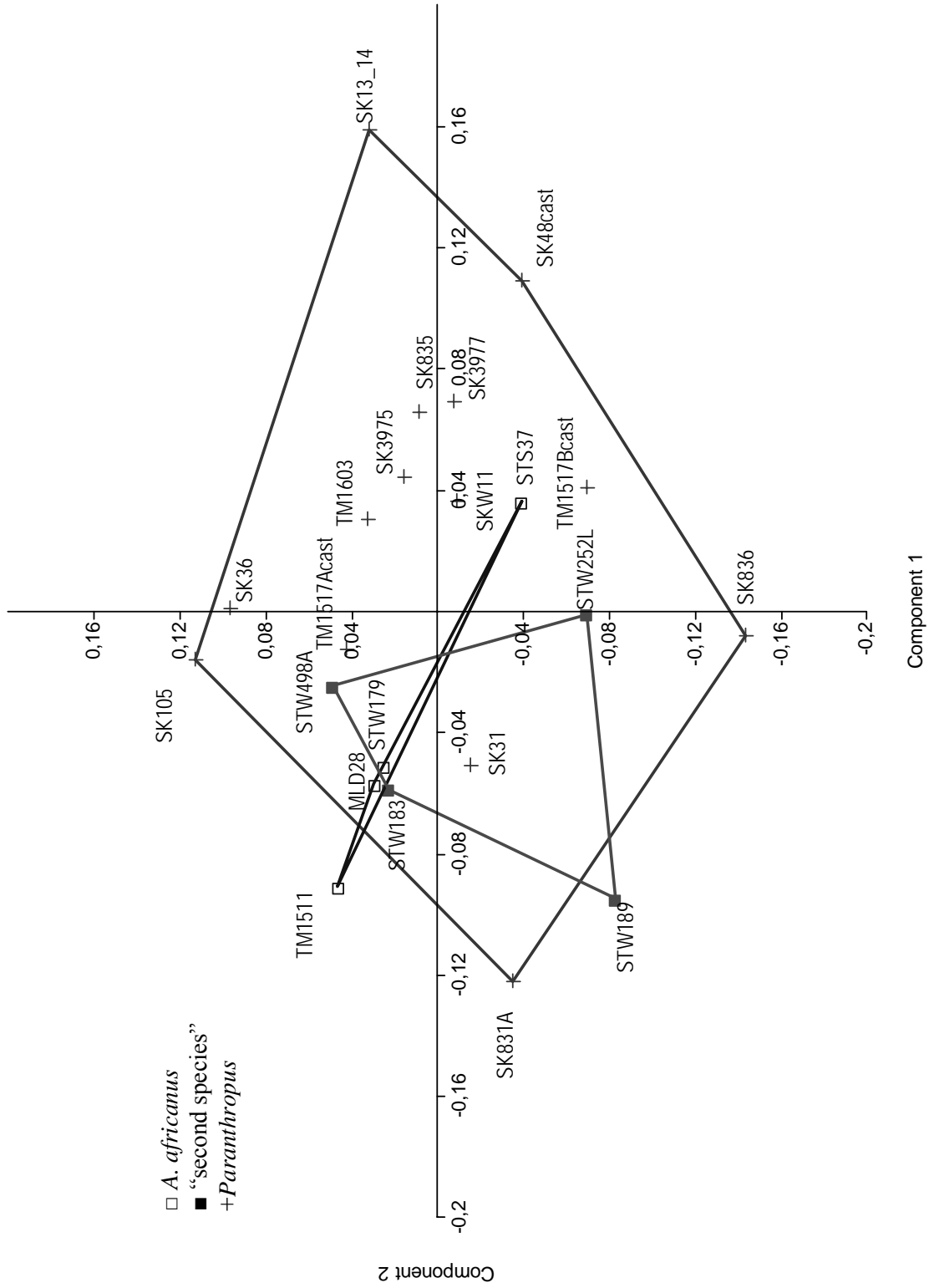


Fig. 8.9 - PCA: M³ – Full sample. Percentage of total variance explained from PC1: 20.81% and PC2 15.78%

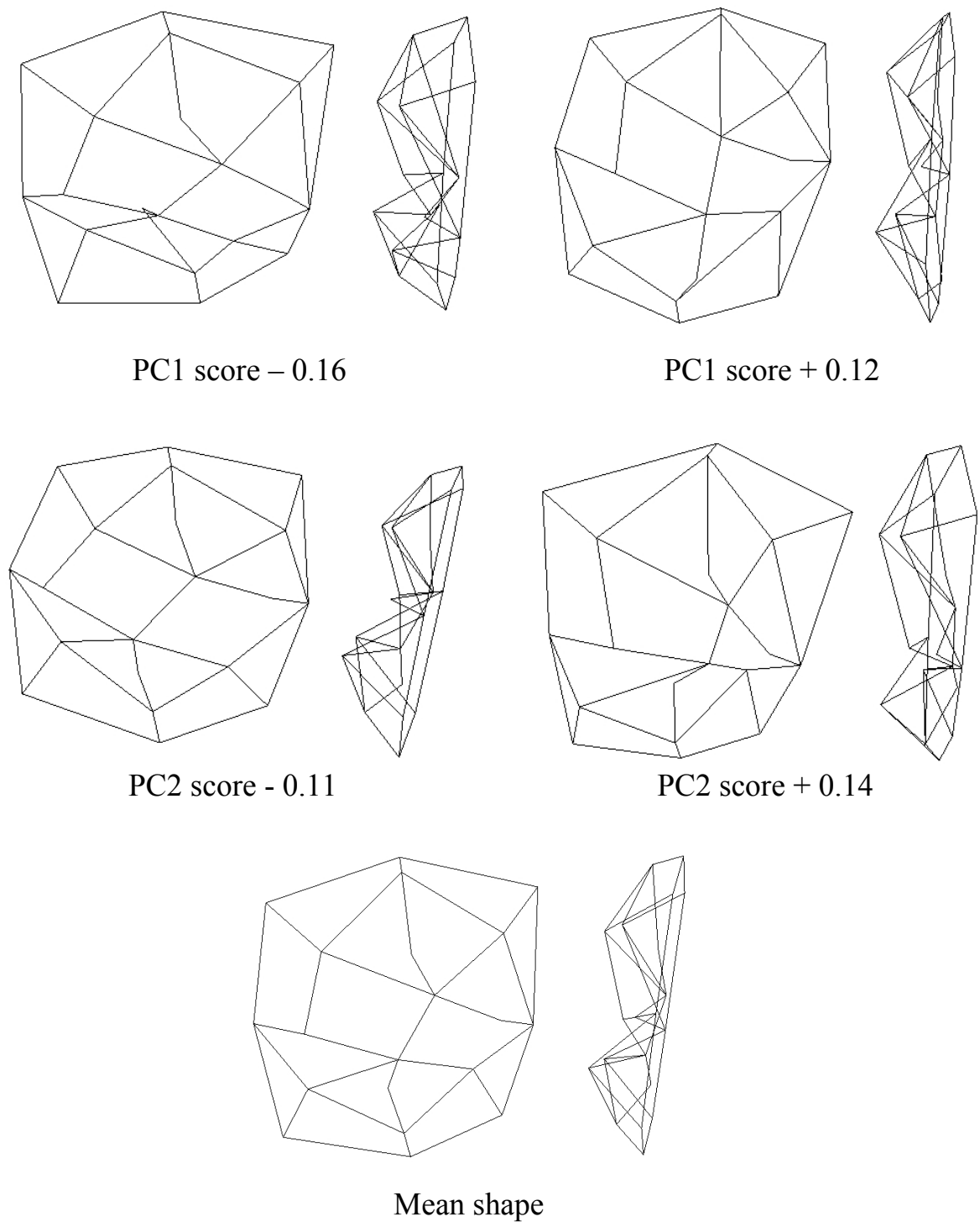


Fig. 8.10 – Wire frame images (as built from *Morphologika* software) showing the mean shapes of the third molars at the extremes scores for PC1 (top line) and PC2 (middle line) as well as the mean shape (bottom line)

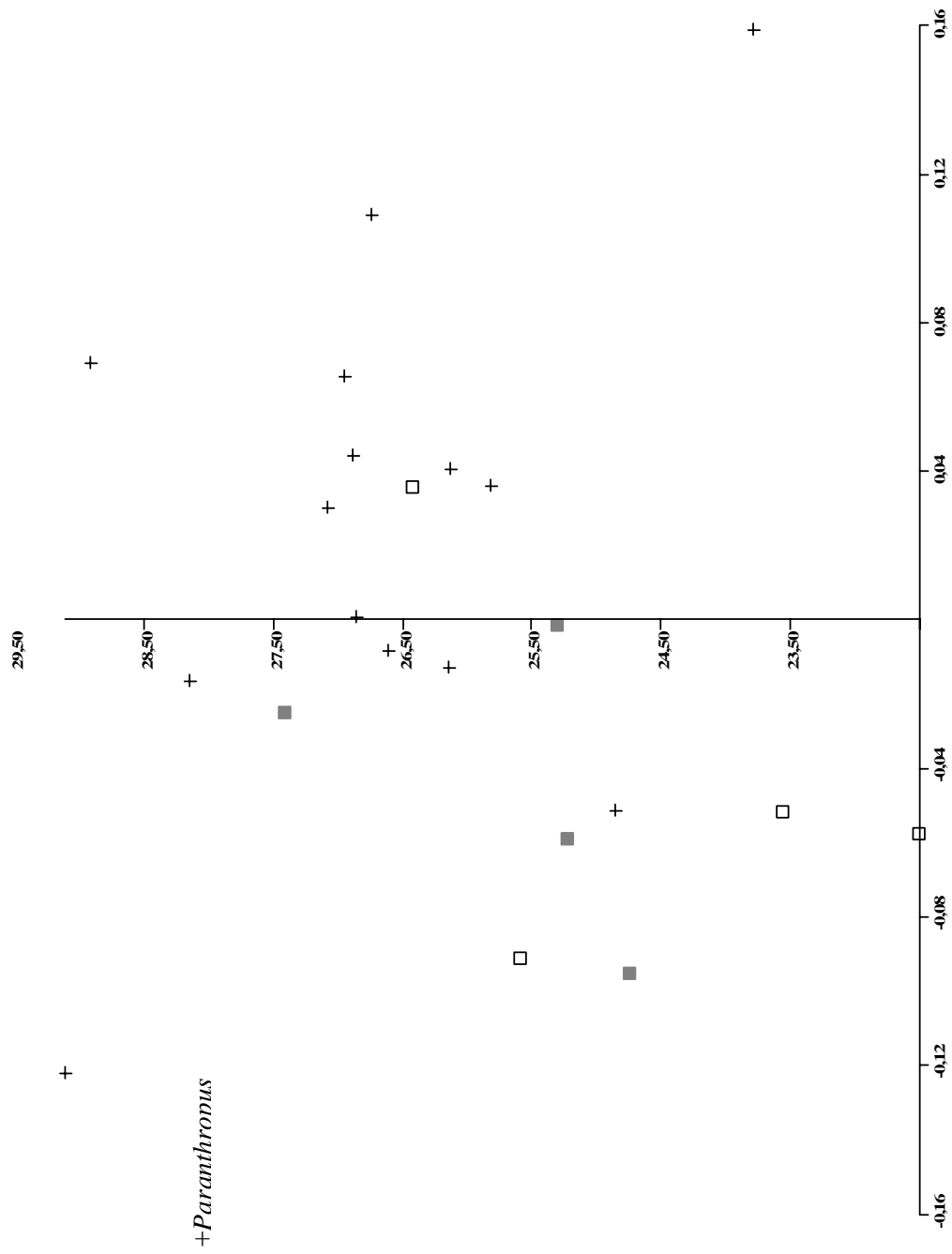


Table 8.3 – Significant linear correlations between centroid size and landmark coordinate for third molars

Landmark coordinate	P
7 z	0.010905
10 z	0.044243
16 y	0.0011154

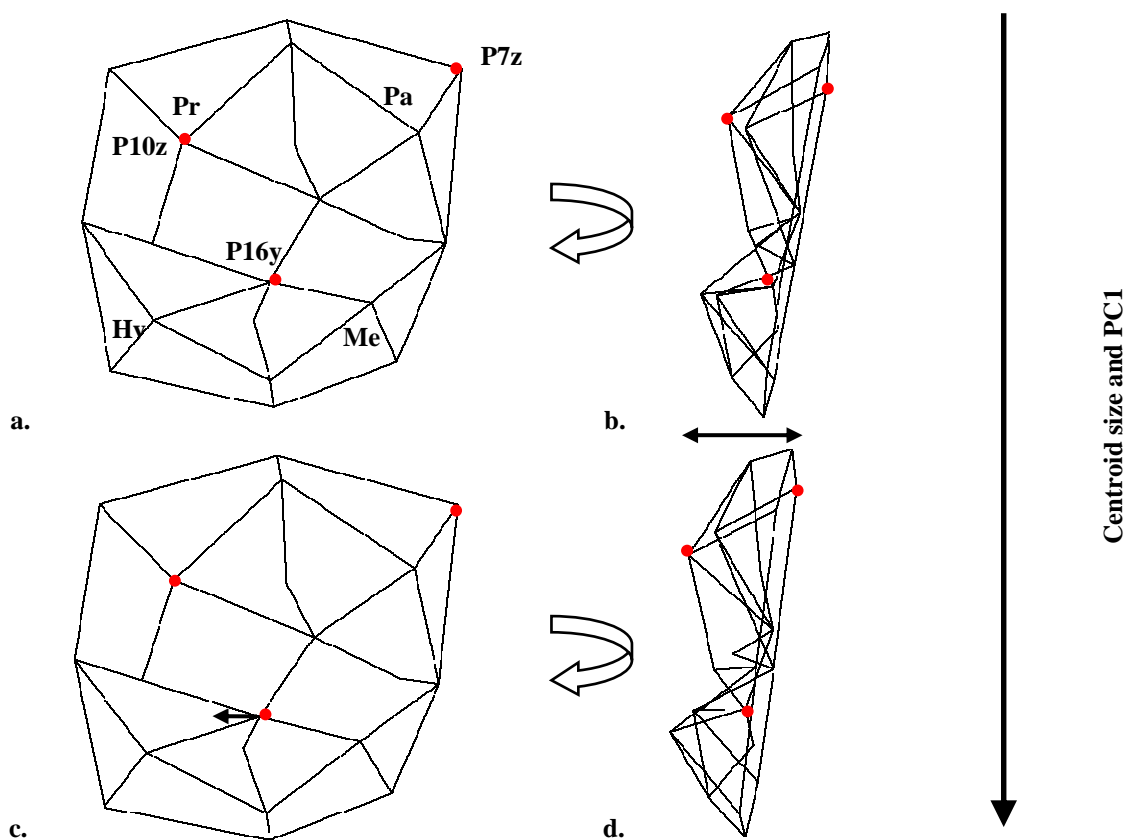


Fig. 8.12 – Morphing along the regression line of centroid size and PC1 for third molars. Red dots represent the landmark coordinates that vary from a. and b. (occlusal and buccal views of the morph for the lowest values of the variables), and c. and d. (occlusal and buccal views of the morph for the highest values of the variables). The black arrow illustrates the direction of the landmark displacement. Further information is provided in the text

8.5 – Joint first and second molars

The opportunity to analyze the joint spatial configurations of more than one tooth belonging to the same individual was considered. However, only M¹ and M² joint spatial configurations could be analyzed, since for all the other combinations (i.e., M¹ + M³, M² + M³, M¹ + M² + M³) the samples were insubstantial. Thus, for five individuals, of which three are considered here as belonging to the “second species” and two are early *Homo* specimens, both M¹ and M² were considered and their spatial configurations of 40 landmarks (20 for each molar type) were analyzed. First of all, GPA was separately performed on the two set of landmark coordinates in order to avoid that M¹ and M² spatial configurations overlapped in different and random ways once the two sets of landmark coordinates are combined (this would have produced artificial and unwanted shape differences). Then, PCA was done on the combined Procrustes residuals.

Figure 8.13 shows a well clear separation between early *Homo* and the “second species” along PC1 which explains 58.24% of the total variance, whilst on PC2 (20.14%) SK 27 and StW 151 are separated by the individuals of the “second species”. The individuals here considered as “second species” cluster tightly.

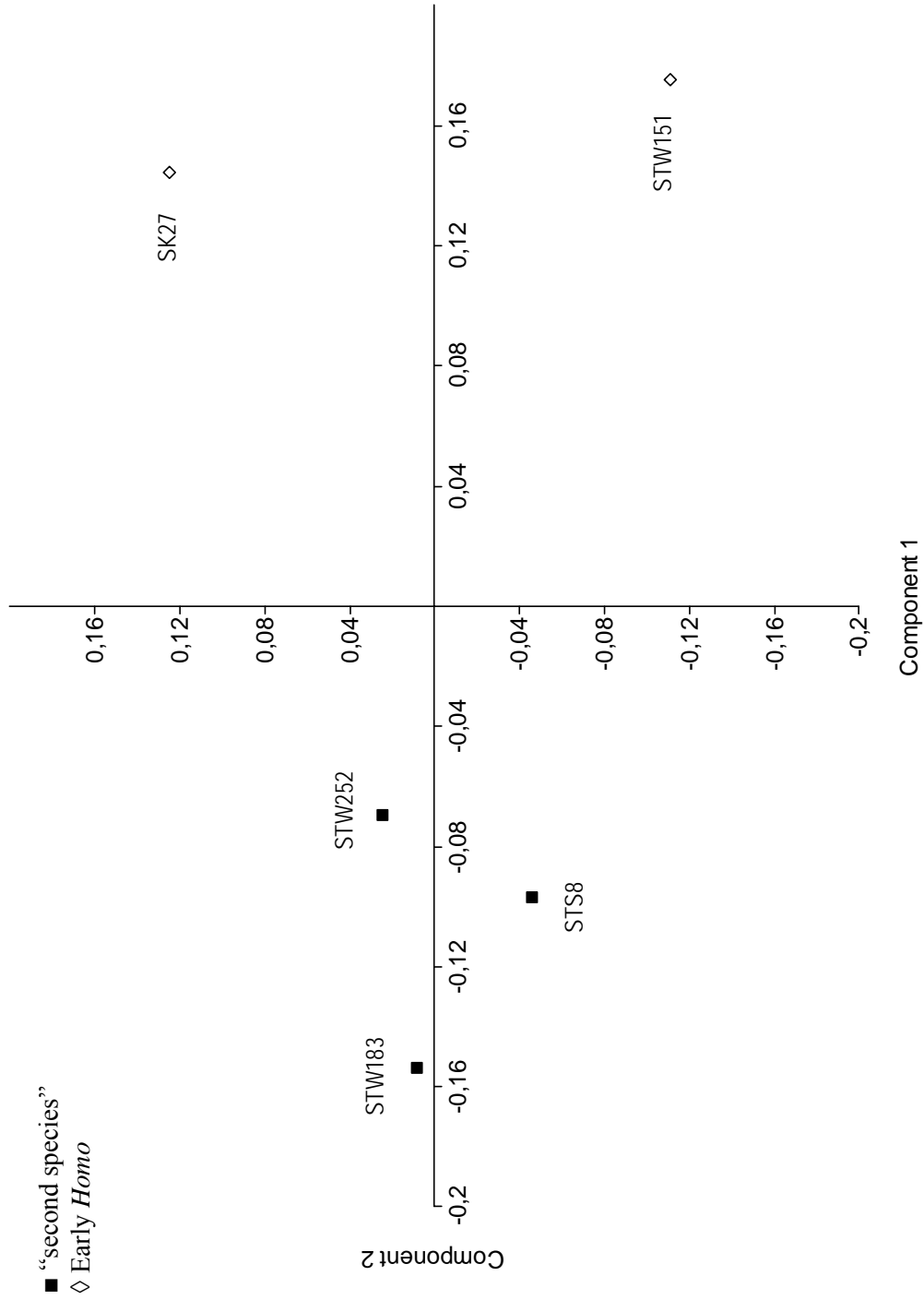


Fig. 8.13 - PCA: M¹ and M² as a single object. Percentage of total variance explained from PC1: 58.24% and PC2 20.14%

8.6 – Final remarks

In this paragraph, a summary of the results presented in the current chapter is provided together with some relevant comments. However, an extensive discussion will be given separately (chapter 9 – *Discussion*).

The results as described above indicate a fairly consistent pattern for the forms under study. *Paranthropus* show a wide range of distribution compared to the other hominid forms, especially but not only along PC1. The specimens attributed to the “second species” always cluster tightly to those of *Paranthropus*. More precisely, (along PC1) they generally set at one extremity of *Paranthropus* scattering, “extending” their range of distribution. Nevertheless, StW 450 (M¹) acts in a different way and fully superimposed to *Paranthropus*. Conversely, along PC2, the “second species” and *Paranthropus* are always completely overlapping.

The specimens attributed to *A. africanus s. s.* and those attributed to the “second species” are generally distinguishable on the plot, except in the case of M³. In the case of M², early *Homo* is well distinct from the others, whilst partially overlaps with *A. africanus* in the case of M¹.

Among the three tooth typologies used, M² has demonstrated to provide the more clear and reliable information. In fact, in spite of the fact that the analysis for first molars provided very convincing results, these teeth are those which present a higher level of wear among the sample. The high variability inherent in the third molar morphology (Robinson, 1956; Sperber, 1974, Wood and Engleman, 1988)

instead, is here clearly reflected on the plot where there is not a clear separation between the hominid taxa considered.

CHAPTER 9

DISCUSSION

9.1 – On the methodology

The aim of this project was twofold: first of all, to establish and validate a new methodology for the study of hominid molar crown morphology; secondly, to test the hypothesis of the occurrence of a second *Australopithecus* species at Sterkfontein Member 4 (and Makapansgat) through the analysis of maxillary molar morphology.

The strength of the methods was corroborated by applying them to two different hominid taxa which are widely recognized to be taxonomically distinct, namely *Paranthropus* and early *Homo* (both from Plio-Pleistocene South African sites).

Through the statistical analysis carried out these taxa were clearly discriminated in terms of crown morphology, thus the first goal of this project has been achieved. The methods and procedures applied presented numerous advantages that made it possible to obtain a good feedback in terms of accuracy of the images, reliability of the data, discriminating power between the different shapes, and, finally, results. The virtual images obtained through reconstruction of the CT-scans provided through the SANRAD facility at Necsa combined two important characteristics: high spatial resolution and volumetric rendering of the objects; thus three-dimensional images representing also the inner structure of the fossils were obtained. Therefore, these virtual images constituted an excellent source for the sampling of the landmark data. This result was achieved through

sophisticated software, VGStudio MAX 2.1 which was suitable not only for the visualization and the handling of the reconstructed images, but very importantly, allowed for accurate and precise collection of the landmark spatial coordinates.

The set of landmarks chosen has also been demonstrated to effectively describe the essential gross morphology of the molar crown, highlighting several aspects of the crown morphology and occlusal surface, but also stressing the relationships between cusps in terms of relative position and size proportions.

Beside the advantages discussed above, another noteworthy aspect of this research is that the nature of the techniques used together with the protocol applied for the transport and handling of the specimens, made them very satisfactory procedures for the safety of the fossil remains. Nevertheless, since the landmark sampling had to be performed at Necca, and the fossils could leave their vault only for the time necessary for the scanning, it was not possible to constantly refer to the original specimens for comparison. In spite of this, the landmark collection resulted in an accurate and precise procedure, as it was statistically quantified through the assessment of the intra-observer error carried out: among the repeats considered only for MLD 28 the error was considered significant. It is noteworthy that this specimen is affected by a moderate degree of wear and this condition was already pointed out as an obstacle to a straightforward identification of the landmarks. This is mainly evident for all the landmarks placed on the occlusal surface, especially cusp tips, but also the highest point of the mesial and distal margins and the points of contacts between mesial and distal cusps. The best way around this problem seemed to be the use of teeth with little or no wear.

One of the major methodological problems dealt with for this project is that of tooth orientation which represents a major issue in the study of tooth morphology.

The procedure adopted here (based on the realignment of teeth according to the four points placed along the cervical margin between the major cusps), has given satisfactory results; however alternative procedures might be tested and their outcomes compared in the attempt to optimize the accuracy of the landmark collection.

In summary, the methods applied for this project have been demonstrated to be scientifically valid as well as effective in the study of hominid molar teeth morphology; therefore they were used for the investigation on the high variability shown among the fossil record of Sterkfontein Member 4.

9.2 - Other potential uses of the methods

Cheek teeth present the same fundamental structure among hominids, which does not differ substantially from that of other hominoids (Robinson 1956; see also appendix A in this work for a general review of hominid molar morphology). Thus, it is conceivable that the methods presented in this work are likely to be effectively applied for additional researches focused on the study of molar morphology within the different taxa of the superfamily Hominoidea. Therefore, it is highly recommended that these methods will be further tested in order to verify the extent of their appropriateness. Nonetheless, adequate changes to the set of landmarks can make of the procedures used in this work a suitable tool for the study of other primates or even mammals, given that molar morphology is a discriminant feature between the taxa considered.

Moreover, other tooth typologies can be taken into account, provided that the set of landmarks is adequately modified in order to effectively describe the shape of the tooth. Other scholars recognized the great potential of geometric

morphometrics in the study of dental morphology (for example, Robinson, *et al.*, 2001; 2002; Martín-Torres, *et al.* 2006; Skinner, *et al.*, 2008). However, Robinson, *et al.*, 2002 and Martín-Torres, *et al.* 2006 both commented on the inadequacy of two-dimensional methods in describing tooth morphology. In fact, a study based on accurate three-dimensional images adds information and improve the quality of data obtained, as demonstrated by some recent works (Olejniczak, *et al.*, 2008; Olejniczak, *et al.*, 2008; Skinner, *et al.*, 2008; Skinner, *et al.*, 2009; Skinner, *et al.*, in press; Skinner, *et al.*, in press). For example, remarkably Skinner, *et al.*, (2008) identified taxonomically relevant differences between samples of mandibular molars of *A. africanus* and *P. robustus* by performing geometric morphometric analysis on data gathered from high-resolution images of the enamel-dentine junction (EDJ) from micro-computed tomographic scanning.

However, one must always keep in mind that the approach used in this project is based on the study of the crown surface and is more taxonomically effective when applied to a sample of unworn teeth, since crown morphology is remarkably altered by wear (see Ungar, 2004 and Skinner, *et al.*, 2008 and their effort to overcome the problem of wear and maximize the sample size). Moreover, other modifications of the original, fully developed tooth morphology such as those produced by pathologies, taphonomic agents or destructive studies may invalidate the results obtained for that specimen. For this research, when a very worn or damaged tooth clearly gave abnormal results (e.g., doubling or trebling the range of variance shown by the rest of the sample altogether) it was then excluded from the analysis. Nevertheless, it seems that a low degree of wear (from slight to moderate) and minor damage (such as cracks that do not produce a significant

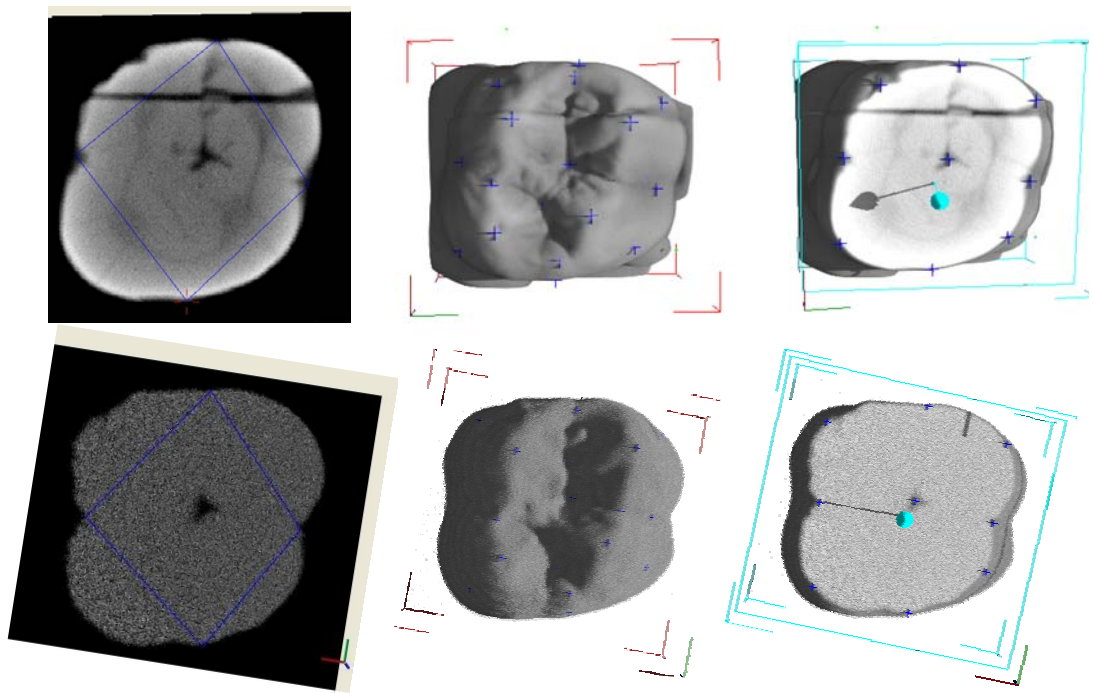


Fig. 9.1 – Top row: axial and three-dimensional views of StW 280 fossil molar as visualized through VGStudio MAX 2.1. The images show the alteration of this specimen’s original morphology due to a previous invasive investigation. Bottom row: axial and three-dimensional views of the cast of the same specimen made before the sampling of dental material, thus showing the original shape of this tooth

displacement of parts of the crown) did not affect the results of this research, as it will be discussed below (paragraph 9.4.1 – *First molars*). However, some of the problematic fossils may be included in the sample by opportunely reducing the set of landmarks analyzed, thus optimizing the sample size.

Some comments with regard to the specimen StW 280 (M²) are given here. The original specimen was previously utilized by Grine and Martin (1988) for an invasive investigation where a vertical slice of tooth approximately 1 mm. thick was removed at the level of the mesial cusps. The current analysis included both the original specimen and a cast of the original, undamaged tooth. Since the original specimen lacks a slice of material in buccolingual direction, a tentative “reconstruction” was done by joining the two halves together for the scanning (Figure 9.1). Thus, a certain bias was introduced for this specimen, as highlighted

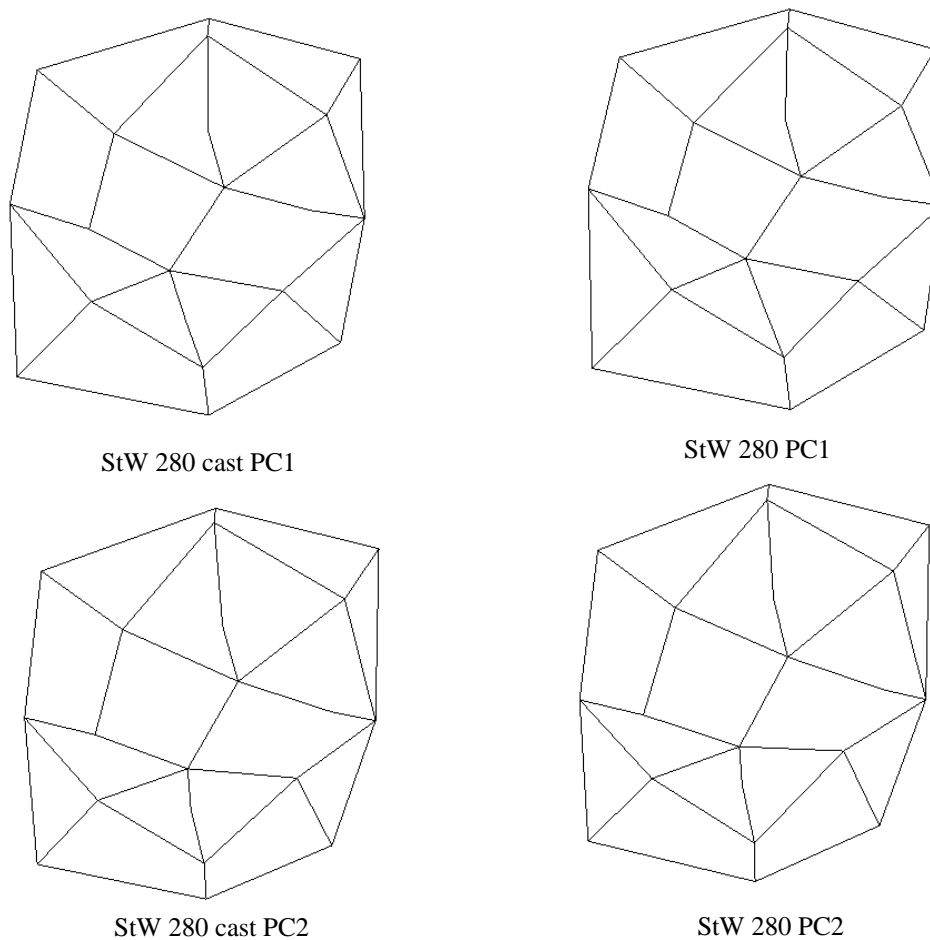


Fig. 9.2 – Visualization features showing the (subtle) differences between the morph of StW 280 cast (on the top and bottom left) and StW original but damaged specimen (on the top and bottom right)

by the visualization features of *Morphologika* in the comparison between the morphing of the original specimens and that of the cast (Figure 9.2). Since the slice was removed from the mesial cusps, these turned out to be smaller compared to the distal ones, as evident along PC1. Conversely, along PC2 the morph for StW 280 original seems more mesiodistally elongated than the cast. This could sound like an inconsistent result in respect of what was said above, however, it must be noted that the slice was removed from the widest section of the mesial cusps, thus the buccolingual breadth of those cusps ended up being proportionally smaller than that of the cast.

It would be interesting however, to assess the error linked to the use of a cast in contrast to an undamaged tooth. Indeed, this was originally one of the aims of this

research, thus a scanning of the cast of StW 151 was done. Unfortunately, such data could not be utilized due to technical problems in the reconstruction of the final image.

9.3 – On the second species hypothesis

Many authors have commented on the polymorphism observed within the *A. africanus* hypodigm (Wood, 1985; Clarke, 1985a,b; 1988; Kimbel and White, 1988; Kimbel and Rak, 1993; Moggi-Cecchi, *et al.*, 2006; Lockwood and Tobias, 2002; Moggi-Cecchi, 2003; Moggi-Cecchi and Boccone, 2007).

Clarke (1985a,b; 1988) explained the unusual degree of variation observed at Sterkfontein Member 4 and Makapansgat Limeworks site with the presence of a new *Australopithecus* species other than *A. africanus*. This hypothesis was formulated on the basis of a descriptive analysis of cranial and dental features and was later enhanced by the finding of the individual StW 252 from Sterkfontein Member 4. After Clarke reconstructed it, he found that this individual showed major differences from *A. africanus* and rather presented strong affinities to *Paranthropus*. However, the anterior dentition remarkably differed from that of *Paranthropus* showing a marked alveolar prognathism and a wide diastema between I² and C, features that may be plesiomorphous to apes.

In Clarke's view, StW 252 shares important similarities with other individuals from the same site, such as Sts 71, StW 183, StW 498A and StW 505. These morphological features can be summarized in: concavity of the frontal squame, anterior position of the encroachment of the temporal lines, thin and flattened supraorbital margin, high and gently curved occipital profile, anterior position of the zygomatic process of the maxilla which curves over P⁴, large cheek teeth.

Clarke distinguished those specimens from others from Sterkfontein Member 4 (Sts 5, Sts 17, Sts 52) which show the following characteristics: a convex frontal squame, reduced sagittal encroachment of the temporal lines, thickened supraorbital margin, angled occipital profile, posterior position of the zygomatic process of the maxilla which starts curving over M¹, relatively small cheek-teeth.

Clarke (1988) argued against the possibility of explaining the variability observed within the Member 4 sample through sexual dimorphism, individual variation or changes through time within the one species *A. africanus*. He noted that among primates, sexual dimorphism is not expressed by the presence of one gender of thick supraorbital margin associated with small teeth, whilst the other gender is characterized by thin supraorbital margin and large teeth. In addition, the dental size variation seemed to be too big in respect to cranial size variation to justify the hypothesis of individual variation. Clarke rejected the explanation which links the two morphotypes through an ancestor-descendent relationship on the basis of the following considerations: it is unlikely that in an evolutionary sequence a specialized, large-toothed *Paranthropus*-like form is ancestral to a less specialized, small-toothed *Homo*-like form; the other possibility is also weak due to the presence of the ancestral morphology of the anterior dentition in the more specialized form.

Kimbel and White (1988) also commented on the variability of *A. africanus* on the basis of a metrical analysis of canine and postcanine dentition combined with the morphological evaluation of different cranial regions. Even though they observed a low variation in canine size, they found that maxillary M² diameters formed two non-overlapping clusters. Moreover, they added that the variability in terms of facial and especially basicranial morphology was too big to be ascribed

to individual variation and sexual dimorphism. They eventually suggested that a further hominid taxon might be present in Sterkfontein Member 4, but also stressed the difficulty to define unequivocally the two species with very similar morphology. Nonetheless, they did not exclude the possibility of a change through time along a lineage, where temporally different populations are represented in the fossil record at Sterkfontein Member 4. It is to be emphasized that they based their morphological analysis of the basicranium mainly comparing Sts 5 and Sts 19, where the latter has been regarded as *Homo* by Kimbel and Rak (1993).

Other scholars explained the polymorphism exhibited within the fossil record at Sterkfontein with the simultaneous occurrence of *A. africanus* and *Homo*; in particular Moggi-Cecchi, *et al.* (1998) considered the specimen StW 151 to trend toward the *Homo* condition. Lockwood and Tobias (2002) supported the view of Kimbel and Rak (1993) and Moggi-Cecchi, *et al.* (1998). Thus, they considered the presence of a further species other than *A. africanus* a possible explanation for the high variability expressed within the assemblage of Sterkfontein Member 4, but did not envisage the occurrence of a new species. Indeed, they agreed with Clarke (1988) some of the specimens from Sterkfontein Member 4 (StW 183, StW 252 and probably related StW 255) possess *Paranthropus*-like features. They disagreed with Clarke (1988) in terms of the diagnostic features to be considered and claimed that Clarke overestimated the number of specimens that diverge from *A. africanus*.

The results achieved by the present research have given further demonstration of the high morphological variability peculiar to the fossil assemblage from Sterkfontein Member 4 in terms of maxillary molar morphology. The geometric morphometric analyses conducted on the full samples (including individuals from

the sites of Sterkfontein Member 4, Makapansgat, Swartkrans, Kromdraai and Cooper's Cave) have led to interesting results in which the individuals considered here as "second species" (Sts 1, Sts 8, StW 183, StW 188, StW 189, StW 252, StW 280, StW 450; StW 498A) are fairly distinguished from those considered as *A. africanus s. s.* (MLD 28, Sts 24a, Sts 37, Sts 56, Sts 57, StW 179, StW 204, StW 402, StW 530, TM 1511; but see paragraph 9.5 – *Uncertain attributions* for further comments).

The geometric morphometric analyses for M¹ and M² do show a fairly distinct pattern in the distribution of the "second species" which is mostly placed at one extremity of the range of variance proper to *Paranthropus*. On the contrary, the maxillary molars of *A. africanus* are close to those of *Homo* on the plots. Thus some of the maxillary molars from Sterkfontein show a gross morphological affinity to those of *Paranthropus*, while the others are more allied to *Homo*. However, whether this picture could be explained through individual or sexual dimorphic variation, change through time or the occurrence of more than one species is to be proved, where the interpretation of the variability observed remains a task.

In M² the "second species" is placed toward an extremity of the horizontal axis and partially superimpose with *Paranthropus*, whilst *A. africanus* extends to the opposite extreme of *Paranthropus* distribution and close to *Homo*, and it seems that an intermediate form is not represented. To explain the picture observed for the M² specimens from Sterkfontein through individual variation implies the acceptance that the variability they express is greater of that of *Paranthropus*. If the individuals labeled as "second species" are regarded as males and those with

smaller teeth are regarded as females of the same species, then *A. africanus* would be a highly dimorphic species (at least in terms of maxillary molar morphology).

Lockwood, *et al.*, (2007) claimed that the southern African *Paranthropus* (from the sites of Swartkrans, Kromdraai and Drimolen) manifested a degree of sexual dimorphism comparable to that of *Gorilla*, with males and females of notably different sizes and degree of robusticity, but not different in morphology.

Moreover, the M² gross morphology seems to be bimodal and non-overlapping. Furthermore, the same bimodal and non-overlapping morphological pattern emerges for M¹, as well, where there seems to be a morphological continuity with the two groups, which are distinct but not separated from each other.

Even though the analysis may be biased by the small sample size, it is worth noting that similar results for M² were achieved by Kimbel and White (1988) on the basis of diameter values, and they argued that such a level of variability is unlikely to be attributed to sexual dimorphism. In addition, they found a preliminary result which, if confirmed, contrasts with the pattern of M², namely a distinct but unimodal distribution of mandibular canine diameters with overlapping values for males and females, which is more likely associated with the *Homo*-like condition (Pilbeam and Zwell, 1973).

In the light of what said above, the hypothesis of sexual variation does not seem convincing. Moreover, individual variation as well does not explain the pictures observed here (especially for M¹ and M²), since it would have implied a gradual change of morphology; thus, individuals with intermediate morphologies, would have been represented.

Alternatively, this picture can be explained with the occurrence of two distinct morphotypes (*sensu* Clarke, 1988) at Sterkfontein Member 4. The presence of a

group of molars morphological close to *Paranthropus* together with another group which shows affinities with *Homo* would fit well the scenario presented by Clarke, where the “second species” is a new *Paranthropus*-like australopithecine species and *A. africanus s. s.* trends toward the *H. habilis* condition. This argument would also explain well the metrical and morphological partial superimposition of the sample of *A. africanus s. l.* to those of *Paranthropus* that recurs in many studies such as Robinson, 1956; Wood and Engleman, 1988; Lockwood and Tobias, 2002; Moggi-Cecchi and Boccone, 2006; Skinner, *et al.*, 2008). Nevertheless, the studies aforementioned used different samples and in some of them the sample is very different from that used here so that a detailed comparison between what was found for the different specimens is not possible. However, there is not unanimous consensus with regard to which specimens present affinities to *Paranthropus*. There are several reasons preventing consensus on the taxonomic attribution of the specimens from these australopithecine-bearing sites. First of all, the limited and fragmented nature of the material represents a constraint to a systematic comparative analysis. In fact, it is a problem to associate the various parts of the skull and mandible with the superior and inferior dentitions, or to associate the postcranial remains with the skulls and dentitions. Therefore, it is difficult to ascertain whether one is dealing with different morphotypes or different parts of the same morphotype.

However, in the sample from Sterkfontein Member 4 there are maxillary molars in place for both cranial morphotypes represented (for example, Sts 52a and StW 183a partial lower faces) and this allows the association between a certain type of cranial morphology and its dentition. This applies to the mandibles and the mandibular molars as well, while there are at present no postcranial remains

proven to be associated with cranial and dental fossils of each morphotypes. For this reason the complete specimen StW 563 from Member 2, which Clarke (2008) suggested may belong to or be closely affiliated to the “second species” will represent a crucial source of information once extracted from the breccia. However, it is noteworthy that Zipfel and Berger (in press) found that the morphologies of two partial tibiae from Sterkfontein Member 4 (StW 396 and StW 514a) differ so greatly that they consider these specimens to belong to different taxa, which may have had a different kinds of locomotor patterns as well. However, they are not able to infer about the taxonomic attribution of the specimens they studied due to the incompleteness of the remains and to the fact that it is impossible to match them either to other skeletal or dental remains. Clarke (personal communication) has previously observed that there are two locomotor patterns represented in two first metatarsals from Sterkfontein Member 4. Another reason why the taxonomic attribution of the fossil materials is not straightforward is that different scholars have used diverse diagnostic features for assessing their systematic grouping (for example, see Clarke 1988 *versus* Lockwood and Tobias, 2002 for the morphological assessment of the Sterkfontein Member 4 fossil record). In some instances, a distinction of the different morphotypes was hampered by the use of methods which were not able to highlight the morphological peculiarity of the different morphotypes and therefore could not discriminate between the various forms present, as in the case of previous dental studies (e.g. Calcagno, *et al.* 1997; 1999; Moggi-Cecchi, 2003). Finally, in some other cases the results of the research can be biased by a wrong or uncertain species attribution of a specimen. For example, Kimbel and Rak (1993) concluded that the high variability shown within the Sterkfontein Member

4 assemblage should be related to the presence at the site of *Homo* where they considered the Sts 19 specimen as early *Homo* while others classified it as *A. africanus* (Ahern, 1998).

Lockwood and Tobias (2002) following Clarke (1988; 1994) identified some characters typically found in *Paranthropus* in the specimens StW 183 and StW 252, although they considered the attribution of StW 183 critical. Moreover, they regarded the position of StW 280 (attributed to the “second species” here) as not effectively resolvable through the fossil evidences available, and attributed StW 505 (in 1999) to *A. africanus* (the latter specimen however is not included here).

As argued by Clarke (1988, 2008) the “second species” presents craniofacial and cheek teeth features that resemble those of *Paranthropus*, and a more ape-like anterior dentition that is unlike that of *Paranthropus*. This concept finds a confirmation in what was found for the maxillary molars with this research. In fact, the cluster formed by the “second species” molar specimens partially overlap the cluster formed by the *Paranthropus* specimens for all the tooth typologies analyzed. Since other authors have stressed the *Paranthropus*-like features observed in both *Australopithecus*-bearing sites of Sterkfontein Member 4 (Johanson and White, 1979; Tobias, 1980; White, *et al.*, 1981; Rak, 1983; Skelton, *et al.*, 1986) and Makapansgat (Aguirre, 1970) one could argue that the “second species” is actually *Paranthropus*. There are several reasons why this is not accepted here. Concerning the fossil assemblage from Sterkfontein Member 4, the differences between the *Paranthropus* specimens and those considered by Clarke as belonging to the second species have been discussed above in this chapter as well as in chapter 1 and find a notable example in the different morphology of the anterior dentition. Other significant differences can be

observed in the shape of the mandible which in side view appears evenly thick in *Paranthropus* while it is more posteriorly tapered in the “second species” as shown by the comparison of MLD 2 and StW 498 (“second species”) to SK 23 and SK 34 (*Paranthropus*). Moreover, both superior and inferior *Paranthropus* premolars and molars are placed in such a way that their bucco-lingual diameter is disto-lingually to mesio-buccally orientated with respect to the sagittal axis of the mandible, while in the “second species” the bucco-lingual diameter is fairly perpendicular to the sagittal axis. The teeth themselves show a different morphology where the *Paranthropus* premolars and molars are bucco-lingually (maxillary molars) or mesio-distally (mandibular molars) elongated and skewed when compared to the much more squared and regular in shape post-canine dentition of the “second species”.

Importantly, the results of the present research show a variability of the specimens attributed to the “second species” that only partially overlap with that of the *Paranthropus* specimens from the different sites considered. It would be rather odd if those specimens from Sterkfontein Member 4 here regarded as “second species” would represent a very selected *Paranthropus* population showing a morphology which not only set at one extremity of the *Paranthropus* range of distribution, but also exceed the variation shown by all the other maxillary molar specimens from Swartkrans, Kromdraai and Cooper’s Cave. This would be even more surprising considering that Lockwood, *et al.* (2007) claimed that *Paranthropus* is a highly sexually dimorphic species on the basis of their study focused on ranking body size and age of the specimens from Swartkrans, Drimolen and Kromdraai.

Boccone's doctoral research (2004) was based on a sample of similar size and composition to that considered here. She studied maxillary molar morphology of South African australopithecines through the analysis of cusp areas and occlusal polygon (namely the geometrical shape obtained connecting each cusp tip with the adjacent ones). Her results were extrapolated and summarized by Moggi-Cecchi and Boccone in 2007. They found higher coefficient of variations for *A. africanus* in respect to that for *Paranthropus*, especially for M². Very importantly, they identified some individuals among those from Sterkfontein Member 4 which possessed maxillary molars of remarkable size and which show a distinct morphology from the rest of the sample (namely a broad cusp area compared to the occlusal basin), and which correspond to some of the specimens indicated by Clarke (1994) as "second species". Thus, they eventually recommended further investigations aimed at evaluating those differences in the crown morphology.

Yet, this project provided new insights with regard to the variability expressed within the *A. africanus* hypodigm and contributed to the subject adding valuable information based on the three-dimensional morphology of the maxillary molar crown morphology.

The hypothesis of change through time seems not plausible because both the morphotypes are represented through the Member 4 breccia (Clarke, 1988). However new studies aimed at elucidating the stratigraphy of Member 4 talus would probably open new perspectives in the interpretation of the morphological variability in Sterkfontein Member 4.

It is noteworthy also that the number of specimens belonging to each of the two groups is approximately the same. Even though the sample considered here is

only a part of that yet recovered at Sterkfontein Member 4, this aspect is still remarkable since the specimens were chosen according to parameters not related to their morphology but based on the state of preservation and degree of wear. The clusters formed (evident especially in M²) may to some observers reflect a normal distribution of males and females of the same species; alternatively if this explanation is rejected they may represent two different species, namely *A. africanus* and a further hominid species (Kimbel and White, 1988; Kimbel and Rak, 1993; Lockwood and Tobias, 2002) or a new australopithecine species (Clarke, 1988). In any case, it seems that this preliminary result supports Clarke's claim that the morphotype divergent from *A. africanus* is represented by a conspicuous number of specimens.

In the case of the Makapansgat Limeworks site, this project does not add valuable information due to the paucity of the sample considered (formed only of MLD 28, M³). However, it is desirable that further researches should be devoted to the study of the fossil record from Makapansgat since it has been suggested that the fossil record is not taxonomically homogenous and probably contains *Paranthropus* or *Paranthropus*-like specimens (Aguirre, 1970; Clarke, 1988; respectively).

In conclusion, the present research provided further demonstration of the variability expressed by the fossil assemblage within Sterkfontein Member 4 and highlighted some of the morphological arguments already stressed by other authors. Moreover, this research not only confirmed the results of previous works (Kimbel and White, 1988; Moggi-Cecchi and Boccone, 2007) with regard to the variability observed within *A. africanus* hypodigm, but most importantly added valuable information to it, investigating the subject through innovative and

accurate methods designed at highlighting the three-dimensional morphology of molar crowns. It is remarkable that the methodologies used in this project detected those dental features that other analytical methods could not capture, such as those based on the analysis of linear dimensions (Calcagno, *et al.*, 1997; 1999; Moggi-Cecchi, 2003; Moggi-Cecchi, *et al.*, 2006), but also those based on the appraisal of cusps' areas (Wood and Engleman, 1988; Moggi-Cecchi and Boccone, 2007), and therefore allowed for a quantitative evaluation of gross morphological differences between the different hominid taxa as would be recognizable through a visual inspection.

The results obtained with the present research suggest that a further species other than *A. africanus* occurred in Sterkfontein Member 4. The morphological variation expressed within the assemblage of Sterkfontein Member 4 is too high to be explained through sexual dimorphism, which is expressed with different molar sizes rather than different molar morphology within the same species. Likewise, the hypothesis of individual variation is rejected since the specimens from Member 4 formed distinct clusters, rather than a cline, as the individuals of the same species would do. In the light of what said above the null hypothesis of a single species at Sterkfontein Member 4 is rejected.

Nevertheless, further studies including also a known sample of closely related primates would be desirable in order to comparatively evaluate the maxillary molar variability expressed in Sterkfontein Member 4.

9.4 – Additional results

The outcomes of this project provided information on the gross molar morphology of the hominid taxon considered, which results will be discussed below with

regards to the different tooth typologies. The discussion provided is based on the observation of the visualization features (as built by *Morphologika* software) and their morphing along PC1 and PC2 (Figures 9.3 for M¹, 9.4 for M² and 9.6 for M³). When it is the case, previous findings will be cited making reference to other works that however are based on different approaches (descriptive analysis, metrical analysis, appraisal of cusp's areas).

9.4.1 – First molars

For M¹ the visualization features highlighted a high difference in cusps's height along PC1, with most of the “second species” characterized by the lowest cusps, and placed at one extremity of the horizontal axis. *A. africanus* and early *Homo* seem to have low cusps as well. Although wear affects this sample more than it does in the samples of M² and M³, it is remarkable that not all of the specimens of the “second species” present a high degree of wear. For example, while StW 252J is moderately worn, in Sts 1, Sts 8 and StW 183 the occlusal attrition is slight, and StW 450, which does not cluster with them on PC1, is unworn.

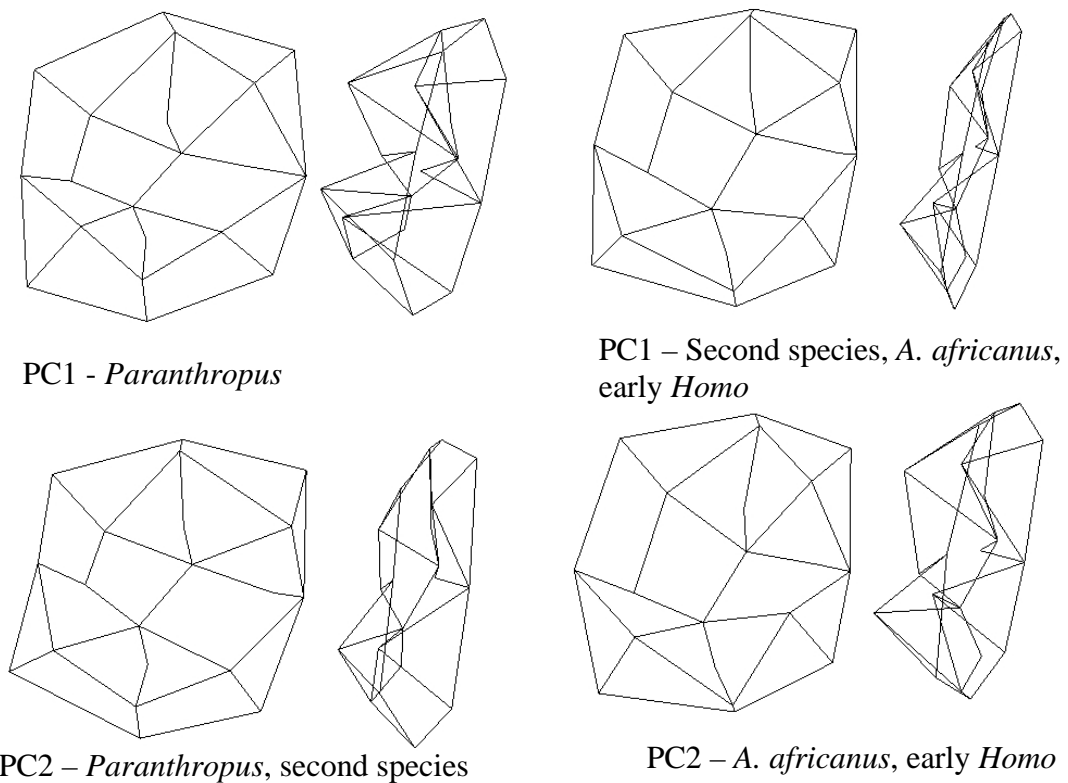


Fig. 9.3 - Wire frame images showing the general morphology of M^1 for the different hominid taxa through the mean shapes at the extremes scores for PC1 (top line) and PC2 (bottom line)

An analogous situation occurs for *A. africanus* and early *Homo*, where SK 27, which is only slightly worn, has lower cusps than SKW 3114 which, conversely, is moderately worn. However, all the specimens of *Paranthropus* taken into account are unworn or slightly worn, and only SK 55A (which is placed closer to the second species) is appreciably worn. These results suggest that a variation in cusp's height is present and it seems to characterize the "second species" more than the others. However, it seems that cusps' height variability is not (entirely) due to wear since teeth with different degree of occlusal attrition presented similar scores (along PC1).

In addition, the morphing along the first principal component emphasized a difference between *Paranthropus* and *A. africanus* as already discussed by Wood and Engleman (1988) on the basis of their appraisal of cusps' areas, namely M^1 in

A. africanus is narrower than that of *Paranthropus*. However, the mean shapes for early *Homo* and “second species” along PC1 seem to present the same characteristic that apparently distinguishes between them and *Paranthropus*.

The second principal component reflects the greatest contribution of Pr to the total crown area, as previously reported by Robinson (1956) and later confirmed by other authors (Sperber, 1974; Wood and Engleman, 1988; Moggi-Cecchi and Boccone, 2007). Conversely, the Pa seems to be bigger in *Paranthropus*, where Moggi-Cecchi and Boccone (2007) found a statistically significant difference with *A. africanus*.

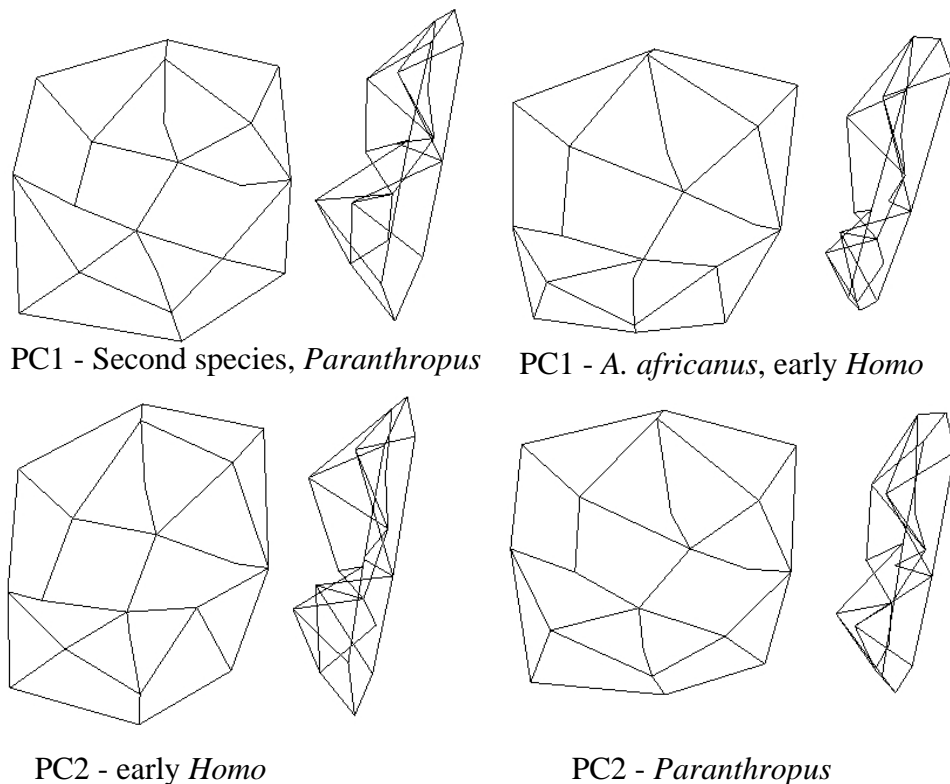


Fig. 9.4 - Wire frame images showing the general morphology of M² for the different hominid taxa through the mean shapes at the extremes scores for PC1 (top line) and PC2 (bottom line)

9.4.2 – Second molars

The analysis of M² highlighted one of the most significant features of molars that distinguishes between both *Paranthropus* and “second species” and *A. africanus* (Clarke, 1988; 1996): the first two are characterized by cusp tips oriented toward the centre of the crown, namely they are more close to each others so that the occlusal basin is small relative to the total crown outline. This characteristic was also stressed by Moggi-Cecchi and Boccone for those specimens from Sterkfontein Member 4 that seem to be distinct from *A. africanus*. By contrast, *A. africanus* has cusps tips more oriented toward the external outline of the crown and the portion of the crown comprised between the perimeter of the occlusal basin and the crown outline is narrower. The molar thus shows less rounded sides (Figure 9.5).

Moreover, the geometric morphometric analysis highlighted a remarkable reduction of distal cusps in M² of early *Homo* (along PC2) in respect to the other hominid taxa. Furthermore, the crown profile in early *Homo* is buccolingually narrower than in the other hominid taxon considered here. This peculiarity of early *Homo* dentition was previously discussed by other scholars (Leakey, *et al.*, 1964; Clarke, 1977).

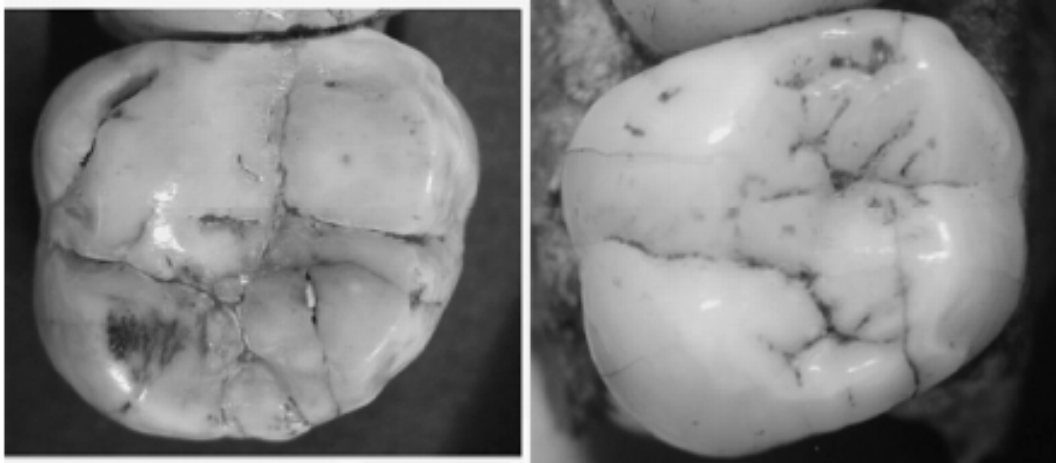


Fig. 9.5 - Occlusal photographs of M² of Sts 22 (on the left) and StW 183 (on the right) which show notable differences in overall crown morphology. Scale=1 cm. (from Moggi-Cecchi and Boccone, 2007)

The visualization features gave emphasis also to a greater contribution of buccal cusps to the total crown area in *Paranthropus* and “second species” respect to *A. africanus* and early *Homo*. The same pattern was found by Moggi-Cecchi and Boccone in the comparison between *Australopithecus* and *Paranthropus* from South African sites.

The reduction of distobuccal angle is evident in M² as well as in M³ as already discussed by Robinson (1956).

9.4.3 – Third molars

The geometric morphometric analysis for M³ did not discriminate between the different hominid taxa. The result reflects the high variability inherent in the morphology of third molars of hominids in general and australopithecines in particular. However, along PC1 a separation between most of the *Paranthropus* specimens and the others is present. The morphological variation that mainly accounts for the variance along the horizontal axis seems to involve the proportions between mesial and distal cusps, with a remarkable reduction of distal cusps relative to the mesial ones in most of the specimens of *Paranthropus*. This

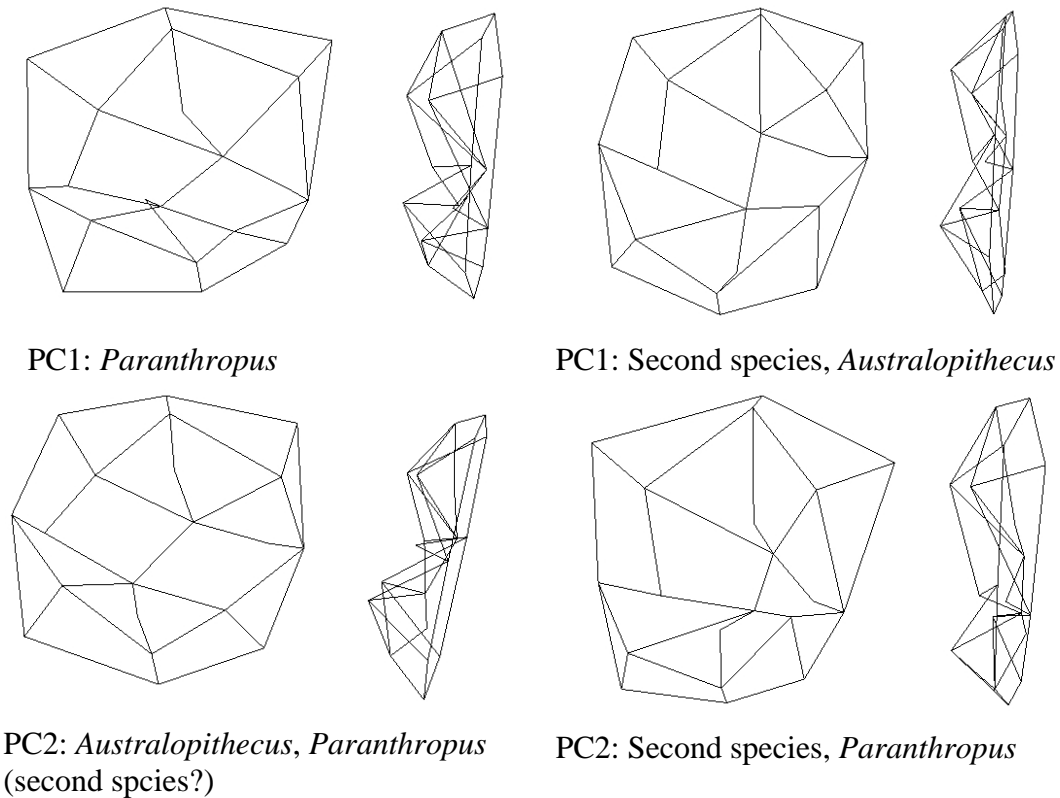


Fig. 9.6 - Wire frame images showing the general morphology of M^3 for the different hominid taxa through the mean shapes at the extremes scores for PC1 (top line) and PC2 (bottom line)

finding is in agreement with what was found by Moggi-Cecchi and Boccone (2007) on the same aspect.

9.4.4 – Remarks on the correlation between size and shape

A significant linear correlation between size and shape for M^1 and M^3 was not found. This can be linked to the well known condition of australopithecine molar crowns where there is a consistent overlap in cusp areas between *Australopithecus* and *Paranthropus* for both tooth typologies. Thus, it is like saying that teeth of approximately the same dimensions can have a substantially different morphology. This phenomenon is also more expressed in M^3 (for which a very low correlation is reported) where the morphological variability is greater.

However, a significant (but not very strong) correlation is shown for M^2 , where other authors did not find a remarkable overlap in crown areas (see Moggi-Cecchi

and Boccone, 2007, for a different point of view). The morphological variation associated to allometry indicates a buccolingual expansion of the distal cusps for bigger teeth. As said above for M¹ and M², this is not confirmed by the analysis on cusps areas conducted by Moggi-Cecchi and Boccone (2007), who observed a relative expansion of mesial cusps in *Paranthropus*.

9.4.5 – Joint first and second molar configurations

This analysis on joint first and second molar configurations was performed on those individuals for which both M¹ and M² were present, namely early *Homo* and “second species”. The results represent a corollary to the outcomes of the analyses conducted on the full sample for M¹, M² and M³. In fact, PC1 separates very clearly the specimens here attributed to the “second species” from those of early *Homo*, whilst, in turn, there is internal unity in the two groups. In conclusion, the outcomes obtained for the M¹ and M² joint landmark configurations gave strength to the results achieved with the other analyses by giving proof of consistency of the methodology applied, where the patterns already found for the same specimens were confirmed.

9.5 – Uncertain attributions

Some of the specimens from Sterkfontein Member 4 (Sts 24a, Sts 37, Sts 56, StW 204, StW 530) were initially considered as *A. africanus* and consequently labeled for the statistical analysis. In fact, some of these teeth (for example Sts 24a and Sts 56 which present small dimensions and crown margins rather vertical) do not exhibit very typical morphological traits that allow for a straightforward

taxonomical attribution. However, the statistical analyses provided some hints on their classification.

Sts 24a and Sts 56 M¹ are placed close to the other *A. africanus* (and early *Homo*). Although PC1 does not discriminate between these two species, PC2 seems to separate Sts 24a and Sts 56 from the second species and place it closer to the group *A. africanus*-early *Homo*.

StW 204 and StW 530 M² are clearly separated from the specimens attributed to the “second species” along PC1. However, PC2 does not discriminate between them and between them and *Paranthropus*, whilst early *Homo* is clearly distinguishable.

Sts 37 M³ is placed within the *Paranthropus* distribution. Nevertheless, nothing can be affirmed with regard to this specimen’s affinity, since the statistical analysis does not clearly separate between all the other specimens as well. The only comment that can be added is that Sts 37 is separated by both PC1 and PC2 from the (other) individuals of *A. africanus*. Provided that the attribution of StW 183 and StW 498a is correct, the specimens belonging to the second species and *A. africanus* overlap along both axes, with *A. africanus* showing a narrower distribution along the negative half of both axes. However, the specimens just mentioned need further comments. The individual StW 183 has been previously regarded as divergent from the typical *A. africanus* (Clarke, 1994; Lockwood and Tobias, 2002; Boccone, 2004; Moggi-Cecchi and Boccone, 2007). The analysis on M² highlighted a morphological affinity to *Paranthropus*; however the result for M³ seems to be not so clear. Nevertheless, it must be noted that this maxillary right M³ was attributed to the individual StW 183 by Moggi-Cecchi, Grine and Tobias (2006), even though it was not found together with its left maxilla and the

left M¹ and M². Thus, the results shown here may suggest that the attribution of this right maxillary molar is incorrect or, alternatively, that the picture observed for M³ is due to the high morphological variability inherent in hominid M³.

The individual StW 498a instead comes from a partly crushed maxilla, thus the evaluation of its morphological features may be difficult. Its third molar presents major damages consisting of a matrix-filled crack which has produced a displacement of parts the crown. Thus, it is hard to say whether there is a bias due to the attribution effectuated here or the result are not reliable due to the damages, or simply the picture presented here reflect the variability typical of third molars.

9.6 – The case of StW 151

StW 151 mixed dentition and cranial remains represent an early hominid recovered at Sterkfontein from the top part of Member 4 or from Member 5 (Tobias, 1983). This specimen has been referred to as *A. africanus* (Smith, 1989), although others (Spor, 1993; Moggi-Cecchi, *et al.*, 1998) considered it to trend towards early *Homo* condition. They found that cranial (Spor, 1993) and both cranial and dental morphology, and dental developmental pattern (Moggi-Cecchi, *et al.*, 1998) show a number of features that have been described as characteristic of *A. africanus* (Robinson, 1956; Grine, 1984), whilst they lack those morphological specialized features proper to *Paranthropus*. However, Moggi-Cecchi, *et al.* (1998) identified also some key traits that make of it a more derived hominid than the rest of the sample from Sterkfontein Member 4.

First and second upper molars (the latter still unerupted) were included in the geometric morphometric analyses performed for the present project in the effort to investigate the variability among Sterkfontein Member 4. In both analyses StW

151 clusters together with the other specimens of early *Homo*; moreover, where *A. africanus* and early *Homo* sets quite close to each others or even overlap, StW 151 is still separated from *A. africanus*, namely in being placed more towards the extremity of the axis further from the specimens of *A. africanus*. Even though this analysis was not conceived for the study of the variability within early *Homo* maxillary molars, nor does it include a sufficient number of early *Homo* specimens, it brings support to the hypothesis of the stronger morphological affinities of StW 151 with early *Homo* rather than *A. africanus*.

9.7 – Morphological variability within *Paranthropus*

As mentioned above, the range of variability of *Paranthropus* is quite wide compared to that shown by the other hominids under study. Moreover, it is wider towards the distal row, along both the first two principal components. Some observations with regards to the debate about the occurrence of one or more species of *Paranthropus* in the South African sites (see Kaszycka, 2002 for a general review) will be given as follows.

The specimens from Swartkrans present a marked scattering along the axes, whilst the individual from Kromdraai is placed within this dispersion and does not show a particular trend (such as clustering together or being placed toward an extremity of the distribution ...). Thus, this analysis does not show evidences in support of a taxonomic distinction within the South African *Paranthropus*. However, further investigation may be necessary in order to highlight those cranial and dental differences that some authors (Robinson, 1954b for distinction at subspecific level; Howell, 1978; Grine, 1981; 1982; 1984; 1985) considered diagnostic for the taxonomic distinction.

The specimen CD 5774 (M²) from Cooper's Cave is placed within the distribution of *Paranthropus*, as has been considered by de Ruiter, *et al.*, (2009) who confidently placed this fossil remain into the species *P. robustus* (*A. robustus* for the authors).

CHAPTER 10

CONCLUSIONS

The issue of the high morphological variability observed among the fossil recovered from Sterkfontein Member 4 and Makapansgat Limeworks sites has attracted the attention of many researchers and has been investigated through different approaches. The polymorphism of *A. africanus* was explained in several ways as different authors have had diverse viewpoints on the matter (Broom, 1947; Johanson and White, 1979; White, *et al.*, 1981; Rak, 1983; Clarke, 1985a,b; 1988; 1994; 1996, 2008; Kimbel and Rak, 1993; Clarke, 1994; 1996; Moggi-Cecchi, *et al.*, 1998; Lockwood and Tobias, 2002). Among these authors, Clarke explained the phenomenon hypothesizing the occurrence of a new *Paranthropus*-like australopithecine species at Sterkfontein Member 4 and Makapansgat. However, there is still an outstanding debate surrounding the matter since there is not a general consensus with regard to the number of specimens that diverge from the typical *A. africanus*, the anatomical features that must be considered and the reason underpinning the variability itself (i.e., individual variation, sexual dimorphism, change through time and occurrence of a further hominid species - either known or new - other than *A. africanus*).

Since the dental features of early hominids are crucial to the interpretation of their phylogenetic position, their morphology and metrical characteristics have been widely investigated (see Robinson, 1956; Johanson, *et al.*, 1982; Tobias, 1991; Wood, 1991; Ward, *et al.*, 2001 among the others). However, previous studies

aimed at elucidating the matter of a new australopithecine species at Sterkfontein Member 4 and Makapansgat and based on statistical, quantitative analyses have led to conflicting (Calcagno, *et al.*, 1997; 1999) or preliminary results (Moggi-Cecchi, 2003; Moggi-Cecchi, *et al.*, 2006; Moggi-Cecchi and Boccone, 2007). That is due to the inadequacy of the methods utilized in describing a complex three-dimensional shape such as that of teeth.

The present project was specifically designed in order to investigate the high variability observed within the *A. africanus* hypodigm through the study of maxillary molars. Moreover, it was conceived in such a way to overcome the limitations proper to other analytical methods. First of all, it used high resolution, three-dimensional images obtained from CT-scan, which represent accurate substitutes of the original teeth. Moreover, by means of this kind of images the problem related to the use of a digitizer for small objects such as hominid teeth was overcome and the three-dimensionality of teeth was preserved. Secondly, a deep investigation of the dental sample was carried out by applying geometric morphometrics, since the latter combines the advantages of both a statistical analysis and a qualitative evaluation of an object shape (molar crown shape in this case).

The methods were considered adequate after testing them on a sample formed of maxillary molars of two taxonomic groups (early *Homo* and *Paranthropus*), which distinction is widely accepted by the scientific community. Thereafter, these methods were applied to a wider sample of maxillary molars from Sterkfontein Member 4, Makapansgat, Swartkrans, Kromdraai and Cooper's Cave in order to investigate their variability and morphological characteristics.

Among M¹, M² and M³, the first two subsamples provided clear evidences of the variability expressed in terms of crown gross morphology. All the specimens considered as candidate for the “second species” (Clarke, 1988; 2008; and personal communication) were discriminated from those regarded as *A. africanus s. s.* through Principal Component Analysis performed on the Procrustes residuals. Conversely, the picture showed by M³ was not so clear, possibly due to the remarkable morphological variability inherent in hominid M³, even though for some specimens other specific causes were discussed.

Important considerations and remarks with regard to the variability expressed by the hominid under study have been given here. This research has provided a further demonstration of the occurrence of a different morphotype in Sterkfontein Member 4. By contrast, the possibility of individual variation and sexual dimorphism are not convincing.

However, it is suggested that the variability observed in the maxillary molar sample studied here should be further investigated and compared to that shown by other closely related taxa. In addition, complementary studies aimed at ascertaining the taxonomic relationships between the two morphotypes in Sterkfontein Member 4 are desirable.

This research provided many additional results with regard to the molar crown morphology of the hominids under study through the use of geometric morphometrics. The latter has represented an outstanding upgrade of this project respect to previous studies. The variance explained by every component was physically observed through the visualization features built from *Morphologika*

software, thus the main morphological differences between taxa were fully highlighted.

Most of these outcomes confirmed the conclusions of previous studies conducted through other methodological approaches (descriptive analysis and metrical analysis: Robinson, 1956; Sperber, 1974; appraisal of crown areas and cusp proportions: Wood and Engleman, 1988; Moggi-Cecchi and Boccone, 2007).

These findings are resumed as follow:

- broadly similar molar crown morphology between the “second species” and *Paranthropus*
- broadly similar molar crown morphology between *A. africanus* and early *Homo*
- Small occlusal basin relative to the crown profile in *Paranthropus* and the “second species” (evident especially for M²)
- M¹ and M² in *A. africanus* and early *Homo* are narrower than in *Paranthropus* and the “second species”
- Greater contribution of Pr to the total crown area of M¹ in *A. africanus*
- Greater contribution of Pa to the total crown area of M¹ in *Paranthropus* and the “second species”
- greater contribution of buccal cusps to the total crown area in *Paranthropus* and “second species” respect to *A. africanus* and early *Homo*
- relative increase in size of mesial cusps for M² and M³ in *Paranthropus* and the “second species”
- remarkable variability of M³ especially in *Paranthropus*

- morphological variability within *Paranthropus* not related to the different site of provenience
- strong affinities between StW 151 and the others specimens classified as early *Homo*

Beside the importance of the data itself, it is remarkable that the methodologies applied here are able to effectively capture the significant features of the hominid dental morphology and therefore discriminate among them.

In conclusion, through the procedures applied it has been possible to effectively highlight the gross morphology of hominid molar crowns. The results achieved with this research not only have found a wide correspondence with those of previous works, but most importantly have added valuable information on the matter: this research substantially contributed to the debate surrounding the high variability observed in the *A. africanus* hypodigm, providing new evidences of the occurrence of a second species in Sterkfontein Member 4.

APPENDIX A

Maxillary molar morphology in the taxa under study

The following review on maxillary molar morphology is mainly based on the 1956 account by Robinson, who mainly focused on the South African remains available at that time from the sites of Swartkrans, Kromdraai, Sterkfontein and Makapansgat. Robinson considered the specimens from the first two sites as representative of the genus *Paranthropus*, and the others as representative of the genus *Australopithecus*. However, the findings of other authors which integrate and sometimes contradict Robinson's view are here included as specified when it is the case.

Maxillary molar morphology is rather uniform among hominids. They are all built upon a same fundamental structure being formed of four main cusps, of which three constitute the trigon, and one is clearly separated from them and represents the talon. Among hominids, *Homo sapiens* shows the greatest tendency of reduction in cusp number, especially in the distal row. However, in maxillary molars small additional cusps (capsules) may occur such as those placed in the back of posterior fovea or along the mesial margin. The main cusps are low and rounded, with the hypocone generally lower than the other cusps. However, Robinson (1962) and Clarke (1996) go farther defining the features that characterized the genus *Paranthropus* and claim that the cusps of *Paranthropus* cheek teeth are more low and bulbous, and situated toward the centre of the crown

than in any other hominid genus; moreover, they found the cheek teeth of this genus are characterised by the formation of flat wear surfaces and smoothly rounded borders between the occlusal surface and the sides of the crown. As assessed by these authors and stressed by Wood (1994) the dentition of *Paranthropus* possesses specialized features (more marked in *P. boisei*) unknown in other genera of the same family which reflect a different adaptation and feeding behaviour.

However, the most evident differences between maxillary molars of *Paranthropus* and *Australopithecus* are in both absolute size and relative sizes of M² and M³, as discussed by Robinson (1956) and reported below. The mean values for breadth and length of *Australopithecus* are smaller than those for *Paranthropus*. Absolute values for M¹ and M³ show little overlap between the two genera, though the overlap is more marked for M². One of the most remarkable differences between the two genera is that M³ is always bigger or at least equal than M² in *Paranthropus*, while in *Australopithecus* it is just the reverse. However, within molars of the same side of a certain individual, in *Paranthropus* M³ is always bigger than M², while it can be from smaller to slightly bigger in *Australopithecus*. In turn, M² is always bigger than M¹ in both genera. These results were confirmed by Sperber (1974), Wood and Engleman (1988) and Moggi-Cecchi and Boccone (2007) who found a considerable overlap in size and shape between *Australopithecus* and *Paranthropus*; but did confirm the size dominance of M³ in *Paranthropus*. Contra Sperber, the results provided by Wood and Engleman suggest also a significant variation in the shape of M¹ between the

two genera, where the first molar of *Australopithecus* appears narrower than that of *Paranthropus*.

In summary, the molar size order is $M^1 < M^2 \leq M^3$ in *Paranthropus*, while it is $M^1 < M^2 \geq M^3$ in *Australopithecus*; conversely, the molar size order in modern humans is $M^1 > M^2 > M^3$ where this pattern seems to have taken rise gradually with the appearance of the genus *Homo* (Robinson, 1956; Sperber, 1974; Wood and Engleman, 1988; Moggi-Cecchi and Boccone, 2007). Moggi-Cecchi and Boccone stated that the differences in the molar sequences between *Australopithecus* and *Paranthropus* seem to be related mostly to a different expansion of mesial cusps, which in *Paranthropus* show a progressive increase in size from M^1 to M^3 .

M^1 and M^2 have a general shape of an equal-sided parallelogram which is progressively more skewed along the tooth row (Robinson, 1956). However, in M^3 the variability is much stronger than in the first two molars, and is extreme in *Paranthropus* where teeth can also be aberrant and have a triangular profile due to a remarkable reduction of distobuccal angle.

In both *Paranthropus* and especially *Australopithecus* the protocone is the largest cusp, and in M^1 the other cusps are sub-equal in size, or sometimes metacone is clearly bigger; however, the metacone progressively reduces from M^1 to M^3 of the same individual and, as mentioned above, in *Paranthropus* M^3 a strong reduction of metacone may occur. Moggi-Cecchi and Boccone (2007) confirmed that the crown base areas are similar in the two genera, and that in M^1 the protocone is significantly larger than in *Paranthropus*. However, they also found that the paracone of M^1 and the protocone of M^2 and M^3 are generally larger in *Paranthropus*.

Beside the differences in shape and dimensions, the maxillary molars of the two genera also present structural variation (Robinson, 1956). One of the features that distinguished between the two genera is the Carabelli complex. Although the Carabelli complex is usually present in both genera, in *Paranthropus* it is often expressed in the form of a small but deep mesiolingual pit associated with several shallow grooves, whilst in *Australopithecus* it is more strongly developed and can be represented by a partial or complete protoconal cingulum. Both Sperber (1974) and Wood and Engleman (1988) confirmed the occurrence of a marked expression of the Carabelli trait in *Australopithecus* than in *Paranthropus* and observed a greater divergence in the expression of this feature in the distal row.

Another dental feature discussed by Robinson (1956) is the buccal groove which is strongly developed in *Paranthropus*, especially in M¹; where it is usually short and terminates abruptly in a pit which can be smooth or edged. Conversely, *Australopithecus* shows a not very marked groove that goes all the way down to the enamel line and ends on a slightly thickened region of enamel.

Another distinctive feature of *Australopithecus*, Robinson (1956) found on a slight parastyle (a protuberance on the mesiobuccal angle of the paracone occlusal surface) which is characteristic of *Australopithecus* but unknown in *Paranthropus*.

In both genera, M³ shows a high degree of variability, though this is more pronounced in *Paranthropus*. The enamel surface is often crenulated, but it is easily smoothed down with a slight wear. Deep accessory grooves and cuspules may alter the characteristic molar structure.

The typical fissure pattern of maxillary molars is simple and symmetrically triradiated in M¹. However, this pattern is variable in the tooth row and can be more complicated in M³. In *Australopithecus*, M³ presents a complex fissure pattern where a U-shaped mesial groove causes the formation of an extra cusp from the protocone. The hypocone may also be subdivided into two cusps.

While a posterior fovea is always present in the maxillary molars of the two genera, differences appear with regard to the anterior fovea. *Paranthropus* does not have a true anterior fovea, although a depressed area is present in the region of interest and the buccal limb of the foveal groove is generally well developed; conversely, *Australopithecus* may or may not show a true anterior fovea.

A certain degree of variability is also present for the trigon crest which connects the protocone and the metacone, but differences in the two genera are not significant (as corroborated by both Sperber, 1974 and Wood and Engleman, 1988), since it can be from poorly to well develop both in *Paranthropus* and *Australopithecus*.

The root system of maxillary molars among hominids is quite uniform and present two buccal and one lingual roots. In both *Paranthropus* and *Australopithecus* there is not a tendency to reduction or fusion and the roots can raise straight or bent distalward. However, aberrant roots may be present in the genus *Homo*, where reduction and fusion is present and is greater toward the end of the distal row.

APPENDIX B

Experiment on animal teeth: testing the risk of enamel damage related to the use of the standard and extra fine tips of the digitizer

In a preliminary stage of this project, I considered the possibility to collect the landmarks directly on the fossils, in order to obtain reliable models of the teeth. It is probably very clear that sampling single points on a surface cannot be dangerous for a fossil specimen. Nevertheless, for the description of the tooth crown in its wholeness, it is necessary to collect landmarks also on its sides (see appendix C for further details). The possibility that the sharp tip of the digitizer could cause some damages on the fossil tooth surface (namely scratches and microwear) was advanced by Dr. Charles A. Lockwood (personal communication).

Preventively, a trial on animal fossil teeth had been done. One tooth of *Gazela vanhoepeni*, from Makapansgat (specimen M8612), and one tooth of *Theropithecus oswaldi*, from Cooper's Cave (specimen CD17753), belonging to the non-Hominid Fossil Collections of the University of the Witwatersrand (housed in the Bernard Price Institute for Paleontological Research), have been photographed before and after the use of the digitizer, equipped, respectively, with the extra fine tip and the standard tip.

The surfaces involved were observed through an OLYMPUS optic microscope at 50X magnification and photographed with an OLYMPUS digital camera. The

equipment was provided by the Department of Archaeology, University of the Witwatersrand and operated by Dr. Geeske Langejans. Comparing the pictures taken (Figure B.1) there is no evidence that any microwear traces or scratches were left on the enamel from the passage of the digitiser tip on the surface. On the contrary, it is very clear the occurrence of a scratch on the layer of Paraloid with which the *Gazela* tooth had been previously treated.

In conclusion, I am able to state that this procedure for data collection cannot consistently damage the enamel. I consider it to be safe for application in further studies on fossil crown specimens.



Fig. B.1 – a. Portion of the tooth surface of the specimen CD17753, *Theropithecus oswaldi* from Cooper’s Cave before the use of the extra-fine tip. b. Same area of the tooth enamel after the use of the microscribe: no traces or damages are visible on the surface. c. extra-fine tip pointing out the scratch left on the Paraloid that covers the surface of the tooth specimen M8612, *Gazella vanhoepeni* from Makapansgat

APPENDIX C

Casting procedures for tooth replicas

The CT-scans were mostly done on the original fossils except for fewer cases where the casts needed to be used. In some instances the cast was already available for replacing specimens that were damaged for the purposes of previous researches (namely, SKX 268, StW 280, StW 402).

For some of the specimens stored at the Transvaal Museum it was necessary to produce replicas being them fossils of particular interest or type specimens. In particular, SK 48 (LM²-M³) is the most complete skull of *P. robustus*, SK 49 (RM²-M³) a quite fragile specimen, TM 1511 (RM³) is the holotype of *A. transvaalensis* (new *A. Africanus*), TM 1517a and TM 1517b (both RM³) are the type specimens of *P. robustus*.

For this purpose, I found suitable the use of a silicone putty with high accuracy and very low degree of deformation, not only for the reliability of the casts, but also for the safety of the fossils. A material such as President® micro light body renders a very accurate mould penetrating even in the smallest interstices, but at the same time once dry, neither sticks to the surface nor leaves greasy residues. Being very soft and flexible it is easily and safely removable from the original. The mould is to be strengthened by applying a thick layer of President® putty which keeps it firm and protected. The cast itself is produced with a two-component epoxy resin which ensures a high quality cast.

A criticism that can be advanced is the lack of accuracy. The answer comes from a test recently made by Prof. J. Moggi-Cecchi and Dr. S. Boccone (personal communication), who verified the reliability of different casting materials and recommend the aforementioned ones. Moreover, the same casting techniques and materials are currently in use for the creation of high resolution casts for the purposes of studies based on three-dimensional objects (Fiorenza, *et al.*, 2009). It is noteworthy that these materials are also preferred for their accuracy from the Prosthodontics Department, at the Oral Health School (Prof. C. P. Owen, personal communication) where dental prostheses should be made with the greatest definitiveness for patients' comfort and health.

APPENDIX D

Landmark collection: image gallery

The procedure applied for the identification and sampling of the points used for tooth alignment and landmark collection are shown below in a series of snapshots (specimen StW 252L, LM3). The views presented reflect those useful for the detection of each point which could be the axial and/or frontal and/or sagittal and three-dimensional views.

The images show 2 cross-like marks in the proximity of each landmark. The green one represents the choice of the operator, while the red one is the point sampled with the help of the software tool “two-dimensional auto snap”. This function joins the cursor to the first pixel(s) available in the nearness of the point manually selected.

Tooth alignment

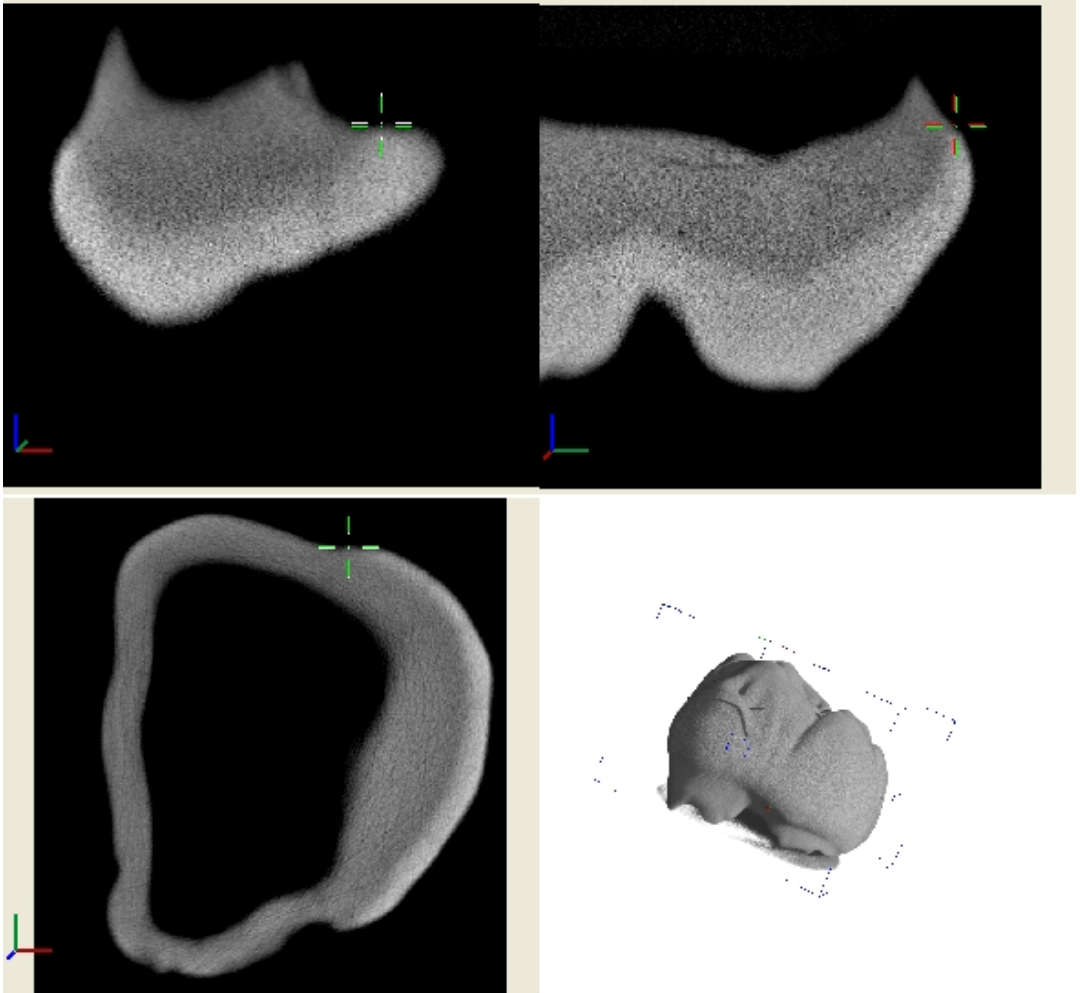


Fig. D.1 - Point i. Palatal aspect

Tooth alignment

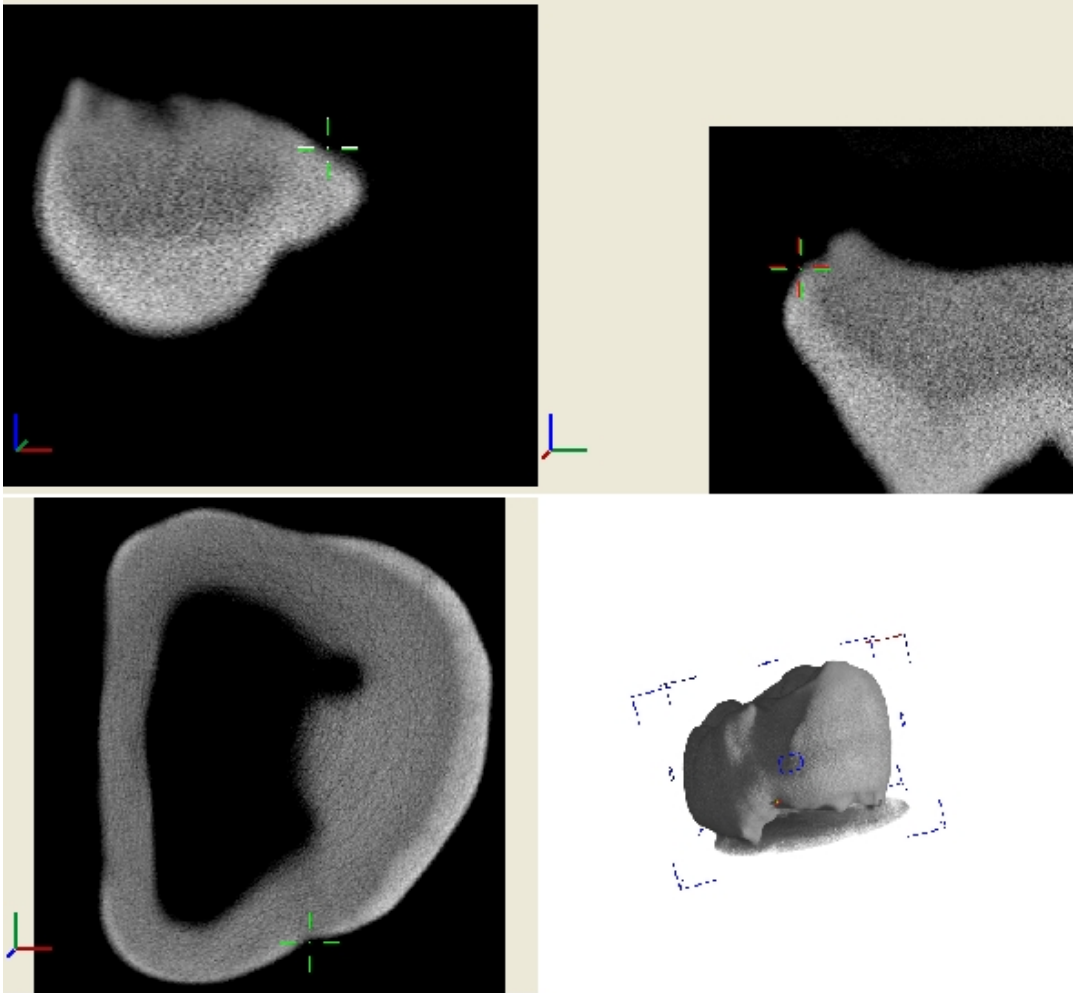


Fig. D.2 - Point ii. Buccal aspect

Tooth alignment

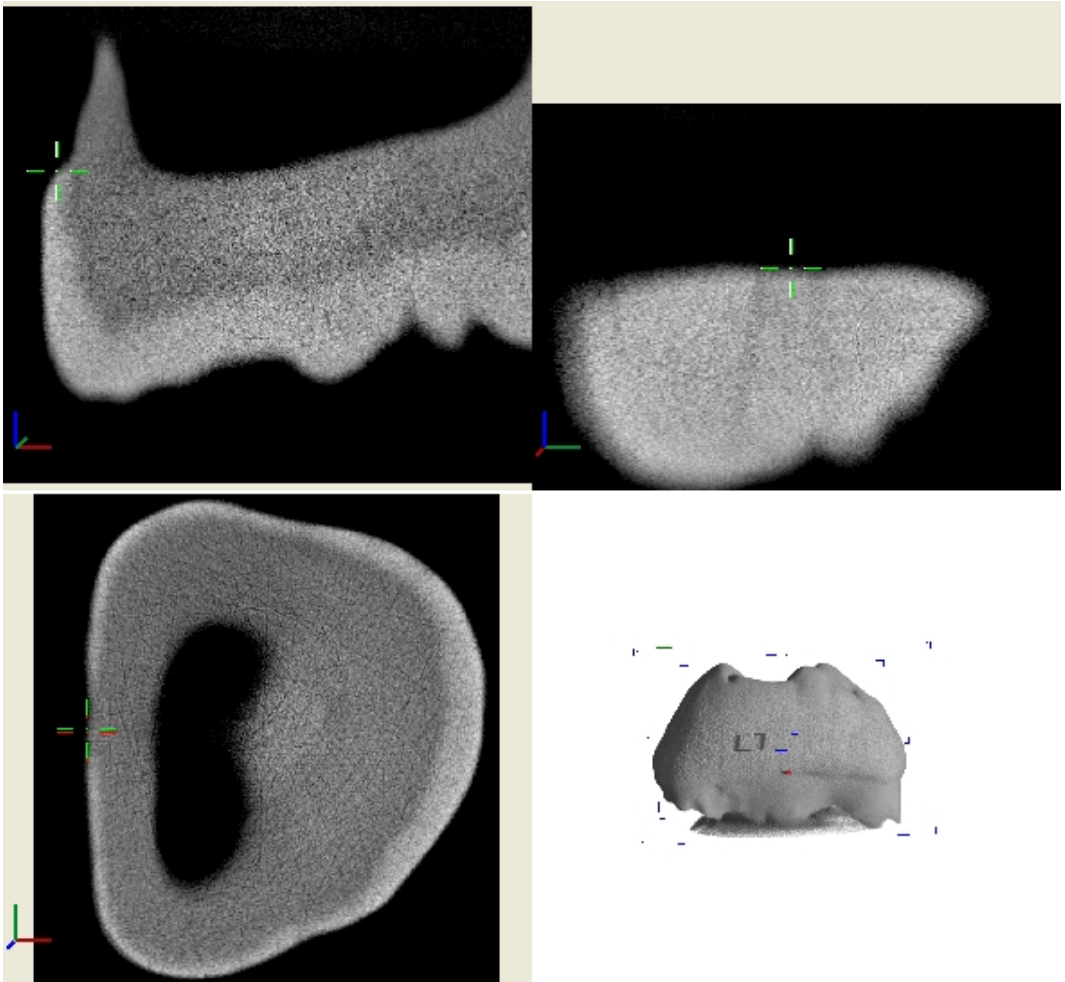


Fig. D.3 - Point iii. Mesial aspect

Tooth alignment

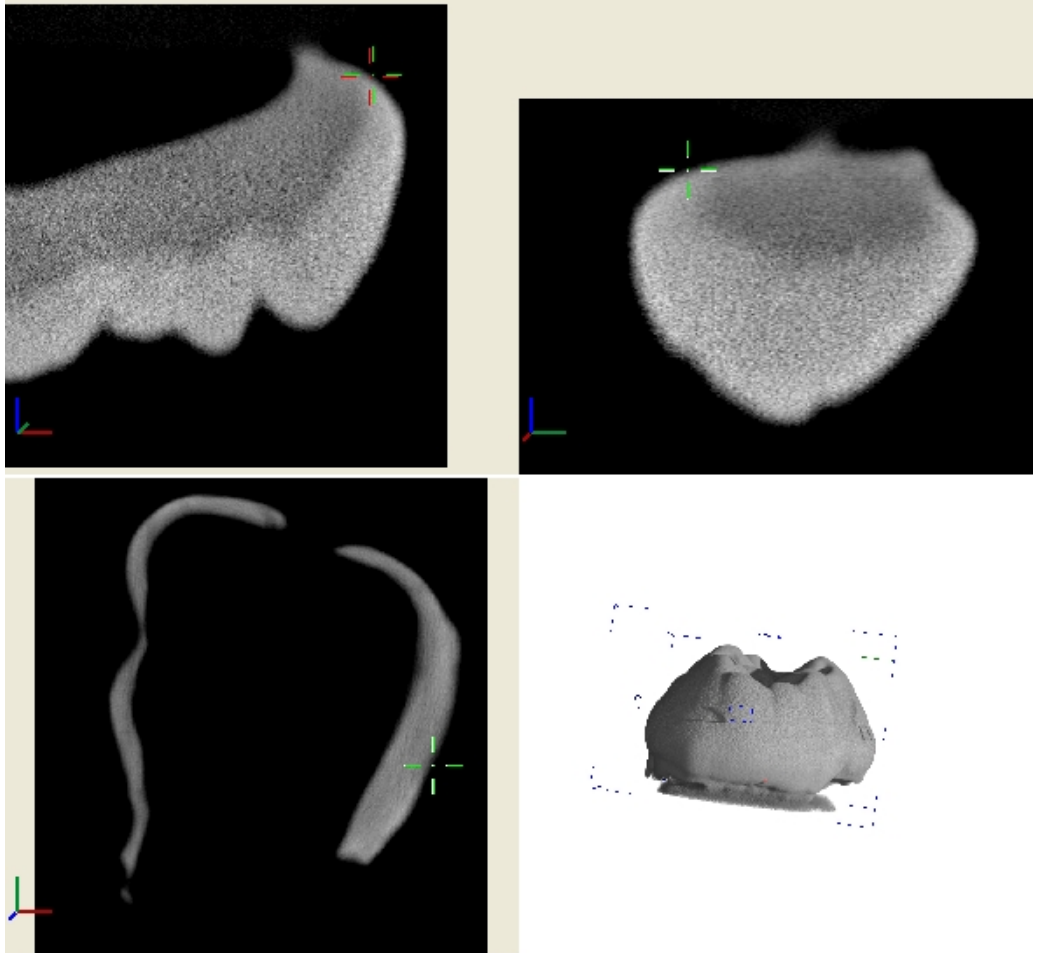


Fig. D.4 - Point iv. Distal aspect

Tooth alignment

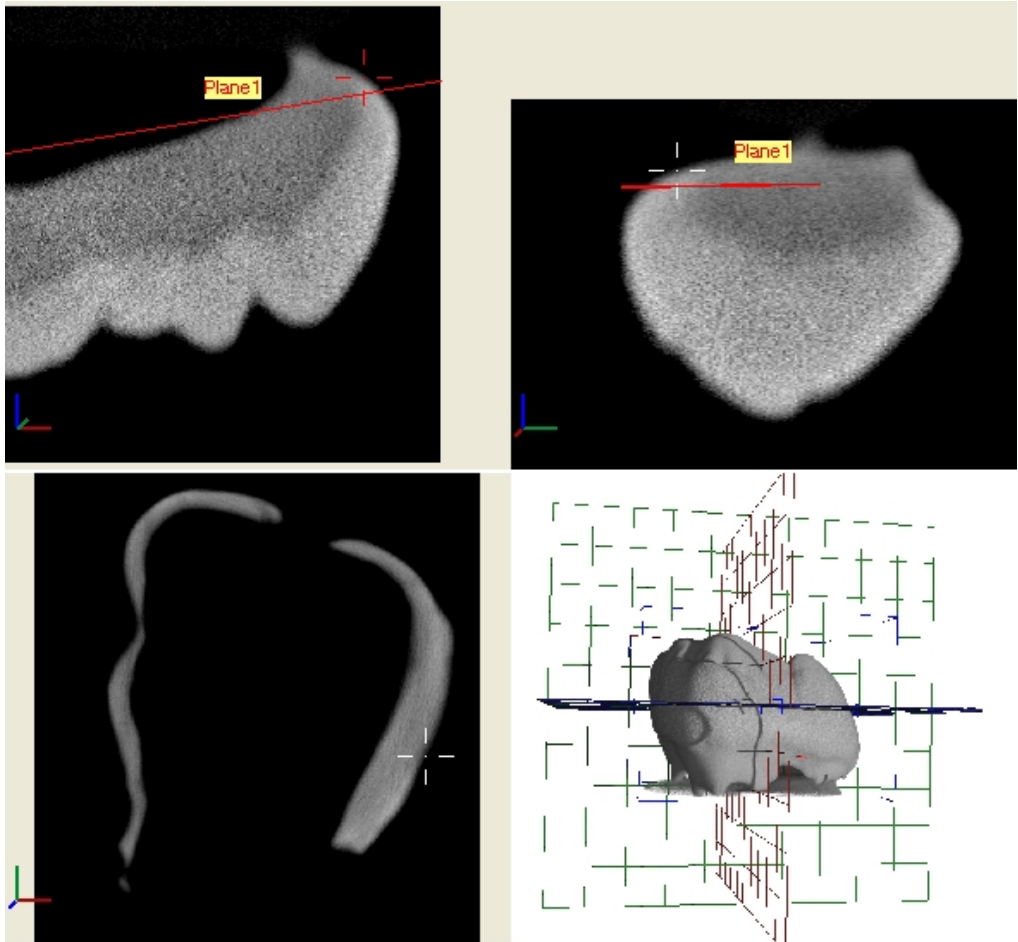


Fig. D.5 – Tooth image before alignment

Tooth alignment

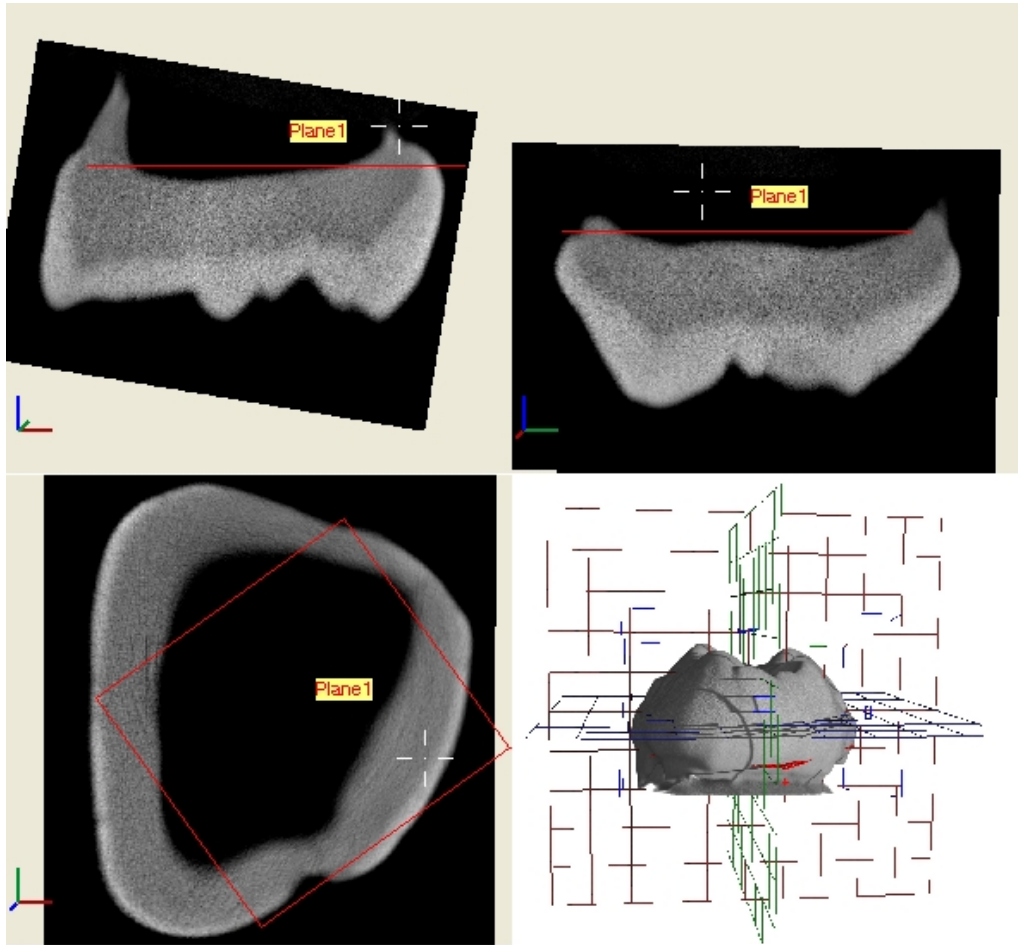


Fig. D.6 – Tooth image after alignment

Landmark coordinates sampling

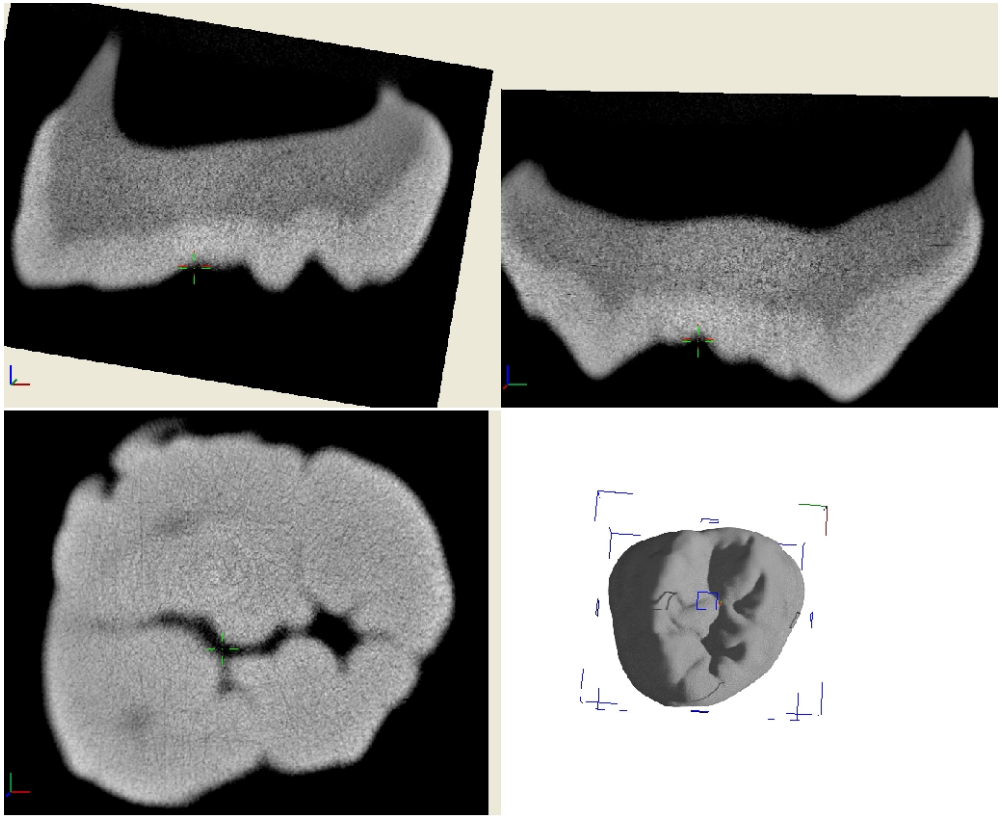


Fig. D.7 - P1. Lowest point of central fossa

Landmark coordinates sampling

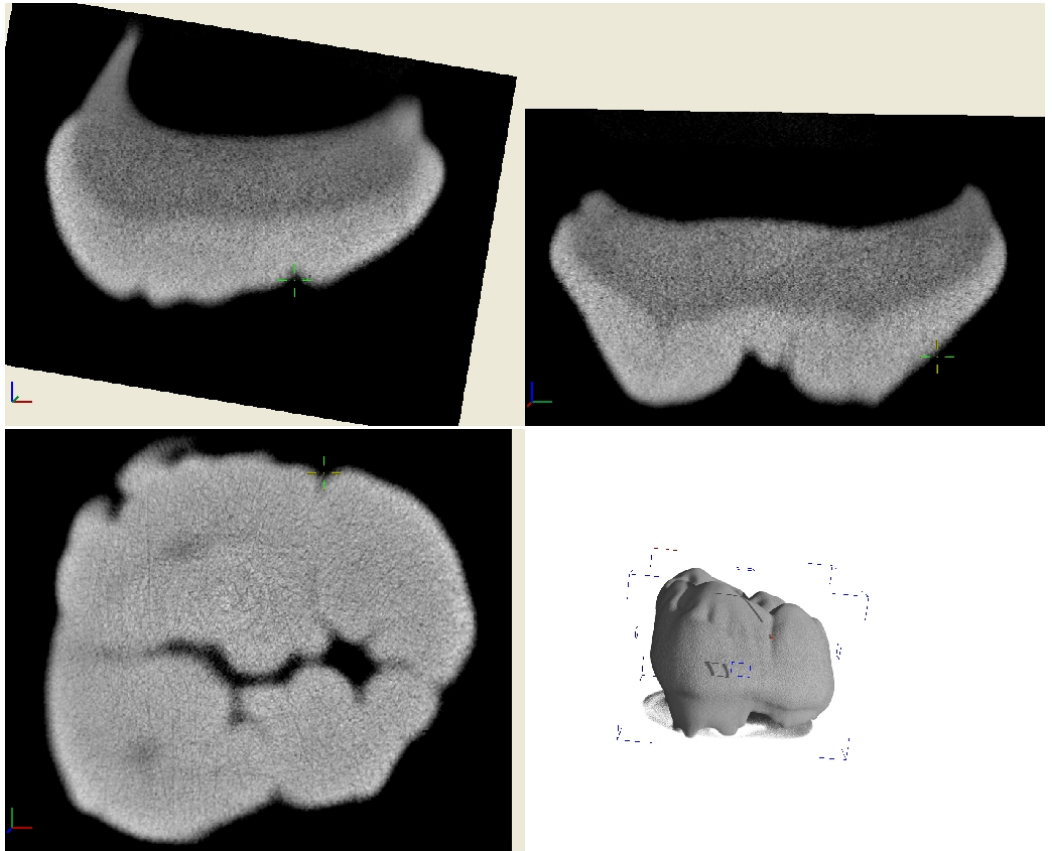


Fig. D.8 - P2. Contact between Pr-Hy on the plane P1 outline

Landmark coordinates sampling

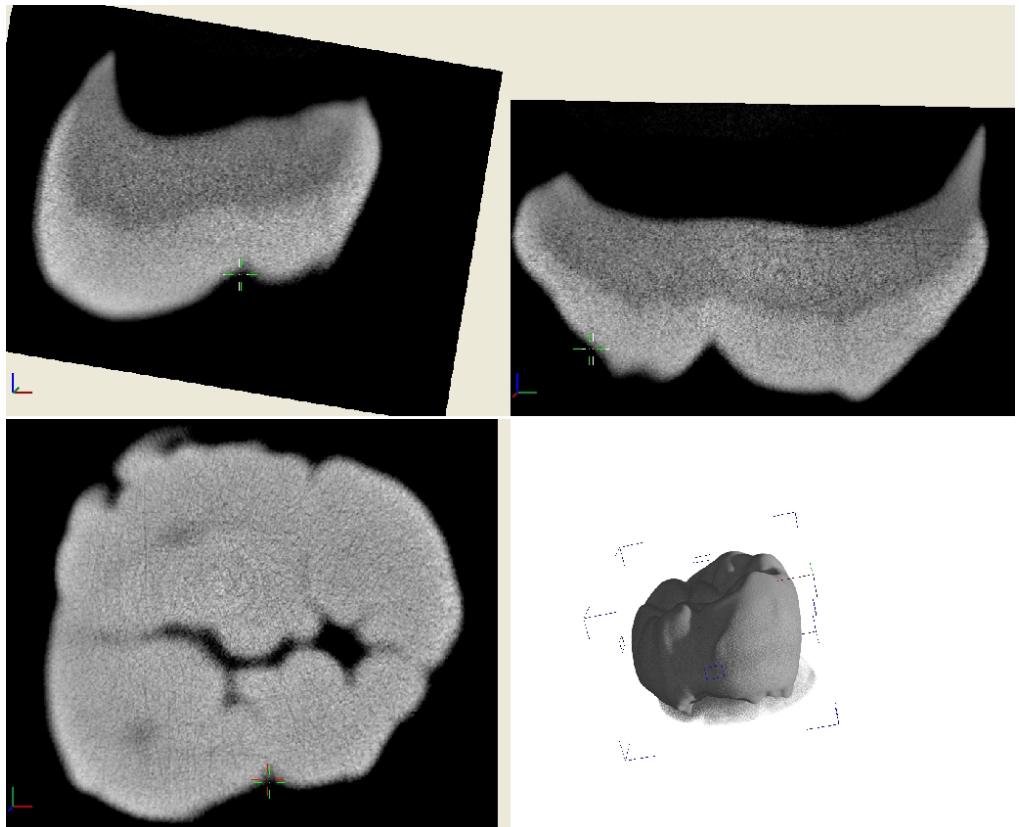


Fig. D.9 - P3. Contact between Pa-Me on the plane P5 outline

Landmark coordinates sampling

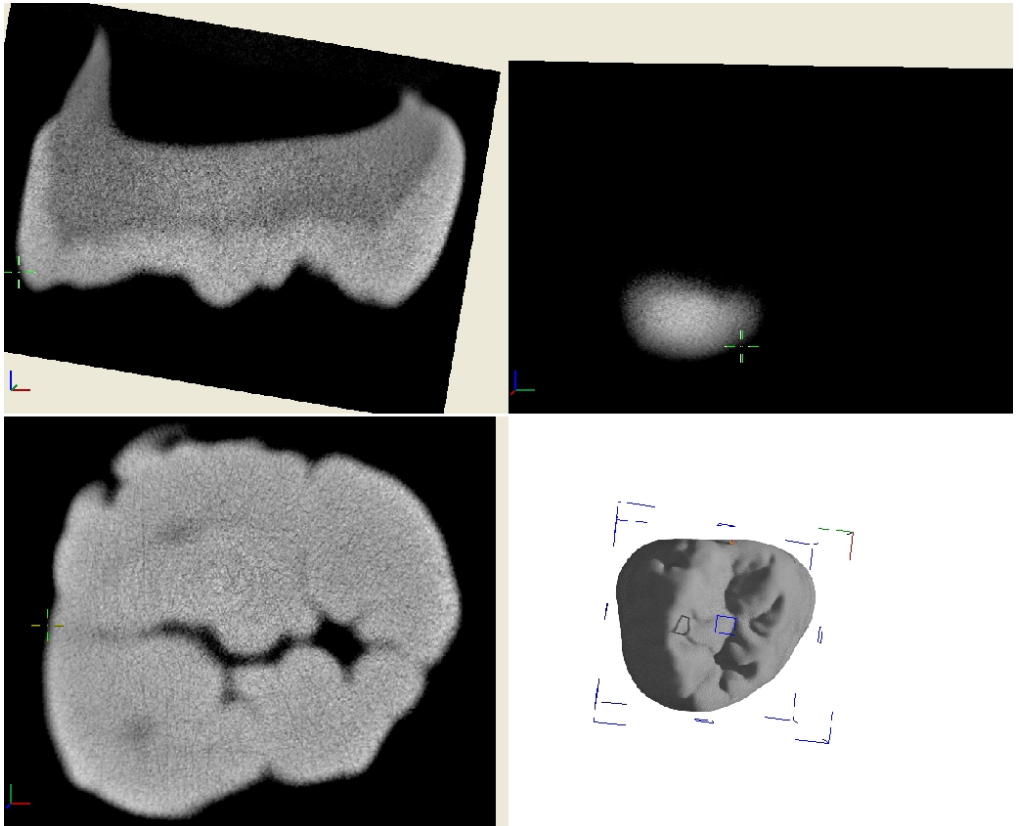


Fig. D.10 - P4. Contact between Pr-Pa on the plane P5 outline

Landmark coordinates sampling

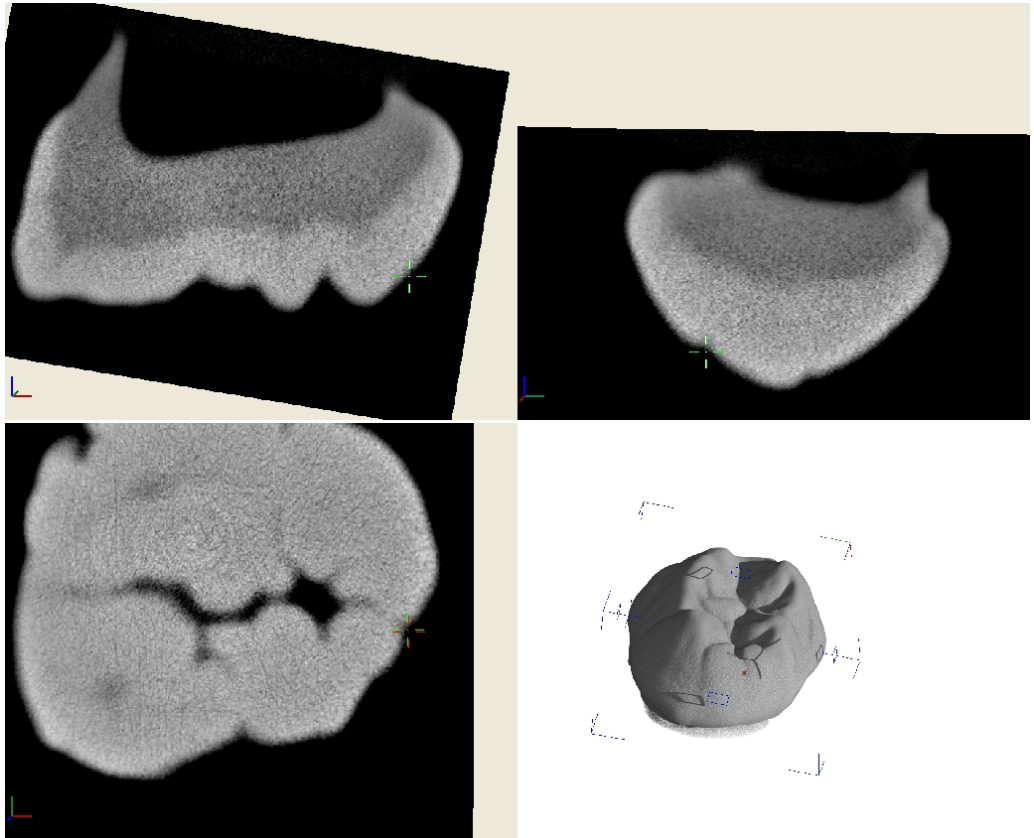


Fig. D.11 - P5. Contact between Hy-Me on the plane P5 outline

Landmark coordinates sampling

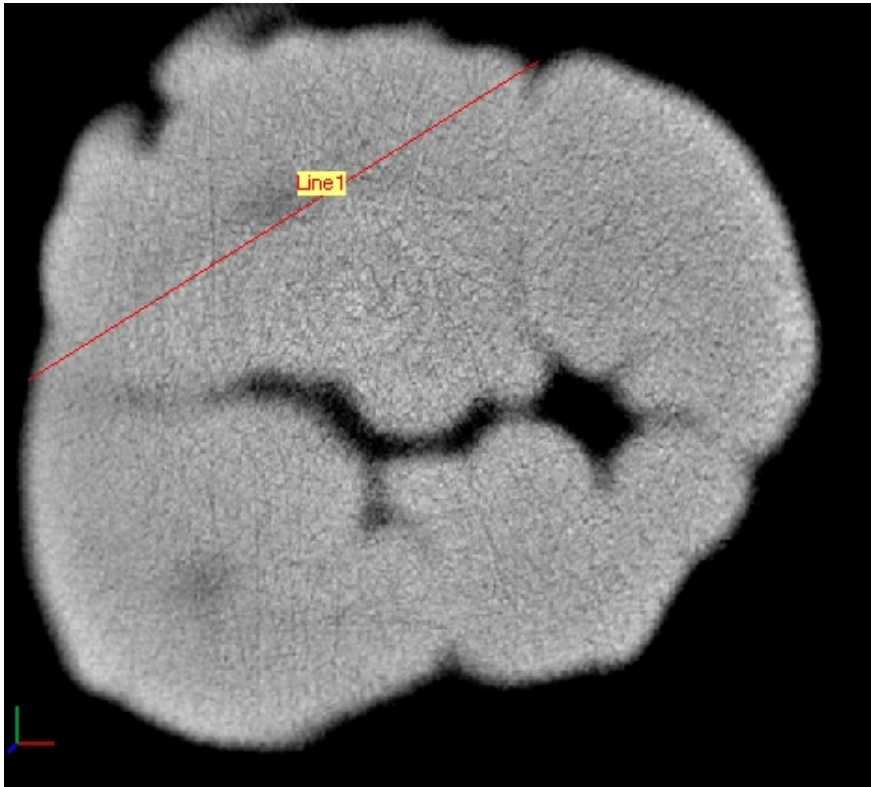


Fig. D.12 - Line 1 (connecting P2-P4)

Landmark coordinates sampling

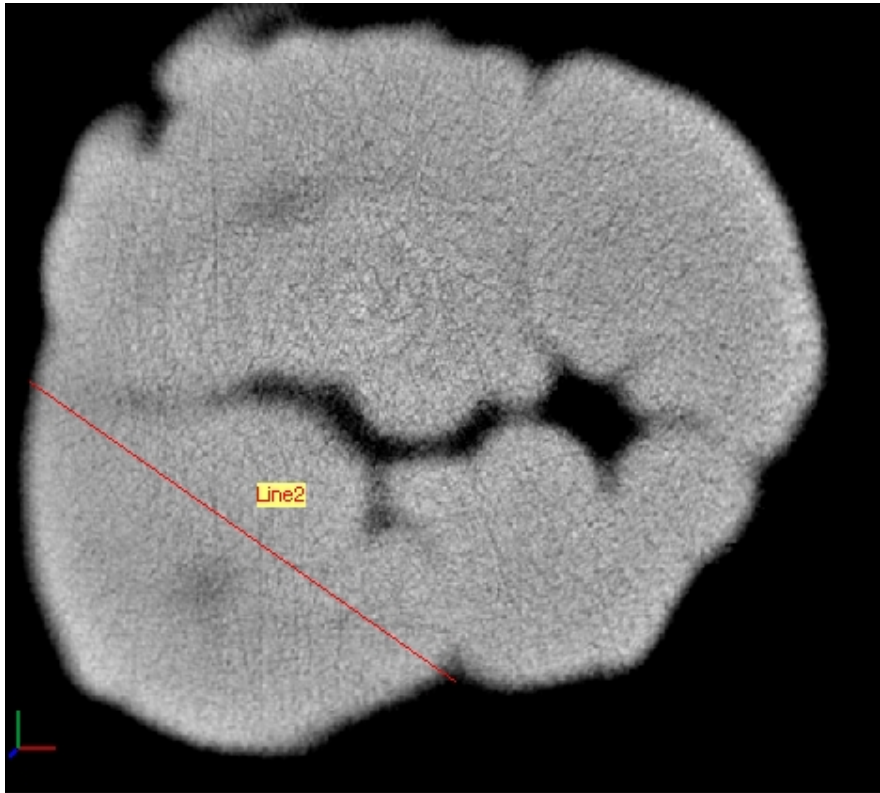


Fig. D.13 - Line 2 (connecting P4-P3)

Landmark coordinates sampling

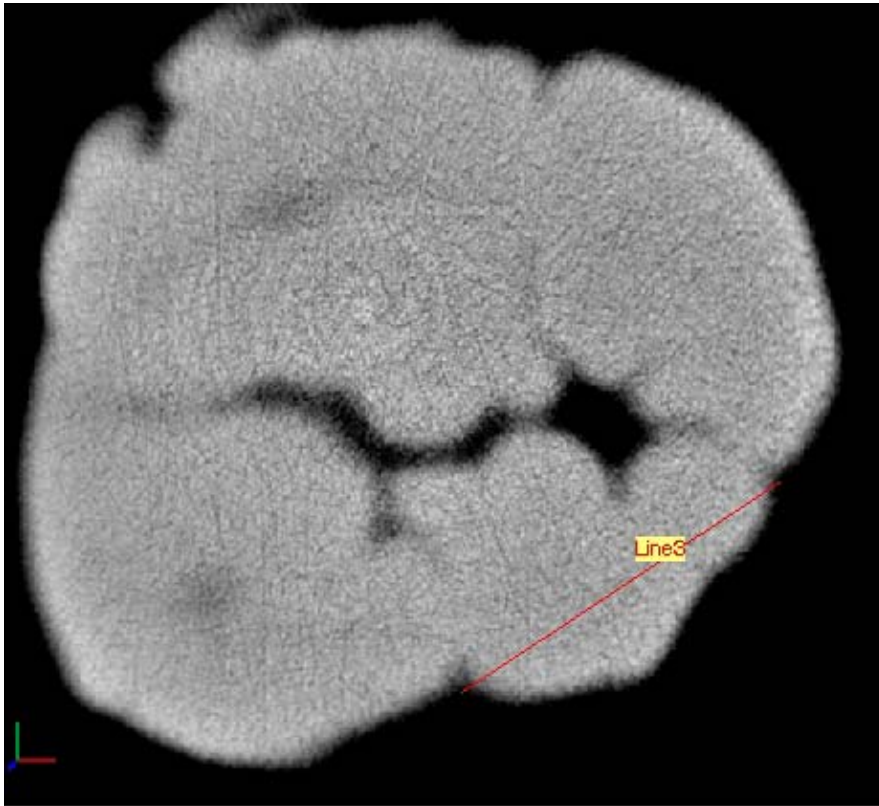


Fig. D.14 - Line 3 (connecting P3-P5)

Landmark coordinates sampling

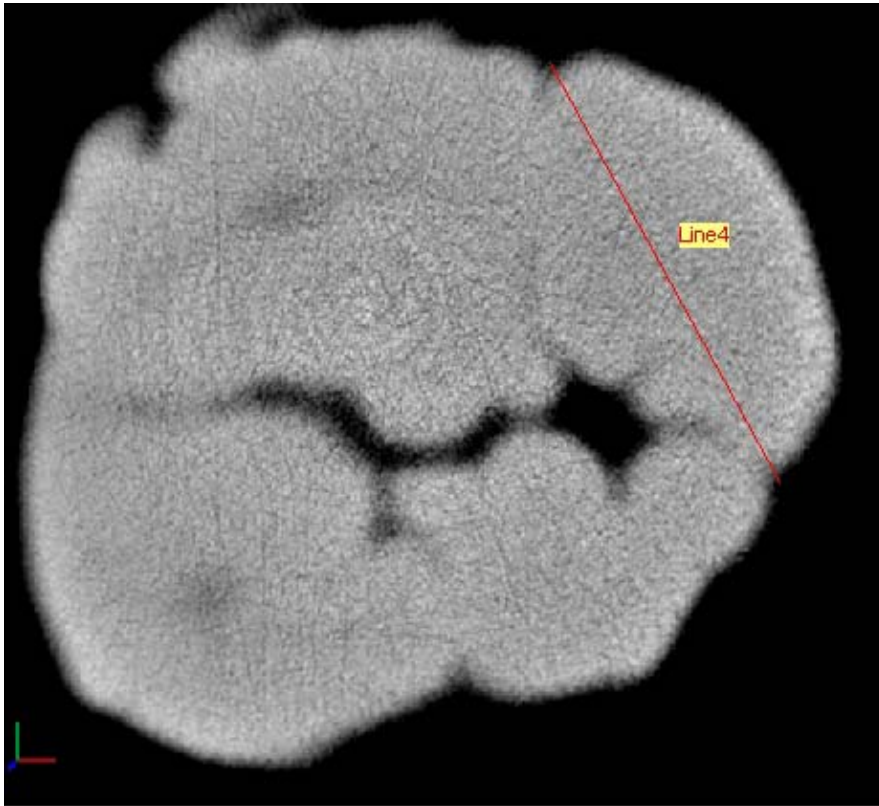


Fig. D.15 - Line 4 (connecting P5-P2)

Landmark coordinates sampling

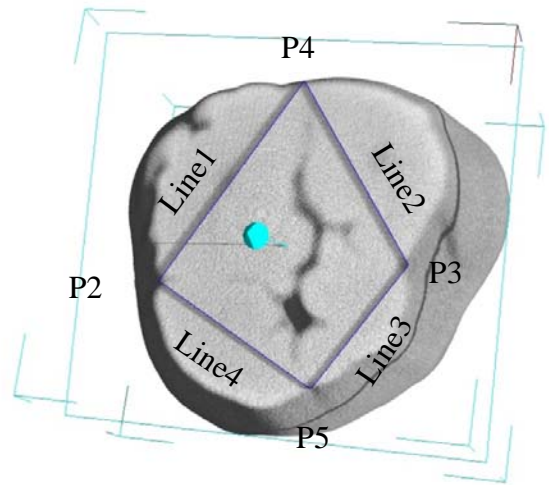
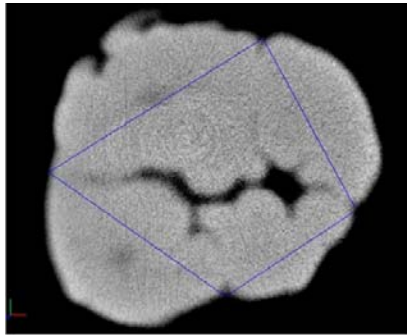


Fig. D.16 - Lines 1-4

Landmark coordinates sampling

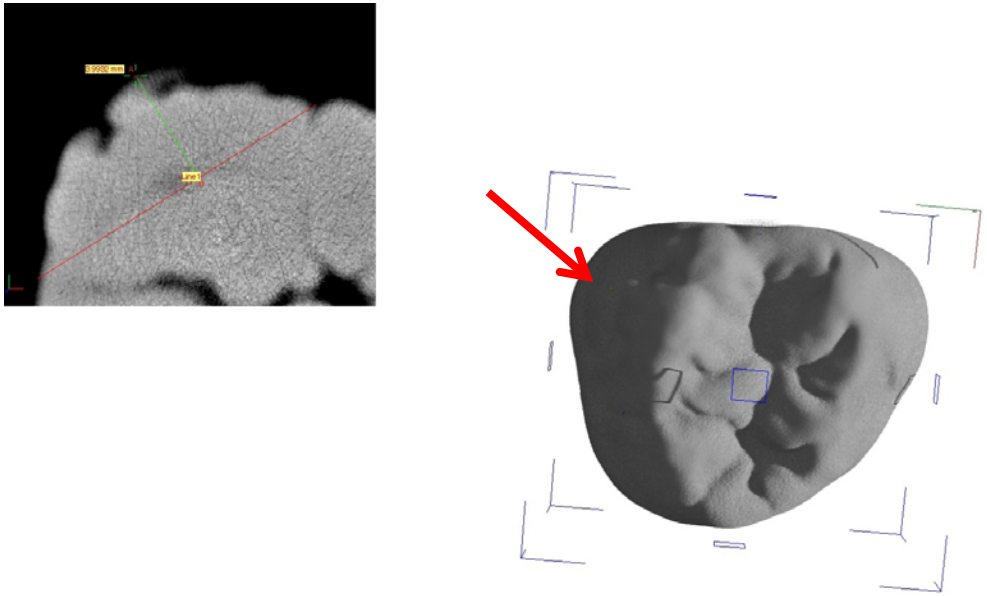


Fig. D.17 - P6. The furthest point projecting from Line 1 to the Pr outline

Landmark coordinates sampling

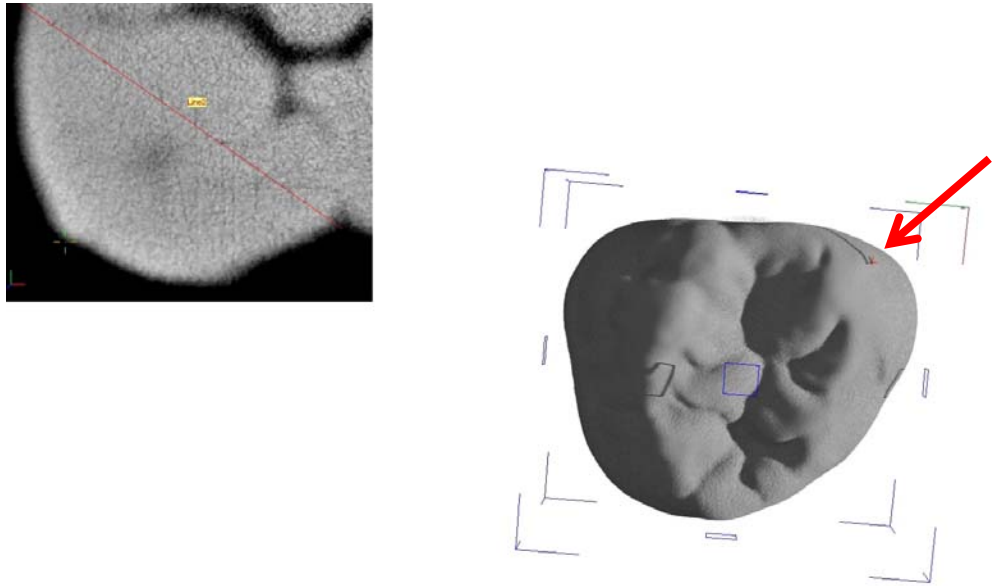


Fig. D.18 - P7. The furthest point projecting from Line 2 to the Pa outline

Landmark coordinates sampling

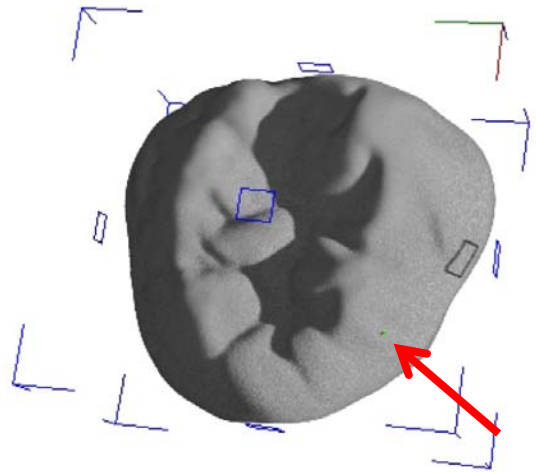
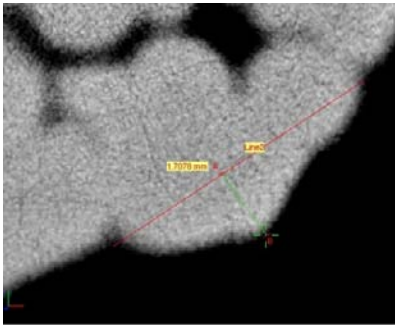


Fig. D.19 - P8. The furthest point projecting from Line 3 to the Me outline

Landmark coordinates sampling

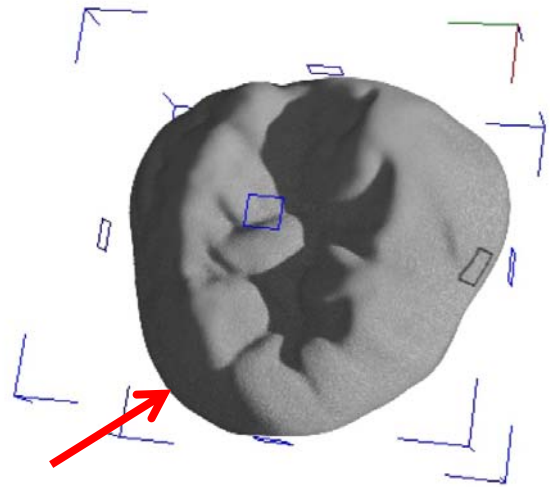
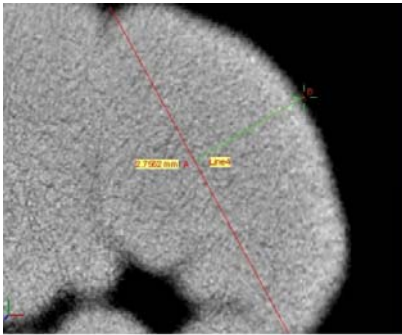


Fig. D.20 - P9. The furthest point projecting from Line 4 to the Hy outline

Landmark coordinates sampling

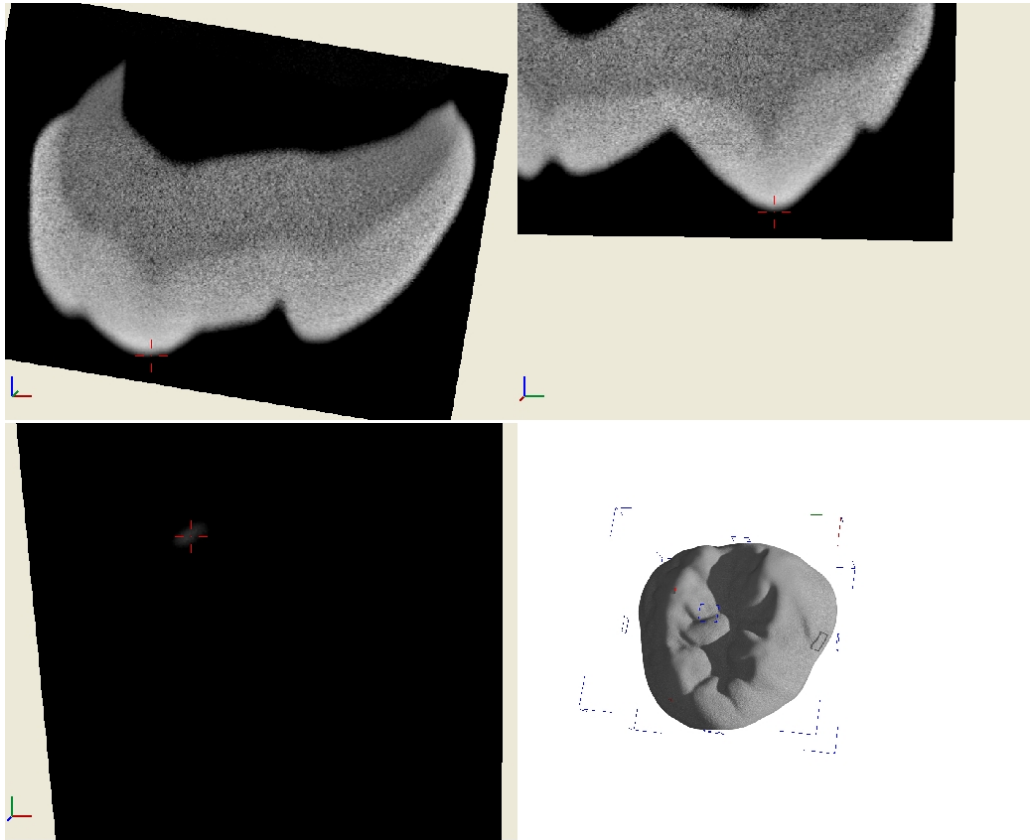


Fig. D.21 - P10. Pr apex

Landmark coordinates sampling

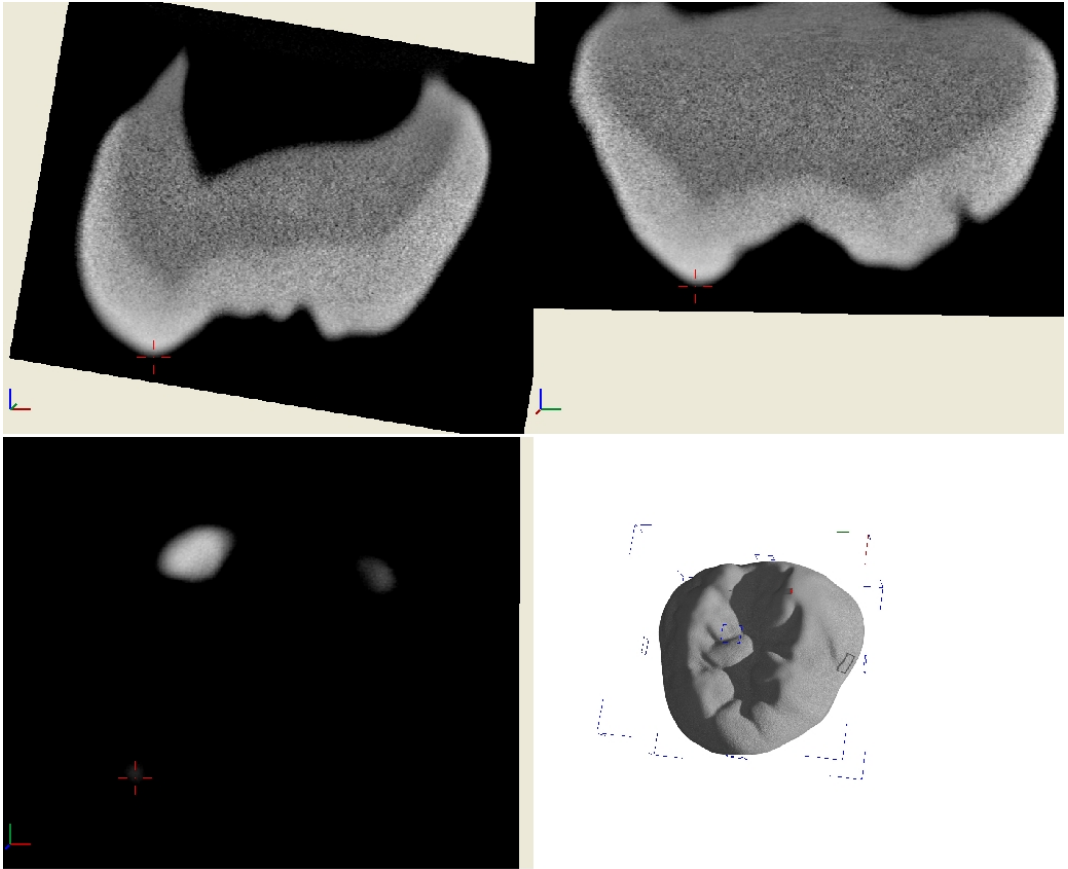


Fig. D.22 - P11. Pa apex

Landmark coordinates sampling

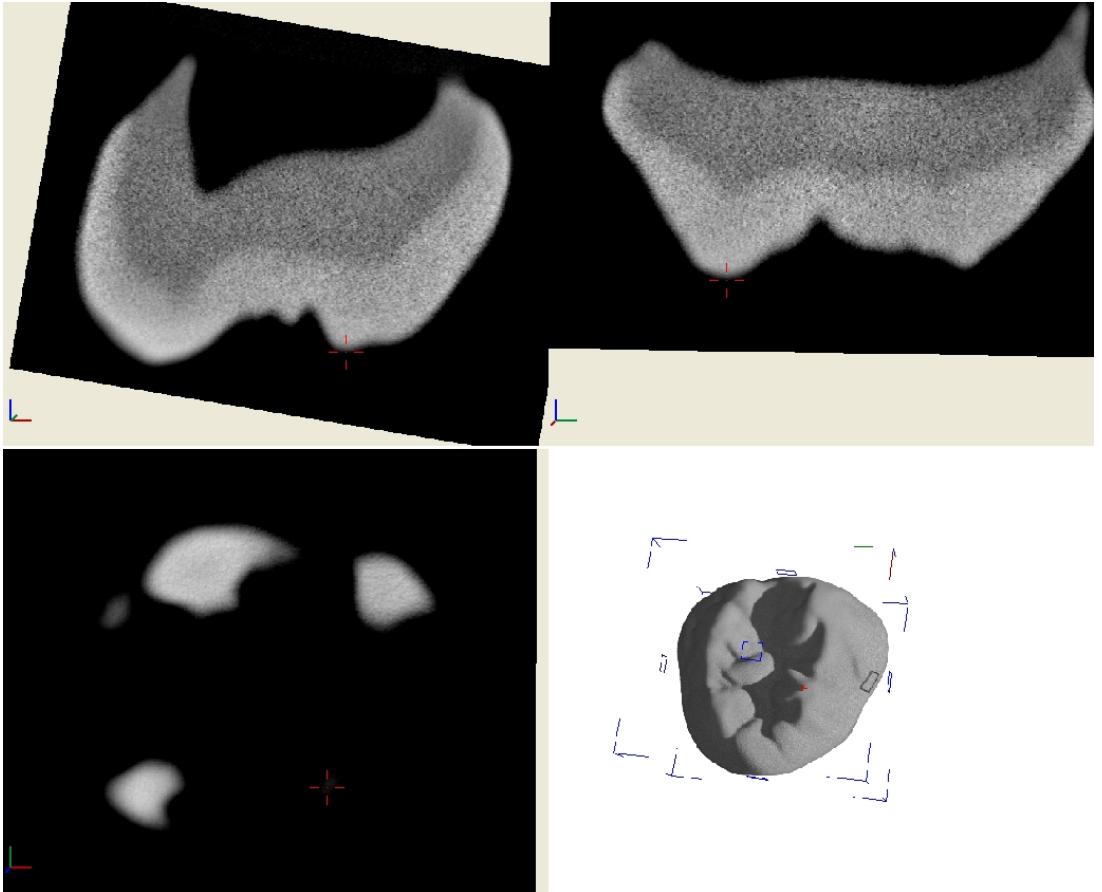


Fig. D.23 - P12. Me apex

Landmark coordinates sampling

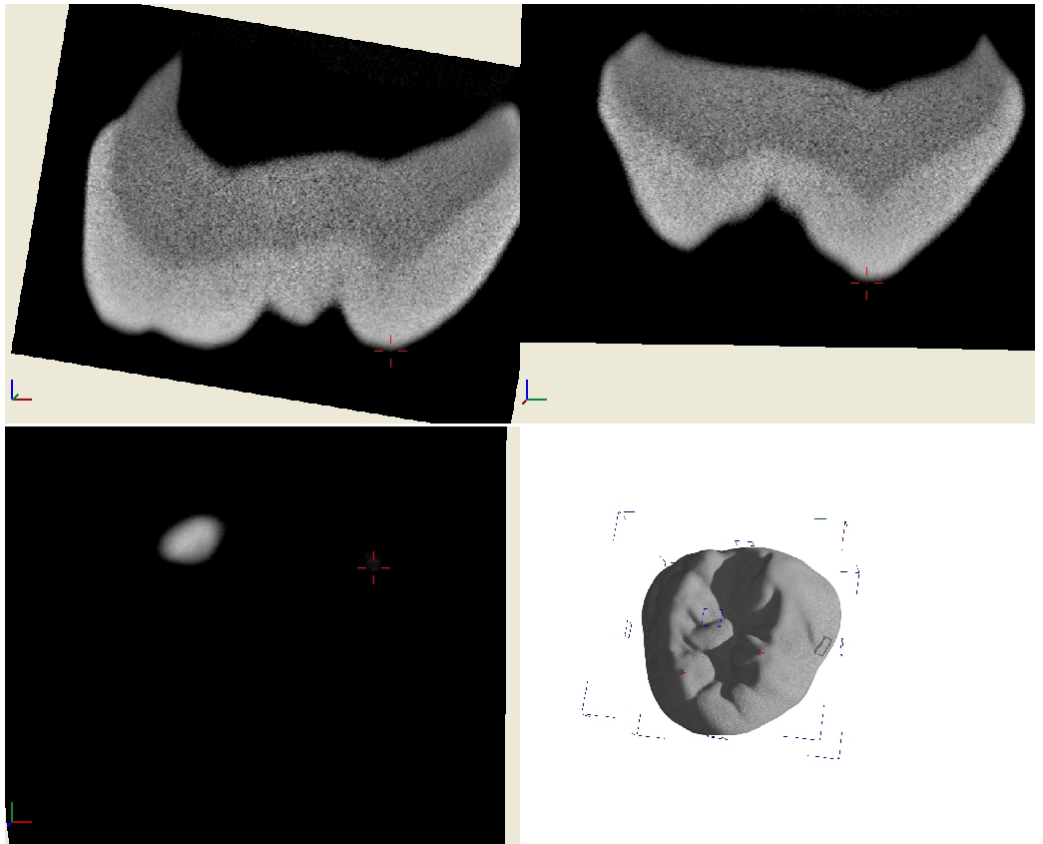


Fig. D.24 - P13. Hy apex

Landmark coordinates sampling

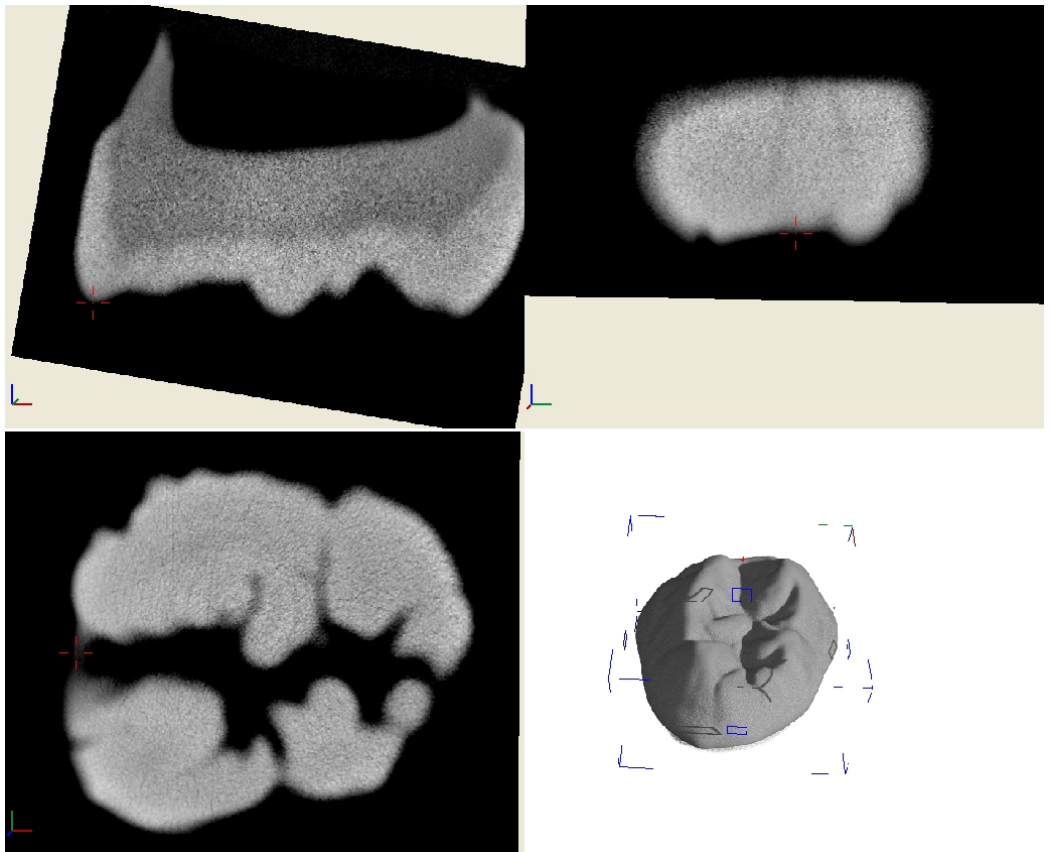


Fig. D.25 - P14. Central groove mesial terminus on the mesial crest

Landmark coordinates sampling

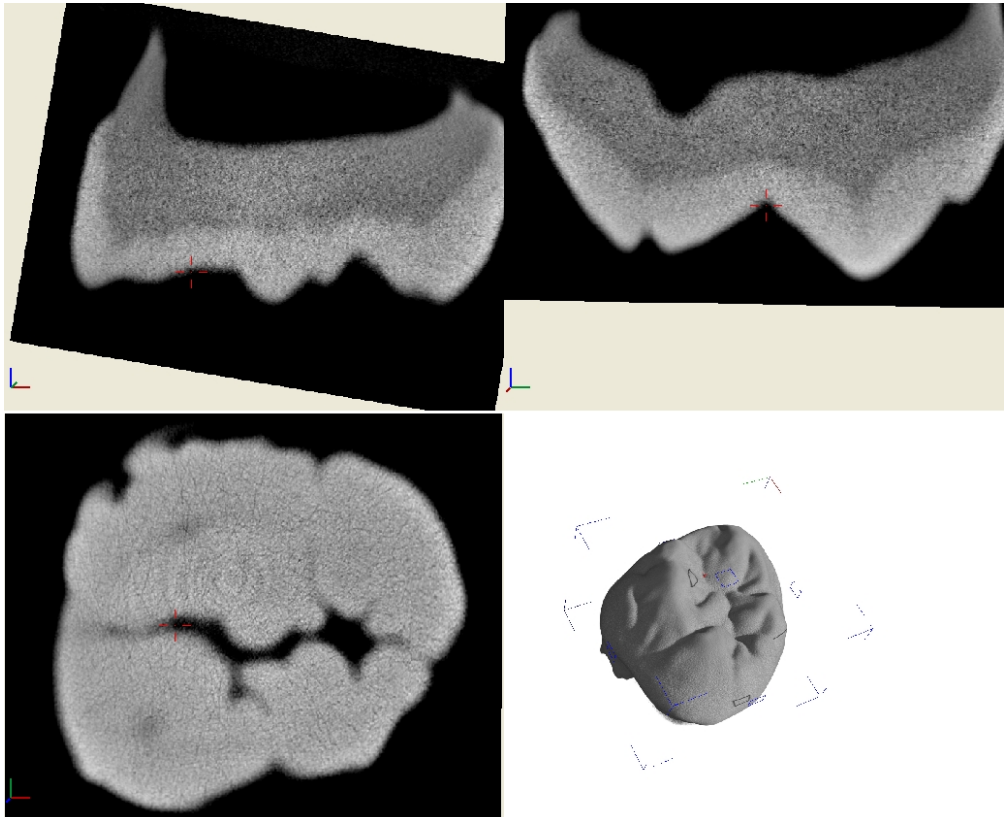


Fig. D.26 - P15. Lowest point on central groove between P1 and P14

Landmark coordinates sampling

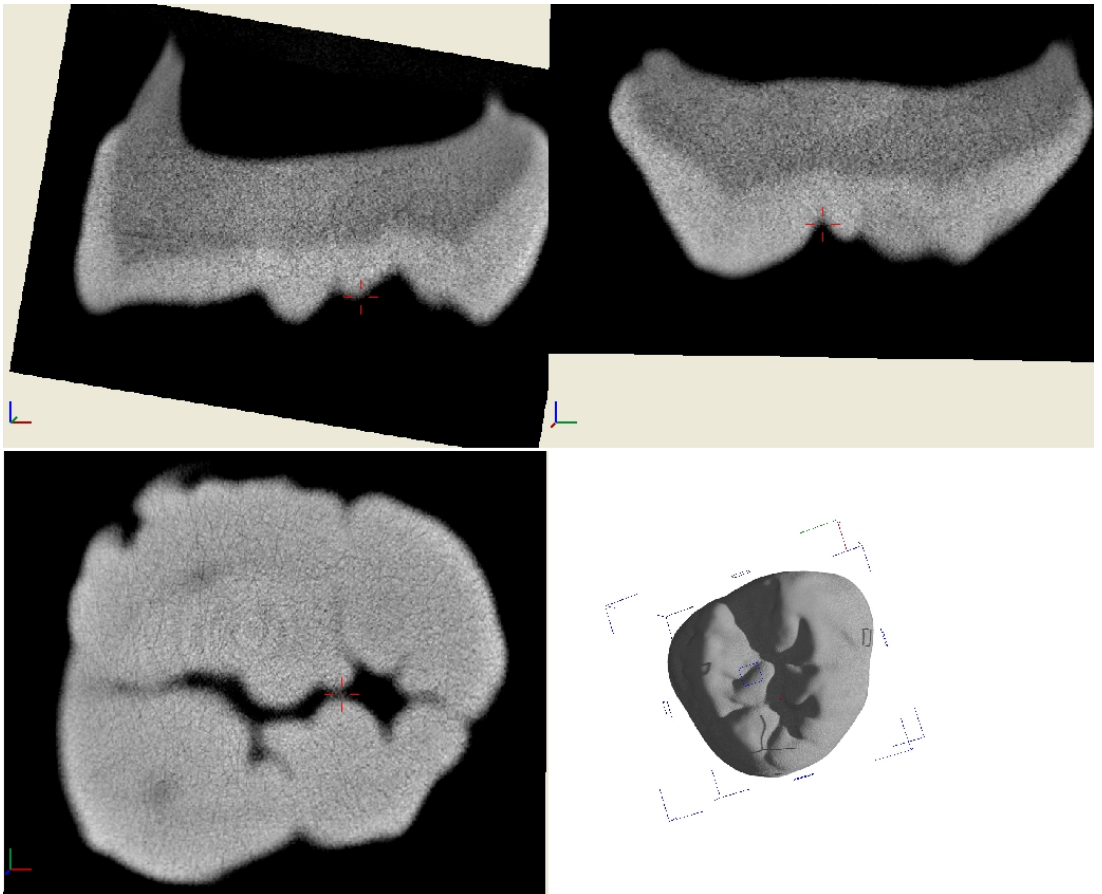


Fig. D.27 - P16. Intersection between the distal central groove and the transverse groove

Landmark coordinates sampling

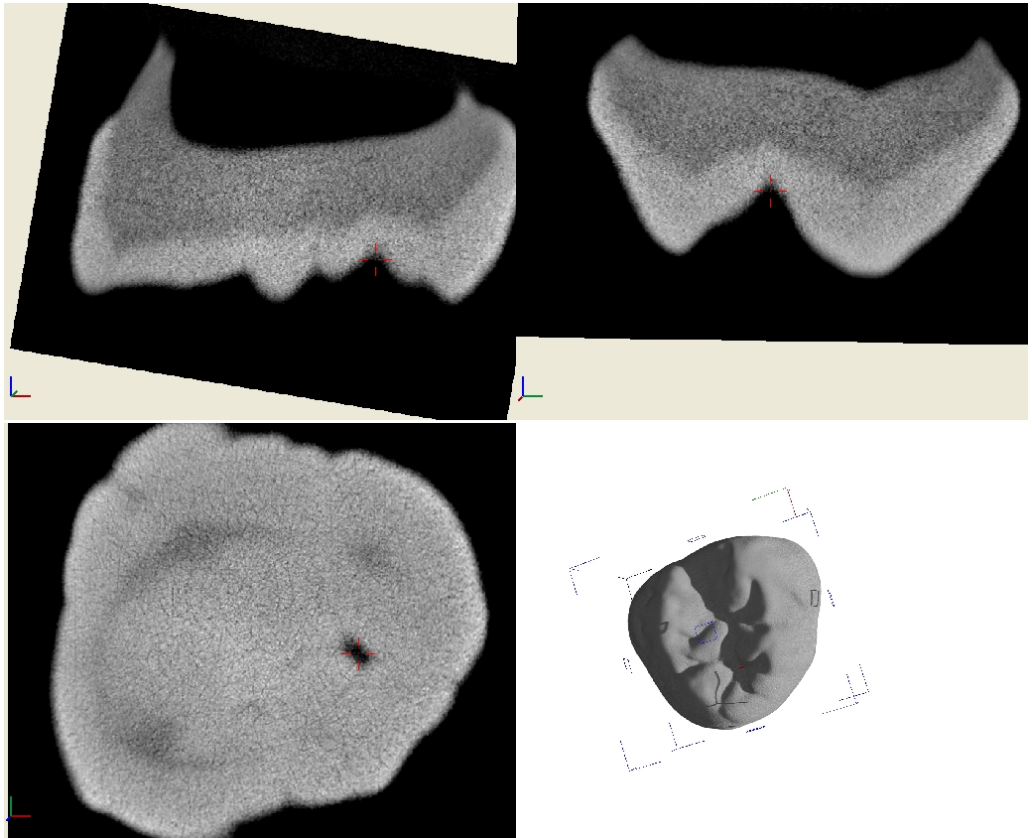


Fig. D.28 - P17. Lowest point of distal fossa

Landmark coordinates sampling

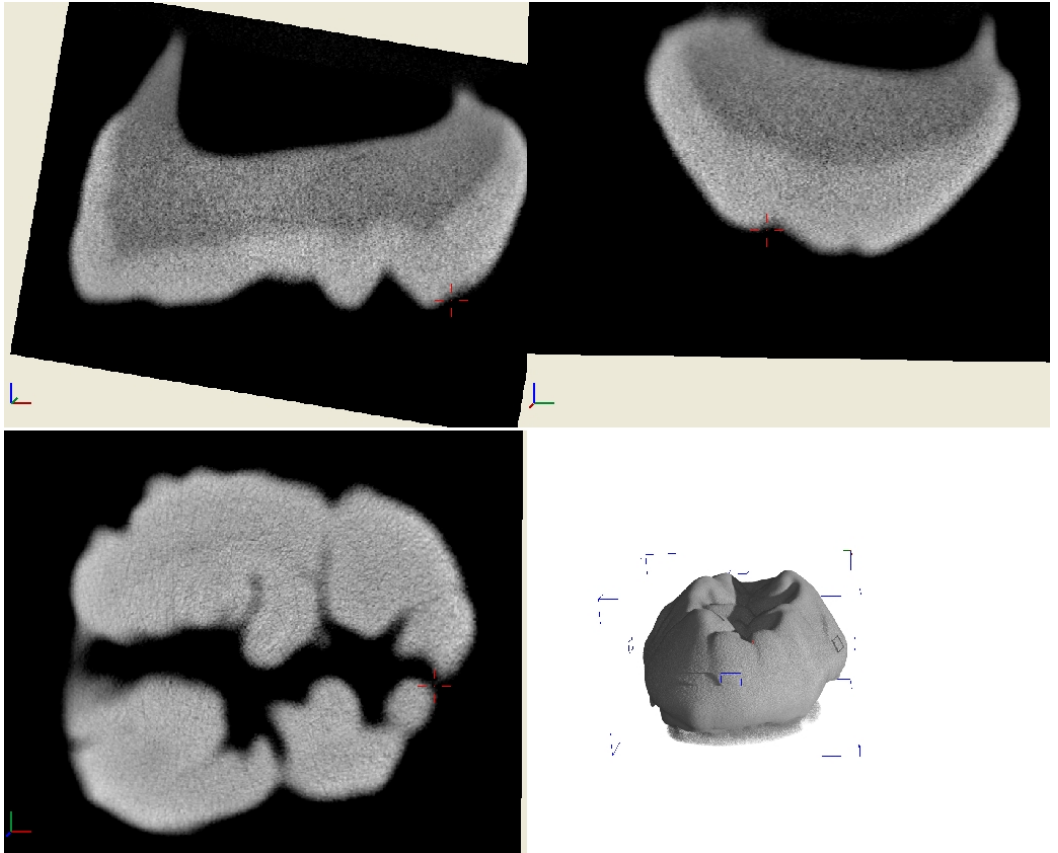


Fig. D.29 - P18. Central groove distal terminus on the distal crest

Landmark coordinates sampling

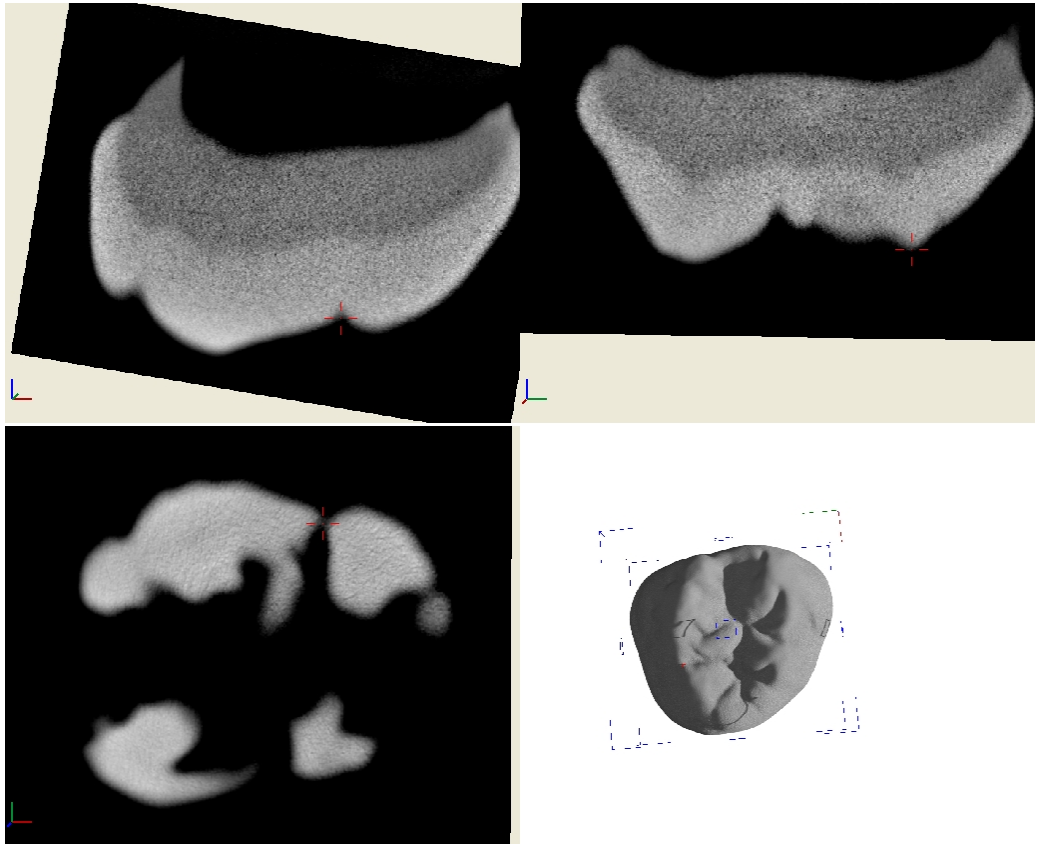


Fig. D.30 - P19. Highest point of contact between Pr and Hy

Landmark coordinates sampling

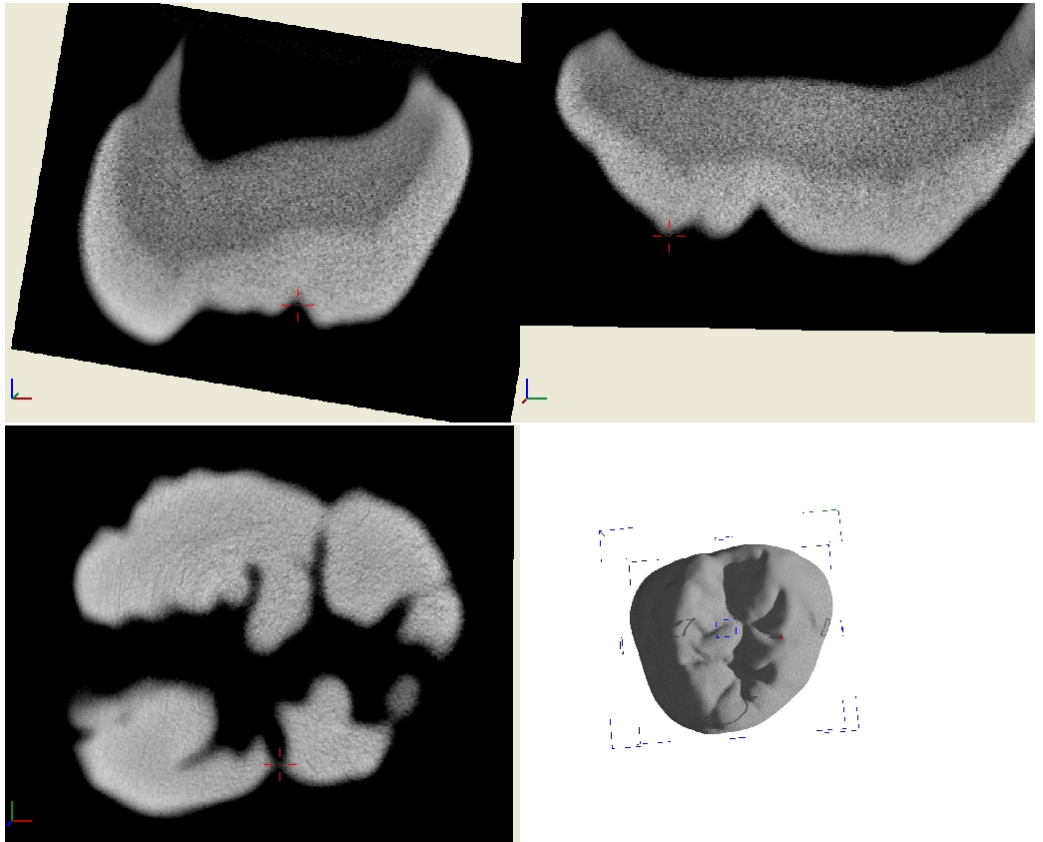


Fig. D.31 - P20. Highest point of contact between Pa and Me

Landmark coordinates sampling

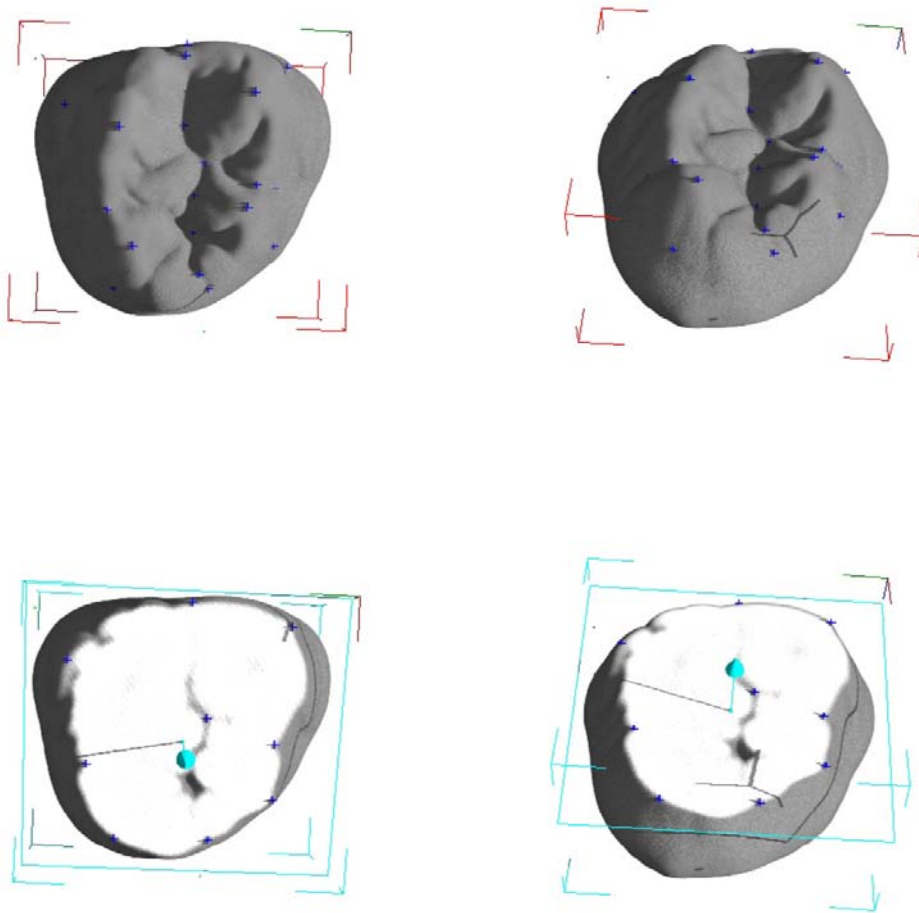


Fig. D.32 – Comprehensive views of the set of landmarks collected. Top row: three-dimensional views showing mostly the occlusal surface. Bottom row: three-dimensional views sectioned at level of plane P1

REFERENCES

- Aguirre, E. (1970). Identification de "Paranthropus" en Makapansgat. *Cronica del XI Congreso Nacional de Arqueologia*, pp. 98-124. Merida.
- Ahern, J. C. M. (1998). Underestimating intraspecific variation: the problem with excluding Sts 19 from *Australopithecus africanus*. *American Journal of Physical Anthropology*, 105, pp. 461-480.
- Aiello, L. C., and Dean, C. (1990). *An Introduction to Human Evolutionary Anatomy*. San Diego: Academic Press.
- Alt, K. W., and Buitrago-Téllez, C. H. (2004). Dental paleoradiology: applications in paleoanthropology and paleopathology. *Canadian Association of Radiologists Journal*, 55 (4), pp. 258-263.
- Bailey, S. E. (2000). Dental morphological affinities among late Pleistocene and recent humans. *Dental Anthropology*, 14, pp. 1-8.
- Bailey, S. E. (2004). A morphometric analysis of maxillary molar crowns of Middle-Late Pleistocene hominins. *Journal of Human Evolution*, 47, pp. 183-198.
- Bailey, S. E., and Lynch, J. M. (2005). Diagnostic differences in mandibular P4 shape between Neandertals and anatomically modern humans. *American Journal of Physical Anthropology*, 126, pp. 268-277.
- Benazzi, S. (2007). Image analysis in the morphological and morphometric study of teeth. *Doctoral thesis*. Bologna: Alma Mater Studiorum, Università di Bologna.
- Berger, L. R. (1992). Early hominid fossils discovered at Gladysvale Cave, South Africa. *South African Journal of Science*, 88, p. 362.
- Berger, L. R., and Pickford, M. (1995). A Plio-Pleistocene hominid upper central incisor from the Cooper's site, South Africa. *South African Journal of Science*, 91 (10).
- Berger, L. R., de Ruiter, D. J., Steininger, C. M., and Hancox, J. (2003). Preliminary results of excavations at the newly investigated Coopers D deposit, Gauteng, South Africa. *South African Journal of Science*, 99, pp. 276-278.

- Berger, L. R., Keyser, A. W., and Tobias, P. V. (1993). Brief communication: Gladysvale: First early hominid site discovered in South Africa since 1948. *American Journal of Physical Anthropology*, 92, pp. 107-111.
- Bernard, D. (2005). Using synchrotron computed microtomography to quantify 3D micro geometrical changes in multimaterials. In C. A. Brebbia, and A. A. Mammoli (Eds.), *Computational Methods and Experiments in Materials Characterisation II*. WIT Press.
- Biggerstaff, R. H. (1970). *A quantitative and qualitative study of the post-canine dentition of twins*. Ann Arbor, MI: University Microfilms.
- Boccone, S. (2004). Alcuni aspetti dello sviluppo dentale nelle Australopithecine Sudafricane. *Doctoral thesis*. Firenze: Università degli Studi di Firenze.
- Bookstein, F. L. (1978). *The Measurement of Biological Shape and Shape Change. Lecture Notes in Biomathematics*. New York: Springer.
- Bookstein, F. L. (1986). Size and shape spaces for landmark data in two dimensions (with discussion). *Statistical Science*, 1, pp. 181-242.
- Bookstein, F. L. (1989). Principal warps: thin-plate splines and the decomposition of deformations. *IEEE Transactions in Pattern Analysis and Machine Intelligence*, 11, pp. 567-585.
- Bookstein, F. L. (1991). *Morphometric Tools for Landmark Data: Geometry and Biology*. Cambridge: Cambridge University Press.
- Bookstein, F. L. (1993). A brief history of the morphometric synthesis. In L. F. Marcus, E. Bello, and A. García-Valdecasas (Eds.), *Contributions to morphometrics* (Vol. 8, pp. 15-40). Madrid: Monografias del Museo Nacional de Ciencias Naturales.
- Brace, C. L. (1979). Krapina, "classic" Neanderthals, and the evolution of the European face. *Journal of Human Evolution*, 8, pp. 527-550.
- Bromage, T. G., Schrenk, F., and Zonneveld, F. W. (1995). Paleoanthropology of the Malawi rift - an early hominid mandible from the Chiwondo beds, northern Malawi. *Journal of Human Evolution*, 28, pp. 71-108.
- Broom, R. (1936). A new fossil anthropoid skull from South Africa. *Nature*, 138, pp. 486-488.
- Broom, R. (1938). The Pleistocene anthropoid apes of South Africa. *Nature*, 142, pp. 377-379.
- Broom, R. (1939). A restoration of the Kromdraai skull. *Annals of the Transvaal Museum*, 19, pp. 327-329.

- Broom, R. (1947). Discovery of a new skull of the South African Ape-man, *Plesianthropus*. *Nature*, 159, p. 672.
- Broom, R. (1949). Another new type of fossil ape-man. *Nature*, 163, p. 57.
- Broom, R. (1950). The genera and species of the South African fossil ape-man. *American Journal of Physical Anthropology*, 8, pp. 1-13.
- Broom, R., and Schepers, G. W. (1946). *The South African ape-men, the Australopithecinae* (Vol. 2). Pretoria: Transvaal Museum Memoir.
- Bruner, E. (2003). Modelli per l'evoluzione. *Sapere*, 69/5 (1028), 49-56.
- Bruner, E., and Manzi, G. (2005). CT-based description and phyletic evaluation of the archaic human calvarium from Ceprano, Italy. *The Anatomical Record*, 285A, pp. 643-658.
- Bruner, E., Manzi, G., and Passarello, P. (2002). The "virtual" endocast of Saccopastore 1. General morphology and preliminary comparisons by geometric morphometrics. In B. Mafart, and H. Delingette (Eds.), *Three-Dimensional Imaging in Paleoanthropology and Prehistoric Archaeology*. Oxford: BAR International Series 1049 Archeopress.
- Calcagno, J. M., Cope, D. A., Lacy, M. G., and Tobias, P. V. (1997). Is *A. africanus* the only hominid species in Sterkfontein Member 4? *American Journal of Physical Anthropology*, S24, pp. 86-87.
- Calcagno, J. M., Cope, D. A., Lacy, M. G., Moggi-Cecchi, J., and Tobias, P. V. (1999). Reinvestigating the number of hominid species in Sterkfontein Member 4. *American Journal of Physical Anthropology*, S28, p. 101.
- Clarke, R. J. (1977). A juvenile cranium and some adult teeth of early *Homo* from Swartkrans, Transvaal. *South African Journal of Science*, 73, pp. 46-49.
- Clarke, R. J. (1985a). Early Acheulean with *Homo habilis* at Sterkfontein. In P. V. Tobias (Ed.), *Hominid Evolution: Past, Present and Future* (pp. 287-298). New York: Alan R. Liss.
- Clarke, R. J. (1985b). *Australopithecus* and early *Homo* in southern Africa. In E. Delson (Ed.), *Ancestors: The Hard Evidence* (pp. 171-177). New York: Alan R. Liss.
- Clarke, R. J. (1988). A new *Australopithecus* cranium from Sterkfontein and its bearing on the ancestry of *Paranthropus*. In F. E. Grine (Ed.), *Evolutionary History of the "Robust" Australopithecines* (pp. 285-292). New York: Aldine de Gruyter.
- Clarke, R. J. (1990). Observations on some restored hominid specimens in the Transvaal Museum, Pretoria. In G. H. Sperber (Ed.), *From Apes to Angels: Essays in*

- Anthropology in Honor of Phillip V. Tobias* (pp. 135-151). New York: Wiley-Riss, Inc.
- Clarke, R. J. (1994). Advances in understanding the craniofacial anatomy of South African early hominids. In R. L. Ciochon (Ed.), *Integrative Paths to the Past: Paleoanthropological Advances in Honor of F. Clark Howell* (p. 20). Englewood Cliffs, NY: Prentice Hall.
- Clarke, R. J. (1996). The genus *Paranthropus*: What's in a name? In W. E. Meikle, F. K. Howell, and N. G. Jablonski (Eds.), *Contemporary Issues in Human Evolution* (Vol. Memoir 21, pp. 93-104). San Francisco, California: California Academy of Sciences.
- Clarke, R. J. (2006). A deeper understanding of the stratigraphy of Sterkfontein fossil hominid site. *Transactions of the Royal Society of South Africa*, 61 (2), pp. 111-120.
- Clarke, R. J. (2008). Latest information on Sterkfontein's *Australopithecus* skeleton and a new look at *Australopithecus*. *South African Journal of Science*, 140, pp. 443-449.
- Conroy, G. C. (1988). Alleged synapomorphy of the M1/I1 eruption pattern in robust Australopithecines and *Homo*: evidence from high-resolution computed tomography. *American Journal of Physical Anthropology*, 75, pp. 487-492.
- Conroy, G. C., and Vannier, M. W. (1987). Dental development of the Taung skull from computerized tomography. *Nature*, 329, pp. 625-627.
- Conroy, G. C., and Vannier, M. W. (1991a). Dental development in South African australopithecines. Part I: problems of pattern and chronology. *American Journal of Physical Anthropology*, 86, pp. 121-136.
- Conroy, G. C., and Vannier, M. W. (1991b). Dental development in South African australopithecines. Part II: dental stage assessment. *American Journal of Physical Anthropology*, 86, pp. 137-156.
- Conroy, G. C., Lichtman, J. W., and Martin, L. B. (1995). Some observations on enamel thickness and enamel prism packing in the Miocene hominoid *Otavipithecus namibiensis*. *American Journal of Physical Anthropology*, 98, pp. 595-600.
- Coppa, A., Cucina, A., Mancinelli, D., Vargiu, R., and Calcagno, J. M. (1998). Dental anthropology of Central-Southern, Iron Age Italy: The evidence of metric versus nonmetric traits. *American Journal of Physical Anthropology*, 107, pp. 371-386.
- Cracraft, J. (1989). Speciation and its ontology: The empirical consequences of alternative species concepts for understanding the patterns and processes of

- differentiation. In D. Otte and J. A. Endler (Eds.), *Speciation and its Consequences* (pp. 28-59). Sunderland, MA: Sinauer Associates.
- Cramon-Taubadel, N., Frazier, B. C., and Lahr, M. M. (2006). The problem of assessing landmark error in geometric morphometrics: theory, methods, and modifications. *American Journal of Physical Anthropology*, 134, pp. 24-35.
- Dahlberg, G. (1926). *Twin births and twins from the hereditary point of view*. Stockholm: Bokförlags: A. B. Tidens Tryckeri.
- Dart, R. A. (1925). *Australopithecus africanus: The Man-Ape of South Africa*. *Nature*, 115, pp. 195-199.
- Dart, R. A. (1948a). The adolescent mandible of *Australopithecus prometheus*. *American Journal of Physical Anthropology*, 6, pp. 391-412.
- Dart, R. A. (1948b). The Makapansgat proto-human *Australopithecus prometheus*. *American Journal of Physical Anthropology*, 6, pp. 259-283.
- Dart, R. A. (1949a). A second adult palate of *Australopithecus prometheus*. *American Journal of Physical Anthropology*, 7, pp. 335-38.
- Dart, R. A. (1949b). Innominate fragments of *Australopithecus prometheus*. *American Journal of Physical Anthropology*, 7, pp. 301-334.
- Dart, R. A. (1949c). The cranio-facial fragment of *Australopithecus prometheus*. *American Journal of Physical Anthropology*, 7, pp. 187-214.
- Dart, R. A. (1954). The Adult Female Lower Jaw from Makapansgat. *American Anthropologist*, 56 (5), pp. 884-888.
- Dart, R. A. (1959). The first *Australopithecus* cranium from the pink breccia at Makapansgat. *American Journal of Physical Anthropology*, 17, pp. 77-82.
- Dart, R. A. (1962). The Makapansgat pink breccia australopithecine skull. *American Journal of Physical Anthropology*, 20 (2), pp. 119-126.
- Davenport, C. B., Steggerda, M., and Drager, W. (1935). Critical examination of physical anthropometry on the living. *Proceedings of the American Academy of Arts and Sciences*, 69, pp. 265-285.
- Day, M. H. (1965). *Guide to Fossil Man*. New York: World.
- De Beer, F. (2005). Characteristics of the neutron/X-ray tomography system at the SANRAD facility in South Africa Nuclear. *Nuclear Instruments and Methods in Physics Research, A* 542, pp. 1-8.
- De Ruiter, D. J., Pickering, R., Steininger, C. M., Kramers, J. D., Hancox, P. J., Churchill, S. E., Berger, L. R., Backwell, L. (2009). New *Australopithecus*

- robustus* fossils and associated U-Pb dates from Cooper's Cave. *Journal of Human Evolution*, 56, pp. 497-513.
- Dryden, I. L., and Mardia, K. V. (1991). General shape distribution in a plane. *Advances in Applied Probability*, 23, pp. 259-276.
- Dryden, I. L., and Mardia, K. V. (1998). *Statistical Shape Analysis*. London: John Wiley.
- Ferrario, V. F., Sforza, C., Tartaglia, G. M., Colombo, A., and Serrao, G. (1999). Size and shape of the human first permanent molar: A Fourier analysis of the occlusal and equatorial outlines. *American Journal of Physical Anthropology*, 108, pp. 281–294.
- Fiorenza, L., Benazzi, S., and Kullmer, O. (2009). Morphology, wear and 3D digital surface models: materials and techniques to create high-resolution replicas of teeth. *Journal of Anthropological Science*, 87, pp. 211-218.
- Goose, D. H. (1963). Dental Measurement: an assessment of its value in anthropological studies. In D. R. Brothwell (Ed.), *Dental Anthropology* (pp. 125-148). London: Pergamon Press.
- Gower, J. C. (1975). Generalized Procrustes analysis. *Psychometrika*, 40, pp. 33-51.
- Grine, F. E. (1981). Trophic differences between “gracile” and “robust” australopithecines: A scanning electron microscope analysis of occlusal events. *South African Journal of Science*, 77, pp. 203-230.
- Grine, F. E. (1982). A new juvenile hominid (mammalia: primates) from Member 3, Kromdraai formation, Transvaal. *Annals of the Transvaal Museum*, 33, pp. 287-290.
- Grine, F. E. (1984). The deciduous dentition of the Kalahari San, the South African Negro and the South African Negro and the South African Plio-Pleistocene Hominids. *Doctoral thesis*. Johannesburg: University of the Witwatersrand.
- Grine, F. E. (1985). Australopithecine evolution: the deciduous dental evidence. In E. Delson (Ed.), *Ancestors: The Hard Evidence* (pp. 153-167). New York: Alan R. Liss.
- Grine, F. E. (2004). Description and preliminary analysis of new hominid craniodental fossils from the Swartkrans formation. In C. K. Brain (Ed.), *Swartkrans. A Cave's Chronicle of Early Man* (II ed.). Pretoria: Transvaal Museum.
- Grine, F. E., and Martin, L. B. (1988). Enamel thickness and development in *Australopithecus* and *Paranthropus*. In F. E. Grine (Ed.), *Evolutionary History of the "Robust" Australopithecines* (pp. 3-42). New York: Aldine de Gruyter.

- Grine, F. E., and Strait, D. S. (1994). New hominid fossils from Member 1 "Hanging Remnant", Swartkrans Formation, South Africa. *Journal of Human Evolution*, 26, pp. 57-75.
- Haeussler, A. (1995). Upper Paleolithic teeth from the Kostenki sites on the Don river, Russia. In J. Moggi-Cecchi (Ed.), *Aspects of Dental Biology: Palaeontology, Anthropology and Evolution* (pp. 315–332). Florence: International Institute for the Study of Man.
- Hall, B. K. (Ed.). (1994). *Homology: The Hierarchical Basis of Comparative Biology*. San Diego: Academic Press.
- Hanihara, K., Tamada, M., and Tanaka, T. (1970). Quantitative analysis of the hypocone in the human upper molars. *Journal of Anthropological Society of Nippon*, 78, pp. 200-207.
- Harmon, E. H. (2007). The shape of the hominoid proximal femur: a geometric morphometric analysis. *Journal of Anatomy*, 210, pp. 170-185.
- Harris, E. F., and Dinh, D. P. (2006). Intercusp relationships of the permanent maxillary first and second molars in American whites. *American Journal of Physical Anthropology*, 130, pp. 514–528.
- Harvati, K. (2003). Quantitative analysis of Neanderthal temporal bone morphology using three-dimensional geometric morphometrics. *American Journal of Physical Anthropology*, 120, pp. 323–338.
- Hillson, S. (1986). *Teeth*. Cambridge: Cambridge University Press.
- Hillson, S., Fitzgerald, C., and Flinn, H. (2005). Alternative dental measurements: Proposals and relationships with other measurements. *American Journal of Physical Anthropology*, 126, pp. 413–426.
- Hounsfield, G. N. (1973). Computerized transverse axial scanning (tomography): Part 1. Description of system. *British Journal of Radiology*, 46, pp. 1016-1022.
- Howell, F. C. (1955). The age of the australopithecines of southern Africa. *American Journal of Physical Anthropology*, 13, pp. 635-662.
- Howell, F. C. (1968). Omo research expedition. *Nature*, 219, pp. 567-572.
- Howell, F. C. (1978). Hominidae. In V. J. Maglio and H. B. S. Cooke (Eds.), *Evolution of African Mammals* (pp. 154-248). Cambridge: Harvard University Press.
- Hrdlička, A. (1920). Shovel-shaped teeth. *American Journal of Physical Anthropology*, 3, pp. 429–465.

- Hublin, J.-J., Spoor, F., Braun, M., Zonneveld, F., and Condemi, S. (1996). A late Neanderthal from Arcy-sur-Cure associated with Upper Palaeolithic artefacts. *Nature*, *381*, pp. 224-226.
- Irish, J. D., and Guatelli-Steinberg, D. (2003). Ancient teeth and modern human origins: an expanded comparison of African Plio-Pleistocene and recent world dental samples. *Journal of Human Evolution*, *45*, pp. 113–144.
- Jamison, P. L., and Ward, R. E. (1993). Brief Communication: measurement size, precision, and reliability in craniofacial anthropometry: bigger is better. *American Journal of Physical Anthropology*, *90*, pp. 495-500.
- Jamison, P. L., and Zegura, S. L. (1974). A univariate and multivariate examination of measurement error in anthropometry. *American Journal of Physical Anthropology*, *40*, pp. 197-204.
- Jernvall, J., and Selänne, L. (1999). Laser confocal microscopy and geographic information systems in the study of dental morphology. *Paleontologia Electronica*, *2* (1), p. 18.
- Johanson, D. C., and White, T. D. (1979). A systematic assessment of early African hominids. *Science*, *202*, pp. 321-330.
- Johanson, D. C., White, T. D., Coppens, Y. (1982). Dental remains from the Hadar Formation, Ethiopia: 1974–1977 collections. *American Journal of Physical Anthropology*, *57*, 545–603.
- Kaszycka, K. A. (2002). Status of Kromdraai. Cranial, Mandibular and Dental Morphology, Systematic Relationships, and Significance of the Kromdraai Hominids. Paris: CNRS Editions.
- Kendall, D. G. (1977). The diffusion of shape. *Advances in Applied Probability*, *9*, pp. 428-430.
- Kendall, D. G. (1984). Shape-manifolds, Procrustean metrics and complex projective spaces. *Bulletin of the London Mathematical Society*, *16*, pp. 81-121.
- Kendall, D. G. (1985). Exact distributions for shapes of random triangles in convex sets. *Advances in Applied Probability*, *17*, pp. 308-329.
- Kendall, D. G. (1986). Comment on F. L. Bookstein, Size and shape spaces for landmark data in two dimensions. *Statistical Science*, *1* (2), pp. 222-226.
- Kendall, D. G. (1989). A survey of the statistical theory of shape. *Statistical Science*, *4*, pp. 87-120.
- Kendall, D. G., and Kendall, W. S. (1980). Alignments in two dimensional random sets of points. *Advances in Applied Probability*, *12*, pp. 380-424.

- Kent, J. T., and Mardia, K. V. (1997). Consistency of Procrustes estimators. *Journal of Royal Statistical Society, Series B* 59, pp. 281-290.
- Kieser, J. A. (1990). *Human adult. Odontometrics*. Cambridge: Cambridge University Press.
- Kimbel, W. H., and Rak, Y. (1993). The importance of species taxa in paleoanthropology and an argument for the concept of the species category. In L. B. Martin (Ed.), *Species, Species Concepts, and Primate Evolution*. New York: Plenum Press.
- Kimbel, W. H., White, T. D. (1988). Variation, sexual dimorphism and the taxonomy of *Australopithecus*. In *Evolutionary History of the "Robust" Australopithecines* (pp. 175–192). New York: Aldine de Gruyter.
- Kimbel, W. H., White, T. D., and Johanson, D. C. (1988). Implications of KNM WT-17000 for the evolution of the robust australopithecines. In *Evolutionary History of the "Robust" Australopithecines* (pp. 259–268). New York: Aldine de Gruyter.
- Kirera, F. M., and Ungar, P. S. (2003). Occlusal relief changes with molar wear in *Pan troglodytes troglodytes* and *Gorilla gorilla gorilla*. *American Journal of Primatology*, 60, pp. 31–41.
- Klingeberg, C. P., and Monteiro, L. R. (2008). Distances and directions in Multidimensional shape spaces: Implications for morphometric applications. *Systematic Biology*, 54, pp. 678-688.
- Kuhl, F. P., and Giardina, C. R. (1982). Elliptic Fourier analysis of a closed contour. *Computer Vision, Graphics, and Image Processing*, 18, pp. 259–278.
- Kuman, K., and Clarke, R. J. (2000). Stratigraphy, artefact industries and hominid associations for Sterkfontein, Member 5. *Journal of Human Evolution*, 38, pp. 827-847.
- Lague, M. R., and Jungers, W. L. (1998). Morphometric variation in Plio-Pleistocene hominid distal humeri. *American Journal of Physical Anthropology*, 101 (3), pp. 401 - 427.
- Leakey, L. S. B., Tobias, P. V., and Napier, J. R. (1964). A new species of the genus *Homo* from Olduvai Gorge. *Nature*, 202, pp. 7-9.
- Le Blanc, S. A., and Black, B. (1974). A long term trend in tooth size in the eastern Mediterranean. *American Journal of Physical Anthropology*, 41, pp. 417-422.
- Le Gros Clark, W. E. (1967). *Man-apes or ape-men? The story of discoveries in Africa*. London: Holt, Rinehart and Winston.
- Lehmann, E. H., Vontobel, P., Schillinger, B., Bücherl, T., Baechler, S., Jolie, J., Treimer, W., Rosa, R., Chirco, P., Bayon, G., Legoupil, S., Körner, S., Böck, H.,

- Micherov, V., Balasko, M., and Kuba, A. (2000). Status and prospect of Neutron Tomography in Europe. Abstract 15th World Conference on Nondestructive Testing, (pp. 1-12). Roma.
- Lele, S. (1993). Euclidean distance matrix analysis: a statistical review. *Mathematical Geology*, 25, pp. 573-602.
- Lestrel, P. E. (Ed.). (1997). *Fourier descriptors and their applications*. Cambridge: Cambridge University Press.
- Lockwood, C. A., and Tobias, P. V. (1999). A large male hominin cranium from Sterkfontein, South Africa, and the status of *Australopithecus africanus*. *Journal of Human Evolution*, 36, pp. 637-685.
- Lockwood, C. A., and Tobias, P. V. (2002). Morphology and affinities of new hominin cranial remains from Member 4 of the Sterkfontein Formation, Gauteng Province, South Africa. *Journal of Human Evolution*, 42, pp. 389-450.
- Lockwood, C. A., Lynch, J. M., and Kimbel, W. H. (2002). Quantifying temporal bone morphology of great apes and humans: an approach using geometric morphometrics. *Science*, 318, pp. 1443-1446.
- Lockwood, C. A., Menter, C. G., Moggi-Cecchi, J., and Keyser, A. W. (2007). Extended male growth in a fossil hominin species. *Journal of Anatomy*, 201, pp. 447-464.
- Macho, G. A., and Thackeray, J. F. (1992). Computed tomography and enamel thickness of maxillary molars of Plio-Pleistocene hominids from Sterkfontein, Swartkrans and Kromdraai (South Africa): an exploratory study. *American Journal of Physical Anthropology*, 89, pp. 133-143.
- Mafart, B., Guipert, G., de Lumley, M.-A., and Subsol, G. (2004). Three-dimensional computer imaging of hominid fossils: a new step in human evolution studies. *Journal of the American College of Radiology*, 55 (4), pp. 264-270.
- Marcus, L. F. (1990). Traditional morphometrics. In F. J. Rolfh, and F. L. Bookstein (Eds.), *Proceedings of the Michigan Morphometrics Workshop* (Vol. Special Publication Number 2, pp. 77-122). Ann Arbor, MI: University of Michigan Museum of Zoology.
- Marcus, L. F., Corti, M., Loy, A., Naylor, G. J., and Slice, D. (Eds.). (1996). *Advanced in Morphometrics*. New York: Plenum Press.
- Martinón-Torres, M., Bastir, M., Bermúdez de Castro, J. M., Gómez, A., Sarmiento, S., Muela, A., and Arsuaga, J. L. (2006). Hominid lower second premolar morphology: evolutionary inferences through geometric morphometric analysis. *Journal of Human Evolution*, 50, pp. 523-533.

- Mayr, E. (1950). Taxonomic categories in fossil hominids. *Cold Spring Harbor Symposia on Quantitative Biology*, 15, pp. 109-118.
- McNulty, K. P. (2005). A geometric morphometric assessment of the hominoid supraorbital region: Affinities of the Eurasian Miocene hominoids *Dryopithecus*, *Graecopithecus*, and *Sivapithecus*. In D. E. Slice (Ed.), *Modern Morphometrics in Physical Anthropology* (pp. 349-373).
- Middleton Shaw, J. C. (1939). Further remains of a Sterkfontein ape. *Nature*, 143, p. 117.
- Moggi-Cecchi, J. (2003). The elusive 'second species' in Sterkfontein Member 4: the dental metrical evidence. *South African Journal of Science*, 199, pp. 268-270.
- Moggi-Cecchi, J., and Boccone, S. (2007). Maxillary molar cusp morphology of South African australopithecines. In S. E. Bailey, and J.-J. Hublin (Eds.), *Dental Perspectives on Human Evolution* (pp. 53-64). Springer.
- Moggi-Cecchi, J., Grine, F. E., and Tobias, P. V. (2006). Early hominid dental remains from Member 4 and 5 of the Sterkfontein Formation (1966-1996 excavations): Catalogue, individual associations, morphological descriptions and initial metrical analysis. *Journal of Human Evolution*, 50, pp. 239-328.
- Moggi-Cecchi, J., Tobias, P. V., and Beynon, A. D. (1998). The mixed dentition and associated skull fragments of a juvenile fossil hominid from Sterkfontein, South Africa. *American Journal of Physical Anthropology*, 106, pp. 425-466.
- Moorrees, C. F., and Reed, R. B. (1954). Correlations among crown diameters of human teeth. *Archives of Oral Biology*, 9, pp. 685-697.
- Nelson, C. T. (1938). The teeth of the Indians of Pecos Pueblo. *American Journal of Physical Anthropology*, 23, pp. 261-293.
- Newton, T. H., and Potts, D. G. (1981). *Radiology of the Skull and Brain (Vol. 5). Technical Aspects of Computed Tomography*. St. Louis: Mosby.
- Nicholson, E., and Harvati, K. (2006). Quantitative Analysis of Human Mandibular Shape Using Three-Dimensional Geometric Morphometrics. *American Journal of Physical Anthropology*, 131, pp. 368-383.
- O'Higgins, P. (2000). The study of morphological variation in the hominid fossil record: biology, landmarks and geometry. *Journal of Anatomy*, 197, pp. 103-120.
- O'Higgins, P., and Jones, N. (1998). Facial growth in *Cercocebus torquatus*: an application of three-dimensional geometric morphometric techniques to the study of morphological variation. *Journal of Anatomy*, 193, pp. 251-272.
- Ohman, J. C., Krocha, T. J., Lovejoy, C. O., Mensforth, R. P., and Latimer, B. (1997). Cortical bone distribution in the femoral neck of hominoids: implications for the

- locomotion of *Australopithecus afarensis*. *American Journal of Physical Anthropology*, 104, pp. 117-131.
- Olejniczak, A. J., Smith, T. M., Feeney, R. N. M., Macchiarelli, R., Mazurier, A., Bondioli, L., Rosas, A., Fortea, J., de la Rasilla, M., Garcia-Taberner, A., Radovčić, J., Skinner, M. M., Toussaint, M., Hublin, J.-J. (2008). Dental tissue proportions and enamel thickness in Neandertal and modern human molars. *Journal of Human Evolution*, 55, pp. 12-23.
- Olejniczak, A. J., Smith, T. M., Skinner, M. M., Grine, F. E., Feeney, R. N. M., Thackeray, J.F., and Hublin, J.-J. (2008). Three-dimensional molar enamel distribution and thickness in *Australopithecus* and *Paranthropus*. *Biology Letters*, 4, pp. 406-410.
- Olson, T. R. (1985). Cranial morphology and systematics of the Hadar Formation hominid and "Australopithecus" africanus. In E. Delson (Ed.), *Ancestors: The Hard Evidence* (pp. 102-119). New York: Alan R. Liss.
- Pan, R., and Oxnard, C. (2004). Craniodental variation in the African Macaque, with reference to various Asian species. *Folia Primatologica*, 75, pp. 355-375.
- Partridge, T. C. (2005). Dating of the Sterkfontein hominids: progress and possibilities. *Transactions of the Royal Society of South Africa*, 60 (2), pp. 107-109.
- Perez, S. I., Bernal, V., and Gonzalez, P. N. (2006). Differences between sliding semi-landmark methods in geometric morphometrics, with an application to human craniofacial and dental variation. *Journal of Anatomy*, 208, pp. 769-784.
- Pilbeam, D. R., and Zwell, M. (1973). The single species hypothesis, sexual dimorphism, and variability in early hominids. *Yearbook of Physical Anthropology*, 16, pp. 69-79.
- Potter, R. H., Alcazaren, A. B., Herbosa, F. M., and Tomaneng, J. (1981). Dimensional characteristics of the Filipino dentition. *American Journal of Physical Anthropology*, 55, pp. 33-42.
- Quam, R., Bailey, S. E., and Wood, B. A. (in press). Evolution of M1 crown size and cusp proportions in the genus *Homo*. *Journal of Anatomy*.
- Rak, Y. (1983). *The Australopithecine face*. New York: Academic Press.
- Rao, C. R., and Suryawanshi, S. (1996). Statistical analysis of shape of objects based on landmark data. *Proceedings of the National Academy of Science of the USA*, 93, pp. 12132-12136.

- Reed, K. E., Kitching, J. W., Grine, F. E., Jungers, W. L., and Sokoloff, L. (1993). Proximal femur of *Australopithecus africanus* from Member 4, Makapansgat, South Africa. *American Journal of Physical Anthropology*, 92, pp. 1-15.
- Robinson, D. L., Blackwell, P. G., Stillman, E. C., and Brook, A. H. (2001). Planar Procrustes analysis of tooth shape. *Archives of Oral Biology*, 46, 191-199.
- Robinson, D. L., Blackwell, P. G., Stillman, E. C., and Brook, A. H. (2002). Impact of landmark reliability on the planar Procrustes analysis of tooth shape. *Archives of Oral Biology*, 47, pp. 545-554.
- Robinson, J. T. (1952). The australopithecines and their evolutionary significance. *Proceedings of the Linnean Society of London*, 163, pp. 196-200.
- Robinson, J. T. (1954a). Phyletic lines in the prehomnids. *Zeitschrift für Morphologie und Anthropologie*, 46, pp. 269-273.
- Robinson, J. T. (1954b). The genera and species of the Australopithecinae. *American Journal of Physical Anthropology*, 12, pp. 181-200.
- Robinson, J. T. (1956). *The Dentition of the Australopithecinae* (Vol. 9). Pretoria: Transvaal Museum Memoir.
- Robinson, J. T. (1962). The origin and adaptive radiation of the Australopithecines. In G. Kurth (Ed.), *Evolution und Hominisation*. Stuttgart, Germany: Gustav Fischer Verlag.
- Robinson, J. T. (1963). Adaptive radiation in the australopithecines and the origin of man. In F. C. Howell, and F. Bourlière (Eds.), *African Ecology and Human Evolution* (pp. 385-416). Chicago, Illinois: Aldine.
- Robinson, J. T. (1967). Variation and taxonomy of the early hominids. In W. C. Steere (Ed.), *Evolutionary Biology* (pp. 69-100). New York: Appleton-Century-Crofts.
- Robinson, J. T. (1972). *Early Hominid Posture and Locomotion*. Chicago, Illinois: University of Chicago Press.
- Rohlf, F. J. (1999). Shape statistics: Procrustes superimpositions and tangent spaces. *Journal of Classification*, 16, pp. 197-223.
- Rohlf, F. J. (2000a). On the use of shape spaces to compare morphometric methods. *Hystrix - Italian Journal of Mammalogy*, (N.S), 11 (1), pp. 8-24.
- Rohlf, F. J. (2000b). Statistical power comparisons among alternative morphometric methods. *American Journal of Physical Anthropology*, 111, pp. 468-478.
- Ross, C. F., and Henneberg, M. (1995). Basicranial flexion, relative brain size, and facial kyphosys in *Homo sapiens* and some fossil hominids. *American Journal of Physical Anthropology*, 98, pp. 575-593.

- Ruff, C. B. (1989). New approaches to structural evolution of limb bones in primates. *Folia Primatologica*, 53, pp. 142-159.
- Ruff, C. B., and Leo, F. P. (1986). Use of computed tomography in skeletal structure research. *Yearbook of Physical Anthropology*, 29, pp. 181-196.
- Schmid, P. (2002). The Gladysvale project. *Evolutionary Anthropology*, 11 (S1), pp. 45-48.
- Schwartz, G. T., Thackeray, J. F., Reid, C., and van Reenan, J. F. (1998). Enamel thickness and the topography of the enamel-dentine junction in South African Plio-Pleistocene hominids with special reference to the Carabelli trait. *Journal of Human Evolution*, 35, pp. 523-542.
- Schwartz, J. H., and Tattersall, I. (Eds.). (2005). *The Human Fossil Record. Craniodental Morphology of Early Hominids (Genera Australopithecus, Paranthropus, Orrorin), and Overview*. New York: Wiley-Liss.
- Schwarz, D., Vontobel, P., Lehmann, E. H., Meyer, C. A., and Bongartz, G. (2005). Neutron Tomography of Internal Structures of Vertebrate Remains: A Comparison with X-ray Computed Tomography. *Palaeontologia Electronica*, 8 (2), pp. 1-11.
- Siegel, A. F., and Benson, R. H. (1982). A robust comparison of biological shapes. *Biometrics*, 38, pp. 341-350.
- Simpson, G. G. (1945). The principles of classification and a classification of mammals. *Bulletin of the American Museum of Natural History*, 85, pp. 1-350.
- Skelton, R. R., McHenry, H. M., and Drawhorn, G. M. (1986). Phylogenetic analysis of early hominids. *Current Anthropology*, 27, pp. 21-43.
- Skinner, M. M., Gunz, P., Wood, B. A., and Hublin, J.-J. (2008). Enamel-dentine junction (EDJ) morphology distinguishes the lower molars of *Australopithecus africanus* and *Paranthropus robustus*. *Journal of Human Evolution*, 55, pp. 979-988.
- Skinner, M. M., Gunz, P., Wood, B. A., Hublin, J.-J. (in press). Discrimination of extant *Pan* species and subspecies using the enamel-dentine junction morphology of lower molars. *American Journal of Physical Anthropology*.
- Skinner, M. M., Gunz, P., Wood, B. A., Hublin, J.-J. (in press). How many landmarks? Assessing classification accuracy of *Pan* lower molars using geometric morphometric analysis of the occlusal basin as seen at the EDJ. In T. Koppe, G. Meyer, K. W., Alt (Eds.). *Interdisciplinary Dental Morphology*. Basel: Karger.
- Skinner, M. M., Wood, B. A., and Hublin, J.-J. (2009). Protostylid expression at the outer enamel surface and at the enamel-dentine junction of mandibular molars of

- Paranthropus robustus* and *Australopithecus africanus*. *Journal of Human Evolution*, 56, pp. 76-85.
- Slice, D. E. (2001). Landmark coordinates aligned by Procrustes analysis do not lie in Kendall's shape space. *Systematic Biology*, 50, pp. 141-149.
- Slice, D. E. (2005). Modern morphometrics. In D. E. Slice (Ed.), *Modern Morphometrics in Physical Anthropology* (pp. 1-45). New York, Boston, Dordrecht, London, Moscow: Kluwer Academic/Plenum Publishers.
- Slice, D. E. (Ed.) (2005). *Modern Morphometrics in Physical Anthropology*. New York: Kluwer Academic/Plenum Publishers.
- Slice, D. E., Bookstein, F. L., Marcus, F. L., and Rohlf, F. J. (1998). A Glossary for Geometric Morphometrics. New York: State University of New York, Stony Brook. <http://life.bio.sunysb.edu/morph/glossary/gloss2.html>
- Smith, B. H. (1989). Growth and development and its significance for early hominid behaviour. *OSSA*, 14, pp. 63-96.
- Sperber, G. H. (1974). Morphology of the cheek teeth of early South African hominids. *Doctoral thesis*. Johannesburg: University of the Witwatersrand.
- Spielman, R. S., Da Rocha, F. J., Weitkamp, L. R., Ward, R. H., Neel, J. V., and Chagnon, N. A. (1972). The genetic structure of a tribal population, the Yanomama Indians. VII. Anthropometric differences among Yanomama villages. *American Journal of Physical Anthropology*, 37, pp. 345-356.
- Spoor, C. F. (1993). The comparative morphology and phylogeny of the human bony labyrinth. *Doctoral thesis*. Universiteit Utrecht, Holland.
- Spoor, F. (1997). Basicranial architecture and relative brain size of Sts 5 (*Australopithecus africanus*) and other Plio-Pleistocene hominids. *South African Journal of Science*, 93, pp. 182-187.
- Spoor, F., and Zonneveld, F. (1998). A comparative review of the human bony labyrinth. *Yearbook of Physical Anthropology*, 41, pp. 211-251.
- Spoor, F., Jeffery, N., and Zonneveld, F. (2000a). Imaging skeletal growth and evolution. In P. O'Higgins, and M. Cohn (Eds.), *Development, Growth and Evolution: Implications for the Study of the Hominid Skeleton*. London: The Linnean Society.
- Spoor, F., Jeffery, N., and Zonneveld, F. (2000b). Using diagnostic radiology in human evolutionary studies. *Journal of Anatomy*, 197, pp. 61-76.

- Spoor, F., Stringer, C., and Zonneveld, F. (1998). Rare temporal bone pathology of the Singa calvaria from Sudan. *American Journal of Physical Anthropology*, 107, pp. 41-50.
- Spoor, F., Zonneveld, F. W., and Macho, G. A. (1993). Linear measurements of cortical bone and dental enamel by Computed Tomography. *American Journal of Physical Anthropology*, 91, pp. 469-484.
- Swindell, W., and Webb, S. (1992). X-ray transmission computed tomography. In S. Webb (Ed.), *The Physics of Medical Imaging* (pp. 98-127). London: IOP.
- Tattersall, I. (1986). Species recognition in human paleontology. *Journal of Human Evolution*, 15, pp. 165-175.
- Tattersall, I. (1992). Species concepts and species identification in human evolution. *Journal of Human Evolution*, 22, pp. 341-349.
- Tattersall, I. (1994). Morphology and phylogeny. *Evolutionary Anthropology*, 3, pp. 40-41.
- Thoma, A. (1985). *Éléments de Paléanthropologie*. Louvain-La-Neuve: Institut Supérieur d'Archéologie et d'Histoire de l'Art.
- Thompson, D. A. (1917). *On Growth and Form*. Cambridge: Cambridge University Press.
- Tobias, P. V. (1967). *The cranium and maxillary dentition of Australopithecus (Zinjanthropus) boisei*. Cambridge, New York: Cambridge University Press.
- Tobias, P. V. (1980). "Australopithecus afarensis" and *A. africanus*: critique and an alternative hypothesis. *Palaeontologia Africana*, 23, pp. 1-17.
- Tobias, P. V. (1983). Seventeenth Annual Report of the Palaeo-Anthropology Research Group September 1982-September 1983). Johannesburg, University of the Witwatersrand, Department of Anatomy and Human Biology.
- Tobias, P. V. (1991). *Olduvai Gorge, Volume IV. The Skulls, Endocasts and Teeth of Homo habilis*. Cambridge: Cambridge University Press.
- Turner, C. G., Nichol, C. R., and Scott, G. R. (1991). Scoring procedures for key morphological traits of the permanent dentition: The Arizona State University Dental Anthropology System. In M. Kelley, and C. Larsen (Eds.), *Advances in Dental Anthropology* (pp. 13-31). New York: Wiley Liss.
- Ungar, P. (2004). Dental topography and diets of *Australopithecus afarensis* and early *Homo*. *Journal of Human Evolution*, 46, pp. 605-622.
- Ungar, P. S., and Kirera, F. M. (2003). A solution to the worn tooth conundrum in primate functional anatomy. *Proceedings of the National Academy of Sciences of the United States of America*, 100, pp. 3874-3877.

- Ungar, P. S., and Williamson, M. (2000). Exploring the effects of tooth wear on functional morphology: a preliminary study using dental topographic analysis. *Palaeontologia Electronica*, 3 (1).
- Van Valen, L. (1982). Homology and causes. *Journal of Morphology*, 173, pp. 305-312.
- Viðarsdóttir, U. S., O'Higgins, P., and Stringer, C. (2002). A geometric morphometric study of regional differences in the ontogeny of the modern human facial skeleton. *Journal of Anatomy*, 201, pp. 211-229.
- Vrba, E. S. (1985). Introductory comments on species and speciation. In E. S. Vrba (Ed.), *Species and Speciation* (pp. ix-xviii). Pretoria: Transvaal Museum.
- Wagner, G. P. (1994). Homology and the mechanisms of development. In B. K. Hall, *Homology: The Hierarchical Basis of Comparative Biology* (pp. 274-301). San Diego: Academic Press.
- Walker, A. C., and Leakey, R. E. (1988). The evolution of *Australopithecus boisei*. In F. E. Grine (Ed.), *Evolutionary History of the "Robust" Australopithecines* (pp. 247-258). New York: Aldine de Gruyter.
- Walker, A. C., Leakey, R. E., and Harris, J. M. (1986). 2.5-Myr *Australopithecus boisei* from west of Lake Turkana, Kenya. *Nature*, 322, pp. 517-522.
- Wallace, J. A. (1972). The Dentition of the South African Early Hominids: A Study of Form and Function. *Doctoral thesis*. Johannesburg: University of the Witwatersrand.
- Ward, S. C., Johanson, D. C., and Coppens, Y. (1982). Subocclusional morphology and alveolar process relationships of hominid gnathic elements from Hadar formation: 1974-1977 collections. *American Journal of Physical Anthropology*, 57, pp. 605-630.
- Ward, C. V., Leakey, M. G., and Walker, A. (2001). Morphology of *Australopithecus anamensis* from Kanapoi and Allia Bay, Kenya. *Journal of Human Evolution*, 41, 255-368.
- White, T. D., and Folkens, P. A. (2000). *Human Osteology* (II ed.). San Diego: Academic Press.
- White, T. D., Johanson, D. C., and Kimbel, W. H. (1981). *Australopithecus africanus*: its phyletic position reconsidered. *South African Journal of Science*, 77, pp. 445-470.
- Williams, L. R. (1979). A photogrammetrical analysis of the pongid molar morphology. *Doctoral thesis*. Toronto: University of Toronto.
- Wolpoff, M. H. (1974). The evidence for two australopithecine lineages in South Africa. *Yearbook of Physical Anthropology*, 17, pp. 113-139.

- Wolpoff, M. H., and Lovejoy, C. O. (1975). A re-diagnosis of the genus *Australopithecus*. *Journal of Human Evolution*, 4, pp. 275-276.
- Wood, B. A. (1984). Interpreting the dental peculiarities of the "robust" australopithecines. In D. J. Chivers, B. A. Wood and A. Bilsborough (Eds.), *Food Acquisition and Processing in Primates* (pp. 535-544). New York and London: Plenum.
- Wood, B. A. (1985). A review of the definition, distribution and relationships of *Australopithecus africanus*. In P. V. Tobias (Ed.), *Hominid Evolution: Past, Present and Future* (pp. 227-232). New York: Alan R. Liss.
- Wood, B. A. (1991). Koobi Fora Research Project IV: Hominid Cranial Remains from Koobi Fora. Oxford: Clarendon Press.
- Wood, B. A., and Abbott, S. A. (1983). Analysis of the dental morphology of Plio-Pleistocene hominids I. Mandibular molars: Crown area measurements and morphological traits. *Journal of Anatomy*, 136 (1), pp. 197-219.
- Wood, B. A., and Engleman, C. A. (1988). Analysis of the dental morphology of Plio-Pleistocene hominids V. Maxillary postcanine tooth morphology. *Journal of Anatomy*, 161, pp. 1-35.
- Wood, B. A., Abbott, S. A., and Graham, S. H. (1983). Analysis of dental morphology of Plio-Pleistocene hominids II. Mandibular molars - study of cusp areas, fissure pattern and cross sectional shape of the crown. *Journal of Anatomy*, 137 (2), pp. 287-314.
- Zelditch, M. L., Swiderski, D. L., Sheets, H. D., and Fink, W. L. (2004). *Geometric Morphometrics for Biologists: A Primer*. San Diego: Elsevier Academic Press.
- Zipfel, B., and Berger, L. R. (in press). Partial hominin tibia (STW 396) from Sterkfontein, South Africa. *Palaeontologia Africana*.
- Zollikofer, P. C., and Ponce de León, M. S. (1995). Tools for rapid processing in the biosciences. *IEEE Computer Graphics and Applications*, 16 (6), pp. 148-155.
- Zonneveld, F. (2002). Applications and pitfalls of CT-based 3D imaging of hominid fossils. In B. Mafart, and H. Delingette (Eds.), *Three-Dimensional Imaging in Paleoanthropology and Prehistoric Archaeology* (pp. 5-9). Oxford: BAR International Series 1049 Archeopress.
- Zuccotti, L. F., Williamson, M. D., Limp, W. F., and Ungar, P. S. (1998). Technical note: Modeling primate occlusal topography using Geographic Information Systems technology. *American Journal of Physical Anthropology*, 107, pp. 137-142.